

Sustainable Textiles: Production, Processing,  
Manufacturing & Chemistry

Subramanian Senthilkannan Muthu *Editor*

# Advances in Textile Waste Water Treatments

 Springer

# **Sustainable Textiles: Production, Processing, Manufacturing & Chemistry**

## **Series Editor**

Subramanian Senthilkannan Muthu, Head of Sustainability, SgT Group and API,  
Kowloon, Hong Kong

This series aims to address all issues related to sustainability through the lifecycles of textiles from manufacturing to consumer behavior through sustainable disposal. Potential topics include but are not limited to:

Environmental Footprints of Textile manufacturing; Environmental Life Cycle Assessment of Textile production; Environmental impact models of Textiles and Clothing Supply Chain; Clothing Supply Chain Sustainability; Carbon, energy and water footprints of textile products and in the clothing manufacturing chain; Functional life and reusability of textile products; Biodegradable textile products and the assessment of biodegradability; Waste management in textile industry; Pollution abatement in textile sector; Recycled textile materials and the evaluation of recycling; Consumer behavior in Sustainable Textiles; Eco-design in Clothing & Apparels; Sustainable polymers & fibers in Textiles; Sustainable waste water treatments in Textile manufacturing; Sustainable Textile Chemicals in Textile manufacturing.

Innovative fibres, processes, methods and technologies for Sustainable textiles; Development of sustainable, eco-friendly textile products and processes; Environmental standards for textile industry; Modelling of environmental impacts of textile products; Green Chemistry, clean technology and their applications to textiles and clothing sector; Eco-production of Apparels, Energy and Water Efficient textiles.

Sustainable Smart textiles & polymers, Sustainable Nano fibers and Textiles; Sustainable Innovations in Textile Chemistry & Manufacturing; Circular Economy, Advances in Sustainable Textiles Manufacturing; Sustainable Luxury & Craftsmanship; Zero Waste Textiles.

More information about this series at <http://www.springer.com/series/16490>

Subramanian Senthilkannan Muthu  
Editor

# Advances in Textile Waste Water Treatments

 Springer

*Editor*

Subramanian Senthilkannan Muthu

Head of Sustainability

SgT Group and API

Kowloon, Hong Kong

ISSN 2662-7108

ISSN 2662-7116 (electronic)

Sustainable Textiles: Production, Processing, Manufacturing & Chemistry

ISBN 978-981-16-0064-7

ISBN 978-981-16-0065-4 (eBook)

<https://doi.org/10.1007/978-981-16-0065-4>

© The Editor(s) (if applicable) and The Author(s), under exclusive license to Springer Nature Singapore Pte Ltd. 2021

This work is subject to copyright. All rights are solely and exclusively licensed by the Publisher, whether the whole or part of the material is concerned, specifically the rights of translation, reprinting, reuse of illustrations, recitation, broadcasting, reproduction on microfilms or in any other physical way, and transmission or information storage and retrieval, electronic adaptation, computer software, or by similar or dissimilar methodology now known or hereafter developed.

The use of general descriptive names, registered names, trademarks, service marks, etc. in this publication does not imply, even in the absence of a specific statement, that such names are exempt from the relevant protective laws and regulations and therefore free for general use.

The publisher, the authors and the editors are safe to assume that the advice and information in this book are believed to be true and accurate at the date of publication. Neither the publisher nor the authors or the editors give a warranty, expressed or implied, with respect to the material contained herein or for any errors or omissions that may have been made. The publisher remains neutral with regard to jurisdictional claims in published maps and institutional affiliations.

This Springer imprint is published by the registered company Springer Nature Singapore Pte Ltd.

The registered company address is: 152 Beach Road, #21-01/04 Gateway East, Singapore 189721, Singapore

*This book is dedicated to:*

*The lotus feet of my beloved Lord  
Pazhaniandavar*

*My beloved late Father*

*My beloved Mother*

*My beloved Wife Karpagam and  
Daughters—Anu and Karthika*

*My beloved Brother—Raghavan*

*Everyone working in sustainable textile waste  
water treatment plants to make our planet  
earth*

**SUSTAINABLE**

# Contents

<b>Reuse of Salt-Containing Dyeing Effluents by Means of an Electrochemical and Ultraviolet Coupled System</b> .....	1
Carmen Gutiérrez-Bouzán, Valentina Buscio, and José-Antonio Tornero	
<b>Application of Sustainable and Low-Cost Sludge-Based Adsorbents for Textile Dye Degradation</b> .....	25
A. Geethakarathi	
<b>Sustainable Approach on the Treatment of Textile Wastewater Using Membrane Techniques</b> .....	89
R. Sivaranjane and P. Senthil Kumar	
<b>Dyestuff Adsorbing Natural Composites for Wastewater Treatments</b> .....	103
E. Emekdar and U. K. Şahin	
<b>Treatment of Textile Waste Water Using Low-Cost and Innovative Materials</b> .....	135
K. Amutha	
<b>Photo-Catalytic-Assisted Method for Treating Industrial Dye House Effluents</b> .....	147
Manickam Parthiban and Gunasekaran Devanand	
<b>Advanced Oxidation Processes (AOP)—Effective Innovative Treatment Methods to Degrade Textile Dye Effluent</b> .....	173
R. Sukanya Devi, Bhaarathi Dhurai, S. Sundaresan, and A. Selvakumar	
<b>Treatment of Textile Wastewater Using Biochar Produced from Agricultural Waste</b> .....	205
R. Sivaranjane and P. Senthil Kumar	

# About the Editor

**Dr. Subramanian Senthilkannan Muthu** currently works for SgT Group as Head of Sustainability, and is based out of Hong Kong. He earned his Ph.D. from The Hong Kong Polytechnic University, and is a renowned expert in the areas of Environmental Sustainability in Textiles & Clothing Supply Chain, Product Life Cycle Assessment (LCA) and Product Carbon Footprint Assessment (PCF) in various industrial sectors. He has five years of industrial experience in textile manufacturing, research and development and textile testing and over a decade's of experience in life cycle assessment (LCA), carbon and ecological footprints assessment of various consumer products. He has published more than 100 research publications, written numerous book chapters and authored/edited around 95 books in the areas of Carbon Footprint, Recycling, Environmental Assessment and Environmental Sustainability.



# Reuse of Salt-Containing Dyeing Effluents by Means of an Electrochemical and Ultraviolet Coupled System



Carmen Gutiérrez-Bouzán, Valentina Buscio, and José-Antonio Tornero

**Abstract** The textile dyeing produces a large volume of wastewater with high salinity and deep colouration. Residual dyes are generally not removed in conventional wastewater treatments, and therefore, specific treatments are required to remove colour. Sometimes, textile mills are not able to accomplish water discharge regulations as salts cannot be removed in the common wastewater treatments. To face both problems, salinity and colour of effluents, a new system has been designed based on a coupled electrochemical and UV process (EC-UV). It is a fast and simple treatment that enables the effluents colour removal. In addition, the wastewater salinity can also be reduced through the reuse of the treated effluents in new productive processes. The treatment is particularly efficient in the reactive dyeing process, although it can also be used for effluents of direct dyes. The implementation of this new system in the textile industry achieves significant benefits. The reuse of effluents containing high amount of salts implies lower consumption of water and salt in the dyeing process, and the removal of colour improves the yield of wastewater treatment plants with less consumption of chemicals. Finally, the reduction of wastewater salinity is also an additional economic and environmental benefit of the treatment, which results in lower wastewater taxes and improvement of the aquatic ecosystems.

**Keywords** Wastewater · Coloured effluents · Exhausted dyebaths · Decolourisation · Colour removal · Reactive dyes · Saline effluents · Water reuse · Electrochemical treatment · Coupled electrochemical–ultraviolet process

---

C. Gutiérrez-Bouzán (✉) · V. Buscio · J.-A. Tornero  
Universitat Politècnica de Catalunya (UPC)-INTEXTER (Textile Research Institute of Terrassa),  
Carrer Colom 15, 08222 Terrassa, Spain  
e-mail: [m.carmen.gutierrez@upc.edu](mailto:m.carmen.gutierrez@upc.edu)

V. Buscio  
e-mail: [valentina.buscio-olivera@upc.edu](mailto:valentina.buscio-olivera@upc.edu)

J.-A. Tornero  
e-mail: [jose.antonio.tornero@upc.edu](mailto:jose.antonio.tornero@upc.edu)

## 1 Introduction

In the last decades, the textile industry has made huge efforts to become more sustainable. It is one of the most important industrial sectors and it uses high amount of water and chemicals [1, 2]. For this reason, the achievement of a lower environmental impact is an important goal. On the one side, the production processes have been improved by using less chemicals or substituting the more hazardous ones by others less aggressive to the environment. On the other hand, the treatment of wastewater has been noticeably improved, which is an important contribution because the textile industry generates up to 20% of industrial wastewater worldwide [3].

Known examples of products substitution by more sustainable ones are, among others, the use of more biodegradable sizing materials, the non-use of certain azo dyes, the change of formaldehyde-based finishing by non-allergenic resins, the replacement of alkylphenols by alcoholethoxylates, the application of more sustainable flame retardants, etc. In addition, all processes have been generally revised and adapted in order to reduce the consumption of chemicals, energy and water. Thus, for instance, in the cotton dyeing processes, new types of reactive dyes with lower salt and water requirements have been developed [4].

As indicated, one of the points that influence the sustainability of the textile industry is that it is a water-intensive sector. The Ellen MacArthur Foundation reported that the different processes of the textile industry spent in total about 93 billion cubic metres of water, of which approximately 6 billion cubic metres are consumed in dyeing and finishing processes [5]. For this reason, different methods and products to reduce the liquor ratio in the in dyeing, washing and finishing processes have been developed. This is the case of Avitera reactive dyeing technology that reduces both water and energy consumption [6].

In any case, the effluents generated in dyeing and washing processes are characterised by a deep colouration due to the unfixed residual dyes, and generally, they have also a high content of salts as a result of the electrolyte added in the dyeing process. Due to this salinity, it is not always possible to reduce more the water consumption in order to accomplish the discharge limits.

On the other hand, the sales of textile products are expected to increase to about 160 million tonnes in 2050; therefore, the amount of discharged wastewater will also increase significantly [5]. For this reason, the reuse of the treated wastewater is becoming an increasing interest for companies with the aim to reduce the environmental impact and to achieve the more efficient use of water resources.

This chapter presents the result of our studies to treat and reuse the coloured effluents of textile industry, which are generally poorly biodegradable. Moreover, the work is especially focussed on those effluents that have a high content of salts, as it is the case of reactive dye effluents [7–11]. With this purpose, a coupled electrochemical and ultraviolet treatment (EC-UV) is used. It is applied to the more coloured and saline effluents, which are segregated at the end of the dyeing or washing process.

This procedure is in accordance with the “Reference Document on BAT for the Textiles Industry” issued by the European Commission where it is recommended to collect and treat separately the effluents containing poorly biodegradable compounds such as dyes [12].

The EC-UV treatment could be carried out with two different purposes: (1) to remove colour to improve the subsequent wastewater treatment or (2) to remove colour and reconstitute the effluent in order to reuse the treated effluent containing salts in new dyeing processes. A general schema of the reuse process is shown in Fig. 1.

The use of the EC-UV process to reuse implies a significant saving of water and salt. The results obtained with the reuse of treated exhausted reactive dyebaths are presented with respect to reference samples (dyed with the usual softened tap water). In addition, the environmental benefits of the EC-UV system, both for colour removal and for reuse, were evaluated through a Life Cycle Assessment (LCA) study.

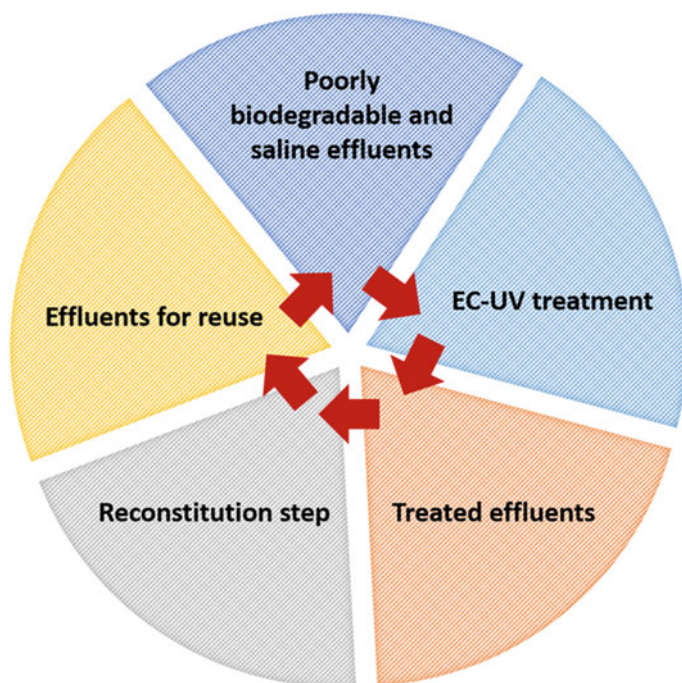
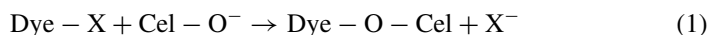


**Fig. 1** General schema of the reuse process applied to poorly biodegradable and saline effluents of the textile industry

## 2 The Problem of Residual Dyes and Salts

The textile industry has a major relevance in developing countries [13]. Nevertheless, it requires an intensive use of water in many processes (a mean of 200–400 L per kg of product) [14] which results in a high generation of wastewater containing salts and a wide range of organic compounds. The amount of produced wastewater and its content of pollutant or harmful compounds is highly dependent on the type of fibre and the process applied [15]. Thus, it is estimated that the dyeing produces about 8% of the total textile wastewater. A high proportion of dyeing effluents is produced by cotton processes as this fibre is the most consumed natural fibre [16]. Cotton dyeing can be performed with many types of dyes but reactive ones are the class mostly used because they have a wide range of shades and brilliant colours [17, 18]. They have also good wet fastness properties because they react with hydroxyl groups of cellulosic fibres, being fixed to them by means of a covalent bond. For instance, reaction 1 illustrates the fixation of the halotriazine reactive group to the cellulose:



However, dyeing of cellulose fibres with reactive dyes has a great inconvenient: meanwhile dyes react with fibres, they also react with water. That is to say, a secondary reaction of hydrolysis (reaction 2) is produced during the fixation of dye.



Then, hydrolysed reactive dyes (Dye-OH) are not able to react with the fibre and should be removed. About 20–40% of reactive dyes could be hydrolysed during the dyeing process, which produces very deeply coloured exhausted dyebaths (Fig. 2).

On the other hand, to ensure a minor hydrolysis, the fixation of the reactive dyes onto the fibre is carried out at alkaline pH and with a high concentration of an electrolyte, generally NaCl or Na<sub>2</sub>SO<sub>4</sub> [19, 20]. The amount of required electrolyte ranges from 0.6 to 0.8 kg salt/kg fibre, according to the type of dye structure, colour intensity and dyeing equipment [17].

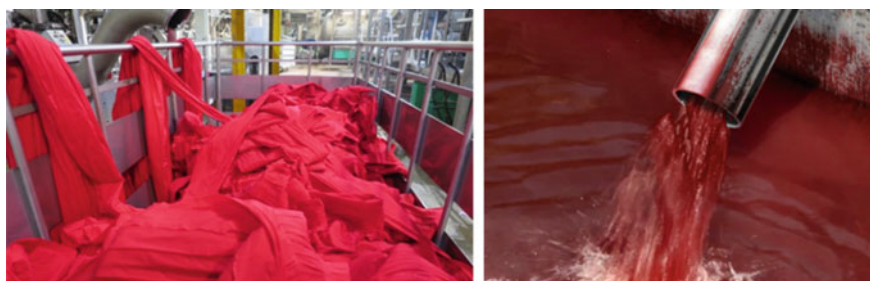


**Fig. 2** Example of exhausted coloured effluent after a reactive dyeing process

Consequently, dyeing processes with reactive dyes produce effluents with:

- High colouration
- High salts content
- Alkaline pH

The treatment of these effluents is very difficult due to both the high salinity and the low biodegradability of dyes. Then, the use of specific treatments is required. The most usual ones are based on the separation of dyes from the effluent. But they generate a waste which requires a further treatment to remove the concentrated pollutants.

On the other hand, there are not feasible treatments able to remove salts. Increasing salinity of riverbeds (due to saline wastewater discharges) is a major concern in most of countries, mainly those with scarce riverbeds. For these reasons, a ground-breaking system, based on an electrochemical-UV combined treatment, able to reuse water and salts is the most appropriate alternative to encourage the circular economy in the textile industry. This system could be applied to any type of saline and coloured effluents. In particular, our studies have been focussed on reactive dye exhausted dyebaths for three reasons: (1) this type of dyes are one of the most used in the textile industry, (2) they have one of the lowest fixation rates onto the fibre and (3) they require the use of a significant amount of salt to be applied, which cannot be further removed from the wastewater.

### 3 Methods for Colour Removal of Textile Effluents

As previously mentioned, the wastewater generated by the textile industry is characterised by containing residual dyes. Modern dyes offer great resistance to chemical and photochemical degradation since the manufacturers are constantly researching to obtain textile dyes with better features: brighter shades and high fastnesses values to light, water, soap, etc. As a consequence, they cannot be effectively removed from the wastewater by traditional methods and wastewater with high colouration could be discharged into the environment. Although many dyes could be non-toxic compounds, small amount of them (about 1 mg/L) is sufficient to produce an intense colouration that can impact or even impede the aquatic life in the riverbeds [21].

The methods currently used for the treatment of textile wastewater can be classified into three categories: biological, chemical and physical processes (Fig. 3). It should be noted that a unique method is not applied to treat the textile wastewater, being required to combine different treatments in order to meet with legislative regulations [22, 23].

Currently, many textile companies use **biological processes** to treat their wastewater. This method shows high efficiency in eliminating biodegradable organic matter with low operational cost. However, due to the structure and high molecular weight of dyes, biological processes provide low colour removal [24]. In fact, the removal of the

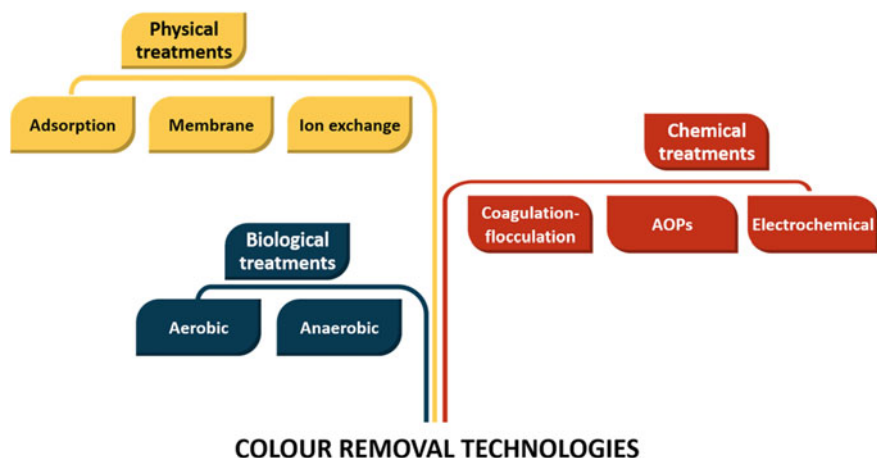


**Fig. 3** Colour removal technologies applied to treat textile effluents (AOPs: advanced oxidation processes)

colour obtained by means of these processes is usually associated to the adsorption of the dyes on the biomass.

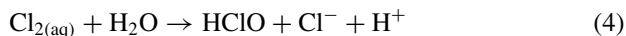
With regard to **physical treatments**, adsorption processes are capable of removing a wide variety of dyes. However, the need to regenerate the adsorbent material increases its operational cost. On the other hand, membranes are increasingly used at industrial level with satisfactory results, but the membrane fouling is still the main drawback of this technology.

The **chemical processes** are based on the addition or generation in situ of chemical reagents capable of degrading dyes. The coagulation–flocculation treatment is the most used chemical process due to its high discolouration rate. Its main disadvantage is the generation of a sludge which must be subsequently dried, collected and treated. The advanced oxidation processes (AOPs) focus on the generation of oxidising species such as hydroxyl radicals ( $\text{OH}^\cdot$ ), which are subsequently used to break down pollutants into smaller and harmless species. Some examples of AOPs are, among others, photocatalysis, Fenton, photo-Fenton, ozonation, etc. The electrochemical processes include treatments as electro-Fenton, electrocoagulation and anodic oxidation. The dye degradation by means of anodic oxidation can be carried out directly on the anode surface or generating indirectly strong oxidant species from hypochlorite/chlorine, hydrogen peroxide and ozone.

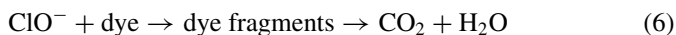
As discussed above, textile wastewater can contain residual salts. As a consequence, the indirect oxidation of the dyes using the ion chloride already present in the effluents has become an interesting alternative to conventional purification processes. In this case, the treatment involves two steps:

1. Generation of oxidant species according to reactions (3)–(5) [25–28]:





2. Degradation of dyes: The oxidant species generated are able to fragment the dye molecule according to the reaction 6:



It should be noted that colour removal is much faster than the degradation of the dye, since the oxidising species attack first the chromophore group of the dye [29–31]. It was observed that colour removal can be enhanced by UV light irradiation. This improvement is attributed to the production of highly efficient radicals (reactions 7 and 8):



Figure 4 shows the steps involved in the indirect oxidation of dyes assisted by UV, which is the base of the EC-UV system.

The EC-UV system has been already validated at industrial scale for the treatment of textile effluents containing reactive dyes. The system not only solves the problem of effluent colouration, but also enables the reuse of the treated water that still contains salts. Therefore, the system allows to reduce the consumption of water and salts in the dyeing processes.

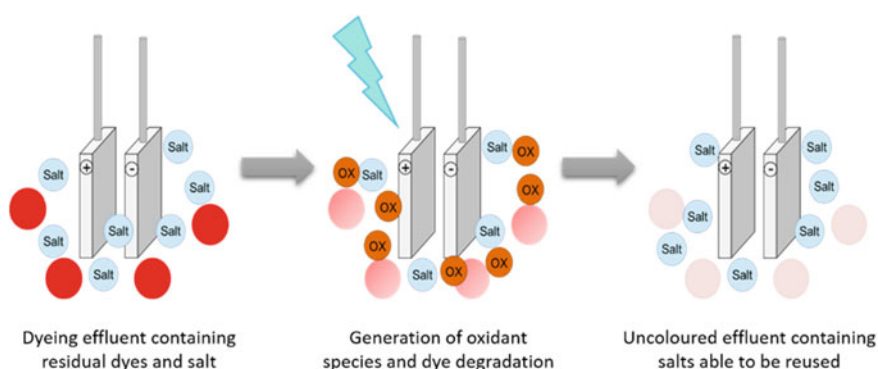


**Fig. 4** Steps involved in the indirect oxidation of dyes

## 4 Advantages of Coupled Electrochemical–Ultraviolet Treatment

Currently, textile effluents are treated by combining biological with coagulation–flocculation processes. Despite this combination is capable of meeting with legislative regulations in terms of organic matter and colour elimination, salts cannot be removed. The treatments used for removing salts (mainly membranes) are based on obtaining a concentrate that must be subsequently removed as a waste. In addition, these treatments have high operational and maintenance cost.

The EC-UV system is an alternative to the current methods applied to treat the textile dyeing effluents. The main advantage of the system is that it enables to degrade organic pollutants without the addition of chemicals and without generating additional wastes. In this treatment, the salts already present in the effluents are used to generate oxidants species that break down the dye molecules into smaller ones. Then, the uncoloured effluents that still contain high amount of salt could be reconstituted and finally reused in new dyeing processes. Currently, there is no technology into the market able to treat the effluents without using chemical reagents and without producing wastes.

Table 1 shows a comparison between the most used methods to treat textile effluents and the EC-UV system.

Taking into account these considerations, it can be stated that the EC-UV system is a green technology that contributes to implement the circular economy in the textile industry.

**Table 1** Advantages and disadvantages of the most used methods to remove colour and comparison with the EC-UV system

Process	Advantages	Disadvantages
Biological	Cost effective	Low colour removal rates
Coagulation–flocculation	High colour removal rates for a wide variety of dyes	Sludge production. Addition of chemicals pH dependent
Adsorption	Simple and effective for a wide variety of dyes	Regeneration of adsorbents materials. Expensive
Membranes	Effective for a wide variety of dyes	Membrane fouling. High operational cost
<b>EC-UV</b>	<b>No sludge production. Does not require the addition of chemicals Reuse of water and salts</b>	<b>Can be applied in the treatment of effluents with a conductivity <math>\geq 20</math> mS/cm</b>



## 5 Description of the EC-UV System

The coupled electrochemical–ultraviolet treatment explained in the previous section has to be implemented through a process that makes it feasible to be applied in the target industry. Beyond the issues related to the industrial implementation (to be explained in the next section), the basic process requires three core steps to remove colour from the effluent and eventually prepare it for its reuse in textile dyeing:

- Generation of oxidant species in an electrochemical cell
- Oxidation (decolouration) reaction
- Water conditioning for reuse (optional).

Therefore, the basic EC-UV system consists of the sequential implementation of the functional elements required to perform the three mentioned steps (Fig. 5).

When the effluent enters in the system flow, it first must pass through an electrochemical cell where the reactions (3)–(5) take place. For this purpose, it is necessary to design the surface of the electrodes in the cell considering the maximum current density allowed to avoid their early damage, and consequently, the intensity and voltage required to run using a power supply commercially available at reasonable cost. Forecasting a wide operative range in order to adjust system operation to effluent conditions will ensure its application with very different effluents in terms of source, colour load and conductivity.

Once the oxidation species are generated in the electrochemical cell, the effluent can remain in a tank while the oxidation (decolouration) takes place. This tank is a suitable place to apply UV irradiation and mechanical stirring, which will speed up reaction (6) by arising reactions (7)–(8). This is a simple step to implement while

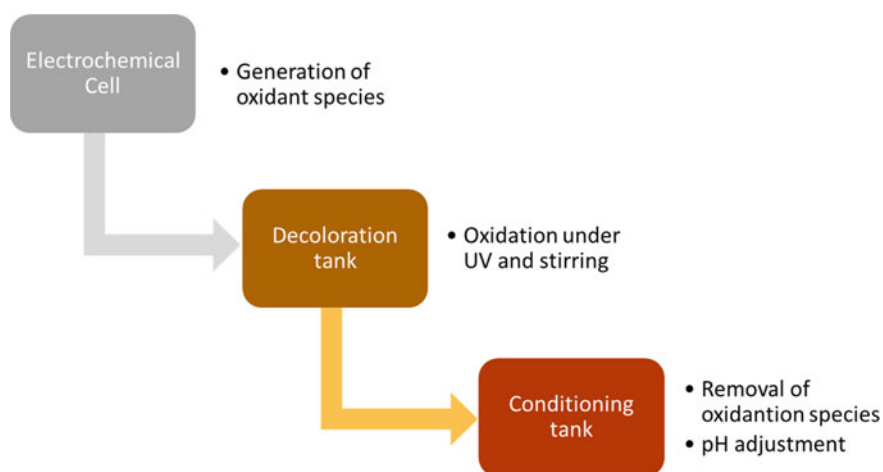


**Fig. 5** Steps of the EC-UV system

their key aspect come from the right tune of staying time and UV application. These variables will have an impact in the overall system's processing efficacy.

In this stage, the system can periodically check the water colour and stop the process when it reaches the desired colour level. Then, it can either:

- Discard the treated effluent (but now with a lower colour load), so the process would end here.
- Prepare it for further reuse in a dyeing process.

In case of preparation for reuse, the system should ensure a low level of oxidant species and adjust the adequate pH level. These operations could be performed either in the same tank or in a different liquid container arranged for such operation.

## 6 Industrial Implementation of the EC-UV System

In addition to the core steps of the EC-UV system, which would form the simplest process at laboratory level, the industrial implementation sets additional requirements in terms of process robustness and efficiency (which leads to cost and competitiveness, in the end). More in detail, industrial process optimisation involves avoiding bottlenecks in the processing flow and also the right arrangement and fine tune of each step. As a part of this optimisation, core steps must be supported by auxiliary operations in its industrial implementation, mainly preparatory checkpoints and in-process checkpoints, although they do not have a relevant impact in the overall productivity of the system.

The industrial implementation of the EC-UV system was tested in an European-funded innovation project (ECO/13/630452) and has been object of two patents [32, 33].

When designing the EC-UV industrial process, the following points, inherent to the electrochemical decolouration, were considered, as well:

1. For the treatment of a fixed volume of water, the required oxidant agent can be generated at higher rate in the electrochemical cells, but it requires more time to perform its oxidation function, which means that it can become a bottleneck
2. Oxidation (decolouration) requires two simultaneous additional actions to be completed: stirring and UV irradiation
3. Eventual preparation for reuse requires additional time for the pH adjustment and residual oxidants removal.

Considering all the above key requirements, EC-UV system was designed consisting of several tanks that are sequentially filled according to the requirements of the process. The system as a whole was developed to work with effluent batches rather than continuous operation. This allows to keep all the elements of the system working continuously in parallel, thus maximising the overall system productivity, although the fine tuning of the operating elements will have an impact on efficacy, energy consumption and processing time.

Also, in order to ensure industrial robustness, the system is equipped with several instruments to ensure that the effluent characteristics are within the system operative constraints.

The effluent is separated into three tanks, each one with UV lamps and a stirring device to homogenise the effluent. The last one is equipped with elements to prepare the effluent before being reused.

After the first step of electrochemical treatment is completed, colour of treated effluent is measured. If the effluent meets the established criteria acceptance, it is directed to tank 3 where the reconstitution step is carried out in order to prepare the effluent to be reused in new dyeing processes.

This approach gives an expanded process which is depicted in Fig. 6 for a system consisting of “n” treatment tanks.

From the equipment point of view, the functional steps are divided into five sub-processes:

1. Analysis of water conditions: During this step, the input valve is opened in order to fill the three treatment tanks passing through a filtre. This filtre will prevent damage or malfunction of the system due to fibres, yarns or solids in suspension that would eventually damage the electrochemical cell and hydraulic elements. The following parameters can be checked in this point to evaluate the suitability of the effluent to be treated: pH, conductivity and temperature. During this operation, the effluent should not go through the electrochemical cell till it is

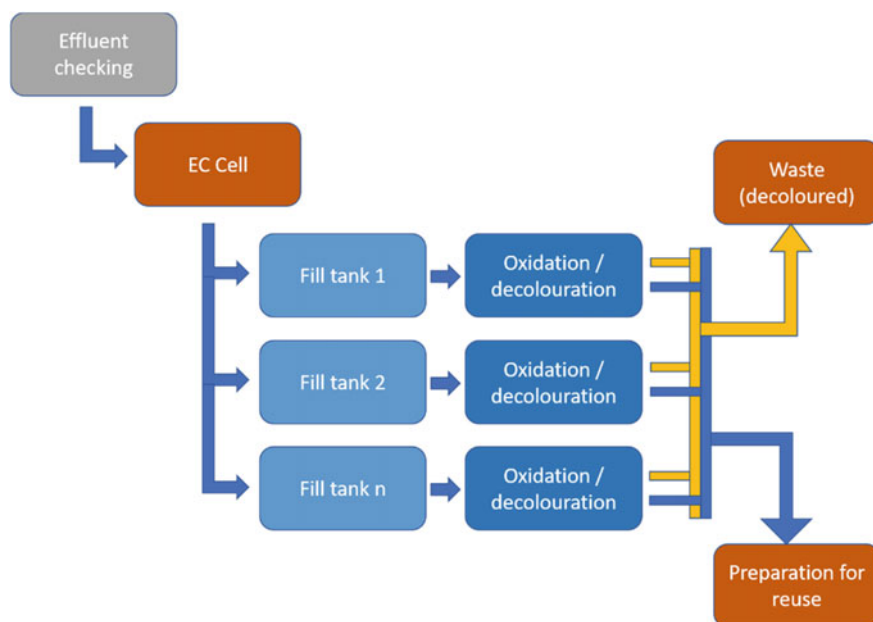


**Fig. 6** Schema of the EC-UV system with n treatment tanks

inside the desired range for the EC-UV system. As long as the effluent does not reach this condition, the effluent can be discarded through a by-pass section. This is intended to reduce the electrodes damage.

2. **Tank filling:** Depending on the effluent volume to be treated, the system is suitable to work with one or more recirculation tanks. The tanks can be filled sequentially with effluent flowing through the electrochemical cell, so the decolouration process will start immediately from the first moment the water enters into the tank.
3. **Tank recirculating:** All the system tanks should be filled at this stage; the oxidation should be taking place in all of them; however, the desired decolouration could have not been achieved. Therefore, a recirculation (for a predefined amount of time) of effluent for each tank, sequentially, though the electrochemical cells can add oxidation agents when required to speed up the decolouration process. While one is recirculating, the other two will be stored. According to the laboratory tests, the storage with stirring and UV lamp irradiation increases the efficiency of the process and reduces the electrical costs. It also achieves the removal of undesirable residual compounds. This recirculating process could be carried out with each tank until the colour sensor indicates that it is decolourised to the pre-defined value.
4. **Preparation for reuse:** When the colour sensor detects that the effluent is into the specified range, the effluent reconstitution can take place in this tank. While this process takes place, the other tanks can be recirculating.
5. **Water flush:** Once the effluent is decolourised and/or ready to be reused (depending on the predefined target), it would be pumped to the output tank. The tank that is empty would be filled to continue the process.

Of course, all these steps must be supported by the appropriate sensors, actuators and electronic control. One of the advantages of the system is that it is suitable to work with predefined recipes based on the characteristics of the effluent (higher or lower conductivity, colour load, etc.). The right design of valves and sensors also allows to implement auxiliary processes like cell cleaning to maximise electrode life, etc.

Joining the maximum system functionality and adaptability to different effluents can generate a moderately complex industrial engineering design, as depicted in patent and Fig. 7, although its industrial implementation is clean, compact and provides an immediate impact in the competitiveness of the dyeing mill when applied.

## 7 Results of EC-UV Treatment

As indicated in the previous sections, the EC-UV system can operate in two ways:

1. decolourisation mode.
2. decolourisation + reuse mode.



**Fig. 7** EC-UV industrial system currently operating in a mill for the treatment of coloured and saline effluents at 4 m<sup>3</sup>/h

In both cases, it is important to select a current density value appropriate to obtain the required decolourisation level. This decolourisation value could be different when the effluent will be discharged to a wastewater treatment plant, to sewer, to a river bed or when it submitted to reconstitution process in order to be reused.

In general, the EC-UV system is appropriate for the treatment of any type of coloured effluents with high conductivity values. In particular, it is especially recommended for the treatment of exhausted dyebaths from reactive dyeing in Jet. These effluents are characterised by their alkaline pH and high content of salts, generally sodium chloride.

### ***7.1 Selection of the Current Density***

The current density required to treat each effluent should be established according to the content of residual dyes and to the conductivity of the effluent. It is an important parameter both from the colour removal yield and from the economic point of view. As can be seen in Fig. 8, the higher the current density, the higher the colour removal yield. But also, an increasing of the current density implies a higher cost of the treatment.

Moreover, it should be noted that when a certain value of colour removal is achieved, the increase of the yield is not so evident when increasing the current density. For this reason, it is important to fix the required decolourisation level and to select the lowest current density that enables to achieve it.

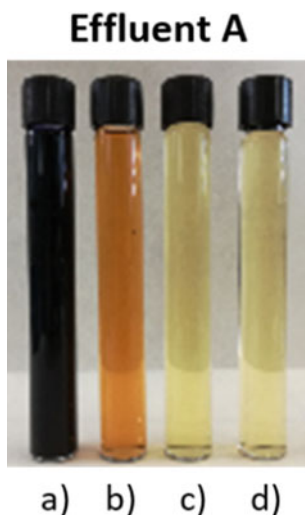


**Fig. 8** Effluent A: influence of current density on the colour removal rate. Applied current density: **a** untreated, **b** treated at  $33 \text{ mA/cm}^2$ , **c** treated at  $66 \text{ mA/cm}^2$ , **d** treated at  $112 \text{ mA/cm}^2$

In addition, there are two characteristics of the effluent that show a clear influence on the decolourisation rate: the initial colouration of the effluent and its conductivity. As expected, when the initial colouration is very deep, it is necessary to work at a high current density value. However, the current to be applied would depend also on the effluent conductivity: the higher the effluent conductivity, the more efficient the EC-UV process, the lower the required current density. It is evident that working at higher current densities provides better results, but it also increases the power consumption.

As an example, in Table 2 are shown different current density values used to treat the exhausted reactive dyebaths that were later discharged to the biological treatment plant of the mill.

As can be observed, the results of the decolourisation tests and the power consumption associated to them lead to the conclusion that it is important to select an intensity value as low as possible, but able to achieve the required decolourisation rate.

**Table 2** Current density required according to the effluent conductivity values (colour removal: 60–80%) and resulting electrical consumption

Effluent Conductivity (mS/cm)	Current density ( $\text{mA/m}^2$ )	Electrical consumption ( $\text{Kwh/m}^3$ )
>120	4	0.5
90–120	16	2.1
60–90	33	4.3
20–60	66	8.5

Although the values presented in Table 2 are indicative and should be adapted to each particular situation, this table can be used as a guide to determine the current density value required to carry out the EC-UV treatment.

## 7.2 Results of Wastewater Colour Removal

The treatment of high conductivity liquor baths with the EC-UV system enables to reach a fast and complete removal of colour of effluents, even in cases of deep colouration, as can be seen in Fig. 9.

During the EC-UV treatment, the dye molecules are broken down into smaller ones, which are also soluble but uncoloured or slightly coloured. Thus, the effluents are decoloured with the advantage that no sludge or solid waste are generated.

As it has been specified before, the effluents must only to meet some characteristics in order to ensure the proper functioning of the EC-UV system:

- pH between 9 and 12
- Conductivity > 30 mS/cm.

When they accomplish these characteristics (or these parameters are adjusted to meet them), the effluents could be directly treated with the EC-UV system. The addition of chemicals is not required as the electrons supplied by the electricity are the only reagent. The salts already contained in the effluents act as an electrolyte to transport the electrons through the solution.

As an example, Fig. 10 shows the results of decolourisation after the application of EC-UV treatment to three residual dyebaths with a wide range of conductivity

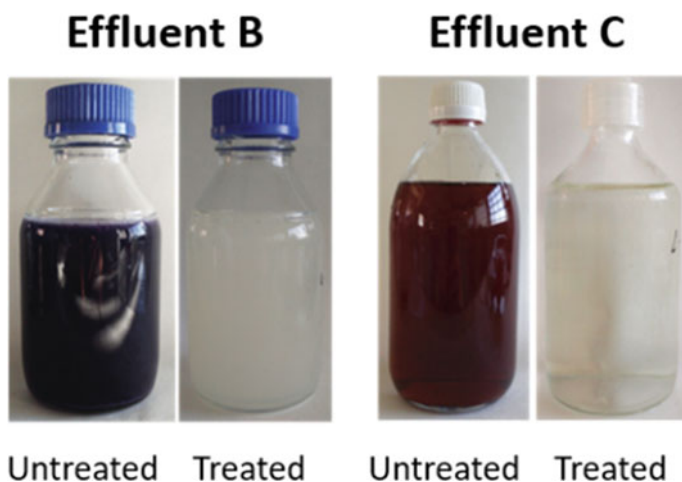


**Fig. 9** Reactive dye effluents treated to 100% colour removal (pH 10.6–10.7, conductivity 60–120 mS/cm)

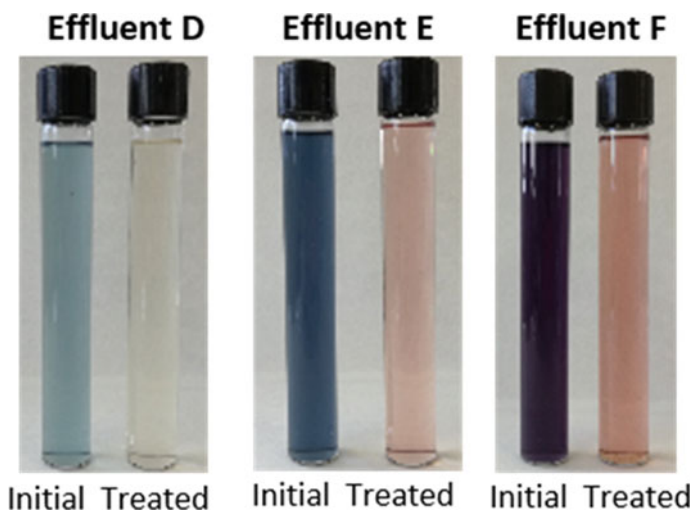


**Fig. 10** Decolourisation results obtained with three reactive dyeing effluents (pH range 9.6–9.8; conductivity: 87–125 mS/cm and  $[Cl^-]$ : 38–52 g  $Cl^-/L$ )

values and containing different types of residual dyes. The effluents were treated at  $33 \text{ mA/cm}^2$  and the colour removal rate was 72%, 88% and 68% for effluents D, E and F, respectively.

In general, most of the exhausted reactive dyebaths met the acceptance criteria established for the EC-UV treatment, and therefore, they were treated by means of this system. In each case, the current should be fixed according to the dye bath conductivity and colour deepness. Also, the decolourisation rate should be established and can depend on whether the EC-UV system will be used to reuse the effluent or to remove colour as a complementary treatment of a biological wastewater treatment plant. In both cases, it is enough to work in a colour removal range between 60 and 80%. The EC-UV treatment can also be used as a final treatment to remove colour. Then, it could be advisable to reach a colour removal level higher than 80%, depending on the particular regulations.

### ***7.3 Results of Dyeing with Reused Salts and Water***

Once the effluents are decolourised, the reconstitution phase of the EC-UV system starts up. The effluent reconstitution is carried out in the following steps:

1. Carbonates and bicarbonates are removed by acid addition and stripping (pH = 5).
2. Neutralisation of the effluent by alkali addition (pH = 7).



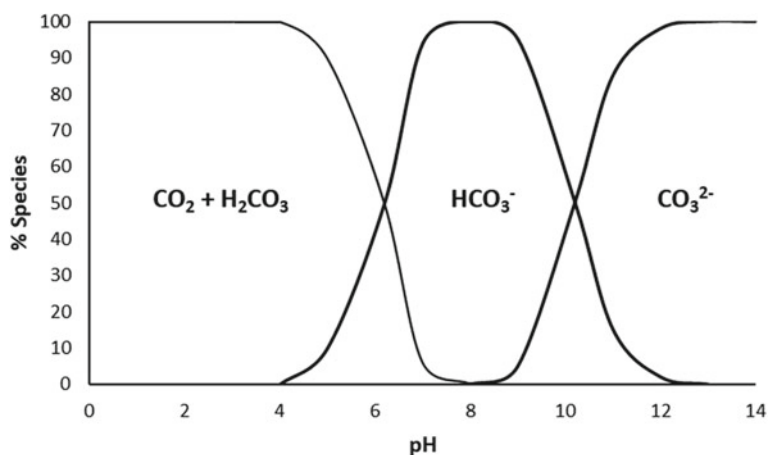


**Fig. 11** Concentration of carbonate, bicarbonate and carbon dioxide depending on the pH

- Residual oxidants removal by UV radiation and, if required, addition of a reducing agent.

As above indicated, the carbonates and bicarbonates are converted into CO<sub>2</sub> when the pH is below 5 (see Fig. 11).

Thus, it was found that when the pH decreases to 5, no HCO<sub>3</sub><sup>-</sup> and CO<sub>3</sub><sup>2-</sup> are present in the effluent and it can be satisfactorily reused in new dyeing processes with reactive dyes. The removal of carbonates and bicarbonates is particularly important in the case of reactive dyeings because these type of dyes are hydrolysed at alkaline pH (see reaction 2 in Sect. 2). Thus, the dyeing process should be started at neutral pH to enable the adsorption of the dye onto the fibre. Once finished the adsorption step, carbonate should be added to favour the reaction of dyes with the fibres.

The reuse of the reconstituted effluents can be performed according to the textile mill procedure. They can be reused directly or mixed with a small proportion of decalcified tap water. If the conductivity of the effluent is insufficient for the next dyeing, the appropriate amount of salt should be added. As a mean, between 30% and 100% of salt can be saved with the EC-UV system when 70% of the treated effluent is reused in new dyeings (depending on the salt contained in the residual bath and the requirements of the new one).

Figure 12 shows the results of several dyeings made with 70% of two reused effluents previously discoloured and reconstituted with the EC-UV system. The salt reused in these processes was 86%. The effluent reuse was carried out both in monochromies and trichromies. Dyeings were carried out on two different cotton fabrics with: 2% Remazol Ultra Yellow RGBN, 2% Remazol Deep Red RGB, 2% Intrafix Navy DSB and a Trichromie of them: 1% Yellow + 1% Red + 1% Navy (% over weight of fibre). After the dyeing process, the usual washing step should be carried out in order to remove the dyes that were not fixed onto the fibre.

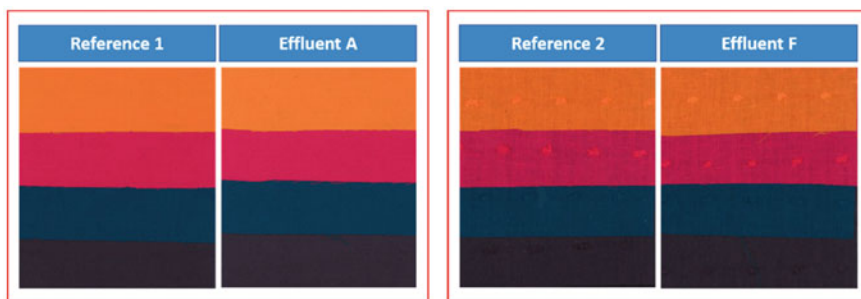


**Fig. 12** Examples of dyeings obtained reusing 70% of two exhausted reactive dyebaths (A and F) both treated at 33 mA/cm<sup>2</sup> (versus a reference dyeing)

The quality of dyed fabrics was studied from colour differences ( $DE_{CMC(l:c)}$ ) with respect to references dyed with decalcified water. The difference in colour was determined in conformity with the Standard UNE-EN ISO 105-J03 [34]. The chromatic coordinates and colour differences obtained with the effluents A and F are presented in Table 3.

As can be seen, in all cases, the effluents were satisfactorily reused. All fabrics showed colour difference values lower than 1, which is the common acceptance criteria established by many companies ( $DE_{cmc(2:1)} < 1$ ). It should be noted that the treated effluents showed a colour removal rate of 80 and 72%, which demonstrates that the full colour removal is not necessary for the effluent reuse. In general, 60–80% colour removal can be an advisable value as an increasing of this rate will imply a higher cost, but not always an improvement of reuse results.

A wide range of reuse trials have been made with the EC-UV system at 70% and 100% reuse ratio, with effluents containing different types of residual reactive

**Table 3** Colour differences obtained in dyeings with the reused effluents A and F

Effluent A				
Dye	DH	DL	DC	$DE_{cmc(2:1)}$
Yellow	0.32	−0.04	−0.64	0.72
Red	−0.59	0.64	−0.14	0.88
Navy	0.78	0.34	−0.29	0.90
Trichromie	−0.74	−0.52	−0.03	0.91
Effluent F				
Dye	DH	DL	DC	$DE_{cmc(2:1)}$
Yellow	0.05	−0.10	−0.38	0.39
Red	−0.13	−0.32	−0.09	0.36
Navy	−0.63	0.03	0.05	0.63
Trichromie	−0.53	0.52	0.07	0.74

dyes, different conductivity values, salt concentration, etc. In many cases, excellent reuse results have been obtained. However, in some cases, colour differences are too high and do not accomplish the acceptance criteria. A specific reason to explain this trouble has not yet been found. For this reason, the combination of factors that can significantly influence or even prevent the reuse of the discoloured effluents is still under research.

## 8 Environmental Impact of EC-UV Treatment

As explained above, EC-UV is a new system that can be applied to treat coloured and saline effluent, being particularly suitable for the purification of the wastewater from the reactive jet dyeing process.

The implementation of the system in the textile industry has clear environmental advantages, both in the wastewater treatment plant of the company [35] and in the dyeing process [36]. A summary of the results obtained in Life Cycle Assessment (LCA) performed according to ISO 14040 standards [37] is presented below.

### 8.1 Environmental Impact on the Wastewater Treatment Plant

The environmental assessment was carried out considering three scenarios:

*Scenario 1: Current situation:* In general, a medium-sized textile company uses a combination of an aerobic biological treatment with activated sludge and a tertiary process before discharging the wastewater (Fig. 13).

*Scenario 2: EC-UV decolourisation mode:* This scenario involves three steps (Fig. 14). In the first one, the EC-UV system is applied to remove the colour of the wastewater generated in the jet dyeing process. Subsequently, the treated effluent is mixed with the wastewater from other processes and the biological treatment is

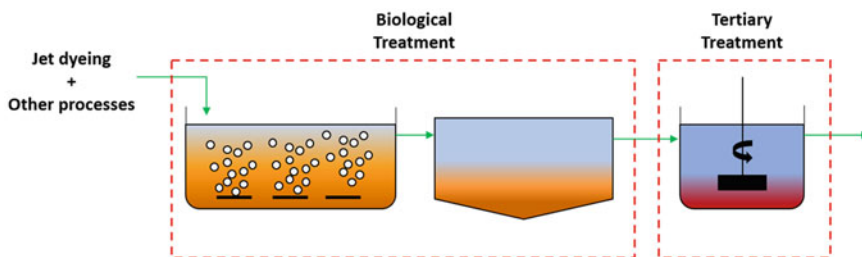
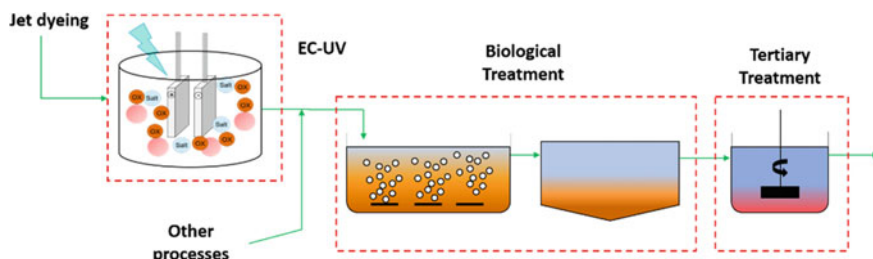
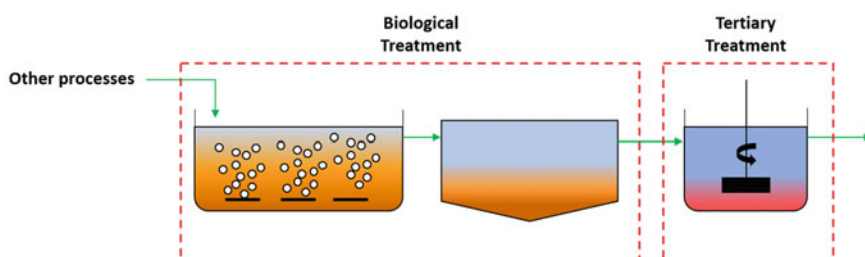


Fig. 13 Scenario 1: Current situation



**Fig. 14** Scenario 2: EC-UV to discoloration mode



**Fig. 15** Scenario 3: EC-UV reuse mode

carried out. The last step is the use of the tertiary treatment to remove residual colour. It should be noted that EC-UV system enables to decrease the electricity consumption of the biological treatment by 10% and the addition of decolourising agent by 35%.

*Scenario 3: EC-UV reuse mode:* In this scenario, the system is applied both to decolourise and to reuse the treated effluents. Consequently, only the wastewater generated in other processes is treated in the wastewater treatment plant (Fig. 15).

The use of the system in this mode results in 70% of water and up to 72% of salt reuse. In addition, the consumption of decolourising agent decreases by 80%.

The three scenarios were evaluated by means of ReCiPe endpoint approach. In comparison to the current situation (Scenario 1), the use of the system in the discoloration mode (Scenario 2) reduces the environmental impact of the textile wastewater treatment in 35%. This improvement can be mainly attributed to the lower consumption of decolourising agent in the tertiary treatment. On the other hand, the reuse of water and salt associated to the Scenario 3 enables to decrease the environmental impact by 60%.

The comparison of the three scenarios was also assessed by means of ReCiPe midpoint approach. Figure 16 shows the significant environmental advantages of applying the system since the impact is decreased for all categories. Especially significant is the reduction observed in Climate Change and Human Toxicity.

The results obtained in the LCA evidence the considerable environmental advantages provided by the application of the EC-UV system in both operation modes.

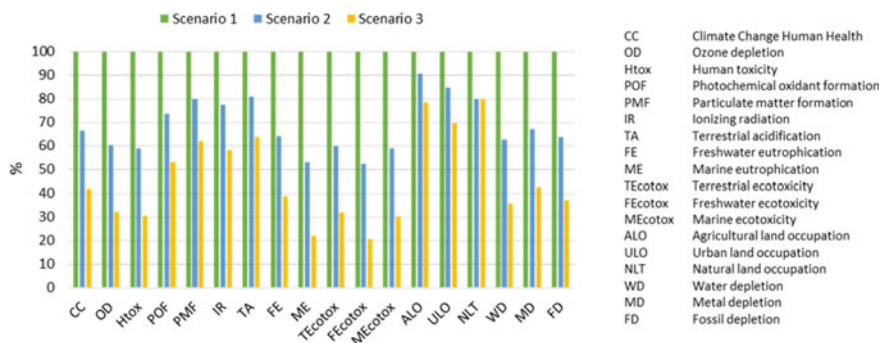


**Fig. 16** ReCiPe midpoint characterisation values for the three scenarios

The reuse of water and salt in new production processes, as well as the decrease in the consumption of reagents associated to the wastewater treatment plant, provides significant economic benefits.

## 8.2 Environmental Impact on the Dyeing Process

Until now, the results obtained in the LCA of the whole wastewater treatment plant were presented. However, it is interesting to separate and quantify the environmental impact on the jet dyeing process and the subsequent treatment of its effluents. With this objective, three scenarios were set:

*Scenario 1: Conventional process:* This scenario involves the dyeing process and a washing step, followed by a biological and tertiary treatments of the wastewater, as previously explained.

*Scenario 2: EC-UV in decolourisation mode:* In this case, the dyeing and first washing processes are followed by the EC-UV treatment to remove colour. Subsequently, the effluent is submitted to a biological treatment to reduce organic matter. As mentioned above, the electrical consumption of biological treatment decreases by 10% as a consequence of the previous use of the EC-UV system. No tertiary treatment is required.

*Scenario 3: EC-UV in reuse mode:* This scenario is formed by the dyeing and washing process followed by the EC-UV system. Neither biological nor tertiary treatment is required. It should be noted that in this case, the dyeing process consumes less water (70%) and salt (72%).

The midpoint analysis shows that the use of the system in decolourisation mode has a lower environmental impact than the reuse mode (Fig. 17). This fact is attributed to the removal of sodium bicarbonate ( $\text{Na}_2\text{CO}_3$ ) present in the effluent before its reuse, which causes carbon dioxide ( $\text{CO}_2$ ) generation.

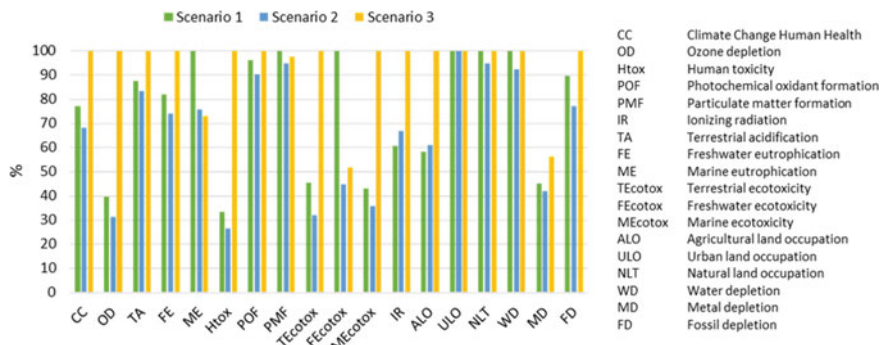


Fig. 17 ReCipe midpoint characterisation values for the three scenarios

Some textile companies use mixtures of  $\text{Na}_2\text{CO}_3$  and  $\text{NaOH}$  to adjust the pH. Based on this, a new LCA was performed considering the total replacement of  $\text{Na}_2\text{CO}_3$  by  $\text{NaOH}$ . In comparison to the conventional process (Scenario 1), the use of the system running in decolourisation mode (Scenario 2 with  $\text{NaOH}$  instead of  $\text{Na}_2\text{CO}_3$ ) decreases by 20% the environmental impact, whereas the reuse of water and salt (Scenario 3) by 60%.

## 9 Conclusions

The EC-UV system, based on the degradation of dyes by combining an electrochemical process with UV radiation, has demonstrated to be an innovative and interesting process for its application in the textile industry.

The EC-UV system has significant advantages with respect to the methods currently used for the treatment of textile wastewater:

- EC-UV is able to treat the more coloured and with high salt content effluents.
- No chemicals are required to carry out the electrochemical process.
- The only cost of the EC-UV treatment is the electric power supply.
- No wastes are produced.
- As the high coloured effluents are segregated to the EC-UV system, the tertiary treatment for colour removal can be suppressed in the wastewater treatment plant. This results in a significant reduction of reagents and sludge disposal costs.
- Discharge taxes are lowered due to the reduction of wastewater salinity.
- The system does not need maintenance since the electrodes are very stable and can be used over 5–10 years.
- Less cost in water due to the reuse of 70–100% dyeing water
- Less cost in salt as a consequence of reusing the treated effluents that still contain salts. Savings up to 100% salt can be achieved.

As a summary, the introduction of the EC-UV system allows to reduce the environmental impact of the textile dyeing process, leading to a more sustainable industry and promoting the implementation of a productive process based on the circular economy.

**Acknowledgements** This research was co-funded by the European Commission within the CIP Eco-Innovation initiative of the Competitiveness and Innovation Framework Programme, CIP: ECUVal project (ECO/13/630452). For more information: [www.ecuval.eu](http://www.ecuval.eu).

## References

1. Al-Mamun MR, Kader S, Islam MS, Khan MZ (2019) *J Environ Chem Eng*
2. Leal Filho W, Ellams D, Boiten VJ, Paco A, Moora H, Han S, Tyler D, Balogun A-L (2019) *J Clean Prod* 218:10–20
3. Tavangar T, Jalali K, Amin M, Shahmirzadi A, Karimi M (2019) *Sep Purif Technol* 216:115–125
4. Jadhav A (2007) Eco-friendly substitution in textiles. <https://www.fibre2fashion.com/industry-article/2524/eco-friendly-substitution>
5. Ellen MacArthur Foundation (2017) A new textiles economy: Redesigning fashion's future. <http://www.ellenmacarthurfoundation.org/publications>
6. Schlaefke H (2018) Reactive dye revolution. <https://www.worldofchemicals.com/media/reactive-dye-revolution/873.html>
7. Sala M, del Río AI, Molina J, Cases F, Gutiérrez-Bouzán C (2012) *Int J Electrochem Sci* 7:12470–12488
8. López-Grimau V, Gutiérrez-Bouzán C, Fu J (ed) (2013) *Dye Process Tech Appl New York*, pp 205–215
9. Sala M, López-Grimau V, Gutiérrez-Bouzán C (2016) *Materials (Basel)* 9:211
10. Sala M, Gutiérrez-Bouzán MC (2014) *J Clean Prod* 65:458–464
11. Gutiérrez-Bouzán C, Buscio V (2018) *Environ Sci* 5:96–104
12. Best Available Techniques for the Textiles Industry (2003)
13. Jaafarzadeh N, Takdastan A, Jorfi S, Ghanbari F, Ahmadi M, Barzegar G (2018) *J Mol Liq* 256:462–470
14. Erkanli M, Yilmaz L, Çulfaz-Emecen PZ, Yetis U (2017) *J Clean Prod* 165:1204–1214
15. Soares PA, Souza R, Soler J, Silva TFCV, Guelli SMA, Boaventura RAR, Vilar VJP (2017) *Sep Purif Technol* 172:450–462
16. Esteve-Turrillas FA, de la Guardia M (2017) *Resour Conserv Recycl* 116:107–115
17. Nallathambi A, Giri Rengaswami Dev V (2017) *Carbohydr Polym* 174:137–145
18. Turcanu A, Bechtold T (2017) *J Clean Prod* 142:1397–1405
19. López-Grimau V, Gutiérrez C, Sala M, Crespi M (2013) *Desalin Water Treat* 51:1527–1532
20. Burkinshaw SM, Salihu G (2018) *Dye Pigment* 149:652–661
21. Collivignarelli MC, Abbà A, Carnevale Miino M, Damiani S (2019) *J Environ Manage* 236:727–745
22. Samsami S, Mohamadi M, Sarrafzadeh MH, Rene ER, Firoozbahr M (2020) *Process Saf Environ Prot* 143:138–163
23. Mcyotto F, Wei Q, Macharia DK, Huang M, Shen C, Chow CWK (2021) *Chem Eng J* 405
24. Verma AK, Dash RR, Bhunia P (2012) *J Environ Manage* 93:154–168
25. Garcia-Segura S, Ocon JD, Nan Chong M (2018) *Process Saf Environ Prot* 113:48–67
26. García-Espinoza JD, Mijaylova-Nacheva P, Avilés-Flores M (2018) *Chemosphere* 192:142–151
27. Klidi N, Clematis D, Delucchi M, Gadri A, Ammar S, Panizza M (2018) *J Electroanal Chem* 815:16–23

28. Buscio V, García-Jiménez M, Vilaseca M, López-Grimau V, Crespi M, Gutiérrez-Bouzán C (2016) *Materials* (Basel) 9
29. Brillas E, Martínez-Huitile CA (2015) *Appl Catal B Environ* 166–167:603–643
30. Medeiros de Araújo D, Cotillas S, Sáez C, Cañizares P, Martínez-Huitile CA, Rodrigo MA (2015) *J Electroanal Chem* 757:144–149
31. Cotillas S, de Vidales MJM, Llanos J, Sáez C, Cañizares P, Rodrigo MA (2016) *J Hazard Mater* 319:93–101
32. Gutiérrez-Bouzán MC, Tornero-García JA, Buscio V, Gutiérrez-Mérida M (2017) Procedimiento Por Lotes Para Tratamiento En Continuo de Efluentes Líquidos Por Técnicas Electroquímicas Para Su Depuración (Spanish Patent), Numer: 201730750
33. Gutiérrez-Bouzán C, Tornero-García JA, Buscio V, Gutiérrez-Mérida M (2018) PCT: batch process for continuous treatment of liquid effluents using electrochemical techniques for purifying, Numer: PCT/ES2018/070395
34. AENOR, UNE-EN ISO 105-J03:2010 - Textiles - Tests for Colour Fastness - Part J03: Calculation of Colour Differences (In Spanish), 2010
35. Buscio V, López-Grimau V, Álvarez MD, Gutiérrez-Bouzán C (2019) *Chem Eng J* 373:161–170
36. Álvarez MD, Buscio V, López-Grimau V, Gutiérrez-Bouzán C (2020) *Chem Eng J* 392
37. AENOR (2006) ISO 14040:2006: Environmental Management—Life Cycle Assessment—Principles and Framework



# Application of Sustainable and Low-Cost Sludge-Based Adsorbents for Textile Dye Degradation



A. Geethakarathi

**Abstract** The industrial development in the last two centuries has led to transfer of pollution by means of environmentally unsafe technology causing serious environmental problems. The concern for the environment has led to the adoption of systematic treatment processes for solid, liquid and gaseous wastes. At present, a number of environmental protection agencies have increased creating a general awareness related to environmental inspection and law enforcement. A demand for low-cost and sustainable treatment methods is adopted. Among the various emerging technologies, the advancement in the preparation of porous activated carbon as fibres or membranes is potential for the remediation of wastewater. This chapter highlights the preparation of activated carbon from sludge discharged from tannery industry in the degradation of synthetic textile dye. The adsorption technique has proved to be an effective method in textile dye degradation, in spite of the stable and complex structure of dyes. The preparation methods of the activated carbon from tannery sludge are discussed under various thermal conditions. Also, the chapter focuses on the dye degradation efficiency of the tannery sludge-based activated carbon under various operating parameter conditions. The adopted adsorption technology elaborated will also have an impact on the rationalization of water and raw material resource consumption, contributing to setting premises for application of sustainable environment management.

**Keywords** Activated carbon · Adsorbent · Adsorption · Commercial activated carbon · Isotherms · Reaction kinetics · Reactive dyes · Tannery sludge

---

A. Geethakarathi (✉)

Department of Civil Engineering, Kumaraguru College of Technology, Coimbatore, Tamil Nadu, India

e-mail: [geethakarathi.a.ce@kct.ac.in](mailto:geethakarathi.a.ce@kct.ac.in)

# 1 Introduction

## 1.1 General

The industrial development in the last two centuries has led to transfer of pollution by means of environmentally unsafe technology. The concern for the environment has led to the adoption of systematic treatment processes for solid, liquid and gaseous wastes. At present, a number of environmental protection agencies have increased creating general awareness related to environmental inspection and law enforcement. Industries, by developing new and appropriate technology, are aiming in the elimination and treatment of wastes, thereby minimizing risks to the environment. Emission of huge volume of lots of industrial wastewater and quantities of hazardous waste materials are being produced in the country. Solid waste discharges from small- and medium-scale industries including leather and textile sector are classified under hazardous category. Disposal of primary chemical sludge containing natural organic, synthetic organic, heavy metals, alkaline earth metal is a major issue confronting leather manufacturing industries and other industries in India. It is important to control them to secure sustainable resources to prevent the ecosystem. This chapter focuses on the development of adsorbent from tannery sludge in treating textile dye effluent.

## 1.2 Indian Tannery Sector

The evidence of leather manufacturing history can be tracked from many Vedic literatures. The leather/tannery has source from animal hides and as a chemical in wide variety of plants and trees (tannin). The Indian leather industry scattered throughout various parts of the country has a major contribution to Indian economy, through its export and employment. The Government of India had planned and promoted export trade by the adoption of the Export Policy Resolution in 1970. Tannery industries exist with about 150 large, 600 medium and over 100,000 cottage units. Central Leather Research Institute (CLRI) survey has reported about 934 units in Tamil Nadu, 538 units in West Bengal and 378 units with Uttar Pradesh accounting for 89% of the tanneries in the country.

### 1.2.1 Manufacturing Process in Tannery Industries

The problem of the environmental pollution due to tannery effluents received serious consideration only in recent years in spite of its historical existence. The pollutants from large numbers of tanneries in the country have caused considerable damage to the surface and sub-surface water sources, thereby affecting drinking water and irrigation. Tannery industry is generally associated with noxious smell arising from

its raw materials, solids, liquids and gaseous wastes emanating from processing. With the increase in number of tanning units and lack of application of suitable methods of disposal of wastes, the problem of environment pollution is likely to aggravate further in coming years with a severe impact on environment, necessitating early measures for control of pollution from tanneries.

The daily production of tannery wastewater in India from roughly 3000 industries is approximately 175,000 m<sup>3</sup>/day. Liquid wastes in tanneries are produced in sufficient quantities during soaking, liming, deliming, pickling, bating, tanning and finishing operations as shown in Fig. 1. In addition to the effluent discharged from different processes, cleaning and washing done in different operations add to the total volume of the factory effluent to an appreciable extent. About 20% of the weight of the raw hides is leather at the end of the process [3], and approximately 40% of the initial raw material is transformed into solid and liquid wastes [2]. For Indian scenario, Kaul et al. [60] have developed a tannery equation, as represented in Eq. (1.1) with an extensive survey of 500 industrial units.

$$\begin{aligned} \text{Hide} + \text{Water} + \text{Chemicals} &= \text{Leather} + \text{Effluents} + \text{Solid Wastes} \\ 1 \text{ kg} + 50 \text{ kg} + 0.5 \text{ kg} &= 0.3 \text{ kg} + 50 \text{ kg} + 1.3 \text{ kg} \end{aligned} \quad (1.1)$$

## 1.2.2 Tannery Effluent Treatment

The generation and characteristics of tannery effluent depend on the tannery processing.

As illustrated in Fig. 1, the effluent nature of beam house processes is highly alkaline with high BOD. The chrome tanning effluent is acidic and contains high amounts of trivalent chromium salts. Effluents from vegetable tanning contain high BOD and COD. The characteristics of combined wastewater before treatment and after treatment are given in Table 1, and the process-wise generation of wastewater and their characteristics are shown in Table 2.

## 1.3 Tannery Solid Waste

### 1.3.1 Sludge Generation

Sludge generated from various tannery operations and treatment processes like equalization and settling tanks are not properly disposed. The dried sludge from the drying beds is disposed nearby the surroundings indiscriminately without any environmental consideration. The advantages and disadvantages of the various sludge disposal methods are summarized in Tables 3, 4, 5 and 6. The disposal methods adopted for the management of tannery solid wastes depend on the tannery operation and

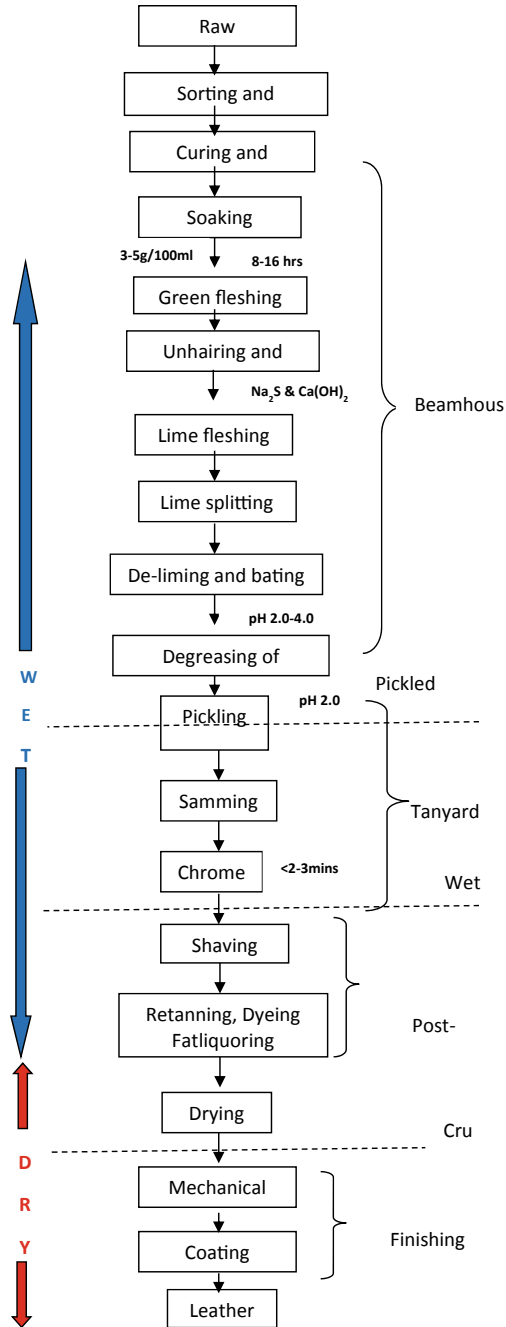


Fig. 1 Manufacturing process of a leather industry

**Table 1** Characteristics of wastewater

S. No.	Parameters	Average effluent concentration before treatment in mg/L	Average effluent concentration after treatment in mg/L
1	Biochemical oxygen demand (BOD)	1850	700
2	Chemical oxygen demand (COD)	4500	3000
3	Chloride	5500	1200
4	Suspended solids	3750	1500
5	Total chromium (Cr)	165	38

Source Minimal National Standard for Tanneries: COINDS/35/1991-92. CPCB, Delhi

process. In recent years, incineration has replaced the old methods. Destruction by incineration is an effective method for solid waste disposal that yields minimal final residues and is attractive on account of the potential recovery of heat from the process.

However, environmental problems arising due to chromium compounds in flue gases and in ashes lead to the production of carcinogenic calcium chromate. The incinerated organic and inorganic residue can ideally be restored in the natural environment by solidification/stabilization methods [110]. In many countries, tannery wastes before or after composting are applied to agricultural land as a source of nitrogen and other trace elements.

So, as the traditional ways of disposal bristle with disadvantages, it is necessary to seek cost-effective and innovative methods to dispose sludge. These huge unused waste resources can be recovered and recycled with useful end products, thereby overcoming both the pollution and waste problems simultaneously. Once, such process is adsorption using porous materials such as activated carbon with excellent properties in separating harmful gases. Highly functional porous materials are therefore in great demand for these purposes [31]. The present work examines the efficacy of a cheaper material in the form of tannery sludge available in large quantities. The sludge developed to an adsorbent is used for the removal of colour from synthetic reactive dyes as an alternate to activated carbon [29].

### 1.3.2 Buffing Dust

The tanned collagenous waste obtained from the finishing operation of the leather processing is the buffing dust. They are microfined solid particulate impregnated with 2.7% chromium (dry weight basis), fat and oil, tanning agents and dye chemicals. Buffing dust is generated in a considerable proportion during processing of raw hides, i.e. 2–6 kg per ton of raw hides. Buffing dust is carcinogenic causing various respiratory tract alignments, dermatitis, ulcers, kidney malfunctions in humans exposed to the environment containing buffing dust particulates. Hence, stringent measures are

**Table 2** Characteristics of tannery effluent

Parameter	Soaking	Beam house operation	Pickling and chrome tanning	Wet finish—rechroming, dyeing and fat liquor	Composite (include washing)
Volume of the effluent in litres/ton of hides	6000–9000	6000–10,000	1500–3000	3000–5000	30,000–40,000
pH	7.5–8.0	8.0–12.0	2.2–4.0	3.5–4.5	7.0–9.0
BOD <sub>5</sub> , mg/L	1100–2500	2000–8000	400–800	1000–2000	1200–3000
COD, mg/L	3000–6000	3000–15,000	1000–3000	2500–7000	2500–8000
Sulphide, mg/L	–	50–200	–	–	30–150
Total solids, mg/L	35,000–55,000	6000–20,000	30,000–60,000	4000–10,000	15,000–25,000
Dissolved solids, mg/L	32,000–48,000	5000–15,000	29,000–58,000	3400–9000	13,000–20,000
Suspended solids, mg/L	3000–7000	3000–15,000	1000–2000	600–1000	2000–5000
Chlorides, mg/L	15,000–30,000	3000–6000	15,000–25,000	500–1000	6000–9500
Total chromium mg/L	–	–	1500–3000	30–60	80–200

Source Central Leather Research Institute, Chennai, India

Note Volume of wastewater applicable for hides (cow and buffalo) and goat skins and not for wool sheep skins

**Table 3** Advantages and limitations of sludge drying

Advantages	Limitations
Volume of sludge is significantly reduced	High energy requirement and intensive
Further disposal/reuse of sludge is needed	Investment cost is very high
Pathogen-free residue can be found in the end sludge with minimal odour	Operational cost is high
Product requires very less area, since the end sludge can be pelletized	Testing, operating and controlling the process are labour-intensive and expensive

**Table 4** Advantages and limitations of aerobic digestion of sludge

Advantages	Limitations
High ratio of volatile reduction	Power cost for aeration is very high
Low BOD in the final supernatant liquor	The digested sludge has poor water loss
The end product is odourless and stable	Temperature change, pH and tank material influence the digestion process
The derived sludge has high fertilizer value	No value material recovered
Operation process is easy with low capital cost	pH fluctuation during digestion process

**Table 5** Advantages and limitations of sludge composting

Advantages	Limitations
Composted product can be stored and is resaleable	Seeding of about 18–30% digested sludge is required
Simple and cheap technique	Large land area is needed
No high operation and capital investment	Seasonal influence affects the compost product without covering

**Table 6** Advantages and limitations of sludge incineration

Advantages	Limitations
Reduced volume of end residue	Causes air pollution problem and requires control of toxic gas emissions
Phosphate recycling	High energy requirement leading to increase in global warming
High contaminant destruction ratio	Installation and capital cost are very high
Minimization of waste transport and disposal	Testing, operating and controlling the process are labour-intensive and expensive
Appropriate and ideally can be used for populated countries	Disposal of ash causes leaching and depletion of groundwater resources

levied by the pollution control authorities for proper collection and safe disposal of buffing dust. Incineration and land co-disposal are the currently practised disposal method for buffing dust [56].

### 1.3.3 Shavings

Putshaka et al. [98] have mentioned about 56–60% fleshing, 35–40% chrome shaving with 2.5–5% chromium, buffing dust, 5–7% trimmings and 2–5% hair in an ideal leather waste. Trivalent chromium forms the major contribution of chrome shaving, which is less toxic compared to  $\text{Cr}^{6+}$ . When being disposed into the environment, this trivalent chromium is converted into hexavalent causing environmental threat

due to leaching in long time period. Every year, 4000–6000 tons of basic chromium is used in tanning process and a discharge of 20–40% is disposed as waste [106]. As buffing dust, shaving is also disposed by means of incineration, pyrolysis and land co-disposal.

## 1.4 Development of Indian Textile Industries

Indian textile industry contributes about 14% to industrial production, 4% to the nation's GDP and 17% to the country's exports. The existence of textiles in ancient Indian period is recorded and well understood from ancient literature and sculpture. The Harappa and Mohenjo-daro civilization has greater evolution in the evolution of cotton textile industry. The intervention of British era during the eighteenth century has augmented with automation in most of the cottage textile industrial process including carding, spinning and weaving.

### 1.4.1 Textile Effluent Flow from Manufacturing Process

A wide fluctuation could be observed from textile effluent discharge based on the customer requirement (Table 7), types of textile raw materials, chemical reagents and additives and process schedules.

The main cause of generation of this effluent is the use of huge volume of water during wet processing such as chemical processing, dyeing, printing and finishing (Fig. 2). In an average, 45% of preparatory processing, 33% of dyeing and 22% of finishing material are reprocessed. The effluent generated in different steps is well beyond the standards. Hence, it is highly polluted and dangerous. Table 8 shows the characteristics of wastewater from a textile plant.

**Table 7** Properties of wastewater from textile chemical processing [32]

Property	Standard	Cotton	Synthetic	Wool
pH	5.5–9.0	9.8–11.8	9.0–10.4	4.8–8.0
BOD <sub>5</sub> , mg/L	30–350	750–900	185–200	4000–11,455
COD, mg/L	250	1400–1700	320–650	12,000–34,500
TDS, mg/L	2100	6000–7000	100–150	4830–20,000



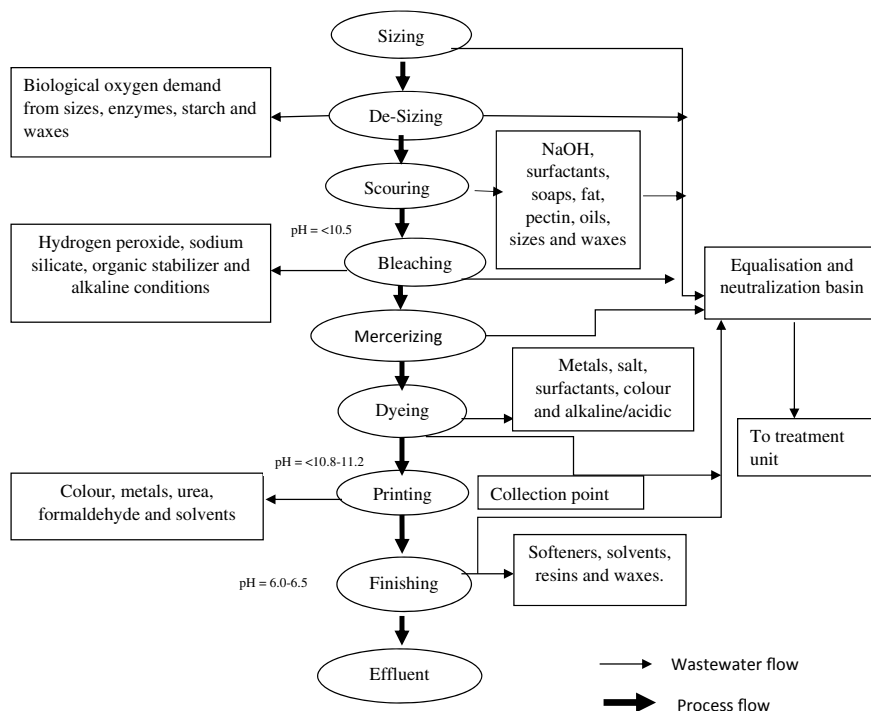


Fig. 2 Flow chart of textile processing industry and generation of effluent flow

## 1.4.2 Textile Dye Degradation

### Physio-chemical Methods

Membrane filtration processes (like nanofiltration, reverse osmosis, electrodialysis) and adsorption techniques are the widely used Physio-chemical methods (Table 9). The life period, high capital and operational cost and membrane fouling are the major disadvantages of membrane processes. Literature suggests liquid-phase adsorption as one of the most ideal methods for pollutant removal with proper design to produce high-quality treated effluent. This process provides an attractive alternative for the treatment of contaminated water, especially if the sorbent is inexpensive and does not require an additional pre-treatment step before its application.

Coagulation–flocculation combined with flotation and filtration, precipitation with Fe(II)/Ca(OH)<sub>2</sub> and other coagulants, electro-flotation and coagulation, conventional oxidation methods by oxidizing agents (ozone) and photo-irradiation processes are some of the predominantly used chemical techniques adopted for various industrial applications. The main disadvantages are the high capital and operational cost, high energy demand, huge accumulation of sludge and their disposal creating secondary pollution due to the excessive usage of chemicals. Recently, advanced

**Table 8** Classification of wastewater treatment process [5]

Treatment	Operations
Primary	Screening
	Sedimentation
	Equalization
	Neutralization
	Mechanical flocculation and chemical coagulation
Secondary	Aerated lagoon
	Trickling filtration
	Activated sludge process
	Oxidation ditch and pond
	Anaerobic digestion
Tertiary	Oxidation technique
	Electrolytic precipitation and foam fractionation
	Membrane technologies
	Electrochemical processes
	Ion exchange method
	Photocatalytic degradation
	Adsorption (activated carbon, etc.)
Thermal evaporation	

oxidation processes have been used for pollution degradation using very powerful oxidizing agents such as hydroxyl radicals.

### Biological Methods

Biological treatment is the most preferred and alternative method compared with physical and chemical processes due to its natural process. Fungal decolourization, adsorption by microbial biomass and bioremediation systems are commonly applied industrial decolorization technologies [26, 77] (Table 10).

However, microbial degradation, large land area and other technical constraints due to seasonal fluctuations and diurnal variation are faced as their major limitations [14]. Biological treatment has less flexibility in design and operation [100]. Although some organic molecules are degraded, it is incapable of obtaining satisfactory colour elimination with current conventional biodegradation processes due to the presence of recalcitrant complex chemicals like azo dyes [99].

**Table 9** Advantages and limitations of physical/chemical decolourization technologies [8, 16]

Technologies	Advantages	Limitations
Adsorption on activated carbon	Economically attractive Good removal efficiency	Cost-intensive regeneration process
Irradiation	Effective removal for a wide range of colourants at low volumes	Dissolved oxygen requirement is high Ineffective light-resistant colourants
Membrane separation	Removes all dye types Produces a high-quality treated effluent	High pressure, expensive, incapable of treating large volumes
Membrane filtration	Recovery and reuse of chemicals and water Wider applications for complex wastes	Dissolved solids are not separated High running cost
Reverse osmosis	Hydrolyses reactive dyes and chemical auxiliaries	High pressure and installation cost
Coagulation–flocculation	Elimination of insoluble dyes Simple and economically feasible	Dewatering and sludge handling Disposal problems
Oxidation	Effective for both soluble and insoluble colourants	Problems with sludge disposal
Ozonation	Effective for azo dye removal	Not suitable for disperse dyes Releases aromatic amines a.
Advanced oxidation process	No sludge production Little or no consumption of chemicals Efficient in removal of recalcitrant dyes	Economically unfeasible Formation of by-products Technical constraints
Photocatalysis	Process carried out at ambient conditions Inputs are toxic and inexpensive Complete mineralization with shorter detention times	Effective for small amount of colourants Expensive process
Fenton's reagent	Capable of decolourizing wide variety of wastes No alternation in volume	Prohibitively expensive

## 2 Adsorption

Adsorption is an equilibrium separation process and an effective method for water decontamination [18]. The primary factors that make adsorption a separation process are the ability to manufacture adsorbents having high surface areas per unit weight and surfaces which are very selective for the materials to be removed from feed stream. Adsorption is superior to other techniques due to its initial cost, flexibility

**Table 10** Advantages and limitations of biological decolourization technologies [8]

Technologies	Advantages	Limitations
Biodegradation	Economically attractive Most commonly acceptable treatment	Slow process, maintenance and nutrient requirements Suitable only in favourable environment
Anaerobic process	Resistant to wide variety of complex colourants Biogas produced is used for steam generation	1. Longer acclimatization phase
Aerobic process	1. Colour removal is facilitated along with COD removal	1. Longer detention period and specific substrate removal 2. Less resistant to recalcitrant dyes
Single cell (fungal, algal and bacteria)	Good removal efficiency for low volumes and concentrations Very effective for specific colourant removal	Culture maintenance is cost-intensive Cannot cope up with large volumes of coloured effluents

and simplicity of design, ease of operation and insensitivity to toxic pollutants. An ideal sorbent meets the following criteria:

1. Large internal surface area to interact and admit the molecules to be adsorbed
2. High affinity and capacity for target compounds
3. High regenerative capacity
4. Long ageing period, thereby maintaining adsorptive capacity through enhanced recycling
5. Possess tolerance for a wide range of effluent parameters
6. Mechanically strong enough to withstand the bulk handling and vibration.

## **2.1 Adsorption Mechanism**

The optimization and design of an adsorption system can only be understood by adsorption mechanism. The effective activation and regeneration of the adsorbents can be achieved only by proper adsorption mechanism. The mechanism involved in colour or ionic removal processes is through the following 3 steps:

1. *Diffusion of the adsorbate molecules through the solution onto surface of the adsorbents*
2. *Adsorption of adsorbate on the surface of materials through molecular interactions and*
3. *Diffusion of molecules to be adsorbed from the surface into the interior of the adsorbent materials.*

Resistance to mass transfer in the adsorption processes can be either resistance caused by external mass transfer through the particle boundary layer or resistance due to intraparticle diffusion. The external mass transfer [74] described by the linear and nonlinear isotherms [108] is differentiated based on their intraparticle diffusion. Solid-phase diffusion is the dominant effect in intraparticle mass transfer during the initial stages of adsorption. These diffusion models developed by various researches [4, 72] have focused on various process parameters including the rate of agitation, dye concentration and phase ratio.

## 2.2 Types of Adsorption

The adsorption phenomena can be classified as physisorption and chemisorption based on the nature of the bonding between the molecule and the adsorbent surface. Physical adsorption results from molecular condensation in the capillaries of the solid and is dominated by the weak-by-weak van der Waals-type forces. There is no significant redistribution of electron density in either the molecule or at the substrate surface. Chemical adsorption results in the formation of monomolecular layer of the adsorbate on the surface through forces of residual valence of the surface molecules. In chemisorption, a strong chemical bond such as covalent bond is formed between the adsorbate and substrate. The bond exhibits substantial rearrangement of electron density. The classification and characteristics between physisorption and chemisorption are shown in Table 11.

**Table 11** Typical characteristics of adsorption processes

Characteristics	Physical adsorption	Chemical adsorption
Binding force	Due to physical force of attraction, thus this process is also called as van der Waals adsorption	Due to chemical forces or bonding, thus this process is also called as activated adsorption
Saturation uptake	Multilayer phenomena	Single-layer phenomena
Activation energy	No activation energy involved	May be involved
Temperature range (over which adsorption occurs)	Adsorption is appreciable at lower temperature below boiling point of adsorbate	Adsorption can take place even at higher temperature
Nature of sorbate	Amount of adsorbate removed depends more on adsorbate than on adsorbent	Depends on both adsorbent and adsorbate
Crystallographic specificity	Virtually independent of surface atomic geometry	Marked variation between crystal planes
Heat of adsorption	1 kcal/mole	50–100 kcal/mole

### 2.3 Adsorption Isotherms

The relationship between the amount of material adsorbed and its concentration in the feed in equilibrium with the adsorbent is called an adsorption isotherm. Langmuir adsorption isotherm equation is one of the most widely used models to describe the equilibrium behaviours of adsorbate uptake. The Langmuir isotherm equation can be theoretically derived based on some fundamental assumptions. The Freundlich [25] isotherm was derived by assuming a heterogeneous surface with a non-uniform distribution of heat of adsorption over the surface, whereas in the Langmuir [66] theory the basic assumption is that the sorption takes place at specific homogeneous sites within the adsorbent. The isothermal equations are mentioned in Table 12.

The Temkin isotherm equation assumes inverse relation between the adsorption heats with adsorbent–adsorbate interaction layers and is characterized by a uniform distribution of the binding energies up to a maximum binding energy [63].

**Table 12** Adsorption isothermal models and equations

Isotherm	Equation	Parameter and dimension	Note	
Linear	$c_s = k_d * c$	$c_s$ $c$ $k_d$	(mg/L) (mg/L)	Concentration in solid phase Concentration in fluid phase Equilibrium distribution coefficient
Langmuir	$q = \frac{q_{\max} K_L C_{eq}}{1 + K_L C_{eq}}$	$q_{\max}$ $K_L$	(mg/g) (mg/L) <sup>-1</sup>	Capacity at monolayer coverage Langmuir coefficient related to the free energy of adsorption
Freundlich	$q = K_F C_{eq}^n$	$K_F$	(mg/g) (mg/L) <sup>-n</sup>	Freundlich affinity coefficient Exponent
Redlich–Peterson	$q = \frac{K_{RP} C_{eq}}{(1 + \alpha_{RP} C_{eq})}$	$K_{RP}$ $\alpha_{RP}$ $n$	(mg/g)(mg/L) <sup>n-1</sup> (-) (-)	Redlich–Peterson affinity coefficient Heterogeneity or shape parameter Exponent
Dubinin–Radushkevich	$q_e = q_s \exp(-B\varepsilon^2)$	$q_s$ $\varepsilon$		Adsorption capacity Rate constant
Temkin	$q_e = \frac{RT}{b} \ln(K_T C_e)$	$K_T$ RT	(Imol <sup>-1</sup> ) (-)	Equilibrium binding constant Gas constant

## 2.4 Adsorption Chemical Kinetics Modelling

The efficiency of the adsorption process describing the mass transfer and chemical reactions is controlled by the kinetic models. Various kinetic models have been used and different systems use different models, but the Lagergren's rate equations [64] for the sorption of a solute from a liquid solution are commonly used. In many cases, the first-order equation of Lagergren does not fit well to the whole range of contact time and is generally applicable over the initial stage of the adsorption processes [75]. In recent years, pseudo-second-order rate law has been considerable as one of the most appropriate models. Linear isothermal regression was widely used to determine the most fitted model throughout the years, and the method of least squares has been frequently used for finding the parameters of the models. However, transformations of nonlinear isotherm equations have implicitly altered their error structure and variance by assumptions of standard least squares.

Several error analysis methods such as the coefficient of determination, the sum of the errors squared, a hybrid error function, Marquardt's per cent standard deviation, the average relative error and the sum of absolute errors have been used to determine the best-fitting isotherm [6, 47]. The linear regression and chi-square analysis of three isotherms, Langmuir, Freundlich and Redlich–Peterson, were compared by Ho. In this study, chi-square ( $\chi^2$ ) tests of the two Langmuir isotherms were similar on the same abscissa and ordinate, whereas the Redlich–Peterson and Freundlich isotherm exhibited identical and lower  $\chi^2$  values than Langmuir.

## 2.5 Adsorbent Precursors

In recent years, preparation and application of non-conventional adsorbents using precursors such as natural materials, biosorbents and waste materials from industry and agriculture with lower cost and high efficiency have gained importance. It is suggested as convenient alternative treatment for the discoloration of wastewaters from the textile industry [16, 24, 36, 61]. Industrial wastes represented as unused resources are to be turned into a useful resource for the colour removal of various dyes. The tannery industry is also inserted into this context. Numerous research works are carried out using waste materials in order to avert an increasing toxic threat to the environment and to streamline the waste disposal techniques.

### 2.5.1 Fly Ash

One of the industrial by-products available in abundance in the world is fly ash. It is a waste substance from thermal power plants and steel plants. The use of fly ash for removal of dyes from aqueous solution was first reported by Khare et al. [62]. The effect of different concentrations and pH on Victoria blue dye was studied under

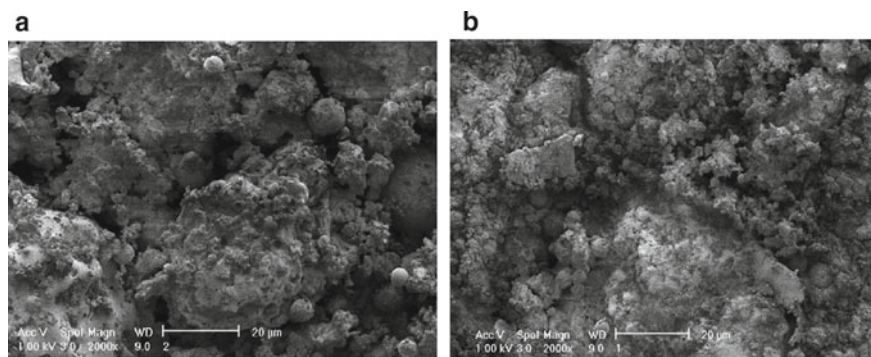


**Fig. 3** **a** Fly ash before adsorption process. **b** Fly ash particle with dye adsorbed

first-order adsorption. The equilibrium data are fitted with the Langmuir model of adsorption.

Brown coal fly ashes tested by Janos et al. [53] showed that both basic (cationic) and acid (anionic) dyes could be sorbed onto fly ash. In this study, the adsorption was described by the multi-site Langmuir isotherm. The sorption capacities were in the range of  $10^{-1}$ – $10^{-3}$  mmol/g and did not differ significantly for basic and acid dyes. Kara et al. [58] used fly ash from a thermal power station for the adsorption of reactive dyes: Reactive Blue 19, Reactive Red 198 and Reactive Yellow 84. The SEM image in Fig. 3a showed that fly ash is mainly composed of irregular and porous particles. The pores in Fig. 3a are more densely packed with dyes than that in Fig. 3b.

The removal efficiencies of the three dyes were 97%, 87% and 82%, respectively, for the particle size of 45–112.5  $\mu\text{m}$  at an optimum dosage. At a particle size range of 45–112.5  $\mu\text{m}$ , the values of saturation capacities were 89–106 mg/g, 48.8–54.6 mg/g and 22.5–33.3 mg/g for Reactive Blue 19, Reactive Red 198 and Reactive Yellow 84, respectively. This increase in adsorption capacity with decreasing particle size range mainly suggested that reactive dyes did not seem to penetrate the whole particle but instead had adsorbed near or on the fly ash surface [55]. Adsorption increased with increasing initial concentration.

### 2.5.2 Bottom Ash

Dincer and Gunes [20] in their study used granular activated carbon and coal-based bottom ash (CBBA) for adsorbing a reactive dye Vertigo Navy Marine (C.I Blue222). The low surface area ( $1.77 \text{ m}^2 \text{ g}^{-1}$ ) of the CBBA tested showed that bottom ash particles were not micropores. The minimum dye colour removal for granular activated carbon (GAC) was observed at the neutral pH. At neutral pH, there is a possibility of oxidation of the surface oxygen complexes present on the surface, which may impart positive charges to the GAC surface [80]. Dye removal efficiency was higher for low dye concentrations because of availability of unoccupied binding sites on



the adsorbents. The amount of dye adsorbed increased with increase in agitation time. In case of GAC, the initial rate of dye uptake was rapid and it rapidly attained equilibrium for low initial dye concentration. Similar results have been reported in the literature on the extent of removal of dyes [57]. The isothermal plot of GAC and CBBA differs from each other since CBBA has not much micro- and macroporous structure. The maximum adsorption capacities of GAC and CBBA were 6.58 mg/g and 4.02 mg/g, respectively.

### 2.5.3 Basic Oxygen Furnace Slag

Basic oxygen furnace slag (BOF slag), a final waste material in the basic oxygen furnace steelmaking process [83], was also used in adsorption studies for the colour removal of synthetic reactive dyes such as Reactive Blue 19, Reactive Black 5 and Reactive Red 120. Reactive Red 120 showed the lowest adsorption due to its large molecular weight and complex structure. The Langmuir and Redlich–Peterson isotherm models fitted the experimental data with higher coefficients than Freundlich model. The first-order kinetic model followed the isothermal plot due to higher correlation coefficient. This is generally in agreement with the published research that the first-order kinetic model was able to describe adsorption process [13]. Amin [7] selected three different activated carbons prepared by chemical and physical activation of sugar bagasse pith in the absence of air at 600 °C for the removal of Reactive orange dye.

### 2.5.4 Other Industrial Inorganic Used Resources

Over the years, a number of workers have used different waste materials such as coal fly ash [53, 105], coal bottom ash [21, 38], bagasse fly ash [39], blast furnace slag [37], deoiled soya [78, 79], red mud [38] and sawdust [35] from industrial and agricultural products, as adsorbent for the removal of different pollutants. Recently, apart from these commonly used waste materials the authors have been trying to utilize waste materials from the boron industry to remove hazardous dyes [11]. The adsorption of both dyes onto boron waste was exothermic in nature with dye removal capacity slightly decreasing with increasing temperature [90]. The maximum adsorption capacities on Basic Yellow 28 and Basic Red 46 were 75.00 and 74.73 mgg<sup>-1</sup>, respectively. From the reported results, it would appear that boron waste is an adsorbent offering greater wastewater treatment potential than other waste materials.

### 2.5.5 Industrial Organic Wastes

Pala et al. [96] conducted a comparative study of activated carbons prepared from solvent extracted olive oil pulp for textile reactive azo dye removal from aqueous streams. These residues showed a surface area of 800 m<sup>2</sup>/g and a pore volume

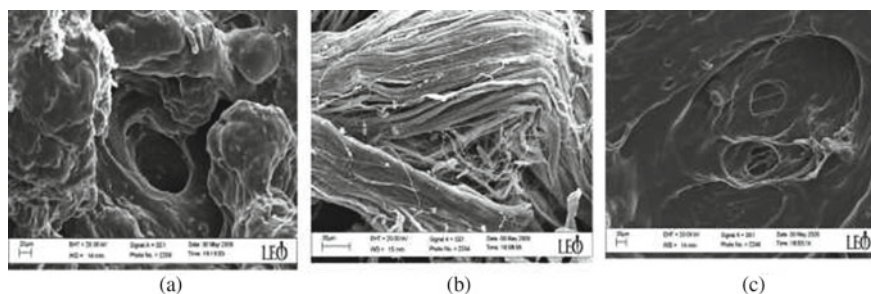


**Fig. 4** (a) Micrograph of the natural leather, (b) chromium-containing leather waste and (c) leather waste after chromium extraction

of  $0.22 \text{ cm}^3/\text{g}$  (micropore volume) and  $0.35 \text{ cm}^3/\text{g}$  (mesopore volume). Activated carbons with relatively high BET surface area ( $1000\text{--}1500 \text{ m}^2/\text{g}$ ) were successfully produced from agricultural wastes by physical activation using steam and  $\text{CO}_2$  [69, 102]. They were also produced by chemical activation [82] [119], and the resulting BET surface area values varied greatly with the chemical activating reagents used. Moreno et al. [82] produced activated carbon from olive-mill waste by both chemical activation using  $\text{KOH}$  and  $\text{H}_3\text{PO}_4$  and physical activation using  $\text{CO}_2$  atmosphere. The reported  $S_{\text{BET}}$  values of activated carbons prepared from these activating reagents were  $\text{H}_3\text{PO}_4$  ( $400 \text{ m}^2/\text{g}$ ) <  $\text{CO}_2$  ( $1040 \text{ m}^2/\text{g}$ ) <  $\text{KOH}$  ( $1800 \text{ m}^2/\text{g}$ ).

The adsorption isotherm pattern for wet blue leather from a tanning industry showed a higher capacity of adsorbing Reactive Red textile dye. The adsorbent materials were characterized by infrared spectroscopy and SEM (Fig. 4a–c) and tested for the dye adsorption (reactive textile and methylene blue dyes). As a low cost abundant adsorbent material with high adsorption ability ( $163 \text{ mgg}^{-1}$  Reactive Red), wet blue leather from a tanning industry is an interesting alternative to costly adsorbent materials. The tanning treatment to produce the wet blue leather yields sludge containing approximately 3% (*w/w*) of chromium [27]. The method commonly used for this waste disposal presents high operational costs [10, 27]. In this work [71], the solid waste from leather industry before and after the chromium extraction is used as an adsorbent for the removal of several organic compounds such as cationic and anionic dyes from aqueous media.

## 2.5.6 Microbial Biomass

The activated sludge process, being the most commonly used in biological wastewater treatment methods, is the most abundant source of microbial biomass. The binding sites present in the sewage sludge and the underlying biosorption mechanism were investigated by many researchers [57, 85, 93]. A study based on regenerability and sorption of four types of sludge were evaluated as biosorbents for the treatment of an anionic reactive dye Reactive Orange 16. The maximum sorption capacities of the four waste sludges estimated by Won et al. [116] using the Langmuir equation at pH

2 were in the order of landfill sludge ( $159.0 \pm 6.0 \text{ mgg}^{-1}$ ) > sewage sludge ( $114.7 \pm 4.7 \text{ mgg}^{-1}$ ) > digested sludge ( $86.8 \pm 4.5 \text{ mgg}^{-1}$ ) > waterworks sludge ( $47.0 \pm 5.8 \text{ mgg}^{-1}$ ). The dye uptake by the landfill sludge was maintained at a significant level, even at pH is higher than 7 compared to the other sludges.

## 2.5.7 Industrial Sludge as Adsorbents

### Chromium Hydroxide Sludge

The sludge precipitates containing chromium hydroxide have shown good adsorptive capacity in the removal of cationic, anionic and disperse dyes. The performance was high at low pH for anion dyes (Reactive Blue and Congo red) and at high pH for methylene blue with zero point surface charge as 10.5 [15]. The monolayer adsorption at the surface of the negatively charged dye species to the positively charged surface of the sludge precipitates through electrostatic attraction and followed first-order reaction.

### Metal Hydroxide Sludge

Studies of waste metal hydroxide sludge from electroplating industry are well suited in the removal of reactive dyes [86, 88], catechol [87]. Adsorption capacity of metal hydroxide sludge generally varied from 44 to 60 mg/g for reactive dyes [88]. High capacity, low-cost adsorbents are still under development to reduce the adsorbent dose and minimize disposal problems. The amphoteric behaviour of the hydroxide sludge by the  $\text{pH}_{\text{zpc}}$  determination was shown by the decrease in pH due to  $-\text{OH}$  adsorption [104]. Particle size distribution and determination, physical textural properties and metal mobility under different pH conditions of the metal sludge were also characterized. The X-ray fluorescence (XRF) showed the presence of mesopores and macropores with an average pore diameter of 32.3 nm. High values of porosity (>50%) were achieved, and possible agglomeration of finer particles in the waste sludge created intraparticle spaces. A homogeneous solid diffusion model (HSDM) was developed for homogenous particles, but has been applied to porous particles in several adsorption systems [76, 113]. Equilibrium data were well described by both Langmuir and Freundlich models. The maximum adsorption capacities obtained varied between 275 mg/g (at 25 °C and pH4.0) and 21.9 mg/g (at 25 °C and pH10.0). A decrease in adsorption capacity from 91.0 to 31.0 mg/g with decrease in pH was studied with simulated textile effluents. The removal of three reactive dyes Reactive Red 2, Reactive Dye 120 and Reactive Red 141 investigated using a metal hydroxide sludge showed a reverse behaviour in the isothermal plot. The adsorption isotherm including the Langmuir constants ( $Q_0$  and  $b$ ) and the Freundlich constants ( $K_f$ ) for Reactive Red 2 decreased with increasing temperature, but reversed for Reactive

Red 120 and Reactive Red 141. This behaviour implied an exothermic process for Reactive Red 2 but an endothermic process for Reactive 120 and Reactive 141. The adsorption of less charged dyes (Reactive Dye 2) was mainly physical but that for more charged dyes (Reactive Red 120 and Reactive Red 141) was chemical based on the enthalpy values of adsorption: 5.5, 2.77 and 6.41 kJ/mol. Decreasing adsorption efficiency of metal hydroxide with higher dye concentration was due to the presence of anionic electrolytes (NaCl and Na<sub>2</sub>SO<sub>4</sub>) in dye solution. Studies have proven the possible effective use for paper sludge ash in the preparation of low-cost sorbents for water purification, using steam and calcination treatments by Hojamberdiev et al. [48].

### Paper Sludge

The press mud, end derivative obtained after the paper sludge treatment process is used in agriculture to improve soil fertility due to its high carbon content [44, 111]. This sludge has very high beneficial effects on soils that are deficient in organic matter. The calcinated paper sludge by mechano-chemical grinding and physical activation in the presence of nitrogen atmosphere showed relatively higher BET surface area (70 m<sup>2</sup>/g at 600 °C) than other samples.

## 2.6 Commercial Activated Carbon

Commercial activated carbon is the most effective adsorbent among the various adsorbents due to its structural characteristics, porous texture, regenerative capacity and chemical nature. The activated carbons are derived from starting materials such as charcoal and coconut husk and have led research towards wide use of pollutant adsorption in both gaseous and liquid phases. Industries like food and beverage processing, chemical, pharmaceutical, petroleum, mining, nuclear, automobile and vacuum manufacturing use adsorbents in their effluent processing units. Commercial activated carbons are prepared from many carbonaceous materials such as biomass and organic wastes. Several recent publications [22, 30, 84, 107, 115] indicate the interest in developing sustainable and environmentally safe recycling processes to produce value products such as activated carbon from wastes. The properties and surface chemistry of these adsorbents play a major role in their industrial applications [109]. The active surface area, characteristics and performance of a particular activated carbon source depend largely on the nature of the material it was manufactured from and the process by which it was activated [43, 67]. This chapter discusses the incineration of tannery sludge into activated carbon by combined activation and their application in degradation of reactive dye.

### 3 Preparation of Adsorbents and Activation Methods

#### 3.1 Activation Methods

Preparation of activated carbons involves two steps:

1. Carbonization of raw precursors in an inert atmosphere and
2. Activation of carbonized material.

Carbonization consists of a thermal decomposition of the carbonaceous material, eliminating non-carbonaceous species (volatilization of the organic compounds) and producing a fixed carbon mass developing pore structures. Volatilization of organic compounds in the precursor is removed at lower temperatures ranging between 300 and 550 °C without inferring the production of carbon during the activation phase. Volatilization is more enhanced in chemical activation due to the treatment of dehydrating chemical agents. Activation can be carried out by chemical or physical means. In chemical activation, carbonization and activation are accomplished in a single step by carrying out thermal decomposition of the raw material impregnated with certain chemical agents. Physical activation involves gasification of the char (obtained from carbonization of the raw material) by oxidation with steam, carbon dioxide, air or any mixture of these gases in the temperature range from 800 to 1100 °C.

Porous carbon materials have attracted much attention in the past decades, and it is believed that the mesoporous activated carbons hold significant potential applications as adsorbents of large molecules [121]. Lin and Teng [67] used waste tyre char as precursor and also employed the steam activation method. The carbon thus obtained had a mean pore size of 50 nm and demonstrated better adsorption capacity for methylene blue than commercial activated carbon, which was also ascribed to the abundant mesopores of this carbon. It should be pointed out that the pore structure of these mesoporous carbons consists of both micropores and mesopores with a broad and disordered pore size distribution, which is an intrinsic trait of porous carbon prepared by steam activation.

##### 3.1.1 Physical Activation and Characterization

The thermal decomposition of the carbonaceous material through oxidation by steam, carbon dioxide, inert gases like nitrogen within a temperature range from 800 to 1100 °C results in the formation of solids, liquids and gaseous products [34]. Kari-fala et al. [59] prepared pyrolysed metal sludge carbon from galvanization industry saturated with spent mineral oil. The variation in the pyrolysis time and temperature influenced the structural and chemical properties of the developed carbon. The waste oil precursor provided active carbonaceous phase which was responsible for development of micropores. Moreover, it contributed to formation of new active surface chemistry either by supplying carbon element or by reducing environment for reactions involving the inorganic compounds. The temperature was maintained between

650 and 950 °C for different pyrolysis times such as 30, 60 or 120 min, respectively. The long holding time and high temperature of pyrolysis stabilized both, organic and inorganic, phases. These phases would undergo aromatization, carbonization, thermal decomposition, incorporation of nitrogen and undefined solid-state reactions. These processes not only change surface chemistry but also significantly affect the porosity and texture of the adsorbents.

### 3.1.2 Chemical Activation and Characterization

The precursors are impregnated with activating agents such as  $\text{ZnCl}_2$ ,  $\text{NaCl}$ ,  $\text{Na}_2\text{CO}_3$ ,  $\text{K}_2\text{CO}_3$ ,  $\text{KOH}$ ,  $\text{NaOH}$ ,  $\text{Al}_2\text{O}_3$ ,  $\text{H}_3\text{PO}_4$ ,  $\text{H}_2\text{SO}_4$ ,  $\text{NH}_4\text{Cl}$ . Orthophosphoric acids [81, Solum et al. 1995; 52, 65], potassium hydroxide [91, 94, 81], zinc chloride [49, 51] and sulphuric acid [17, 101] are the most commonly used chemical activating agents used before incineration of the adsorbent precursors. Best results are obtained in an inert atmospheric condition in the absence of air or oxygen ( $\text{N}_2$ , Ar and  $\text{CO}_2$  atmosphere). Types of activating agent, impregnation ratio, activation temperature and activation time are related to different physical and chemical characteristics of the products.

#### Alkali and Zinc Chloride Activation

The most commonly used activating agents are  $\text{KOH}$  and  $\text{ZnCl}_2$ , where the prepared carbon has high surface area. These alkali agents are effective and influence the structure of activated carbon due to their strong chemical base. Alkali activation is advantageous because of their higher carbon yield at low activation temperatures (500–800 °C) and less activation time. At higher temperature, the development of micropores could be obtained due to steam activation. The corrosive nature of  $\text{KOH}$  and higher cost are the setbacks of using this activating alkali agent [117].

#### Acid Activation

The acid activation can be carried out with strong and weak inorganic acids. Studies conducted by Yanping and Rockstraw [120] used orthophosphoric acid as a activation reagent for activating pecan shell. The characterized carbon showed well-developed pore structure at temperatures  $\geq 250$  °C and reached 1130  $\text{m}^2/\text{g}$  and 0.34  $\text{cm}^3/\text{g}$ , respectively, at 500 °C. The pore development was influenced by the impregnation ratio and soaking time [19, 33]. The data indicated that reactions between the activation agent (existing as phosphorus pentoxide, a strong acid and dehydration agent, at 400 °C) and precursor matrix also contributed the development of porosity.

## 3.2 Factors Affecting Activation of Adsorbent Preparation

### 3.2.1 Nature of Activating Agent

Chemical agents and carbonization temperature have an impact on the development of the pore volume and pore formation. The activated carbon prepared by chemical activation of lignin by Hayashi et al. [42] using  $\text{ZnCl}_2$  and  $\text{H}_3\text{PO}_4$  showed an increase in pore volume with an increase in temperature over the range 500–600 °C. At the temperature above 600 °C, the carbon structure shrank showing the decrease in surface area and hence the pore volume. Above 800 °C, the excess pore enlargement induced combination of pores, resulting in an increase in mesopores for all alkali metal salts and a decrease of micropore volume and of surface area. In a study conducted by John Kennedy et al. [54], porous carbon was prepared from rice husk using phosphoric acid activation through pre-carbonization and chemical activation. The method adopted produced carbons with micro- and mesoporous structure.

A wide range of chemical agents is used in the activation of carbons. The chemical agents used in the chemical process are normally alkali and alkaline earth metal containing substances and some acids such as KOH,  $\text{K}_2\text{CO}_3$ , NaOH,  $\text{Na}_2\text{CO}_3$ ,  $\text{ZnCl}_2$ ,  $\text{MgCl}_2$  and  $\text{H}_3\text{PO}_4$ . Although phosphoric acid is shown to be the most environmentally sound chemical for the activation processes, most studies have used zinc chloride due to its effective activating capability [97]. Also, it has been found that the effect of some chemicals on the carbon precursor yields more char and less tar than the untreated sample [1]. A very few carbon activation works are carried out using sulphuric acid.

### 3.2.2 Impregnation Ratio

The increase in impregnation ratio intensifies the reaction of the activating agent resulting in pore widening. Yanping and Rockstraw [120] activated pecan shell using orthophosphoric acid and developed micropore and mesopore activated carbons. The development of surface area and pore distribution followed the same trend with the increase of impregnation ratio with micro- and mesopore volumes as 1.5, 1.5 and 2.0  $\text{cm}^3/\text{g}$ , respectively: The initial increase followed by decrease after reaching a maximum was observed due to calcination of the developed carbon.

### 3.2.3 Activation Temperature

Low impregnation ratio (less than 1.5) and activation temperature (less than 300 °C) were favourable in the formation of acidic surface functional groups, which consisted of temperature-sensitive (unstable at high temperature) and temperature-insensitive (stable at high temperature) parts. At an impregnation ratio of 1.5, activated carbon with BET surface area and micropore volume as high as 861  $\text{m}^2/\text{g}$  and 0.289  $\text{cm}^3/\text{g}$

was obtained at 400 °C [33]. The surface area, pore volume and pore size distribution of carbon samples activated at three different temperatures 700, 800 and 900 °C have been carried out using nitrogen adsorption isotherms at 77 K. The production yield was observed to decrease with increase in activation temperature. The average pore size distribution was dependent mainly on the concentration of chemical impregnation and heat treatment temperature. The average pore diameter of 38.8 Å was obtained at activation temperature 700 °C and later on increased with activation temperature up to 800 °C but reversed at further higher temperature. The decrease in the pore diameter was due to the suppression of the pore widening of stable carbon structures formed during pre-carbonization process and coalescence of pores in the carbon matrices.

### 3.2.4 Pore Development and Specific Surface Area

Wang et al. [105] carried adsorption of a basic dye, methylene blue, from aqueous solutions onto three activated carbons: one derived from coconut shell and the other two coal-based carbons. The physical and surface chemical properties of the activated carbons are characterized using BET-N<sub>2</sub> adsorption, X-ray photoelectron spectroscopy (XPS) and mass titration. It was found that acid treatment had little effect on carbon textural characteristics but significantly changed the surface chemical properties, resulting in an adverse effect on dye adsorption. The physical properties of activated carbon, such as surface area and pore volume, have little effect on dye adsorption, while the pore size distribution and the surface chemical characteristics play an important role in dye adsorption. The pH value of the solution also influences the adsorption capacity significantly. For methylene blue, a higher pH of solution favoured the adsorption capacity. The kinetic adsorption of methylene blue on all carbons followed a pseudo-second-order equation.

## 4 Development of Tannery Sludge-Activated Carbon

### 4.1 Characterization of Tannery Sludge

The preliminary tannery sludge collected from common effluent treatment plant throughout different seasons of the year was dried in an oven at 105 °C ± 2 °C until the mass of the sludge remained constant. The dried sludge was crushed and sieved in IS sieves. The sludge retained in the sieve sizes 300 μm and 600 μm was arbitrarily chosen for experimentation. The proximate and ultimate analysis of the raw sludge was conducted in the laboratory as per the ASTM standards (D3172-07 and 3176-89). Table 13 shows the proximate and ultimate analysis of the raw tannery sludge in dry basis.



**Table 13** Characterization of raw tannery sludge

Parameters	Values
<i>(i) Proximate analysis</i>	
pH	7.2 ± 0.01
Moisture content	3.6 ± 0.02
Volatile content	32.5 ± 0.03
Ash content	28.36 ± 0.02
Fixed carbon	35.54 ± 0.03
<i>(ii) Ultimate analysis</i>	
Carbon	36.77
Hydrogen	3.79
Nitrogen	3.54

## 4.2 Tannery Sludge Carbon

The dried raw sludge was subjected to physical activation, chemical activation and a combination of physical and chemical activation. The pyrolysis was carried out in the presence of nitrogen atmosphere under varying temperatures: 600 °C, 650 °C and 750 °C for 3 h. The chemical activation was done by acid treatment succeeded by pyrolysis under the same conditions as done in physical activation. A strong acid (sulphuric acid) and a weak acid (acetic acid) were selected for the acid activation of the sludge. The acid and water were combined in ratios such as 1:1, 2:1 and 5:1.

The sludge was mixed with different proportions of acid to mass ratios of 1 and 2 and kept for an impregnation period of 12 h. To remove the effect of excess acid, the samples were washed several times with deionized water and dried in oven for 4 h and desiccated before use.

## 4.3 Comparison of Commercial Activated Carbon and Tannery Sludge Carbon

### 4.3.1 Proximate and Ultimate Analysis

The proximate analysis of the various sulphuric acid-impregnated activated carbons is shown in Table 14.

The sludge-derived activated carbons were categorized based on two particle sizes (600 and 300 µm). The activated carbons having higher carbon content from each particle size under various impregnation ratios are recommended for further instrumental analysis. Thus, the sludge carbons CAH652650 or SC600 from particle size 600 µm and CAH352650 or SC300 from particle size 300 µm were recommended for further adsorption studies discussed in Chapter “[Dyestuff Adsorbing](#)”

**Table 14** Proximate analysis and iodine number of tannery sludge-derived activated carbon (results are expressed in a dry basis, except for the moisture content)

Activated carbon	pH	Moisture content (%)	Volatile content (%)	Ash content (%)	Fixed carbon (%)	Iodine number
CAC	7.30 ± 0.05	2.60 ± 0.01	22.75 ± 0.06	18.20 ± 0.00	56.45 ± 0.02	370.00 ± 0.50
SC600	6.95 ± 0.00	2.10 ± 0.00	32.15 ± 0.05	14.25 ± 0.05	49.40 ± 0.00	253.5 ± 0.50
SC300	6.90 ± 0.00	2.4 ± 0.25	33.60 ± 0.25	15.60 ± 0.20	46.10 ± 0.45	377.5 ± 0.50

**Table 15** Ultimate analysis of tannery sludge-derived activated carbons

Adsorbent	C	H	N
CAC	77.17	0.93	0.21
SC600	41.9	1.24	1.08
SC300	43.07	0.97	1.12

**Natural Composites for Wastewater Treatments**". These activated carbons have higher volatile content but lower ash content, which are the two key requirements in the production of adsorbents [12]. They also have a higher carbon content than the other activated carbons prepared from their respective particle sizes. The volatile content and ash content of SC300 > SC600, but the carbon content of SC300 and SC600 was  $46.10 \pm 0.45\%$  and  $49.40 \pm 0.20\%$ , respectively. Hence, the carbon content increased with increasing particle size of the activated carbon. The iodine number of SC600 and SC300 was  $253.0 \pm 0.50$  and  $377.5 \pm 0.50$ , respectively. The iodine number of activated carbons was found to be less than those suggested by ASTM standards (600–1500). Iodine number is a relative indicator of porosity for an activated carbon. It does not necessarily provide a measure of activated carbon capacity to absorb other species. Iodine number may be used as an approximation of surface area, but the relationship between surface area and iodine number cannot be generalized. Iodine number varies with changes in carbon raw material, processing conditions and pore volume distribution. The presence of adsorbed volatiles, sulphur and water extracts may also affect the measured iodine number of an activated carbon.

Table 15 shows the ultimate analysis of the developed activated carbon from tannery sludge in comparison with the commercial activated carbon. Commercial activated carbon had higher carbon content when compared to SC600 and SC300.

### 4.3.2 Surface Chemistry and Characterization

The surface morphology of the raw tannery sludge and the activated carbons produced was analysed using SEM images. Figures 5, 6 and 7 depict the SEM micrographs of the raw tannery sludge and the activated carbons (SC600 and SC300) obtained at an activation temperature of 650 °C and an impregnation ratio 2. The SEM micrographs revealed micropores and mesopores on the external surface of the carbons during the

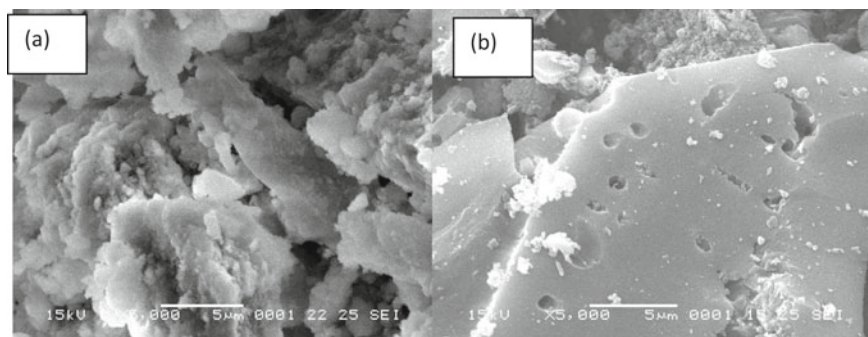


**Fig. 5** SEM images of **a** raw tannery sludge and **b** commercial activated carbon

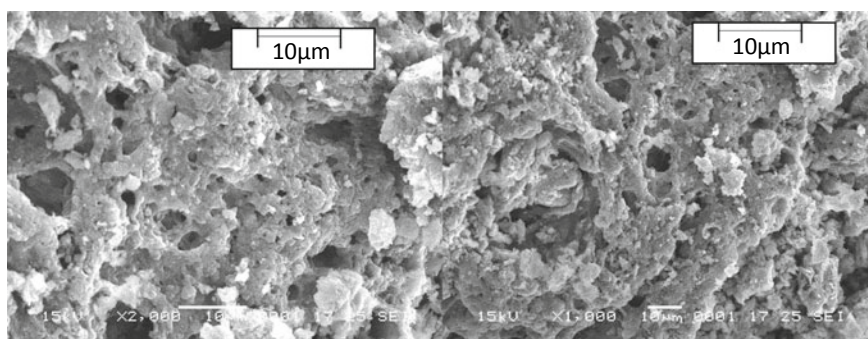


**Fig. 6** SEM images of tannery sludge carbon (SC600) activated at 650 °C

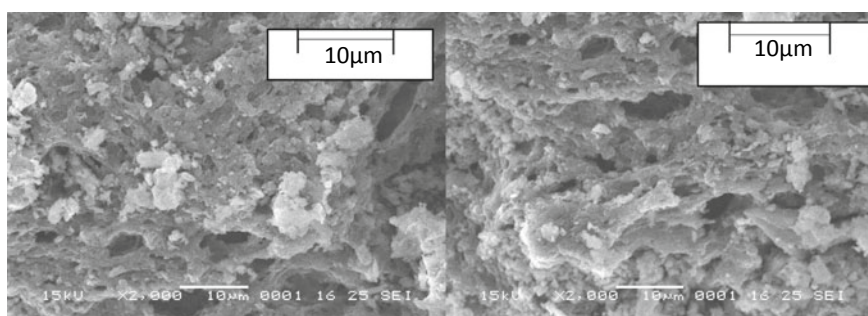


**Fig. 7** SEM images of tannery sludge carbon (SC300) activated at 650 °C

activation process. The pores are due to the release of volatile matter and the reaction between the chemical agent (sulphuric acid) and the carbon atom in precursor. From the analysis of these surface images, it was concluded that the adsorbents under the study were porous in nature and the pore development confirmed the sludge carbons

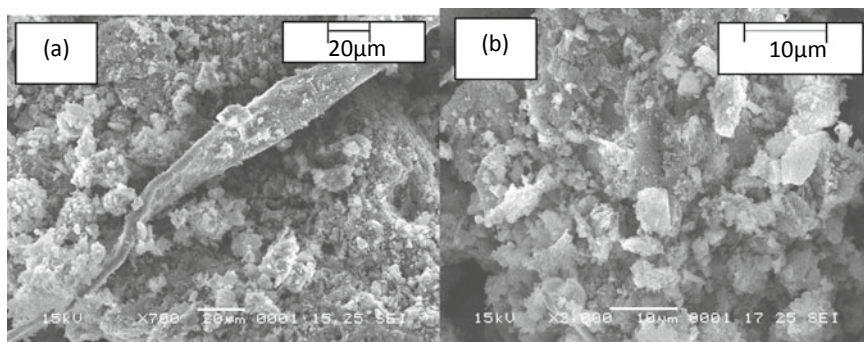


**Fig. 8** SEM images of SC600 after adsorption on **a** Reactive Red 31 and **b** Reactive Red 2

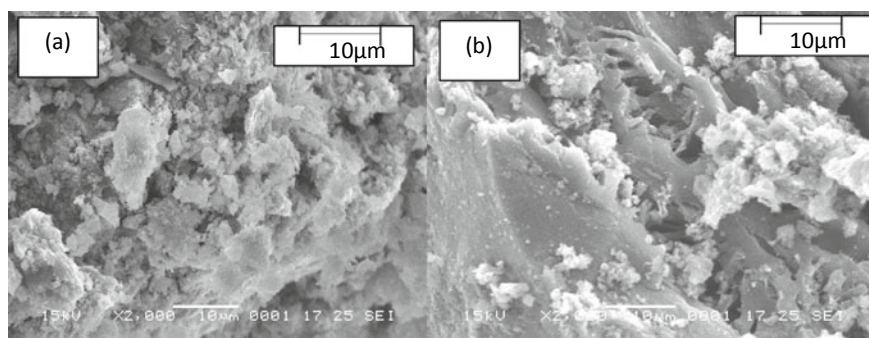


**Fig. 9** SEM images of SC300 after adsorption on **a** Reactive Red 31 and **b** Reactive Red 2

to be a potential adsorbent (Figs. 5 and 9). The sludge-developed carbons favoured adsorption due to the presence of active sites and a layer of gaps and cavities. The structures of adsorbents were also compared with the commercial activated carbon.

The morphological changes in the surface of the developed adsorbents (SC600 and SC300) by the adsorption of RR31 and RR2 were also obtained. Figures 8 and 9 show the surface coverage of the activated carbons SC600 and SC300 on Reactive Red 31 and Reactive Red 2 due to adsorption of the dye molecule over the adsorbent surface. The adsorption process was evident from the formation of white layer over the surface and the absence of the pores. The micrograph showed that the dye had densely and homogeneously adhered to the surface of the adsorbent, as a result of either natural entrapment into the porous sludge carbon, due to physical adsorption by electrostatic forces or by covalent binding between the reactive dye and the activated carbon. The uniform distribution was an important criterion for the proper adsorption of the reactive dyes on the whole surface area of the adsorbents.

### 4.3.3 Analysis of Specific Surface Area and Pore Development

The adsorptive capacity of activated carbon is related to its specific surface area, pore volume and pore size distribution. Generally, as the surface area of the activated carbon increases, its adsorptive capacity also increases.

The effects of activation temperatures on the BET surface area of the activated carbons are shown in Fig. 10. Increasing the activation temperature from 600 °C up to an optimum value caused an increase on the BET surface area, and a sharp decline in the BET surface area was observed when the activation temperature increased from 650 to 750 °C. This phenomenon was largely due to the excessive burn-off of carbon constituents at these higher temperatures. Increase in activation temperature can cause an increase in porosity by increasing the release of volatile matter. However, the constant decrease in the surface area with increasing temperature from 750 and 800 °C indicated the sintering effect of volatiles and the shrinkage of carbon structure, resulting in narrowing and closing up of some of the pores.

Lua and Yang [70] reported similar effect of temperature on the characteristics of activated carbon and attributed this to excessive carbon burn-off, resulting in the widening of pores and even the loss of some walls between the pores. The BET surface area of SC600 and SC300 reached an optimum at 188.250 m<sup>2</sup>/g and 212.32 m<sup>2</sup>/g, respectively. The porous nature of the different activated carbons analysed by BET isotherm is shown in Table 16.

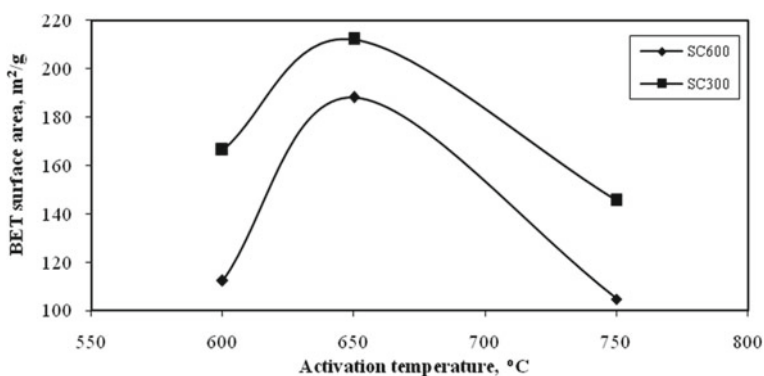


**Fig. 10** Effect of activation temperature on BET surface area of various activated carbons

**Table 16** Porosity characterization of the activated carbons by BET isotherm

Activated carbon	Surface area (m <sup>2</sup> /g)	Pore volume (cm <sup>3</sup> /g)	Pore width (Å°)	
			BJH method	HK method
CAC	693.35	0.380042	19.01	5.25
SC600	188.25	0.134239	19.77	5.15
SC300	212.32	0.132500	19.73	5.07

The pore size distribution was calculated by Barrett–Joyner–Halenda (BJH) method and Horvath–Kawazoe (HK) method. N<sub>2</sub> isotherms at 77 K are used for practical reasons (e.g. simultaneous determination of the BET surface area). The method proposed by Barrett–Joyner–Halenda (1951), known as BJH method, continued to be used even today. In the BJH method, desorption branch of isotherm is used, which is the desorption branch of the usual hysteresis loop of the isotherm for the mesoporous sorbents and hence employed to deduce the mesopore size distribution. A simple and popular method for evaluating pore size distribution of microporous materials was proposed by Horvath and Kawazoe.

This technique has been successfully used for the determination of pore size distribution in microporous sorbents such as activated carbons and zeolites. The adsorption–desorption plot of the isotherm distribution showed the dominance of the microporous carbon and the presence of mesoporous carbon (Figs. 11, 12 and 13). The optimum activation temperature was 650 °C after 180 min at a burn-off level of 29% and 26% for SC300 and SC600, respectively.

## **5 Adsorption of Reactive Dyes onto Tannery Sludge-Activated Carbons: Equilibrium Kinetic Studies**

### **5.1 Reactive Dyes**

The removal of colour from dye house liquid effluents is one of the main problems in textile industries. Reactive dyes are one of the largest problematic groups of dyes used in the textile industries. As the reactive dyes are highly water soluble and practically non-biodegradable, they are not degraded in municipal activated sludge treatment plants; nor are they substantially removed via adsorption onto the biomass. Removal of reactive dyes is necessary for preventing the recalcitrant compounds from getting released into the environment and for efficient and complete dye removal. Various types of reactive dyes are commercially available. Their common feature is a chemical reaction with the textile fibre to achieve a covalent dye–fibre bond. Reactive dyes are typically azo-based chromophores combined with different types of reactive groups. Reactive dyes interact with the active groups on the cell surface by surface adsorption, ion exchange, complexation, chelation and microprecipitation [50]. They are characterized by nitrogen to nitrogen double bonds, azo bonds used mainly for dyeing cellulose fibres. They differ from all other classes of dyes in that they get bound to the textile fibres such as cotton to form covalent bonds. They have the favourable characteristics of bright colour, simple application techniques and low energy consumption and are used extensively in textile industries. The reactive systems of these dyes react with ionized hydroxyl groups on the cellulose substrate [68]. However under alkaline conditions, the hydroxyl ions compete with the cellulose substrate resulting in a percentage of hydrolysed dyes which can no longer react with the fibre [3, 68]. Hence, their removal is of great importance. Dyes with two

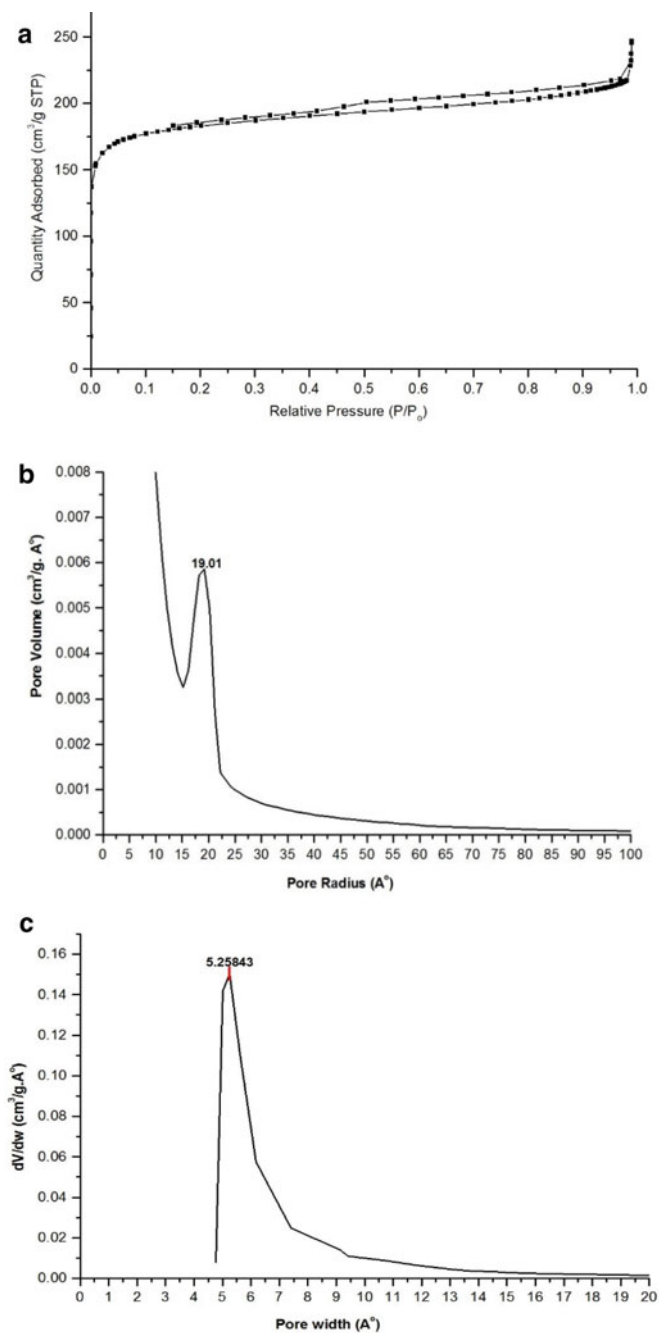


**Fig. 11** a BET isothermal adsorption-desorption linear plot of commercial activated carbon. b BJH desorption pore distribution of commercial activated carbon. c HK desorption pore distribution of commercial activated carbon

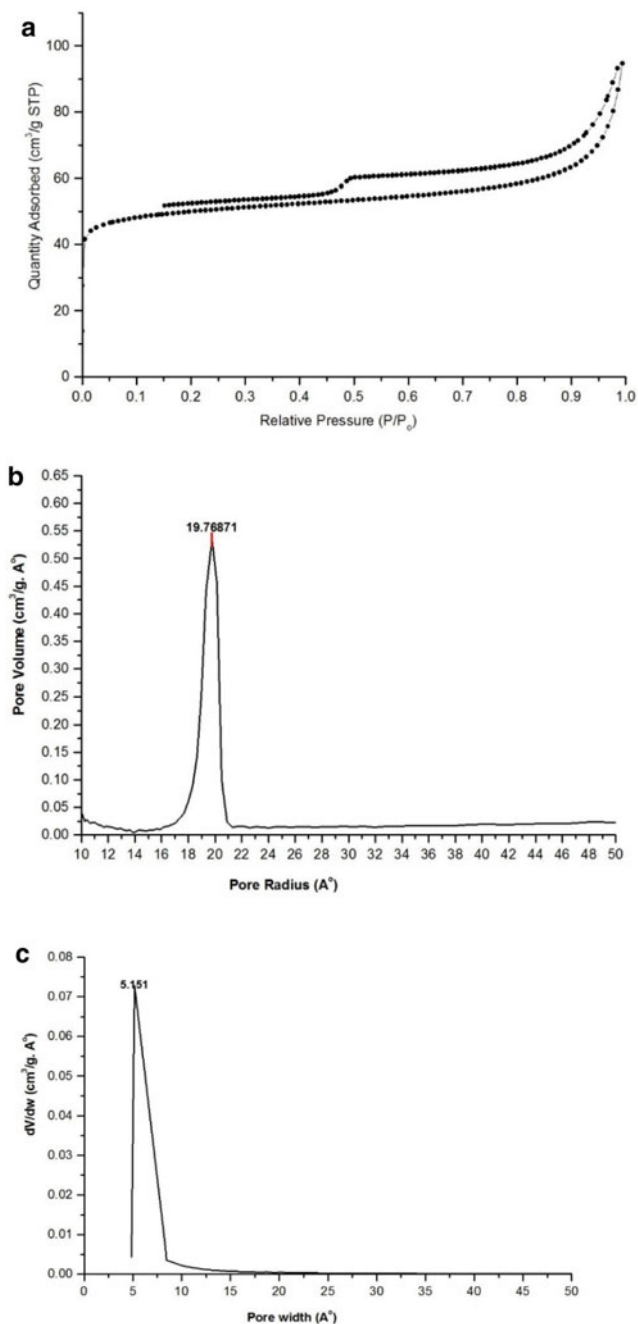


**Fig. 12** a BET isothermal adsorption–desorption linear plot of tannery sludge-activated carbon (SC600). b BJH desorption pore distribution of tannery sludge-activated carbon (SC600). c HK desorption pore distribution of tannery sludge-activated carbon (SC600)



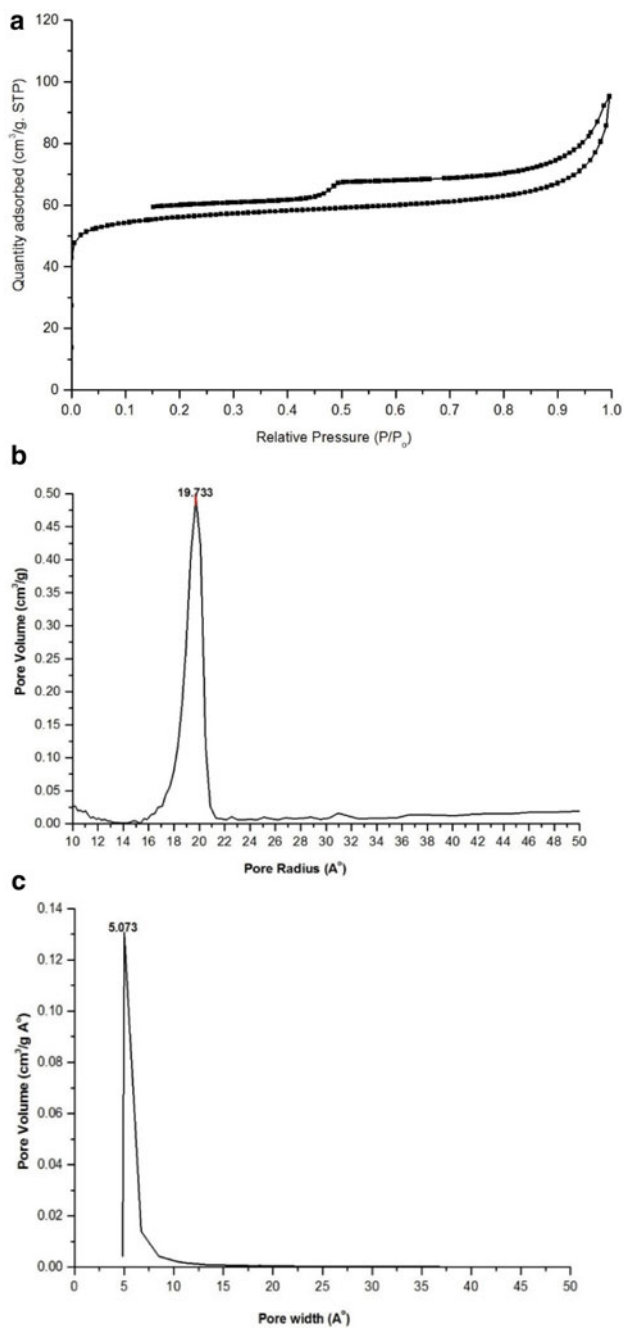


**Fig. 13** a BET isothermal adsorption-desorption linear plot of tannery sludge-activated carbon (SC300). b BJH desorption pore distribution of tannery sludge-activated carbon (SC300). c HK desorption pore distribution of tannery sludge-activated carbon (SC300)

of the most commonly used anchors—the monochlorotriazine and the vinylsulphone group—were chosen for this study. Reactive dyes have a relatively low fixation degree on the textile substrate, and the corresponding wastewaters may be highly coloured.

## 5.2 Adsorption Studies by Batch Mode

### 5.2.1 Equilibrium Time and Removal Efficiency

The adsorption equilibrium studies for the removal of Reactive Red 31 and Reactive Red 2 on the commercial activated carbon (CAC) and the tannery sludge-developed activated carbon (SC600 and SC300) were performed under a temperature of 30 °C, 120 rpm maintained under a pH-7.0. The equilibrium times for CAC in the removal of RR31 and RR2 were 90 min and 120 min, respectively. The equilibrium adsorption times of SC600 on RR31 and RR2 were 180 min and 240 min and that for SC300 on RR31 and RR2 were 150 min and 210 min, respectively. The dye adsorption on the different activated carbons was in the order CAC > SC600 > SC300. The equilibrium condition for RR31 was reached earlier compared to RR2, due to the presence of more number of sulphonate ions in RR31. The quicker adsorption was due to the greater surface area of CAC (693 m<sup>2</sup>/g).

The adsorption of reactive dyes by CAC is shown in Figs. 14 and 15. The removal efficiency of SC300 was greater than SC600. Thus, with decrease in particle size of the adsorbent, an increase in surface area had occurred, thereby increasing the removal efficiency. The removal efficiencies of the reactive dyes on the activated carbons at the equilibrium time were as follows. The RR31 removal efficiency of SC600 and SC300 was 65.04% and 71.95%, respectively (Figs. 16 and 18). The RR2

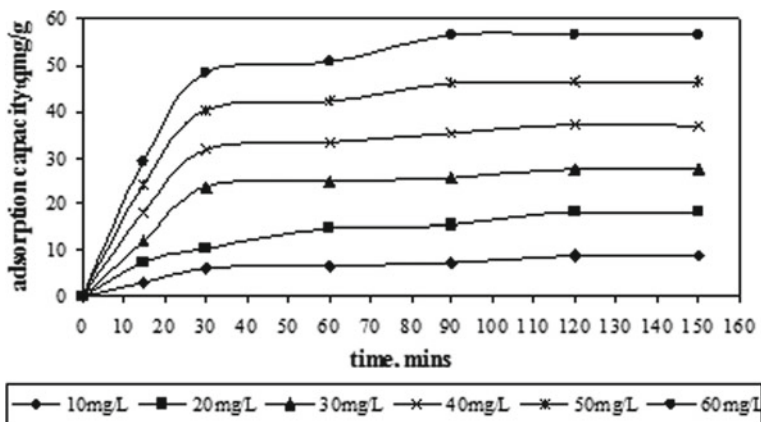


**Fig. 14** Adsorption capacity of CAC on Reactive Red 31 to reach equilibrium time at 120 rpm, 30°C and pH = 7.0

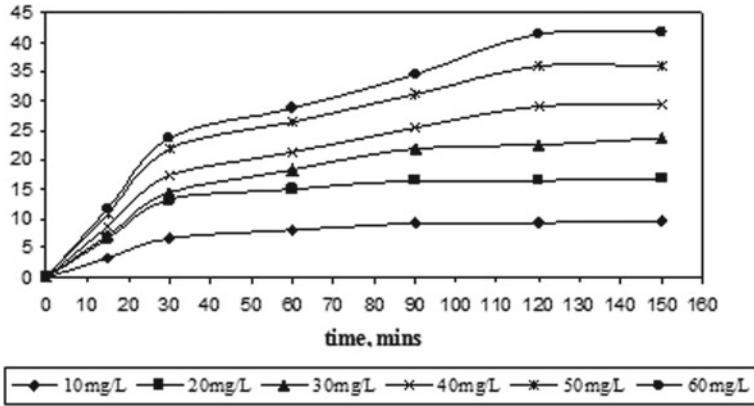


**Fig. 15** Adsorption capacity of CAC on Reactive Red 2 to reach equilibrium time at 120 rpm, 30°C and pH = 7.0

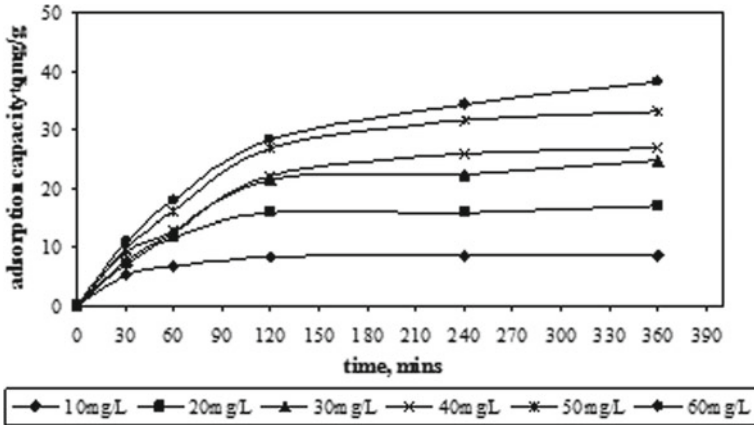


**Fig. 16** Adsorption capacity of SC600 on Reactive Red 31 to reach equilibrium time at 120 rpm, 30°C and pH = 7.0

removal efficiencies of SC600 and SC300 were found to be 78.83% and 80.10% (Figs. 17 and 19), respectively. The diazo RR31 dye had higher colour removal efficiency than the monoazo dye RR2. This can be attributed to the size of the dye molecule and the number of  $SO^{-3}$  ions present.

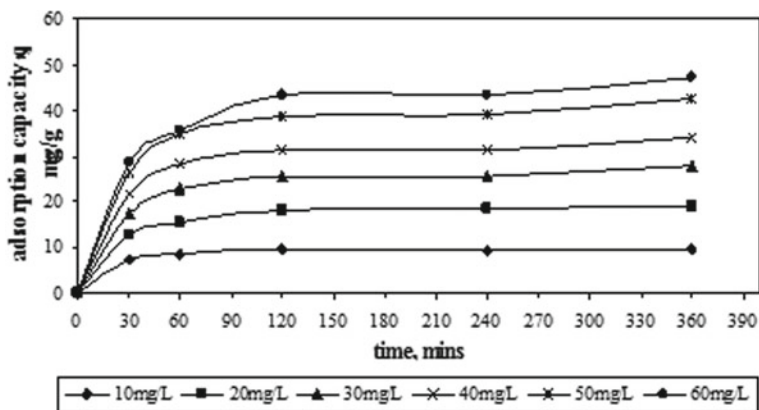


**Fig. 17** Adsorption capacity of SC600 on Reactive Red 2 to reach equilibrium time at 120 rpm, 30°C and pH = 7.0

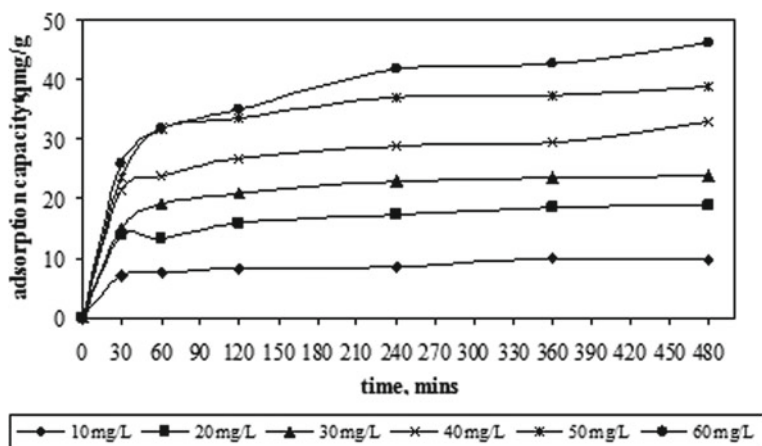


**Fig. 18** Adsorption capacity of SC300 on Reactive Red 31 to reach equilibrium time at 120 rpm, 30°C and pH = 7.0

### 5.2.2 Effect of Contact Time and Initial Dye Concentration on Adsorption Kinetics

The influence of initial dye concentration on adsorption of RR31 and RR2 onto CAC, SC600 and SC300 was investigated in the concentration range of 10–60 mg/L at pH = 7.0, temperature 30 °C and an adsorbent dosage of 1 g/100 mL. When the initial dye concentration increased from 10 mg/L to 60 mg/L, the amount of dye adsorbed increased from 9.36 mg/g to 34.58 mg/g for CAC on RR31, 6.44 mg/g to 50.64 mg/g for CAC on RR2, 8.51 mg/g to 34.27 mg/g for SC600 on RR31, 9.48 mg/g to 43.20 mg/g for SC600 on RR2, 8.48 mg/g to 41.88 mg/g for SC300 on RR31 and

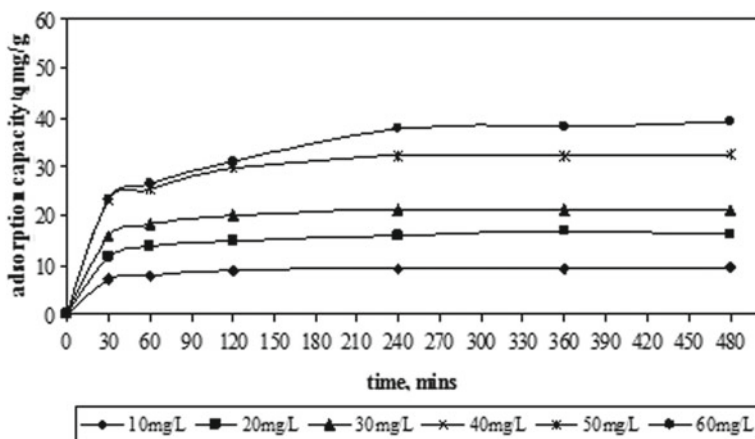


**Fig. 19** Adsorption capacity of SC300 on Reactive Red 2 to reach equilibrium time at 120 rpm, 30°C and pH = 7.0

9.07 mg/g to 37.86 mg/g for adsorption of SC300 on RR2, respectively. The dye removal capacities of CAC, SC600 and SC300 on RR31 and RR2 with initial dye concentrations up to 30 mg/L are 88.46% and 75.46%, 74.53% and 84.66%, and 69.21% and 66.61%, respectively. For dye concentrations greater than 40 mg/L, the per cent removal of RR31 and RR2 is 85.283% and 72.853% for CAC, 65.04% and 78.53% for SC600 and 66.903% and 61.52% for SC300. From these observations, it is evident that the adsorption was very fast at lower concentrations of dyes. The per cent removal of dyes decreased with increase in initial concentration and took longer time to reach equilibrium. No significant change on the extent of adsorption was observed, beyond the equilibrium time of the dyes.

### 5.2.3 Effect of Adsorbent Dosage on Adsorption Kinetics

The adsorbent dosage of the various adsorbents varied from 0.5 g/100 mL to 2.5 g/100 mL. For an initial dye concentration of 40 mg/L, the reactive dyes adsorbed on various A similar trends were reported in the adsorption of a dye Reactive Red 241 onto a commercial activated carbon [92]. The variation in percentage removal of dye with contact time at different initial concentrations ranging from 10 to 60 mg/L is presented in Figs. 20 and 21. From the illustrations (Figs. 14, 15, 16, 17, 18, 19, 20 and 21), it was observed that the maximum amount of dye adsorption took place within the contact time of 30 min and becomes gradual thereafter. This indicated a quicker adsorption rate during the initial contact period. Adsorbent dosages increased from 21.60 mg/g to 37.40 mg/g for RR31 on CAC; 13.25 mg/g to 40 mg/g for RR2 on CAC; 19.71 mg/g to 38.09 mg/g for RR31 on SC600; 21.29 mg/g to 38.92 mg/g for RR2 on SC600; 15.16 mg/g to 35.29 mg/g for RR31 on SC300; and 21.04 mg/g to 38.92 mg/g for RR2 on SC300, respectively. Figure 22 shows that, the dye uptake

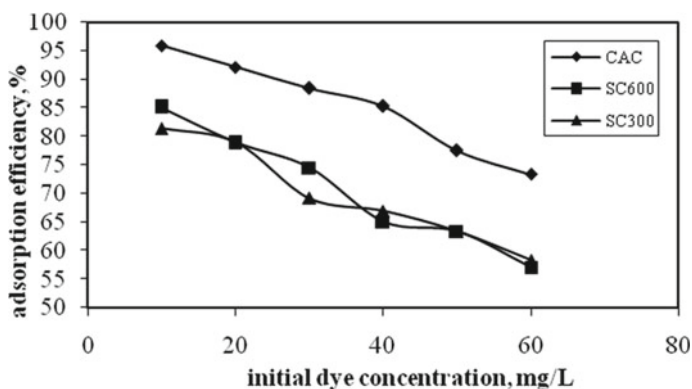


Fig. 20 Dye removal efficiency of RR31 dye for various activated carbons at equilibrium time

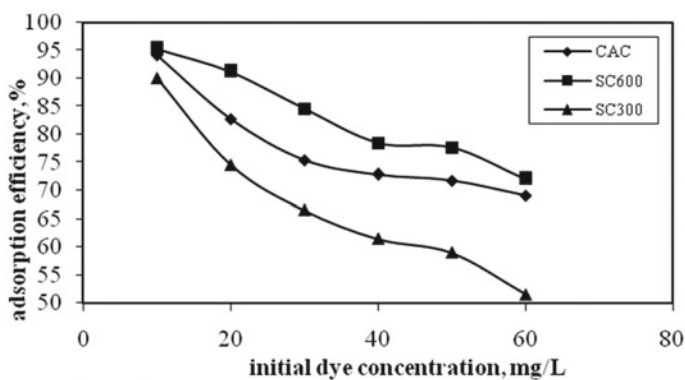


Fig. 21 Dye removal efficiency of RR2 dye for various activated carbons at equilibrium time

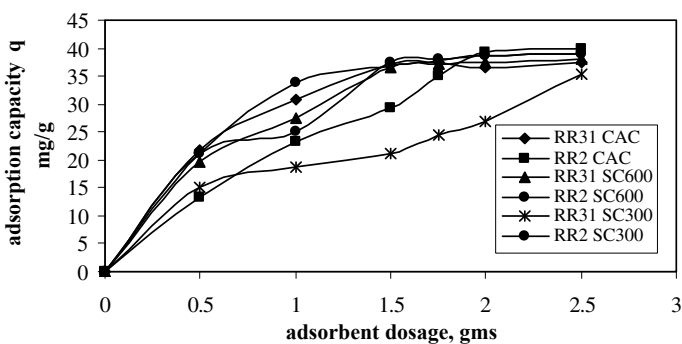


Fig. 22 Effect of adsorbent dosage at 40 mg/L of adsorbate concentration at 120 rpm, 30 °C and pH = 7.0

increased with the increase in carbon dosage at constant initial dye concentration and hence increased the overall removal efficiency of the dyes.

For an increase in dye concentration, there would be increased competition for the active adsorption sites. The strong chemical binding of the adsorbate slows down the adsorption process. A similar trend was reported in the adsorption of a dye Reactive Red 241 onto a commercial activated carbon [92]. The variation in percentage removal of dye with contact time at different initial concentrations ranging from 10 to 60 mg/L is presented in Figs. 20 and 21. From the illustrations (Figs. 14, 15, 16, 17, 18, 19, 20 and 21), it was observed that the maximum amount of dye adsorption took place within the contact time of 30 min and becomes gradual thereafter. This indicated a quicker adsorption rate during the initial contact period.

#### 5.2.4 Effect of Agitation Speed on Adsorption Kinetics

Agitation is an important parameter in adsorption phenomena because it influences the distribution of the solute in the bulk solution and the formation of the external boundary film. Figure 23a, b, respectively, shows the adsorption capacity of the reactive dyes, Reactive Red 31 and Reactive Red 2, using three activated carbons (CAC, SC600 and SC300) at different agitation speeds (100, 120 and 140 rpm). It is clear from Fig. 23a, b that the uptake of dyes increased from 100 rpm to 120 rpm and decreased slightly at the agitation speed of 140 rpm.

The slight decrease in adsorption capacity at 140 rpm was due to desorption at the equilibrium time. Difference in agitation speed caused changes in kinetics of the adsorption as well as the equilibrium adsorption capacity. The increase in dye uptake at the optimum speed of 120 rpm reduced the film boundary layer surrounding the particles, thus increasing the external film transfer coefficient and thereby the percentage dye removal. Mckay [73] also found that the degree of agitation reduced the boundary layer resistance and increased the mobility of the system and the external mass transfer coefficient resulting in quicker adsorption of dye molecules with agitation speed.

#### 5.2.5 Effect of pH on Adsorption Kinetics

The initial pH of the dye solution is an important parameter which controls the adsorption process in general and the adsorption capacity in particular. pH of the solution influences the following factors:

1. The surface charge of the adsorbent
2. The degree of ionization of the adsorbate molecule and
3. The extent of dissociation of functional groups on the active sites of the adsorbent.

Experimental results showed that the removal of dye increased with the decrease in pH as shown in Fig. 24. The variation of adsorption capacity with pH, shown in

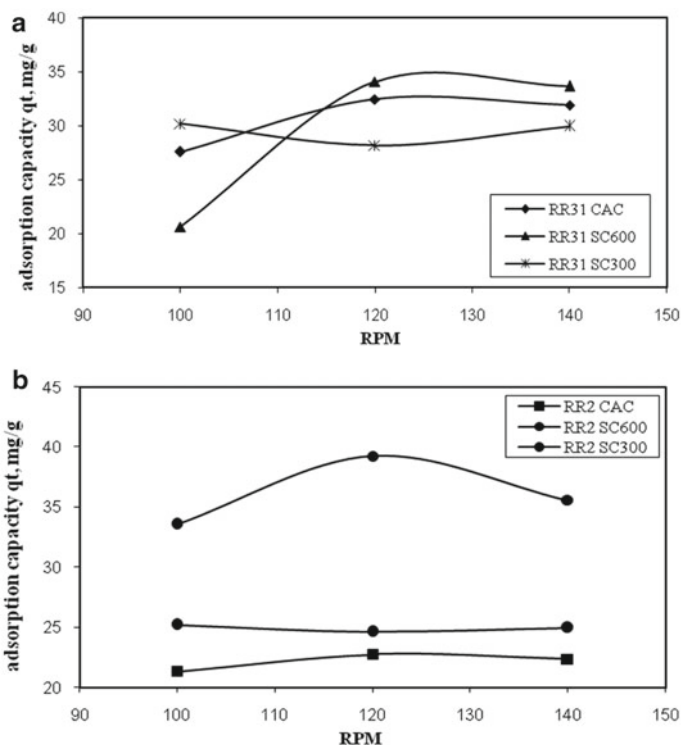


**Fig. 23** **a** Effect of varying agitation speed at 40 mg/L of RR31 dye concentration at 30 °C. **b** Effect of varying agitation speed at 40 mg/L of RR2 dye concentration at 30 °C

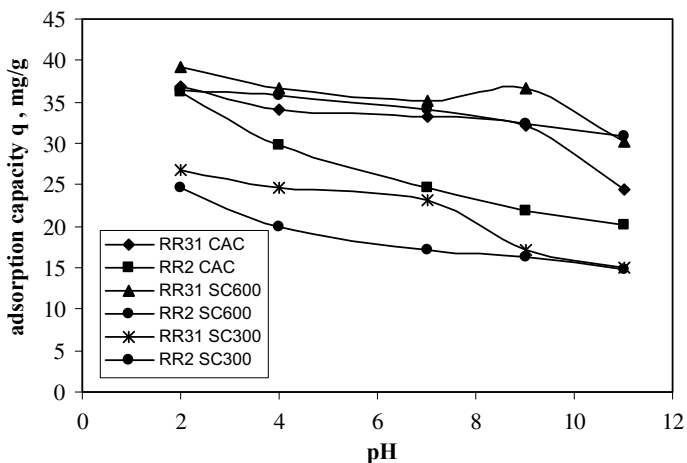


**Fig. 24** Effect of pH at 40 mg/L of adsorbate concentration @ 120 rpm and 30 °C



Fig. 24, can be explained from the fact that the anions are favourably adsorbed by the adsorbent at lower pH due to the presence of  $H^+$  ions. The removal of dyes at lower pH (2.0–7.0) decreased from 92.05% to 85.40% for RR31 on CAC; 90.70% to 74.20% for RR2 on CAC; 75.44% to 69.28% for RR31 on SC600; 81.06% to 77.07% for RR2 on SC600; 66.22% to 61.87% for RR31 on SC300; and 61.58% to 49.70% for RR2 on SC300.

The percentage removal of the reactive dyes at lower pH increased in the order of  $CAC > SC600 > SC300$ . Similar results were reported by Santhy and Selvapathy [103] in the removal of Reactive Red dye. Moreover, lower sorption of the anionic dye at alkaline pH can be attributed to the abundance of  $OH^-$  ions, which will compete with the dye anions for the sorption sites [28, 95] (Khaled et al. 2009). Similar observations have been reported by previous work for sorption of reactive dyes on activated carbon prepared from sugarcane bagasse pith, coir pith and orange peel (Khaled et al. 2009) [7, 103]. A useful index that shows whether the surface is likely to become negatively or positively charged as a function of pH is pH value at which the net electric charge of the surface is zero. This value is called the zero point charge ( $pH_{zpc}$ ) or the pH value of isoelectric point of zeta potential ( $Z_{IEP}$ ). Figures 25, 26 and 27 show that the  $pH_{zpc}$  of CAC on both the reactive dyes was 8.75 and  $pH_{zpc}$  of SC600 and SC300 for Reactive Red 31 and Reactive Red 2 was 9.0 and 7.0, respectively. The pH values of the dye solutions at equilibrium were  $6.6 \pm 0.4$ . As the equilibrium pH is lower than the  $pH_{zpc}$ , an effective removal of the anionic reactive dyes RR31 and RR2 onto the different activated carbons is confirmed. Low pH values strongly indicated that the activated carbons had a positive charge in the external layer (at equilibrium  $pH < pH_{zpc}$ ) during the adsorption process.

This positive charge attracted the negative portions of the reactive dyes. Similar results were reported in the adsorption of commercial activated carbon F-400 on three reactive dyes. A similar behaviour was also reported by Netpradit et al. [89]

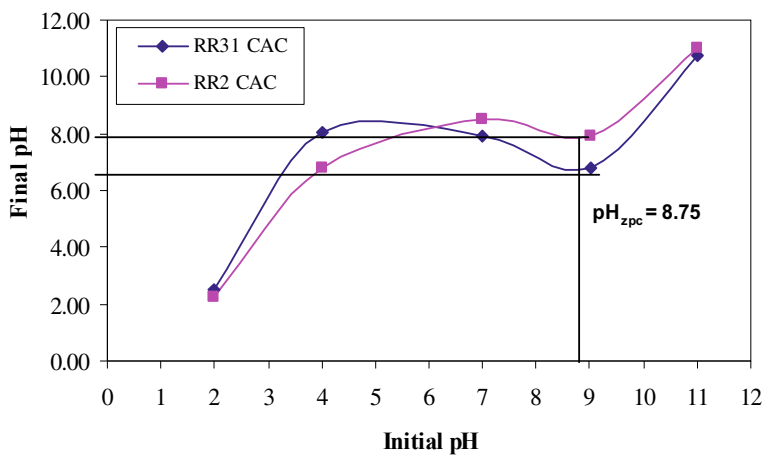
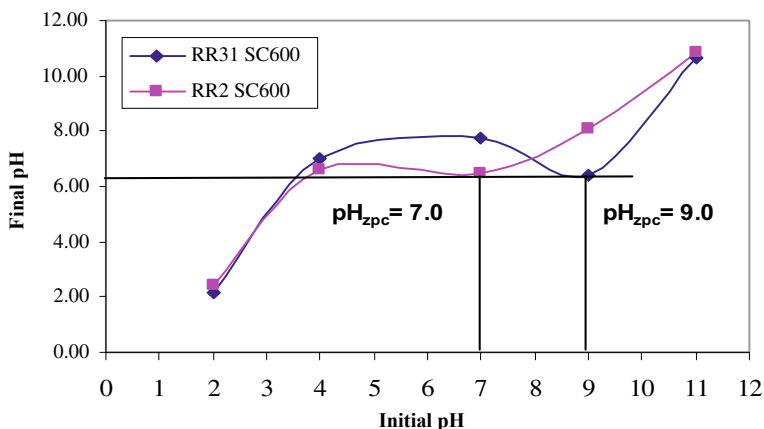
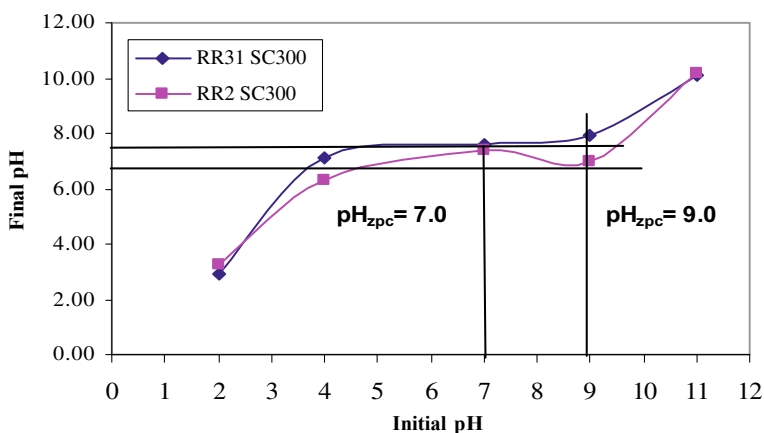


Fig. 25 Experimental determination of  $pH_{zpc}$  of reactive dyes on CAC



**Fig. 26** Experimental determination of  $pH_{zpc}$  of reactive dyes on SC600



**Fig. 27** Experimental determination of  $pH_{zpc}$  of reactive dyes on SC300

who obtained a  $pH_{zpc}$  of around 8.7, favouring the uptake of the negative charge of the reactive dyes.

### 5.3 Equilibrium Adsorption Isotherms

For any adsorption investigation, one of the most important parameters required to understand the behaviour of the adsorption process is the adsorption isotherm. Adsorption isotherm is of fundamental importance in the design of adsorption systems. The isotherm expresses the relation between the mass of the dye adsorbed

at a particular temperature, the pH, particle size and liquid phase of the dye concentration. The shape of an isotherm provides information about the affinity of the dye molecules for adsorption and also reflects the possible mode for adsorbing dye molecules. Several attempts have been made to find the adsorbed amount of the dye concentration. The most common method used for obtaining an adsorption isotherm is by determining the concentration of the dye solution before and after the adsorption experiments. An adsorption isotherm shows how the adsorbate molecules partition between the liquid and solid phases when the adsorption process reaches equilibrium conditions. The analysis of the isotherm data by fitting them to different isotherm models is an important step to find a suitable model that can be used for the design of adsorption systems. Two adsorption isotherm models, namely Langmuir and Freundlich models, have been used in this work. The applicability of the isotherm models to the adsorption study was compared by judging the maximum adsorption capacity and the correlation coefficients ( $R^2$  values).

### 5.3.1 Langmuir Isotherm

The Langmuir isotherm assumes monolayer adsorption onto a surface containing a finite number of adsorption sites of uniform strategies of adsorption with no transmigration of adsorbate in the plane of surface [66]. The Langmuir equation can be expressed in mathematical form as

$$C_e/q_e = 1/Q_o b + C_e/Q_o \quad (5.1)$$

where  $C_e$  is the equilibrium concentration (mg/L),  $q_e$  is the amount adsorbed at equilibrium (mg/g),  $Q_o$  is the adsorption capacity (mg/g) and  $b$  is the energy of adsorption (Langmuir constant, L/mg). The maximum adsorption capacity ( $Q_o$ ) and Langmuir constant ( $b$ ) were calculated from the slope and intercept of the linear plots  $C_e/q_e$  versus  $C_e$ . The results are presented in Tables 17 and 18. The maximum adsorption capacity  $Q_o$  was found to increase with temperature, thereby enhancing the mobility of the dye ions. This led to a higher chance of the reactive dyes being

**Table 17** Langmuir isotherm constants for adsorption of Reactive Red 31 on commercial activated carbon and tannery sludge-developed activated carbons

Temperature (°C)	Adsorbents											
	CAC RR31				SC600 RR31				SC300 RR31			
	$Q_o$	$B$	$R^2$	$R_L$	$Q_o$	$b$	$R^2$	$R_L$	$Q_o$	$B$	$R^2$	$R_L$
20	31.25	0.28	1.00	0.90	31.35	0.21	0.94	0.87	47.62	2.23	0.98	0.99
30	41.67	0.27	0.95	0.92	43.10	0.22	0.94	0.90	52.36	10.05	0.96	1.00
40	43.29	1.01	1.00	0.98	45.46	0.71	0.95	0.83	52.63	13.01	0.96	0.99
50	44.05	0.52	0.99	0.97	47.02	0.94	0.98	0.87	55.87	22.07	0.96	1.00

**Table 18** Langmuir isotherm constants for adsorption of Reactive Red 2 on commercial activated carbon and tannery sludge-developed activated carbons

Temperature (°C)	Adsorbents																	
	CAC RR2						SC600 RR2						SC300 RR2					
	$Q_o$	$B$	$R^2$	$R_L$	$Q_o$	$B$	$R^2$	$R_L$	$Q_o$	$B$	$R^2$	$R_L$	$Q_o$	$B$	$R^2$	$R_L$		
20	35.84	0.078	0.972	0.737	23.15	0.969	0.984	0.957	36.63	0.134	0.952	0.831						
30	37.88	0.122	0.983	0.823	25.58	1.412	0.993	0.973	37.74	0.331	0.973	0.926						
40	38.91	0.213	0.993	0.892	35.84	0.782	0.966	0.966	41.50	0.610	0.960	0.962						
50	41.49	0.142	0.984	0.855	39.37	3.175	0.991	0.992	41.84	0.759	0.955	0.969						

adsorbed onto the carbon adsorbents and an increase in its adsorption capacity which resulted in the enlargement of pore size or activation of the adsorbent surface.

The isotherm showed no linear variation for the Langmuir constant  $b$ , and hence the kinetic energy of the dye molecules was independent. The observed linear relationship was statistically significant (at the 95% confidence level) as evidenced by the  $R^2$  values (which were close to unity). This indicated the applicability of the isotherm and the surface. The order of increase in adsorption capacity for RR31 was as  $CAC > SC300 > SC600$ . The tannery sludge-activated carbon had greater adsorption capacity at a particle size of 300  $\mu\text{m}$  than at 600  $\mu\text{m}$ . In the adsorption of RR2, the adsorption capacity was in the order of  $CAC < SC600 < SC300$ . These adsorption capacities showed the complex nature of the adsorption. The lower adsorption of dyes towards CAC was due to the lesser anionic charge of the dyes causing weaker attraction towards the site of cationic charge of the CAC. Hence, the dye molecule had to escape from the solid phase to the bulk phase. The pore size of the CAC could not accommodate quicker adsorption as compared to the tannery-activated carbons SC600 and SC300. The maximum monolayer adsorption capacity of SC300 was greater than SC600 for both the reactive dyes. The adsorption capacity  $Q_o$  increased with the temperature throughout the isothermal studies.

The maximum adsorption capacity was 55.87 mg/g for RR31 on SC300 and 41.84 mg/g for RR2 on SC300. Figures 28, 29, 30, 31, 32, 33 show the linear Langmuir isotherm plot for the reactive dyes on the three different activated carbons. Weber and Chakraborti [114] expressed the essential characteristics and the feasibility of the Langmuir isotherm in terms of a dimensionless constant separation factor or equilibrium parameter  $R_L$ , which is defined by Hall et al. [40].

$$R_L = \frac{1}{1 + bC} \quad (5.2)$$

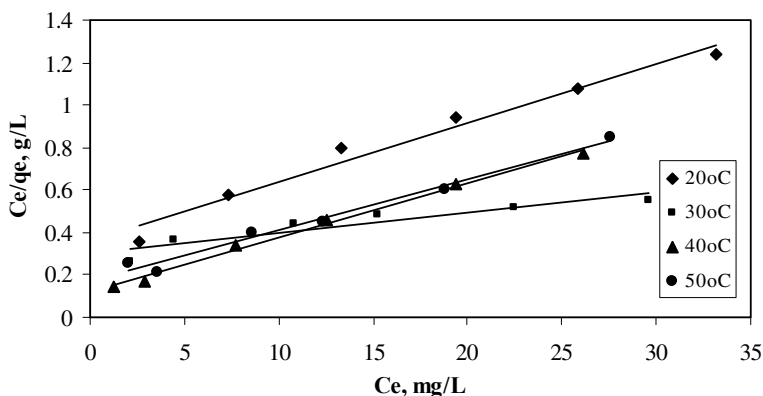


**Fig. 28** Langmuir isotherm for the adsorption of dye Reactive Red 31 using CAC for different temperatures at 120 rpm and pH = 7.0

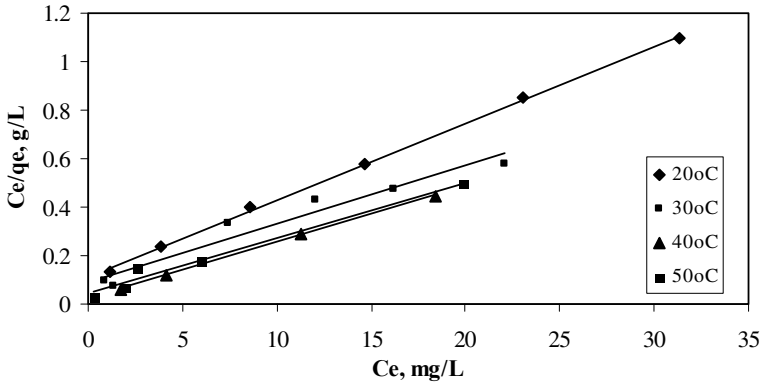


Fig. 29 Langmuir isotherm for the adsorption of dye Reactive Red 2 using CAC for different temperatures at 120 rpm and pH = 7.0

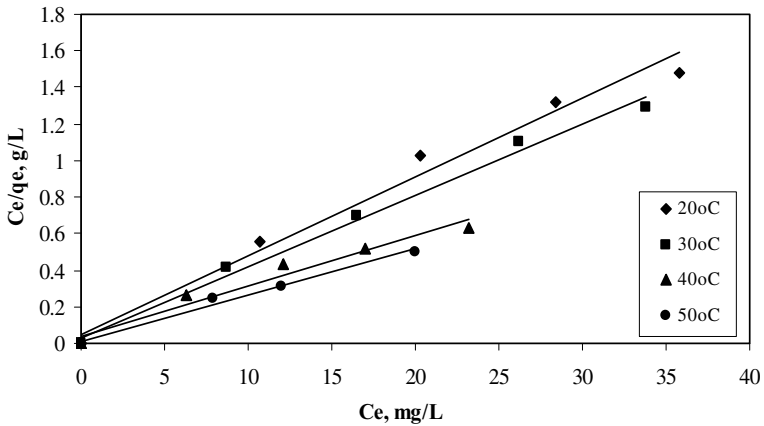
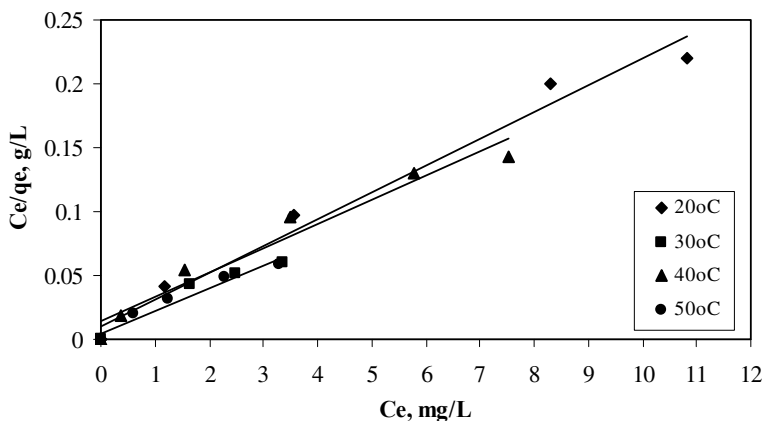
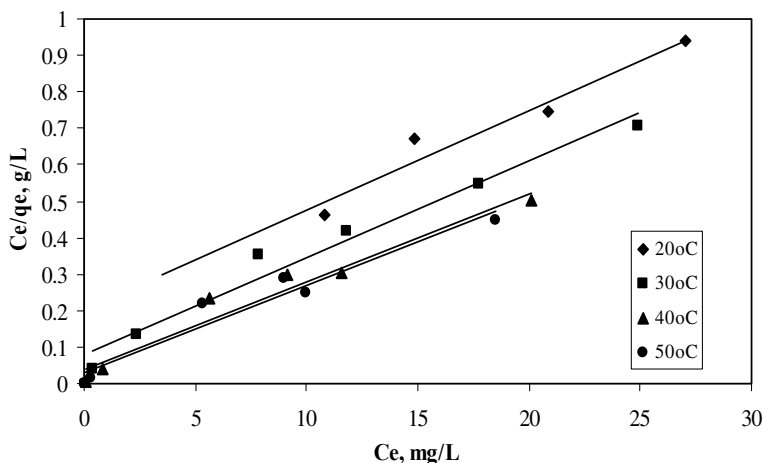


Fig. 30 Langmuir isotherm for the adsorption of dye Reactive Red 31 using SC600 for different temperatures at 120 rpm and pH = 7.0

where  $C$  is the highest initial concentration of the adsorbate and  $b$  is the Langmuir constant (mg/L).  $R_L$  value indicates the shape of the isotherm such that  $R_L > 1$  indicates unfavourable isotherm;  $R_L = 1$  indicates linear isotherm;  $0 < R_L < 1$  indicates favourable isotherm; and  $R_L = 0$  indicates irreversible isotherm. The range of  $R_L$  value is significant in defining the nature of adsorption. The  $R_L$  values determined from Tables 17 and 18 lie between 0 and 1, indicating that the adsorption systems were favourable for both the dyes (Reactive Red 31 and Reactive Red 2) using different adsorbents (CAC, SC600 and SC300).



**Fig. 31** Langmuir isotherm for the adsorption of dye Reactive Red 2 using SC600 for different temperatures at 120 rpm and pH = 7.0



**Fig. 32** Langmuir isotherm for the adsorption of dye Reactive Red 31 using SC300 for different temperatures at 120 rpm and pH = 7.0

### 5.3.2 Effect of Temperature

Various textile dye effluents are produced at relatively high temperatures. In practical application, temperature plays an important factor in the removal of dyes. To determine the nature of adsorption process as either endothermic or exothermic in nature, adsorption studies of reactive dyes onto the activated carbon adsorbents were carried out at 20 °C (293 K), 30 °C (303 K), 40 °C (313 K) and 50 °C (323 K) for an initial dye concentration of 10 mg/L to 60 mg/L, pH of 7.0 and an adsorbent dose of 1 g/100 mL at their respective equilibrium times. The adsorption of dyes increased

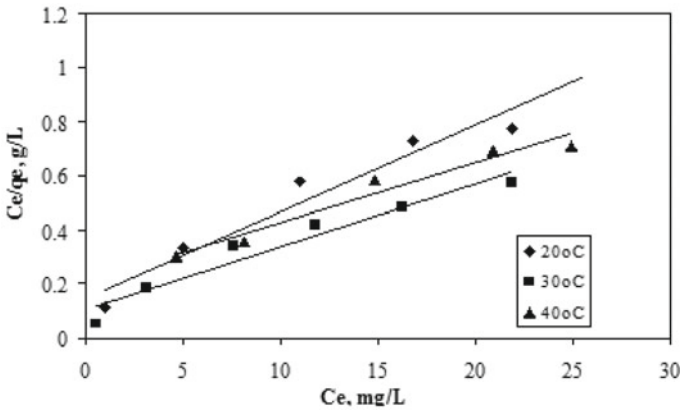


**Fig. 33** Langmuir isotherm for the adsorption of dye Reactive Red 2 using SC300 for different temperatures at 120 rpm and pH = 7.0

with increase in temperature for all the adsorbents as shown in Fig. 34 indicating that the adsorption process was endothermic in nature. The effect of temperature on batch adsorption studies can be correlated based on the thermodynamic studies (Fig. 34).

The apparent heat per net enthalpy ( $\Delta H^0$ ) of adsorption is related to the Langmuir constant ( $b$ ). The Langmuir constant ( $b$  or  $k_d$ ) is related to energy consumption and the ratio of adsorption rate to desorption rate [23]. In thermodynamics equation, change of Gibbs free energy ( $\Delta G^0$  in kJ/mol) was calculated by using Eqs. (5.3) and (5.4). Change in entropy ( $\Delta S^0$  in J/Kmol) and change in enthalpy ( $\Delta H^0$  in kJ/mol) for the adsorption were calculated and estimated by using Eq. (5.5).  $K_d$  represents equilibrium distribution constant, and  $R$  is the universal gas constant (8.314 J/Kmol).

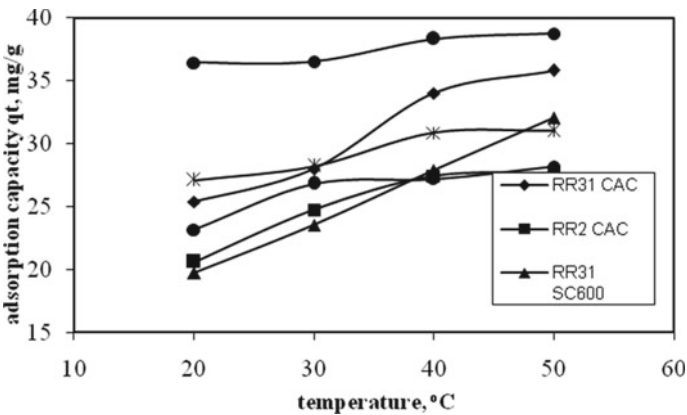


**Fig. 34** Effect of temperature at 40 mg/L of adsorbate concentration at 120 rpm and pH = 7.0



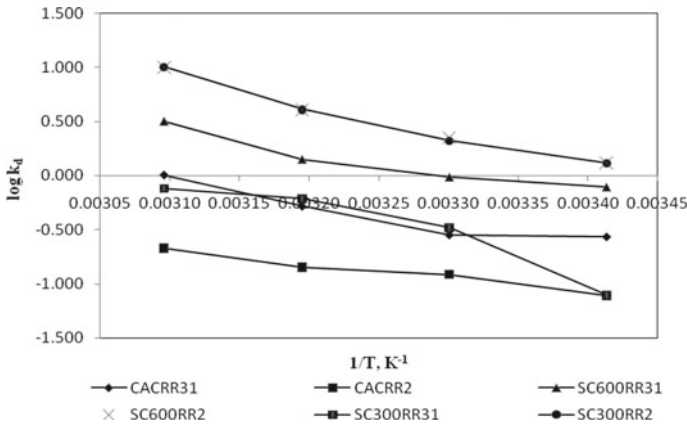


**Fig. 35** Van't Hoff plots of adsorption of reactive dyes onto activated carbons at different temperatures, pH = 7.0 and carbon dosage = 1 g/mL

$$\Delta G^0 = -2.303RT \log K_d \tag{5.3}$$

$$\Delta G^0 = \Delta H^0 - T \Delta S^0 \tag{5.4}$$

$$\ln K_d = \frac{-\Delta H^0}{2.303R} \left( \frac{1}{T} \right) + \frac{\Delta S^0}{2.303R} \tag{5.5}$$

If the equilibrium constants for an adsorption reaction at different temperatures are known, the standard enthalpy changes for adsorption can be estimated from the slope of a Van't Hoff plot ( $\log K_d$  vs.  $1/T$  in Fig. 35). Thus, the enthalpy and entropy changes ( $\Delta H^0$  and  $\Delta S^0$ ) are calculated from the slope and intercept of the Van't Hoff plot (Fig. 35). The thermodynamic parameters for the adsorption of RR31 and RR2 reactive dyes in aqueous solutions of CAC, SC600 and SC300 at various temperatures are summarized in Tables 19 and 20. The positive values of  $\Delta H^0$  indicated the endothermic nature of the chemical adsorption process. The free energy of the process at all temperatures for RR31 adsorption onto CAC, SC600 and SC300 adsorbents was positive. The positive Gibbs free energy indicated the reluctance in adsorption of RR31 onto different activated carbons due to the diazo nature of Reactive Red 31 (RR31) with more number of  $\text{SO}_3^{3-}$  ions. The negative  $\Delta G^0$  value observed in the adsorption of RR2 onto SC600 and SC300 indicated the spontaneous adsorption of the Reactive Red 2. The positive values of  $\Delta S^0$  observed in the adsorption process showed the increased randomness at the carbon–dye solution interface [41].

**Table 19** Thermodynamic parameters for the adsorption of Reactive Red 31 onto commercial and sludge-based activated carbons

Adsorbent	Temperature (K)	$\Delta G^0$ (kJ/mol)	$\Delta H^0$ (kJ/mol)	$\Delta S^0$ (J/K mol)	$R^2$
CAC RR31	293	2.875	3.772	-2.776	0.903
	303	2.903			
	313	2.931			
	323	2.959			
SC600 RR31	293	7.707	3.810	-12.063	0.919
	303	7.586			
	313	7.465			
	323	7.345			
SC300 RR31	293	4.142	6.146	-6.204	0.878
	303	4.204			
	313	4.267			
	323	4.329			

**Table 20** Thermodynamic parameters for the adsorption of Reactive Red 2 onto commercial and sludge-based activated carbons

Adsorbent	Temperature (K)	$\Delta G^0$ (kJ/mol)	$\Delta H^0$ (kJ/mol)	$\Delta S^0$ (J/K mol)	$R^2$
CAC RR2	293	5.969	2.623	-10.359	0.970
	303	5.865			
	313	5.762			
	323	5.658			
SC600RR2	293	-53.345	5.285	181.515	0.976
	303	-51.530			
	313	-49.714			
	323	-47.899			
SC300 RR2	293	-2.076	5.648	23.915	0.980
	303	-1.837			
	313	-1.598			
	323	-1.359			

### 5.3.3 Freundlich Isotherm

The Freundlich isotherm describes equilibrium on heterogeneous adsorbent surfaces and hence does not assume monolayer capacity as in Langmuir plot. It relates the adsorbed concentration to the power functions of solute concentration. One of the limitations of the Freundlich model is that the amount of adsorbed solute increases indefinitely with the concentration of solute in the solution.

This empirical equation takes the form as Eq. 5.6:

$$q_e = K_F C_e^{1/n} \quad (5.6)$$

The logarithmic form of the equation is represented in Eq. 5.7

$$\log(q_e) = \log K_F + \frac{1}{n} \log(C_e) \quad (5.7)$$

where  $K_F$  and  $n$  are the Freundlich constants of the system.  $K_F$  and  $n$  are the indicators of the adsorption capacity and adsorption intensity, respectively. The slope and the intercept of the linear Freundlich equation are equal to  $1/n$  and  $\ln K_F$ , respectively. It has been shown that  $n$  values between 1 and 10 represent good adsorption potential of the adsorbent. The values of the Freundlich constants at different temperatures are shown in Tables 21 and 22.

The experimental data showed correlation coefficients ( $R^2$ ) close to unity. But there was no linear correlation between the Freundlich constants ( $K_F$  and  $n$ ) and the adsorption capacities shown in Tables 21 and 22. Hence, the adsorption of the solute concentration was not evident. Though the  $n$  values were between 0 and 1, the adsorption process showed the complex nature of the adsorption of reactive dyes onto the activated carbon adsorbents. The experimental data were well suited to the Langmuir isotherm than the Freundlich model. Therefore, the adsorptions of the reactive dyes under consideration are linear in Langmuir isotherm plot.

**Table 21** Freundlich isotherm constants and correlation coefficients for adsorption of RR31 on commercial activated carbon and tannery sludge-developed activated carbons

Temperature (°C)	Adsorbents								
	CAC RR31			SC600 RR31			SC300 RR31		
	$N$	$K_F$	$R^2$	$N$	$K_F$	$R^2$	$n$	$K_F$	$R^2$
20	1.965	4.549	0.999	2.801	6.671	0.968	0.869	1.119	0.933
30	1.374	4.414	0.996	7.348	15.844	0.894	3.263	12.995	0.989
40	1.960	6.915	0.908	2.899	12.290	0.981	4.529	19.696	0.964
50	2.375	9.138	0.950	4.268	20.271	0.871	5.631	24.047	0.916

**Table 22** Freundlich isotherm constants and correlation coefficients for adsorption of RR2 on commercial activated carbon and tannery sludge-developed activated carbons

Temperature (°C)	Adsorbents								
	CAC RR2			SC600 RR2			SC300 RR2		
	$N$	$K_F$	$R^2$	$N$	$K_F$	$R^2$	$n$	$K_F$	$R^2$
20	6.485	3.294	26.940	2.649	35.616	0.997	1.520	5.000	0.962
30	2.843	2.773	15.999	2.693	23.755	0.978	2.573	8.496	0.969
40	2.818	2.502	12.203	4.488	27.511	0.962	2.705	11.516	0.987
50	3.062	2.247	9.457	1.816	28.983	1.000	1.835	86.125	0.975

## 5.4 Adsorption Kinetics

The prediction of batch sorption kinetics gives the most important information for designing batch sorption systems. Adsorption kinetics explains how fast the sorption process occurs and also the factors affecting the reaction rate. It is important to establish the time dependence of adsorption systems under various process conditions. The principle behind the adsorption kinetics involves the search for a best model that well represents the experimental data. Numerous kinetic models have been used for describing the reaction order of the system and to express the mechanism of solute sorption onto a sorbent. In order to investigate the mechanism of sorption, characteristic constants of sorption were determined using two simplest kinetic models, a pseudo-first-order equation of Lagergren based on solid capacity and a pseudo-second-order equation based on solid phase sorption [46, 45].

A linear form of pseudo-first-order model Eq. (5.8) is:

$$\log(q_e - q) = \log(q_e) - \frac{k_{1,ad}}{2.303}t \quad (5.8)$$

where  $q_e$  is the amount of adsorbed dye at equilibrium (mg/g),  $q$  is the amount of dye adsorbed at time  $t$  (min) ( $\text{mgg}^{-1}$ ) and  $k_{1,ad}$  is the rate constant of first-order sorption ( $\text{min}^{-1}$ ). A linear plot of  $\log(q_e - q)$  against time ( $t$ ) allows obtaining the rate constant. The rate constants for the pseudo-first-order model were calculated from the slopes and intercepts of the plots from Eq. (5.8) and are illustrated in Figs. 36, 37, 38, 39 and 40. The  $q_e$  values increased with increase in concentration for all the dye adsorption onto the different activated carbons. The correlation coefficients ( $R^2$ ) were closer to unity except for the adsorption of RR2 onto SC300. In case of the pseudo-first-order kinetic model, the calculated  $q_e$  was not equal to the experimental  $q_e$  suggesting the insufficiency of the model to fit the kinetic data for the initial

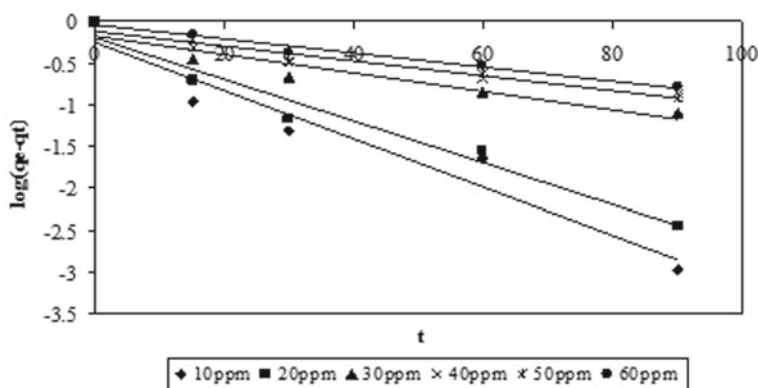


**Fig. 36** First-order Lagergren plot for the adsorption of dye Reactive Red 2 using SC600 at different initial dye concentrations at 120 rpm and pH = 7.0

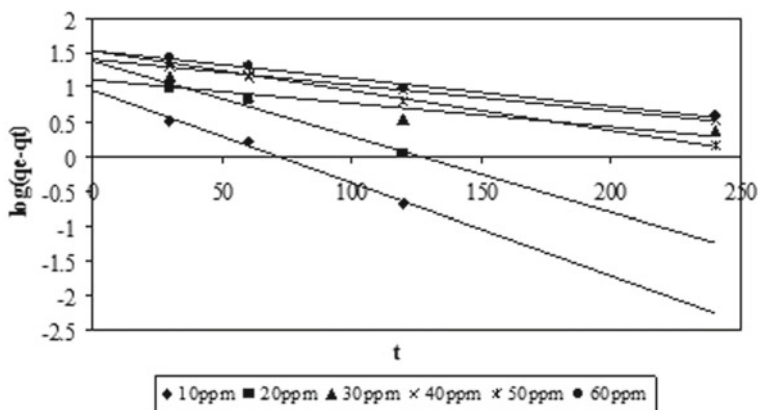


**Fig. 37** First-order Lagergren plot for the adsorption of dye Reactive Red 31 using CAC at different initial dye concentrations at 120 rpm and pH = 7.0

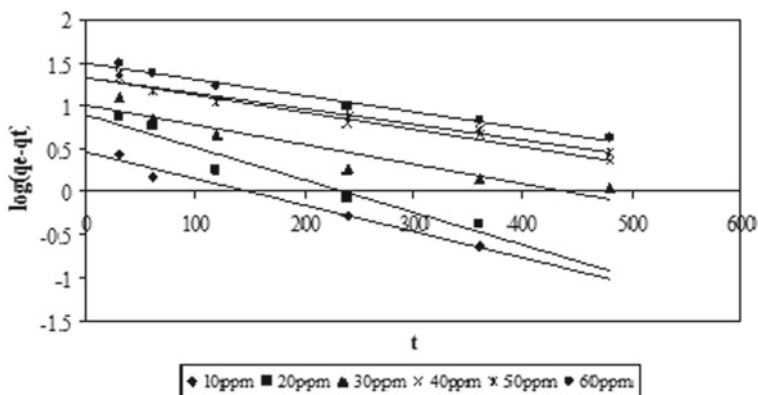


**Fig. 38** First-order Lagergren plot for the adsorption of dye Reactive Red 2 using SC600 at different initial dye concentrations at 120 rpm and pH = 7.0

concentrations examined. The reason for these differences in the  $q_e$  values was due to a time lag, possibly as a result of a boundary layer or an external resistance controlling the beginning of the sorption process [75]. Existing literature shows that the pseudo-first-order model does not fit the kinetic data well over the entire contact time range [112]. Thus, a good linearity of the Lagergren plots is no guarantee that the interactions will follow first-order kinetics. Contrary to the pseudo-first-order model, pseudo-second-order model predicts the sorption behaviour over the entire study range.

The pseudo-second-order model is based on the sorption capacity of the solid phase. The pseudo-second-order kinetic model is linearly expressed as

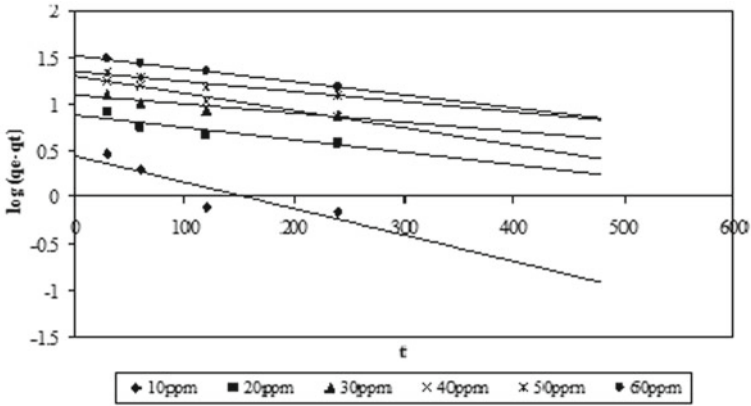


**Fig. 39** First-order Lagergren plot for the adsorption of dye Reactive Red 31 using SC300 at different initial dye concentrations at 120 rpm and pH = 7.0

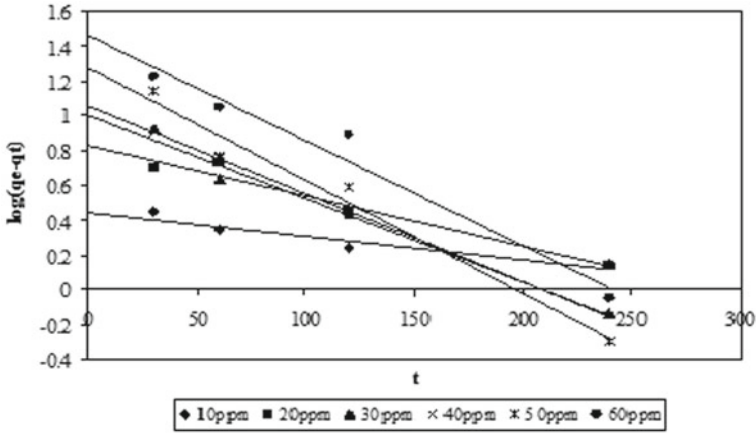


**Fig. 40** First-order Lagergren plot for the adsorption of dye Reactive Red 2 using CAC at different initial dye concentrations at 120 rpm and pH = 7.0

$$\frac{t}{q} = \frac{1}{k_{2,ad}q_e^2} + \frac{1}{q_e}t \tag{5.9}$$

where  $k_{2,ad}$  is the rate constant of the second-order sorption ( $\text{min}^{-1}$ ) and is illustrated in Figs. 41, 42, 43, 44 and 45. The adsorption capacity ( $q_e$ ) at equilibrium increased with increase in concentration as first-order kinetic models. The rate constants ( $q_e$  and  $k_d$ ) of the pseudo-second-order kinetic model were higher than that of the pseudo-first-order kinetic model. The correlation coefficients ( $R^2$ ) were also higher in the pseudo-second-order kinetic models. Hence, the second-order correlation can

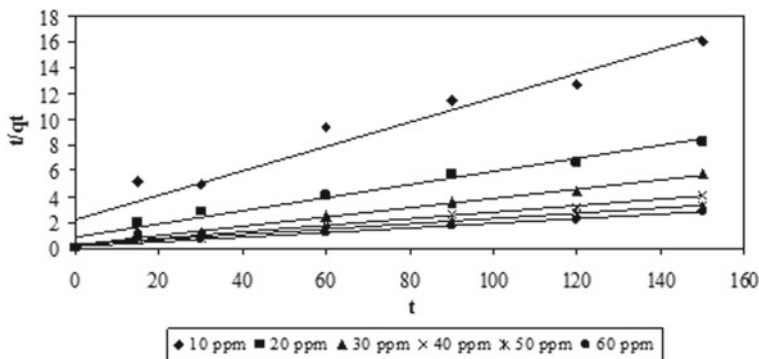


**Fig. 41** Second-order Lagergren plot for the adsorption of dye Reactive Red 31 using SC300 at different initial dye concentrations at 120 rpm and pH = 7.0

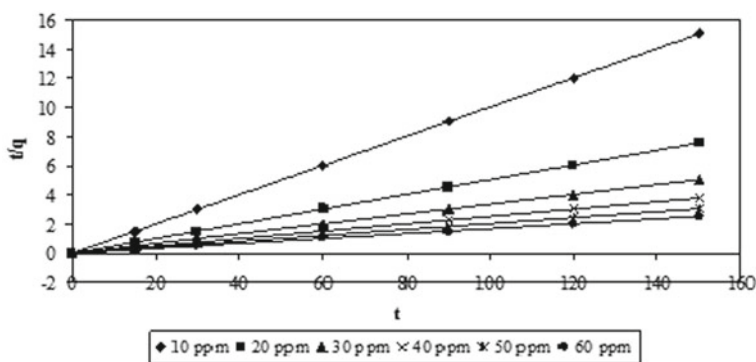


**Fig. 42** Second-order Lagergren plot for the adsorption of dye Reactive Red 2 using SC600 at different initial dye concentrations at 120 rpm and pH = 7.0

best describe the kinetics and the adsorption capacity is much closer to the experimental value. These suggest that the pseudo-second-order adsorption mechanism was predominant for the sorption of the reactive dyes onto the activated carbon. This indicated that adsorption of Reactive Red dyes onto the activated carbons, CAC, SC600 and SC300, is controlled by chemical processes. Similar phenomenon was observed in relation to the adsorption of Reactive Red 120 [9, 118].

## 6 Summary

In this chapter, development and effluent treatment process of two major industrial sectors, tannery and textile industries, are discussed. Tannery sludge generated as end product of effluent treatment is discharged as unused by-product. The development

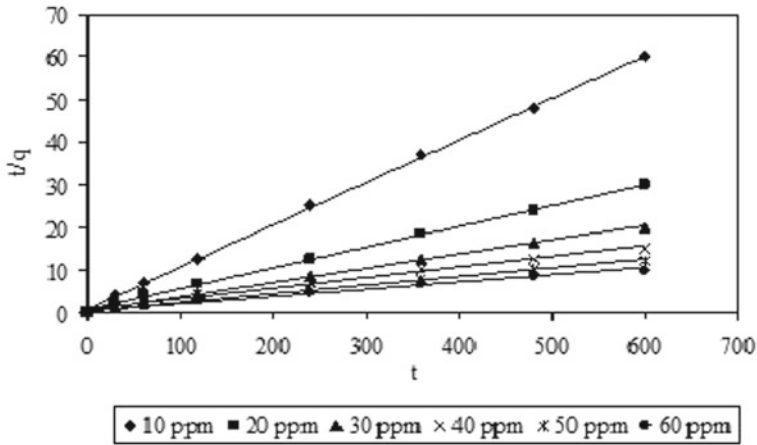


Fig. 43 Second-order Lagergren plot for the adsorption of dye Reactive Red 31 using CAC at different initial dye concentrations at 120 rpm and pH = 7.0

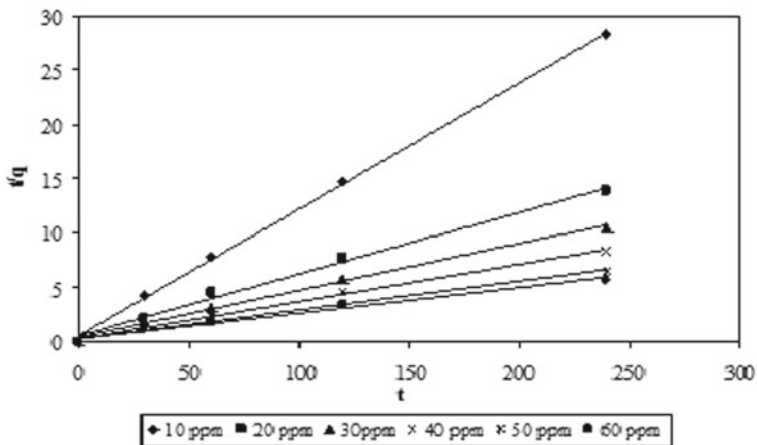
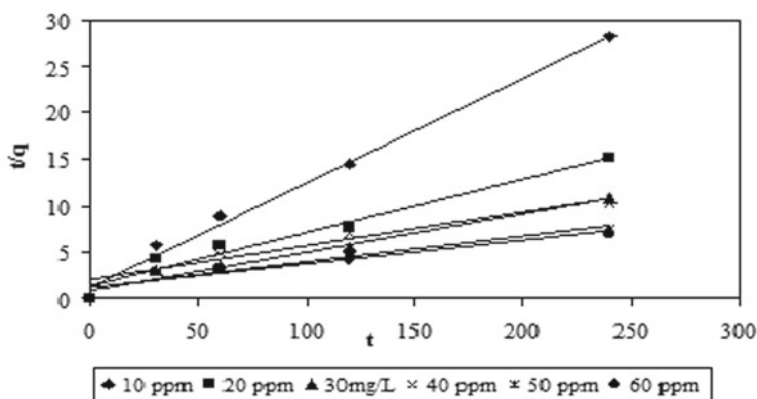


Fig. 44 Second-order Lagergren plot for the adsorption of dye Reactive Red 2 using SC300 at different initial dye concentrations at 120 rpm and pH = 7.0

of raw tannery sludge into a useful resource and an activated carbon through physical and chemical activation under various activation conditions was discussed. The strong acid activation using sulphuric acid as a chemical agent resulted in the lower burn-off and higher yield percentage. The burn-off of SC600 and SC300 was 29% and 26%, and the yield percentages of the two carbons were 71% and 74%, respectively. The chemically activated sludge carbon showed the development and distribution of micropores compared to the physical activation of the sludge carbon. Of the various





**Fig. 45** Second-order Lagergren plot for the adsorption of dye Reactive Red 31 using SC600 at different initial dye concentrations at 120 rpm and pH = 7.0

carbons developed from the raw tannery sludge, two carbons were chosen based on their carbon content and the particle size (SC600 and SC300).

The combined activation on the sludge has led to the development of micropores and mesopores on the external surface of the carbons. Also, the presence of active sites and a layer of gaps and cavities confirmed that the sludge-developed carbons favoured adsorption. The surface areas of the various carbons were in the order of  $S_{CAC}$ :  $693.35 \text{ m}^2/\text{g} > S_{SC300}$ :  $212.32 \text{ m}^2/\text{g} > S_{SC600}$ :  $188.205 \text{ m}^2/\text{g}$ , respectively. The pore size distributions were dominated with mesopores, and micropore was also uniformly distributed. The micropore widths of the activated carbons were  $5.15 \text{ \AA}$  and  $5.07 \text{ \AA}$ , and the mesopore widths were  $19.77 \text{ \AA}$  and  $19.73 \text{ \AA}$ , respectively. The cationic nature of the developed activated sludge carbons was confirmed by the Boehm titration methods with higher acidic functional groups. The higher surface area of the sludge carbons obtained by the BET isotherm plot suggested the application of the produced carbon for adsorption of dyes. The Langmuir isotherm with higher correlation coefficients best suited compared to the Freundlich isotherm. The maximum monolayer adsorption capacities were  $55.87 \text{ mg/g}$  and  $41.49 \text{ mg/g}$  for adsorbents SC300 on RR31 and RR2, respectively. The application of sludge carbons produced in the removal of reactive dye solution and their batch kinetics showed that pseudo-second-order adsorption mechanism was predominant for the sorption of the reactive dyes onto the activated carbon indicating the adsorption of Reactive Red dyes onto the activated carbons: CAC, SC600 and SC300 to be controlled by chemical processes.

## Appendix

This appendix enumerates a short description of the articles (journals/books/chapters/standards) referred for relevant data in preparing this chapter including tables. All the graphs mentioned were the worked out results carried over by the author.

S. No.	Journal title	Volume/issue article title	Year of publication	Page no.	Content referred in the current chapter
1	Minimal National Standard for Tanneries: CPCB, New Delhi	COINDS/35	1991–92		Table 1: Characteristics of wastewater
2	Central Leather Research Institute, Chennai, India				Table 2: Characteristics of tannery effluent
3	A Critical Review. Journal of Chemical Eng. & Process Technology	5	2014	182	Table 7: Properties of wastewater from textile chemical processing
4	Journal of Chemistry	2020	2020	1–13	Table 8: Classification of wastewater treatment process
5	Reviews in Environ. Sci. and Biotech.	4	2005	245–273	Table 9: Advantages and limitations of physical/chemical decolourization technologies
6	Bioresour. Technol.	97	2006	1061–1085	
7	Reviews in Environ. Sci. and Biotech.	4	2005	245–273	Table 10: Advantages and limitations of biological decolourization technologies

## References

1. Ahmadpour A, Do DD (1997) The preparation of activated carbon from macadamia nutshell by chemical activation. Carbon 12:1723–1732

2. Al-Degs YS, Khraisheh MA, Allen SJ, Ahmad M (1999) Adsorption of remazol reactive black B on activated carbon: adsorption on H and L carbon. *Adv Environ Res* 3:132–138
3. Al-Degs YS, Khraisheh MA, Allen SJ, Ahmad M (2001) Sorption behaviour of cationic and anionic dyes from aqueous solution on different types of activated carbons. *Sep Sci Technol* 36:91–102
4. Al-Duri B, McKay G, El Geundi MS, Abdul Wahab MZ (1990) Three resistance transport model for dye adsorption onto bagasse pith. *J Environ Eng* 116:487–502
5. Al-Sakkaf BM, Nasreen S, Ejaz N (2020) Degradation pattern of textile effluent by using bio and sono chemical reactor. *J Chem* 2020:1–13
6. Allen SJ, Gan Q, Matthews R, Johnson PA (2003) Comparison of optimised isotherm models for basic dye adsorption by kudzu. *Bioresour Technol* 88:143–152
7. Amin NK (2008) Removal of reactive dye from aqueous solutions by adsorption onto activated carbons prepared from sugarcane bagasse pith. *Desalination* 223:152–161
8. Anjaneyulu Y, Sreedhara Chary N, Samuel Sumanraj D (2005) Decolourization of industrial effluents—available methods and emerging technologies—a review. *Rev Environ Sci Biotechnol* 4:245–273
9. Annadurai G, Ling LY, Lee J-F (2008) Adsorption of reactive dye from an aqueous solution by chitosan: isotherm, kinetic and thermodynamic analysis. *J Hazard Mater* 152:337–346
10. Aravindhan R, Madhan B, Rao JR, Nair BU, Ramasami T (2004) Bioaccumulation of chromium from tannery wastewater: an approach for chrome recovery and reuse. *Environ Sci Technol* 38:300–306
11. Atar N, Olgun A (2007) Removal of Acid Blue 062 on aqueous solution using calcinated colemanite ore waste. *J Hazard Mater* 146:171–179
12. Bansal RC, Donnet J, Stoeckli HF (1988) *Active carbon*. Dekker, New York
13. Bhatnagar A, Jain AK (2005) A comparative adsorption study with different industrial wastes as adsorbents for the removal of cationic dyes from water. *J Colloid Interface Sci* 281:49–55
14. Bhattacharyya KG, Sharma A (2003) Adsorption characteristics of the dye. *Brill Green Neem Leaf Powder Dyes Pigments* 57:211–222
15. Chaudhary AJ, Ganguli B, Girmes SM (2002) The use of chromium waste sludge for the adsorption of colour from dye effluents streams. *J Chem Biotech* 77:767–770
16. Crini G (2006) Non-conventional low-cost adsorbents for dye removal: a review. *Bioresour Technol* 97:1061–1085
17. Cureda-Correa EM, Diaz-Diez MA, Macias-Gracia A, Ganan-Gomez J (2006) Preparation of activated carbons previously treated with sulfuric acid—a study of their adsorption capacity in solution. *Appl Surface Sci* 252:6042–6045
18. Dabrowski A (2001) Adsorption—from theory to practice. *Adv Coll Interface Sci* 93:135–224
19. Dastgheib SA, Rockstraw DA (2001) Pecan shell activated carbon: synthesis, characterization, and application for the removal of copper from aqueous solutions. *Carbon* 39:1849–1855
20. Dincer AR, Gunes Y (2007) Comparison of activated carbon and bottom ash for removal of reactive dye from aqueous solution. *Bioresour Technol* 98:834–839
21. Dincer AR, Gunes Y, Karakaya N (2007) Coal-based bottom ash (CBBA) waste material as adsorbent for removal of textile dyestuffs from aqueous solution. *J Hazard Mater* 141:529–535
22. El-Sheikh AH, Newman AP, Al-Daffae HK, Phull S, Cresswell N (2004) Characterization of activated carbon prepared from a single cultivar of Jordanian olive stone by chemical and physicochemical techniques. *J Anal Appl Pyrolysis* 71:151–154
23. Faust SD, Aly OM (1987) *Adsorption process for water treatment*. Butterworths, Boston, pp 14–22
24. Forgacs E, Cserhati T, Oros G (2004) Removal of synthetic dyes from wastewaters: a review. *Environ Int* 30:953–971
25. Freundlich HMF (1906) Over the adsorption in solution. *J Phys Chem* 57:385–470
26. Fu Y, Viraraghavan T (2001) Fungal decolorization of dye wastewaters: a review. *Biores Technol* 79:251–262
27. Galatik A, Duda J, Minarik L (1988) Pressure hydrolysis of leather waste with sodium hydroxide. *Czech Patent CS* 252:382

28. Geethakarthis A, Phanikumar BR (2011) Adsorption of reactive dyes from aqueous solutions by tannery sludge developed activated carbon: Kinetic and equilibrium studies. *Int J Environ Sci Technol* 8:561–570
29. Geethakarthis A, Phanikumar BR (2011) Industrial sludge based adsorbents/industrial by-products in the removal of reactive dyes—a review. *Int J Water Resources Environ Eng* 3:1–9
30. Geethakarthis A, Phanikumar BR (2011a) Adsorption of two azo reactive dyes by tannery sludge activated carbon: effect of temperature and pH. In: International conference on environmental science and development (ICESD-2011), vol 4, pp 154–157
31. Gergova K, Petrov N, Minkova V (1993) A comparison of adsorption characteristics of various activated carbons. *J Chem Technol Biotechnol* 56:77–82
32. Ghaly AE, Ananthashankar R, Alhattab M, Ramakrishnan VV (2014) Production, characterization and treatment of textile effluents: a critical review. *J Chem Eng Process Technol* 5:182
33. Girgis BS, El-Hendawy AA (2002) Porosity development in activated carbons obtained from date pits under chemical activation with phosphoric acid. *Microporous Mesoporous Mater* 52:105–117
34. Goutam C, Macdonald DG, Bakhshi NN, Mohammadzadeh JSS, Dalai AK (2006) Preparation and characterization of chars and activated carbons from Saskatchewan lignite. *Fuel Processing Technol* 87:997–1006
35. Grag VKC, Amita M, Kumar R, Gupta R (2004) Basic dye (methylene blue) removal from simulated wastewater by adsorption using Indian rosewood sawdust: a timber industry waste. *Dyes Pigments* 63:243–250
36. Gregorio C, Lichtfouse E, Wilson LD, Morin-Crini N (2019) Conventional and non-conventional adsorbents for wastewater treatment. *Environ Chem Lett* 17:195–213
37. Gupta VK, Ali I Suhas, Mohan D (2003) Equilibrium uptake and sorption dynamics for the removal of basic dye (basic red) using low-cost adsorbents. *J Colloid Interface Sci* 265:257–264
38. Gupta VK, Mittal A, Krishnan L, Gajbe V (2004) Adsorption kinetics and column operations for the removal and recovery of malachite green from waste water using bottom ash. *Sep Purif Technol* 40:87–96
39. Gupta VK, Mohan D, Sharma S, Sharma M (2000) Removal of basic dyes (rhodamine B and methylene blue) from aqueous solutions using bagasse fly ash. *Sep Sci Technol* 35:2097–2113
40. Hall KR, Eagleton LC, Acrivos A, Vermeulen T (1966) Pore and solid diffusion kinetics in fixed bed absorption under constant pattern conditions. *Ind Eng Chem Fundam* 5:212–223
41. Hameed BH, Ahmad AA, Aziz N (2009) Adsorption of reactive dye on palm-oil industry waste: equilibrium, kinetic and thermodynamic studies. *Desalination* 247:551–560
42. Hayashi J, Kazehaya A, Muroyama K, Paul Watkinson A (2000) Preparation of activated carbon from lignin by chemical activation. *Carbon* 38:1873–1878
43. Helleur R, Popovic N, Ikura M, Stanculescu M, Liu D (2001) Characterization and potential applications of pyrolytic char from ablative pyrolysis of used tires. *J Anal Appl Pyrolysis* 58:813–824
44. Henry CL (1991) Nitrogen dynamics of pulp and paper sludge amendment to forest soils. *Water Sci Technol* 24:417–423
45. Ho YS (2001) Sorption studies of acid dye by mixed sorbents. *Adsorption* 7:139–147
46. Ho YS, McKay G (1999) Pseudo-second order model for sorption processes. *Process Biochem* 34:451–465
47. Ho YS, Porter JF, McKay G (2002) Equilibrium isotherm studies for the sorption of divalent metal ions onto peat: copper, nickel and lead single component systems. *Water Air Soil Pollut* 141:1–33
48. Hojamberdiev M, Kameshima Y, Nakajima A, Okada K, Kadirova Z (2008) Preparation and sorption properties of materials from paper sludge. *J Hazard Mater* 151:710–719
49. Hourieh MA, Alaya MN, Youssef AM (1997) Carbondioxide adsorption and decolorizing power of activated carbons prepared from pistachio shells. *Adsorpt Sci Technol* 15:300–303

50. Hu TL (1996) Removal of reactive dyes from aqueous solution by different bacterial genera. *Water Sci Technol* 34:89–95
51. Ibarra JV, Moliner R, Palacios JM (1991) Catalytic effects of zinc chloride in the pyrolysis of spanish high sulfur coals. *Fuel* 70:727–732
52. Jagtoyen M, Thwaites M, Stencil J, McEnaney B, Debyshire F (1992) Adsorbent carbon synthesis from coals by phosphoric acid activation. *Carbon* 30:1089–1096
53. Janos P, Buchtova H, Ryznarova M (2003) Sorption of dyes from aqueous solutions onto fly ash. *Water Res* 37:4938–4944
54. John Kennedy L, Judith Vijaya L, Kayalvizhi K, Sekaran G (2007) Adsorption of phenol from aqueous solutions using mesoporous carbon prepared by two-stage process. *Chem Eng J* 132:279–287
55. Juang RS, Tseng RL, Wu FC, Lee SH (1997) Adsorption behaviour of reactive dyes from aqueous solutions on chitosan. *J Chem Technol Biotechnol* 70:391–399
56. Kanagaraj J, Velappan KC, Chandra Babu NK, Sadulla S (2006) Solid wastes generation in the leather industry and its utilization for cleaner environment—a review. *J Sci Ind Res* 65(7):541–548
57. Kannan N, Sundaram MM (2001) Kinetics and mechanism of removal of methylene blue by adsorption on various carbons—a comparative study. *Dyes Pigments* 51:25–40
58. Kara S, Aydinera C, Demirbas E, Kobya M, Dizge N (2007) Modeling the effects of adsorbent dose and particle size on the adsorption of reactive textile dyes by fly ash. *Desalination* 212:282–293
59. Karifala K, Qiu J, Zhao Z, Cheng Y, Bandosz TJ (2008) Development of surface porosity and catalytic activity in metal sludge/waste oil derived adsorbents: effect of heat treatment. *Chem Eng J* 138:155–165
60. Kaul SN, Nandy T, Szpyrkowicz L, Gautam A, Khanna DR (2005) Waste water management with special reference to tanneries. Discovery Publishing House, New Delhi
61. Kaushik P, Malik A (2009) Fungal dye decolourization: recent advances and future potential. *Environ Int* 35:127–141
62. Khare SK, Panday KK, Srivastava RM, Singh VN (1987) Removal of victoria blue from aqueous solution by fly ash. *J Chem Technol Biotechnol* 38:99–104
63. Kim Y, Kim C, Choi I, Rengraj S, Yi J (2004) Arsenic removal using mesoporous alumina prepared via a templating method. *Environ Sci Technol* 38:924–931
64. Lagergren S (1898) About the theory of so-called adsorption of soluble substances. *Vetenskapsakad Handl* 24:1–39
65. Laine J, Calafat A, Labady M (1989) Preparation and characterization of activated carbons from coconut shells impregnated with phosphoric acid. *Carbon* 27:191–195
66. Langmuir I (1918) Adsorption of gases on plain surfaces of glass mica platinum. *J Am Chem Soc* 40:1361–1403
67. Lin YR, Teng H (2002) Mesoporous carbons from waste tire char and their application in wastewater discoloration. *Microporous Mesoporous Mater* 54:167–174
68. Low K, Lee C, Tan B (2000) Quaternized wood as sorbent for reactive dyes. *Appl Biochem Biotechnol* 87:233–245
69. Lua AC, Guo J (2000) Activated carbon prepared from oil palm stone by one-step CO<sub>2</sub> activation for gaseous pollutant removal. *Carbon* 38:1089–1097
70. Lua A, Yang T (2004) Effect of activation temperature on the textural and chemical properties of potassium hydroxide activated carbon prepared from pistachio-nut shell. *J Colloid Interface Sci* 274:594–601
71. Luiz CAO, Goncalves M, Oliveira DQL, Guerreiro MC, Guilherme LRG, Dallago RM (2007) Solid waste from leather industry as adsorbent of organic dyes in aqueous-medium. *J Hazard Mater* 141:344–347
72. Matthews AP, Weber WJ (1977) Predictive model for designing adsorption rates in slurry reactors. *AIChE Symp Ser* 73:91–98
73. McKay G (1982) Adsorption of dyestuffs from aqueous solutions with activated carbon. Part I. Equilibrium and batch contact-time studies. *J Chem Technol Biotechnol* 32:759–772

74. McKay G (1984) Mass transfer processes during the adsorption of solutes in aqueous solutions in batch and fixed bed absorbers. *Chem Eng Res Des* 62:235–246
75. McKay G, Ho YS (1999) The sorption of lead (II) on peat. *Water Res* 33:578–584
76. McKay G (1998) Application of surface diffusion model to the adsorption of dyes on bagasse pith. *Adsorption* 4:361–372
77. McMullan G, Meehan C, Conneely A, Kirby N, Robinson T, Nigam P, Banat IM, Marchant R, Smyth WF (2001) Microbial decolourisation and degradation of textiles dyes. *Appl Microbiol Biotechnol* 56:81–87
78. Mittal A, Krishnan L, Gupta VK (2005) Removal and recovery of malachite green from wastewater using and agricultural waste material, de-oiled soya. *Sep Sci Technol* 43:125–133
79. Mittal A, Kurup (Krishnan) L, Gupta VK (2005) Use of waste materials-bottom ash and de-oiled soya, as potential adsorbents for the removal of Amaranth from aqueous solutions. *J Hazard Mater B* 117:171–178
80. Mohan D, Singh KP, Singh G, Kumar K (2002) Removal of dyes from wastewater using fly ash, a low-cost adsorbent. *Ind Eng Chem Res* 41:3688–3695
81. Molina-Sabio M, Rodriguez-Reinoso F, Caturla F, Selles MJ (1995) Porosity in granular carbons activated with phosphoric acid. *Carbon* 33:1105–1113
82. Moreno-Castilla C, Carrasco-Marin F, Lopez-Ramon MV, Alvarez-Merino MA (2001) Chemical and physical activation of olive-mill waste water to produce activated carbons. *Carbon* 39:1415–1420
83. Motz H, Geiseler J (2001) Products of steel slag an opportunity to save natural resource. *Waste Manage* 21:285–293
84. Murillo R, Navarro MV, Lopez JM, Garcia T, Callen MS, Aylon E, Mastral AM (2004) Activation of pyrolytic tire char with CO<sub>2</sub>: Kinetic study. *J Anal Appl Pyrolysis* 71:945–957
85. Mykola S, Bandosz TJ (2007) Sewage sludge as a single precursor for development of composite adsorbents/catalysts. *Chem Eng J* 128:59–67
86. Namasivayam C, Jeyakumar R, Yamuna RT (1994) Dye removal from wastewater by adsorption on waste Fe(III)/Cr(III) hydroxide. *Waste Manage* 14:643–648
87. Namasivayam C, Sumithra S (2004) Adsorptive removal of catechol on waste Fe(III)/Cr(III) hydroxide: equilibrium and kinetic study. *Ind Eng Chem Res* 43:7581–7587
88. Netpradit S, Thiravetyan P, Towprayoon S (2003) Application of waste metal hydroxide sludge for adsorption of azo reactive dyes. *Water Res* 37:763–772
89. Netpradit S, Thiravetyan P, Towprayoon S (2004) Adsorption of three azo reactive dyes by metal hydroxide sludge: effect of temperature, pH and electrolytes. *J Colloid Interface Sci* 270:255–261
90. Olgun A, Atar N (2009) Equilibrium and kinetic adsorption study of Basic Yellow 28 and Basic Red 46 by a boron industry waste. *J Hazard Mater* 61:148–156
91. Olivares-Marin M, Fernandez-Gonzalez C, Macias-Gracia A, Gomez-Serrano V (2006) Preparation of activated carbons from cherry stones by activation with KOH. *Appl Surf Sci* 252:5980–5983
92. Orfao JJM, Silva AIM, Pereira JCV, Barata SA, Fonseca IM, Faria PCC, Pereira MFR (2006) Adsorption of a reactive dye on chemically modified activated carbons—Influence of pH. *J Colloid Interface Sci* 296:480–489
93. Otero M, Rozada F, Calvo LF, Garcia AI, Moran A (2003) Kinetic and equilibrium modelling of the methylene blue removal from solution by adsorbent materials produced from sewage sludges. *Biochem Eng J* 15:59–68
94. Otowa T, Nojima Y, Miyazaki T (1997) Development of KOH activated high surface area carbon and its application to drinking water purification. *Carbon* 35:1315–1319
95. Ozcan AS, Erdem B, Ozcan A (2004) Adsorption of acid blue 193 from aqueous solutions onto Na-bentonite and DTMA—bentonite. *J Colloid Interface Sci* 280:44–54
96. Pala A, Galiatsatou P, Tokat E, Erkaya H, Israilides C, Arapoglou D (2006) The use of activated carbon from Olive oil mill residue for the removal of colour from textile wastewater. *Eur Water* 13:29–34

97. Park S, Jung W (2003) KOH activation and characterisation of glass fibers supported phenolic resin. *J Colloid Interface Sci* 265:245–250
98. Putshaka JD, Yakubu A, Aliyu Jauro HH, Kolo M (2015) Effect of alkali and acid concentration in extraction of chromium III from tannery soild waste. *Am J Chem Appl* 2(6):89–94
99. Ravikumar MNV, Sridhar TR, Bhavani KD, Dutta PK (1998) Trends in colour removal from textile mill effluents. *Colourage* 40:25–34
100. Robinson T, McMullan G, Marchant R, Nigam P (2001) Remediation of dyes in textile effluent: a critical review on current treatment technologies with a proposed alternative. *Bioresour Technol* 77:247–255
101. Rozada F, Otero M, Moran A, Gracia AI (2005) Activated carbons from sewage sludge and discarded tyres: production and optimization. *J Hazard Mater B* 124:181–191
102. Sanchez AR, Elguezabal AA, Saenz LLT (2001) CO<sub>2</sub> activation of char from *Quercus agrifolia* wood waste. *Carbon* 39:1367–1377
103. Santhy K, Selvapathy P (2006) Removal of reactive dyes from wastewater by adsorption on coir pith activated carbon. *Bioresour Technol* 97:1329–1336
104. Santos SCR, Vilar VJP, Boaventura ARR (2008) Waste metal hydroxide sludge as adsorbent for a reactive dye. *J Hazard Mater* 153:999–1008
105. Shaobin W, Zhu ZH, Coomes A, Haghseresht F, Lu GQ (2005) The physical and surface chemical characteristics of activated carbons and the adsorption of methylene blue from wastewater. *J Colloid Interface Sci* 284:440–446
106. Sharaf SA, Gasmeeled GA, Musa A (2013) Extraction of chromium six from chrome shavings. *Int J Adv Ind Eng* 1:24–27
107. Skodras G, Orfanoudaki T, Kakaras E, Sakelaropoulos GP (2002) Production of special activated carbon from lignite for environmental purposes. *Fuel Process Technol* 77:75–87
108. Spahn H, Schlunder EU (1975) The scale-up of activated carbon columns for water purification, based on results from batch tests—I: theoretical and experimental determination of adsorption rates of single organic solutes in batch tests. *Chem Eng Sci* 30:529–537
109. Stavropoulos GG, Zabaniotou AA (2005) Production and characterization of activated carbons from olive-seed waste residue. *Microporous Mesoporous Mater* 82:79–85
110. Swarnalatha S, Ramani K, Geethakarathi A, Sekaran G (2006) Starved air combustion–solidification/stabilization of primary chemical sludge from a tannery. *J Hazardous Mater B* 137:304–313
111. Tripepi RR, Zhang X, Campbell AG (1996) Use of raw and composted paper sludge as a soil additive or mulch for cottonwood plants. *Comp Sci Util* 4:26–30
112. Vijayaraghavan K, Yeung-Sang Y (2007) Utilization of fermentation waste (*Corynebacterium glutamicum*) for biosorption of Reactive Black 5 from aqueous solution. *J Hazard Mater* 141:45–52
113. Vilar VJP, Botelho CMS, Boaventura RAR (2006) Equilibrium and kinetic modelling of Cd(II) biosorption by algae *Gelidium* and agar extraction algal waste. *Water Res* 40:291–302
114. Weber TW, Chakraborti RK (1974) Pore and Solid diffusion models for fixed bed adsorbents. *J Am Inst Chem Eng* 20:228–238
115. Williams PT, Reed AR (2004) Higher grade activated carbon matting derived from the chemical activation and pyrolysis of natural fibre textile waste. *J Anal Appl Pyrolysis* 71:971–986
116. Won SW, Choi SB, Yun Y-S (2006) Performance and mechanism in binding of Reactive Orange 16 to various types of sludge. *Biochem Eng J* 28:208–214
117. Wang X, Zhu N, Yin B (2008) Preparation of sludge-based activated carbon and its application in dye wastewater treatment. *J Hazard Mater* 153:22–27
118. Yakup Arica M, Gulay Bayramoglu (2007) Biosorption of reactive Red-120 dye from aqueous solution by native and modified fungus biomass preparations of *Lentinus sajor-caju*. *J Hazard Mater* 149:499–507
119. Yalcin N, Sevinc V (2000) Studies of the surface area and porosity of activated carbons prepared from rice husks. *Carbon* 38:1943–1945

120. Yanping GD, Rockstraw A (2007) Physicochemical properties of carbons prepared from pecan shell by phosphoric acid activation. *Bioresour Technol* 98:1513–1521
121. Yu LL, Zhong Q (2006) Preparation of adsorbents made from sewage sludges for adsorption of organic materials from wastewater. *J Hazard Mater B* 137:359–366



# Sustainable Approach on the Treatment of Textile Wastewater Using Membrane Techniques



R. Sivaranjane and P. Senthil Kumar

**Abstract** Membrane technology seems to be the most eminent advancement in recent years. Among the various physical and chemical treatments available for water treatment, membrane separation process has proved to be a very good alternative for water treatment. This technique allows separation process to be carried out without the utilization of heat. Separation is mainly due to the difference in particle size and shape by the application of pressure. Separation process plays a very vital role in chemical industries. Membrane behaves as a barrier between any two bulk phases of separation. Membranes can be broadly classified based on their nature, structure and pore geometry. Various separation process which can be employed for evacuating the dyes present in wastewater. A few such separation processes include ultrafiltration, microfiltration and nanofiltration. Initially, nanofiltration membrane was employed to retrieve water, salts and dye from textile effluent which is highly saline in nature. Inorganic membranes offer a wide range of advantages over the organic ones in terms of their pH and chemical resistance. Membrane technology is widely used because of its cost-effective nature and also due to its easy operation on the contrary. This chapter will highlight about the overview of the membrane separation process, the various types of separation techniques and the application of membranes for the expulsion of dye from wastewater.

**Keywords** Dye removal · Microfiltration · Nanofiltration · Reverse osmosis · Ultrafiltration · Reverse osmosis

---

R. Sivaranjane  
Department of Chemical Engineering, St. Joseph's College of Engineering, Chennai 600119, India

P. Senthil Kumar (✉)  
Department of Chemical Engineering, Sri Sivasubramaniya Nadar College of Engineering,  
Chennai 603110, India  
e-mail: [senthilchem8582@gmail.com](mailto:senthilchem8582@gmail.com); [senthilkumarp@ssn.edu.in](mailto:senthilkumarp@ssn.edu.in)

## 1 Introduction

Water is the establishment of life. Due to the fast development of total population across the globe, water contamination and water lack issue turns out to be a genuine issue [1]. The release of a lot of wastewater has carried along with it incredible difficulties to the natural environment and human wellbeing [2]. The contaminants present in wastewater may originate from various sources like oil contamination, herbicides, pesticides, pathogens, plastic and heavy metals [3]. Wastewater released from textile industries if not effectively treated would establish a genuine ecological issue for water contamination [4]. Wastewater treatment is broadly grouped under three main categories, namely the physical, chemical and biological method. Of these methods, the membrane process plays a vital role and it finds its application in the purification of residential and industrial wastewater [5]. The interest for water is expanding, and consequently, careful examination of different methodologies for production of high grade water is essential [6].

Membrane technology has gone through a fast improvement in accordance with most applications and specifically in accordance with purification of water [7]. Membrane technology has been broadly applied in water and wastewater treatment for the total partition of particulate issue and microbial microorganisms, having a size bigger than the pore size membrane [8]. Membrane technology finds its application in various fields like petrochemical industry, wastewater treatment and also in sea water desalination [9]. Membranes will dispense high grade quality of water at a reasonable cost and with minimum amount of energy consumption. Membranes with various physical and porosity attributes can viably eliminate a degree of toxins [10]. On the contrary, membranes are widely classified into two broad categories based on the type of material that is utilized in the membrane. The membrane materials can be classified as organic or inorganic membrane material [11]. In terms of characteristic, membranes can be categorized as isotropic and anisotropic membranes [12]. Polymeric membranes have a definite pore structures and they are most commonly employed. Apart from membranes, the different water purification technologies which are available for eliminating the impurities from wastewater will include electrosorption, precipitation, chemical disinfection, ion exchange and distillation [13]. Sleek wastewaters are one of the significant toxins of the sea-going condition. This is because of the emanation of oily waters released from a variety of origin which includes petrochemical plants and refineries [14]. Membrane filtration is generally preferred for the treatment of sleek wastewater because of its preferences: no synthetic added substances are expected to break the emulsion, high COD evacuation efficiencies are accomplished, and treatment methodologies are much minimized and completely mechanized [15]. The film-based methods like pervaporation, microfiltration, nanofiltration, ultrafiltration are often utilized to eliminate oil water emulsion [16].

## 2 Membrane Separation Process

Membrane technology is one of the most encouraging methods for purification of wastewater and it also enhances the production of high grade water quality [17]. Membrane separation process utilizes a membrane which in turn acts as a semipermeable barrier to effect the separation of two or more components. This membrane hinders the motion of chemical species either in partial or total manner [18]. Membrane technology has been widely utilized to isolate fluid/fluid or fluid/strong blends because of the adaptability and capacity to eliminate the contaminant from wastewater to low levels [19]. Separation processes by employing membranes have shown powerful exhibitions in desalination, recovery and water treatment applications [20].

Membrane technology allows us to separate very small size particles to the molecular and ionic level. This is in turn similar to the conventional separation systems also called as dead end filtration, where we employ filtration to separate suspended particles that are typically larger than 10  $\mu\text{m}$ . In this process, the particles are retained by the filter and they in turn build up with time as a cake layer resulting in the increased resistance to filtration. The common requirements include frequent cleaning and replacement of the filters. In this method, gravity is the main force for separation to take place, and here, the feed flows in a perpendicular direction to the filter medium. This system remains open to the atmosphere.

Thin membrane filters are generally employed for the purpose of separation to occur. The liquid is made to flow under pressure and it is forced to flow along the surface of the membrane. The commonly used membrane technologies include microfiltration, ultrafiltration, nanofiltration, reverse osmosis. Membranes possessing antifouling and self-cleaning properties can be a more powerful and an eco-friendly methodology [21].

The most commonly used membrane system used in food industry includes microfiltration, ultrafiltration, nanofiltration and reverse osmosis. These systems are differentiated based on their membrane pore size. The smallest pore size is for reverse osmosis ranging from  $10^{-4}$  to  $10^{-3}$   $\mu\text{m}$ . For nanofiltration membranes, the pore size varies from  $10^{-3}$  to  $10^{-2}$ . For ultrafiltration, the pore size varies from  $10^{-2}$  to  $10^{-1}$ . The microfiltration has the largest pore size ranging anywhere from  $10^{-1}$  to  $10^1$   $\mu\text{m}$ . Also, the pressure used in these systems varies, fairly the pressure used in microfiltration is around 1 bar, ultrafiltration requires around 1–12 bars, nanofiltration requires 10–40 bars, and in reverse osmosis, we require very high pressures ranging from 30 to 60 bars (Fig. 1).

## 3 Microfiltration

Microfiltration is often used to remove bacteria and to separate a larger size molecule. They are commonly used in skimmed milk to reduce bacteria, whey, brine, and it

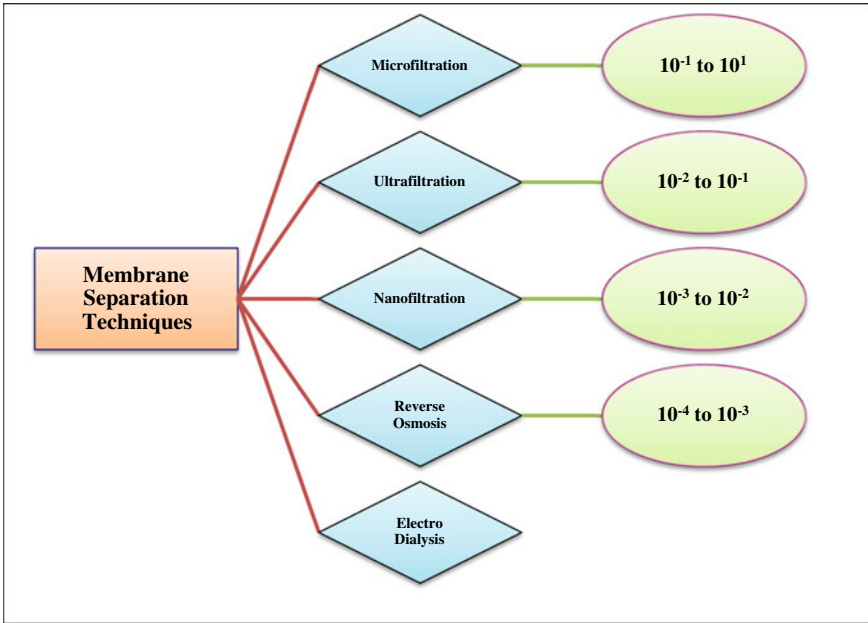


**Fig. 1** Various membrane separation techniques and their respective pore size

is also used to make whey proteins and to concentrate proteins. The most regularly utilized membrane films are comprised of permeable material and have a pore size in the size of 0.1–1.0 Lm, with a normal pore size of 0.2 Lm. The operating pressure for microfiltration membranes is typically 5 bar [22]. The process of microfiltration is often utilized as a pre-treatment action before the reverse osmosis and ultrafiltration process so as to diminish film fouling [23]. Notwithstanding the more customary points of eliminating fats and microbes from the whey, the utilization of MF has been applied for different purposes. The impact of MF measure on the taste, color and usefulness of whey protein concentrate, which was later acquired by ultrafiltration (UF) and spray drying measures, was assessed [18]. Gravity-driven microfiltration (GDM) has been demonstrated to be successful in pre-treating seawater as a synthetic free and low vitality choice, in which the dismissed natural substances are biodegraded by the biofilm on the film of the membrane [24]. The coal-based microfiltration carbon layer with minimal effort for the treatment of sleek wastewater was set up via carbonization of tubular carbonaceous precursor acquired by expulsion technique [25].

## 4 Ultrafiltration

Ultrafiltration is a pressure-driven process that separates particulate matter from soluble components. Ultrafiltration film has an extensive application possibility in wastewater purging and for the producing drinking water [26]. Ultrafiltration is a measure of expanding the heed for color and salt fractionation, since it permits high salt penetration with improved saturation transition [27]. Ultrafiltration was utilized to additionally diminish microbial load, chemical oxygen demand, turbidity and total suspended solids present in wastewater [28]. Ultrafiltration has been effectively utilized in oil-in-water partitions [14]. Ultrafiltration can give apparent specific detachment and it works at a encompassing and low temperature [29]. Microfiltration works out for eliminating suspended and colloidal particles; ultrafiltration permits the expulsion of particles and molecules larger than 10 nm [30]. In ultrafiltration, transport of solutes through films can be accomplished by convection because of the variation in pressure and also it is attributed due to the solution diffusion by concentration gradient [31]. Ultrafiltration film innovation has attained significant importance for cleansing drinking water and sleek wastewaters [32]. Ultrafiltration has been widely utilized in the area of pure water manufacture as well as in pharmaceutical industries and also it finds its application in the field of sleek wastewater treatment [33]. Membrane fouling happens to be the major disadvantage of ultrafiltration in oil water division [34].

It was reported that of the various methodologies available, the polymeric ultrafiltration membrane was utilized to handle oily wastewater and this method popped up to be the most cost-effective technique and a high level of separation was achieved using this method on comparing it with other traditional methods available used to manage oily wastewater [35]. Utilization of tight ultrafiltration (UF) layers has made another pathway in fractionation of salt or dye blends from textile effluent for manageable asset recuperation [36]. Ultrafiltration has been effectively applied in numerous businesses; however, it has not been generally acknowledged by the textile industry [37].

## 5 Nanofiltration

Nanofiltration is a pressure-driven process and it has a capacity to dismiss ionic and molecular species. Ceramic membranes, organic membranes and nanofiltration membranes can be either thick or permeable. Membranes employed in nanofiltration have bigger space, little pores and nanovoids that are accessible for transport [38]. Partitioning and diffusion, hydrophobic interactions, electrostatic repulsion and steric effect are the various expulsion mechanisms exhibited by nanofiltration method and they are in turn subjected to feed water qualities, film properties and physico-substance properties of solutes [39]. The partition system of this method incorporates size prohibition and Donnan avoidance that can be ideal in eliminating colors [20].

Nanofiltration is profitable over other processes of filtration because of the reality that it tends to be worked at lower transmembrane pressure on comparison with than reverse osmosis and it is adequately used to eliminate monovalent and divalent particles. Utilization of nanofiltration could adequately decrease the convergence of particles present in the wastewater [40]. Nanofiltration membranes possessing a molecular weight cut off of about 500–100 Da have allured great attention in portioning the salts and dyes [41]. Nanofiltration membranes have been employed widely in the purification of effluent released from textile industries on the basis of COD retention, permeate flux, salt rejection and dye retention [42]. On comparing with reverse osmosis, NF displays a bigger pore size and higher porousness and a lower transmembrane pressure, bringing about lower vitality utilization of NF measure [43]. The various benefits of nanofiltration on comparison with other methodologies include low power utilization and low partition cost [44]. The execution of nanofiltration membranes can be seriously restricted by concentration polarization and film fouling [45].

## 6 Reverse Osmosis

Reverse osmosis measure includes the constrained section of water through a film against the normal osmotic strain to isolate water and particles. Upon the application of high osmotic pressure, the water particles passes through the films and the salts are abandoned as a briny concentrate. Reverse osmosis membranes are constructed from a membrane flat sheet and it is comprised of three layers, namely a polyester fabric support base, a microporous polysulphone layer and a point two micron thick polyamide barrier layer.

## 7 Electro Dialysis

The process of movement of ions from one solution to another solution by passing them through a selective ion exchange membrane by using electric potential difference to attract ions toward the electrodes is known as electro dialysis [46]. It is based on the principle that when an electric field is applied to the electrodes, the salt solution containing the ions enters into the electro dialysis unit. When these ions flows through the electrodes, the cations will go to the anode and the anions will go to the cathode. It is a substitute to reverse osmosis process as a desalinization system. While reverse osmosis utilizes constrain drop to drive the detachment, electro dialysis uses a voltage potential [47].

## 8 Membrane Fouling

Membrane fouling is a term in which the solution or particle settles on the surface of the membrane or the membrane pores in the process such as in membrane bioreactor so that the performance of the membrane is degraded. Membrane fouling causes a downfall in flux and it in turn transforms the quality of the water produced. Severe fouling requires chemical cleaning or replacement of the membrane. Fouling can be classified as reversible and irreversible fouling. Reversible fouling can be expelled by strong shear force or backwashing. Physical cleaning does not prove effective in eliminating irreversible fouling. Fouling can be controlled by air scour, relaxation, by the addition of adsorbent or coagulant and by mechanical cleaning.

## 9 Application of Membrane for the Removal of Dye

The PI-based membrane displayed a dismissal of 98.65% against the Direct Red 23 color with a concentration of 100 ppm at 0.1 MPa. Consequently, this PI-based UF film is profoundly advantageous and served as a powerful material for color expulsion from wastewater released by the textile industry [48]. The expulsion of Alizarin red-S was examined by filtration methodology in which AT1-500 membrane was employed for the purpose of expulsion of the dye [49]. The filtration execution of bentonite layer was assessed by unrelated filtration of Direct Red 80 and Rhodamine B at 4 bar pressure. The impact of initial concentration and time for filtration was observed and it demonstrated the dismissal of Direct Red 80 and Rhodamine B could accomplish an estimation of 97.0 and 80.1% individually [50]. CHI upgraded ultrafiltration accomplished within the sight of CHI demonstrated that the rate of retention expanded upto 86% for methyl orange and 89% for Direct Blue 71 [51]. The conduct of a polyvinyl chloride hollow fiber ultrafiltration membrane for the expulsion of methyl green dye from hydrous solution was assessed by examining the impact of fluctuating the activity conditions like the flow rate and initial concentration to decide upon the effect of separation processes at constant pressure and temperature [52]. Ultrafiltration membranes were prepared from natural Moroccan clays. The acquired membrane films were subjected to digressive filtration of Direct Red 80 dye solution having a concentration of 50 ppm under tension of 3 bar. Test results show that color dismissal could accomplish an estimation of 99 and 97% individually for the clays [53]. Ceramic membrane employed for ultrafiltration was utilized to remove Reactive Black 5 dye has a wide range of initial concentrations from 50 to 500 mg/L [54]. Methyl green dye was expelled by adopting hybrid adsorption-membrane technique in which a mesoporous material MCM-41 was utilized as an adsorbent which in turn was combined with ultrafiltration technique and the rejection coefficient was determined to be 94.79% [55].

Two monomers, namely 1,3,5-benzenetricarbonyl trichloride and 4,4'-diaminodiphenylmethane, were utilized to produce polyamide-based nanofiltration (NF) membranes which in turn was used to expel dye. The as prepared membrane demonstrated a flux of  $36.81 \text{ L m}^{-2} \text{ h}^{-1}$  and a rejection rate of 99% for Congo Red dye solution [56]. The acquired membrane (H-PAN-ETA) was utilized for color expulsion and it demonstrated both an astounding enemy of color fouling and a decent dismissal property for anionic dyes [57]. The GO-PCS nanofiltration membrane was utilized to expel salt containing anionic dyes and it exhibited good antifouling property along with good separation [58]. The covalent organic frameworks (COFs) membrane proved to be very potential in expelling Chrome Black T and it demonstrated a rejection rate of 97.4% [59]. Graphene oxide composite loose nanofiltration membrane was utilized to expel methyl blue and Congo Red dye solution and the rejection rate for Congo Red dye was observed to be >97% [60]. A study affirmed that the membrane employed for the purpose of nanofiltration showed excellent performance toward desalination as well as expulsion of dye solution. These membranes discarded 99.4% of Congo Red dye solution and 2.5% NaCl [61]. Nanofiltration hollow fiber membrane retrieved from rubber demonstrated an excellent outcome by expelling methylene blue dye upto 93.1% [62]. Nanofiltration membrane system and reverse osmosis were used to expel acid red, reactive black and reactive blue dyes. By using nanofiltration membrane systems, the expulsion of dye was inferred to be 97% for blue dye, 95.67% for black dye and 93.77% for red dye, respectively. The removal using reverse osmosis membrane was reported as 99.9% for reactive blue dye, 99.58% for reactive black and 97.2% for acid red dye [63]. The MfSNPs/PVDF/PTFE films were exceptionally effective in eliminating Congo Red color from water and 99% expulsion productivity was accomplished was reported by Khumalo et al. [64] (Table 1).

## 10 Case Study

A contextual investigation of oleochemical wastewater treatment utilizing a serious cycle that contains reverse osmosis and ultrafiltration was inferred in a case study. The amount and nature of the penetrate stream of the membrane system were occasionally observed more than 43 days. The outcomes demonstrated that the framework worked adequately in decreasing the COD, hardness content and TDS content in it. This membrane framework began to break down following 15 days of activity. Film biofouling was suspected to have happened in the RO layer. In any case, the fouling issue could be settled by synthetically cleaning the RO layer utilizing a sodium hydroxide solution for about 3–5 days [71].



**Table 1** Different type of membranes for the expulsion of dye

Membrane type	Dye	Flux ( $L m^{-2} h^{-1}$ )	Permeability ( $L m^{-2} h^{-1} bar^{-1}$ )	Rejection rate %	Pressure	Refs.
PI-based UF membrane	Direct red dye23	345.10 305.58	–	98.65	0.1 MPa	[48]
AT1-500 membrane	Alizarin Red-S	–	9.6	96.9		[49]
UF bentonite membrane	Direct Red 80 Rhodmine B	–	30	97 80.1	4 bar	[50]
PEUF	Methyl Orange Direct Blue 71	–	–	86 71	–	[51]
Ceramic ultrafiltration membranes	Direct Red 80	–	14.7 16.4	99 97	3 bar	[53]
UF ceramic membranes	Reactive Black 5	266.81	–	79.8	3 bar	[54]
UF membrane coupled with adsorbent	Methyl Green	42.5		94.79	–	[55]
Polyamide-based nanofiltration (NF) membranes	Congo Red	36.81	–	99	–	[56]
Polyetherimide based NF	Reactive Red 120	0.013	–	98	60 psi	[65]
PVDF	Congo Red	$202.51 \pm 9.63$	–	97.93	0.1 MPa	[66]
UiO-66 incorporated NF membranes	Congo Red	102	14.8	99.9	–	[67]
DS5 DK type nanofiltration membranes	RB5 RO16 RB19	–	–	99	–	[68]
EGCg/PEI 600 co-deposited membrane	Congo Red	–	19	99	2 bar	[69]
NF membrane	Safranin O dye	–	9–14	99.98	–	[70]

## 11 Conclusion

Membranes are able to eliminate a variety of organic and non-natural substances from fluid suspension. Membrane separation technology proves to be one of the most effective methodologies for effective treatment of waste effluent discharged by the textile industry. It is a separation process which employs a semi-permeable membrane for the effective separation of one or multiple components by employing electric potential, concentration polarization or hydrostatic pressure. The filtration process that is carried out by utilizing a membrane produces predominant quality water.

The coloring matter (dye) which is present in the system can be eliminated on subjecting them to either of the above mentioned membrane separation techniques for recovering them from the textile effluents. On the contrary, the reverse osmosis membrane plays a very vital role in expelling the salt from the solution and the rejection rate has shot up from 97% to almost 99.5%.

## 12 Future Scope

Enhancing the exploration of membrane innovation demonstrates that the membranes unquestionably will turn into another option for industrial purpose. A ceaseless examination to deal with properties associated with membrane and the underlying feature of transport phenomena operating the membrane is significant for the fate of membrane science and technology. The innovation using membrane technology will expand with immense advantage of water treatment in the filtration equipment. There is an enormous arrangement of materials right now under scrutiny with potential for application as membranes. The following decades will disclose to us the advances reachable with new film of membranes and the assembling measures.

## References

1. Yin J, Deng B (2015) Polymer-matrix nanocomposite membranes for water treatment. *J Membr Sci* 479:256–275. <https://doi.org/10.1016/j.memsci.2014.11.019>
2. Feng X, Zongxue Yu, Long R, Sund Y, Wang M, Li X, Zeng G (2020) Polydopamine intimate contacted two-dimensional/two-dimensional ultrathin nylon basement membrane supported RGO/PDA/MXene composite material for oil-water separation and dye removal. *Sep Purif Technol* 247:116945. <https://doi.org/10.1016/j.seppur.2020.116945>
3. Yalcinkaya F, Boyraz E, Maryska J, Kucerova K (2020) A review on membrane technology and chemical surface modification for the oily wastewater treatment. *Materials* 13(2). <https://doi.org/10.3390/ma13020493>
4. Li X, Jin X, Zhao N, Angelidaki I, Zhang Y (2017) Novel bio-electro-Fenton technology for azo dye wastewater treatment using microbial reverse-electrodialysis electrolysis cell. *Biores Technol* 228:322–329. <https://doi.org/10.1016/j.biortech.2016.12.114>

5. Karami P, Khorshidi B, McGregor M, Peichel JT, Soares J, Sadrzadeh M (2020) Thermally stable thin film composite polymeric membranes for water treatment: a review. *J Clean Prod* 250:119447. <https://doi.org/10.1016/j.jclepro.2019.119447>
6. Madaeni SS (1999) The application of membrane technology for water disinfection. *Water Res* 33(2):301–308. [https://doi.org/10.1016/S0043-1354\(98\)00212-7](https://doi.org/10.1016/S0043-1354(98)00212-7)
7. Nicolaisen B (2002) Developments in membrane technology for water treatment. *Desalination* 153:355–360. [https://doi.org/10.1016/S0011-9164\(02\)01127-X](https://doi.org/10.1016/S0011-9164(02)01127-X)
8. Kim H-S, Takizawa S, Ohgaki S (2007) Application of microfiltration systems coupled with powdered activated carbon to river water treatment. *Desalination* 202:271–277. <https://doi.org/10.1016/j.desal.2005.12.064>
9. Vatanpour V, Khorshidi S (2020) Surface modification of polyvinylidene fluoride membranes with ZIF-8 nanoparticles layer using interfacial method for BSA separation and dye removal. *Mater Chem Phys* 241:122400. <https://doi.org/10.1016/j.matchemphys.2019.122400>
10. Moattari RM, Mohammadi T (2020) Nanostructured membranes for water treatments. In: *Nanotechnology in the beverage industry*, pp 129–150. <https://doi.org/10.1016/B978-0-12-819941-1.00005-5>
11. Pichardo-Romero D, Garcia-Arce ZP, Zavala-Ramírez A, Castro-Muñoz R (2020) Current advances in biofouling mitigation in membranes for water treatment: an overview. *Processes* 8(2):182. <https://doi.org/10.3390/pr8020182>
12. Obotey Ezugbe E, Rathilal S (2020) Membrane technologies in wastewater treatment: a review. *Membranes* 10(5). <https://doi.org/10.3390/membranes10050089>
13. Liu Y, Zhang F, Zhu W, Dong Su, Sang Z, Yan X, Li S, Liang Ji, Dou SX (2020) A multifunctional hierarchical porous SiO<sub>2</sub>/GO membrane for high efficiency oil/water separation and dye removal. *Carbon* 160:88–97. <https://doi.org/10.1016/j.carbon.2020.01.002>
14. Salahi A, Mohammadi T, Pour AR, Rekabdar F (2009) Oily wastewater treatment using ultrafiltration. *J Desalin Water Treat* 6(1–3):289–298. <https://doi.org/10.5004/dwt.2009.480>
15. Li YS, Yan Lu, Xiang CB, Hong LJ (2006) Treatment of oily wastewater by organic–inorganic composite tubular ultrafiltration (UF) membranes. *Desalination* 196:76–83. <https://doi.org/10.1016/j.desal.2005.11.021>
16. Ahmad T, Guria C, Mandal A (2018) Synthesis, characterization and performance studies of mixed-matrix poly(vinyl chloride)-bentonite ultrafiltration membrane for the treatment of saline oily wastewater. *Process Saf Environ Prot* 116:703–717. <https://doi.org/10.1016/j.psep.2018.03.033>
17. Benkhaya S, M'rabet S, Hsissou R, El Harfi A (2020) Synthesis of new low-cost organic ultrafiltration membrane made from polysulfone/polyetherimide blends and its application for soluble azoic dyes removal. *J Mater Res Technol* 9(3):4763–4772. <https://doi.org/10.1016/j.jmrt.2020.02.102>
18. Argenta AB, De Paula Scheer A (2019) Membrane separation processes applied to whey: a review. *J Food Rev Int* 36(5):499–528. <https://doi.org/10.1080/87559129.2019.1649694>
19. Yuliwati E, Ismail AF, Matsuura T, Kassim MA, Abdullah MS (2011) Effect of modified PVDF hollow fiber submerged ultrafiltration membrane for refinery wastewater treatment. *Desalination* 283:214–220. <https://doi.org/10.1016/j.desal.2011.03.049>
20. Ong YK, Li FY, Sun S-P, Zhao B-W, Liang C-Z, Chung T-S (2014) Nanofiltration hollow fiber membranes for textile wastewater treatment: lab-scale and pilot-scale studies. *Chem Eng Sci* 114:51–57. <https://doi.org/10.1016/j.ces.2014.04.007>
21. Lv Y, Zhang C, He Ai, Yang S-J, Guang-Peng Wu, Darling SB, Zhi-Kang Xu (2017) Photocatalytic nanofiltration membranes with self-cleaning property for wastewater treatment. *Adv Func Mater* 27(7):1700251. <https://doi.org/10.1002/adfm.201700251>
22. Ahmad A, Azam T (2019) Water purification technologies. *Bottled Packaged Water* 4:83–120. <https://doi.org/10.1016/B978-0-12-815272-0.00004-0>
23. Masoudnia K, Raisia A, Aroujalian A, Fathizadeh M (2014) A hybrid microfiltration/ultrafiltration membrane process for treatment of oily wastewater. *J Desalin Water Treat* 55(4):901–912. <https://doi.org/10.1080/19443994.2014.922501>

24. Wua B, Suwamo SR, Tan HS, Kim LH, Hochstrasser F, Chong TH, Burkhardt M, Pronk W, Fane AG (2017) Gravity-driven microfiltration pretreatment for reverse osmosis (RO) seawater desalination: microbial community characterization and RO performance. *Desalination* 418:1–8. <https://doi.org/10.1016/j.desal.2017.05.024>
25. Song C, Wang T, Pan Y, Qiu J (2006) Preparation of coal-based microfiltration carbon membrane and application in oily wastewater treatment. *Sep Purif Technol* 51:80–84. <https://doi.org/10.1016/j.seppur.2005.12.026>
26. Li P, Cheng X, Zhou W, Luo C, Tan F, Zixiao Ren Lu, Zheng XZ, Daoji Wu (2020) Application of sodium percarbonate activated with Fe(II) for mitigating ultrafiltration membrane fouling by natural organic matter in drinking water treatment. *J Cleaner Prod* 269:122228. <https://doi.org/10.1016/j.jclepro.2020.122228>
27. Ye W, Ye K, Lin F, Liu H, Jiang M, Wang J, Liu R, Lin J (2020) Enhanced fractionation of dye/salt mixtures by tight ultrafiltration membranes via fast bio-inspired co-deposition for sustainable textile wastewater management. *Chem Eng J* 379:122321. <https://doi.org/10.1016/j.cej.2019.122321>
28. Hashemi F, Hashemi H, Shahbazi M, Dehghani M, Hoseini M, Shafei A (2020) Reclamation of real oil refinery effluent as makeup water in cooling towers using ultrafiltration, ion exchange and multioxidant disinfectant. *Water Resour Ind* 23:100123. <https://doi.org/10.1016/j.wri.2019.100123>
29. Yong M, Zhang Y, Sun S, Liu W (2019) Properties of polyvinyl chloride (PVC) ultrafiltration membrane improved by lignin: Hydrophilicity and antifouling. *J Membr Sci* 575:50–59. <https://doi.org/10.1016/j.memsci.2019.01.005>
30. Barredo-Damas S, Alcaina-Miranda MI, Bes-Piá A, Iborra-Clar MI, Iborra-Clar A, Mendoza-Roca JA (2010) Ceramic membrane behavior in textile wastewater ultrafiltration. *Desalination* 250:623–628. <https://doi.org/10.1016/j.desal.2009.09.037>
31. Srivastava HP, Arthanareeswaran G, Anantharaman N, Starov VM (2011) Performance of modified poly(vinylidene fluoride) membrane for textile wastewater ultrafiltration. *Desalination* 282(87):94. <https://doi.org/10.1016/j.desal.2011.05.054>
32. Adib H, Hassanajili S, Sheikhi-Kouhsar MR, Salahi A, Mohammadi T (2015) Experimental and computational investigation of polyacrylonitrile ultrafiltration membrane for industrial oily wastewater treatment. *Korean J Chem Eng* 32:159–167. <https://doi.org/10.1007/s11814-014-0218-9>
33. Wu TY, Mohammad AW, Jahim JMd, Anuar N (2007) Palm oil mill effluent (POME) treatment and bioresources recovery using ultrafiltration membrane: effect of pressure on membrane fouling. *Biochem Eng J* 35:309–317. <https://doi.org/10.1016/j.bej.2007.01.029>
34. Li H-J, Cao Y-M, Qin J-J, Jie X-M, Wang T-H, Liu J-H, Yuan Q (2006) Development and characterization of anti-fouling cellulose hollow fiber UF membranes for oil–water separation. *J Membr Sci* 279:328–335. <https://doi.org/10.1016/j.memsci.2005.12.025>
35. Ahmad T, Guria C, Mandal A (2020) A review of oily wastewater treatment using ultrafiltration membrane: a parametric study to enhance the membrane performance. *J Water Process Eng* 36:101289. <https://doi.org/10.1016/j.jwpe.2020.101289>
36. Jiang M, Ye K, Deng J, Lin J, Ye W, Zhao S, Van der Bruggen B (2018) Conventional ultrafiltration as effective strategy for dye/salt fractionation in textile wastewater treatment. *Environ Sci Technol* 52(18):10698–10708. <https://doi.org/10.1021/acs.est.8b02984>
37. Tang C, Chen V (2002) Nanofiltration of textile wastewater for water reuse. *Desalination* 143:11–20. [https://doi.org/10.1016/S0011-9164\(02\)00216-3](https://doi.org/10.1016/S0011-9164(02)00216-3)
38. Nagy E (2012) Nanofiltration. In: *Basic equations of the mass transport through a membrane layer*, pp 249–266. <https://doi.org/10.1016/B978-0-12-416025-5.00010-7>
39. Azaïs A, Mendret J, Gassara S, Petit E, Deratani A, Brosillon S (2014) Nanofiltration for wastewater reuse: counteractive effects of fouling and matrix on the rejection of pharmaceutical active compounds. *Sep Purif Technol* 133:313–327. <https://doi.org/10.1016/j.seppur.2014.07.007>
40. Deepti A, Sinhab P, Biswas S, Sarkar U, Bora MKP (2020) Separation of chloride and sulphate ions from nanofiltration rejected wastewater of steel industry. *J Water Process Eng* 33:101108. <https://doi.org/10.1016/j.jwpe.2019.101108>

41. Ye W, Liu R, Chen X, Chen Q, Lin J, Lin X, Van der Bruggen B, Zhao S (2020) Loose nanofiltration-based electro dialysis for highly efficient textile wastewater treatment. *J Membr Sci* 608:118182. <https://doi.org/10.1016/j.memsci.2020.118182>
42. Liu M, Lü Z, Chen Z, Sanchuan Yu, Gao C (2011) Comparison of reverse osmosis and nanofiltration membranes in the treatment of biologically treated textile effluent for water reuse. *Desalination* 281:372–378. <https://doi.org/10.1016/j.desal.2011.08.023>
43. Cao X-L, Yan Y-N, Zhou F-Y, Sun S-P (2020) Tailoring nanofiltration membranes for effective removing dye intermediates in complex dye-wastewater. *J Membr Sci* 595:117476. <https://doi.org/10.1016/j.memsci.2019.117476>
44. Guo D, Xiao Y, Li T, Zhou Q, Shen L, Li R, Yanchao Xu, Lin H (2020) Fabrication of high-performance composite nanofiltration membranes for dye wastewater treatment: mussel-inspired layer-by-layer self-assembly. *J Colloid Interface Sci* 560:273–283. <https://doi.org/10.1016/j.jcis.2019.10.078>
45. Lin J, Tang CY, Ye W, Sun S-P, Hamdan SH, Volodin A, Van Haesendonck C, Sotto A, Luis P, Van der Bruggen B (2015) Unravelling flux behavior of superhydrophilic loose nanofiltration membranes during textile wastewater treatment. *J Membr Sci* 493:690–702. <https://doi.org/10.1016/j.memsci.2015.07.018>
46. Aghaeinejad-Meybodi A, Ghazemzadeh K (2017) Silica membrane application for desalination process. In: *Current trends and future developments on bio-membranes*, pp 181–216. <https://doi.org/10.1016/B978-0-444-63866-3.00008-X>
47. Hutten IM (2016) Filtration mechanisms and theory. In: *Handbook of nonwoven filter media*, 2nd edn., pp 53–107. <https://doi.org/10.1016/B978-0-08-098301-1.00002-2>
48. Yang C, Weixing Xu, Nan Y, Wang Y, Yunxia Hu, Gao C, Chene X (2020) Fabrication and characterization of a high performance polyimide ultrafiltration membrane for dye removal. *J Colloid Interface Sci* 562:589–597. <https://doi.org/10.1016/j.jcis.2019.11.075>
49. Huang X, Tian C, Qin H, Guo W, Gao P, Xiao H (2020) Preparation and characterization of Al<sup>3+</sup>-doped TiO<sub>2</sub> tight ultrafiltration membrane for efficient dye removal. *Ceram Int* 46(4):4679–4689. <https://doi.org/10.1016/j.ceramint.2019.10.199>
50. Saja S, Bouazizi A, Achiou B, Ouaddari H, Karim A, Ouammou M, Aaddane A, Bennazha J, Alami Younssi S (2020) Fabrication of low-cost ceramic ultrafiltration membrane made from bentonite clay and its application for soluble dyes removal. *J Eur Ceram Chem* 40:2453–2462. <https://doi.org/10.1016/j.jeurceramsoc.2020.01.057>
51. Fradj AB, Boubakri A, Hafiane A, Hamouda SB (2020) Removal of azoic dyes from aqueous solutions by chitosan enhanced ultrafiltration. *Results Chem* 2:100017. <https://doi.org/10.1016/j.rechem.2019.100017>
52. Alardhi SM, Alrubaye JM, Albayati TM (2020) Hollow fiber ultrafiltration membrane for methyl green dye removal. *Eng Technol J* 38(7A):1077–1083. <https://doi.org/10.30684/etj.v38i7A.653>
53. Ouaddari H, Karim A, Achiou B, Saja S, Aaddane A, Bennazha J, El Amrani El I, Hassani M, Ouammou AA (2019) New low-cost ultrafiltration membrane made from purified natural clays for direct Red 80 dye removal. *J Environ Chem Eng* 7:103268. <https://doi.org/10.1016/j.jece.2019.103268>
54. Alventosa-deLara E, Barredo-Damas S, Alcaina-Miranda MI, Iborra-Clar MI (2012) Ultrafiltration technology with a ceramic membrane for reactive dye removal: optimization of membrane performance. *J Hazard Mater* 209–210:492–500. <https://doi.org/10.1016/j.jhazmat.2012.01.065>
55. Alardhi SM, Albayati TM, Alrubaye JM (2020) A hybrid adsorption-membrane process for removal of dye from synthetic and actual wastewater. *Chem Eng Process Process Intensification* 157:108113. <https://doi.org/10.1016/j.cep.2020.108113>
56. Yang C, Weixing Xu, Nan Y, Wang Y, Chen X (2020) Novel negatively charged nanofiltration membrane based on 4,4'-diaminodiphenylmethane for dye removal. *Sep Purif Technol* 248:117089. <https://doi.org/10.1016/j.seppur.2020.117089>

57. Yun J, Wang Y, Liu Z, Yujie Li Hu, Yang Z-L (2020) High efficient dye removal with hydrolyzed ethanalamine polyacrylonitrile UF membrane: rejection of anionic dye and selective adsorption of cationic dye. *Chemosphere* 259:127390. <https://doi.org/10.1016/j.chemosphere.2020.127390>
58. Song Y, Sun Y, Chen M, Huang P, Li T, Zhang X, Jiang K (2020) Efficient removal and fouling-resistant of anionic dyes by nanofiltration membrane with phosphorylated chitosan modified graphene oxide nanosheets incorporated selective layer. *J Water Process Eng* 34:101086. <https://doi.org/10.1016/j.jwpe.2019.101086>
59. Wang Ze, Si Z, Cai Di, Li GLS, Qin P (2020) Synthesis of stable COF-300 nanofiltration membrane via in-situ growth with ultrahigh flux for selective dye separation. *J Membr Sci* 615:118466. <https://doi.org/10.1016/j.memsci.2020.118466>
60. Kang X, Cheng Y, Wen Y, Qi J, Li X (2020) Bio-inspired co-deposited preparation of GO composite loose nanofiltration membrane for dye contaminated wastewater sustainable treatment. *J Hazard Mater* 400:123121. <https://doi.org/10.1016/j.jhazmat.2020.123121>
61. Jin J, Xilan Du, Jie Yu, Qin S, He M, Zhang K, Chen G (2020) High performance nanofiltration membrane based on SMA-PEI cross-linked coating for dye/salt separation. *J Membr Sci* 611:118307. <https://doi.org/10.1016/j.memsci.2020.118307>
62. Lin Y-T, Kao F-Y, Chen S-H, Wey M-Y, Tseng H-H (2020) A facile approach from waste to resource: reclaimed rubber-derived membrane for dye removal. *J Taiwan Inst Chem Eng* 112:286–295. <https://doi.org/10.1016/j.jtice.2020.06.004>
63. Abid MF, Zablouk MA, Abid-Alameer AM (2012) Experimental study of dye removal from industrial wastewater by membrane technologies of reverse osmosis and nanofiltration. *J Environ Health Sci Engineer* 9:17. <https://doi.org/10.1186/1735-2746-9-17>
64. Khumalo NP, Nthunya LN, De Canck E, Derese S, Verliefe AR, Kuvarega AT, Mamba BB, Mhlanga SD, Dlamini DS (2019) Congo red dye removal by direct membrane distillation using PVDF/PTFE membrane. *Sep Purif Technol* 211:578–586. <https://doi.org/10.1016/j.seppur.2018.10.039>
65. Gunawan FM, Mangindaan D, Khoiruddin K, Gede Wenten I (2018) Nanofiltration membrane cross-linked by m-phenylenediamine for dye removal from textile wastewater. *Polym Adv Technol* 30(2):360–367. <https://doi.org/10.1002/pat.4473>
66. Zhang Y, Weiming Yu, Li R, Yanchao Xu, Shen L, Lin H, Liao B-Q, Guosheng Wu (2019) Novel conductive membranes breaking through the selectivity-permeability trade-off for Congo red removal. *Sep Purif Technol* 211:368–376. <https://doi.org/10.1016/j.seppur.2018.10.008>
67. Wang K, Qin Y, Quan S, Zhang Y, Wang P, Liang H, Ma J, Cheng XQ (2019) Development of highly permeable polyelectrolytes (PEs)/UiO-66 nanofiltration membranes for dye removal. *Chem Eng Res Des* 147:222–231. <https://doi.org/10.1016/j.cherd.2019.05.014>
68. Koyuncu I (2002) Reactive dye removal in dye/salt mixtures by nanofiltration membranes containing vinylsulphone dyes: effects of feed concentration and cross flow velocity. *Desalination* 143:243–253. [https://doi.org/10.1016/S0011-9164\(02\)00263-1](https://doi.org/10.1016/S0011-9164(02)00263-1)
69. Zhang Na, Jiang B, Zhang L, Huang Z, Sun Y, Zong Y, Zhang H (2019) Low-pressure electroneutral loose nanofiltration membranes with polyphenol-inspired coatings for effective dye/divalent salt separation. *Chem Eng J* 359:1442–1452. <https://doi.org/10.1016/j.cej.2018.11.033>
70. Zhong PS, Widjojo N, Chung T-S, Weber M, Maletzko C (2012) Positively charged nanofiltration (NF) membranes via UV grafting on sulfonated polyphenylenesulfone (sPPSU) for effective removal of textile dyes from wastewater. *J Membr Sci* 417–418:52–60. <https://doi.org/10.1016/j.memsci.2012.06.013>
71. Koo CH, Mohammad AW, Suja F (2011) Recycling of oleochemical wastewater for boiler feed water using reverse osmosis membranes—a case study. *Desalination* 271:178–186. <https://doi.org/10.1016/j.desal.2010.12.025>

# Dyestuff Adsorbing Natural Composites for Wastewater Treatments



E. Emekdar and U. K. Şahin

**Abstract** Environmental concerns gain importance with the increase in the lack of sources on the world. Especially, the textile industry has many contaminating effects on the environment, and the most important one is wastewater problems related to the high chemical load that is coming from textile processes and high water consumption. To eliminate the adverse results of textile wastewater discharges and high usages, wastewater must refine before discharging and must reuse in suitable processes. Refining processes are very valuable for decreasing the contaminants in wastewater, but these processes need extra cost, time, production place, and investments. Multifunctional agents as adsorbing composites can provide many advantages to refining processes and alternative reuse strategies and environmental conservation. In this chapter, the needs for refinement and types of refining processes are evaluated first. Then, adsorbent materials and their composites are detailed with properties, production stages, and usages. Finally, this chapter offers an alternative adsorbent composite production and usage study based on clay and modified chitosan.

**Keywords** Textile wastewater · Refining processes · Dyestuff adsorbing composites · Clay · Chitosan · Cellulose derivatives · Biochar · Biopolymers

## 1 Introduction

Water sources are decreasing day by day with various reasons as increasing human population, global warming, uncontrolled water consumption, water contamination, etc. The human population increase and global warming are indirect reasons and more related to the balance of nature. Water consumption and contamination are direct reasons for source decrease, and they are related to human behavior directly and can be controlled or limited by environmental awareness. Water consumption was 1041 billion liters per day for surface water sources and 3002 billion liters per

---

E. Emekdar (✉) · U. K. Şahin

Textile Engineering Department, Textile Technologies and Design Faculty, Istanbul Technical University, İnönü Cad. No: 65, Beyoğlu, İstanbul, Turkey

e-mail: [emekdar@itu.edu.tr](mailto:emekdar@itu.edu.tr)

© The Author(s), under exclusive license to Springer Nature Singapore Pte Ltd. 2021

103

S. S. Muthu (ed.), *Advances in Textile Waste Water Treatments*, Sustainable Textiles: Production, Processing, Manufacturing & Chemistry, [https://doi.org/10.1007/978-981-16-0065-4\\_4](https://doi.org/10.1007/978-981-16-0065-4_4)

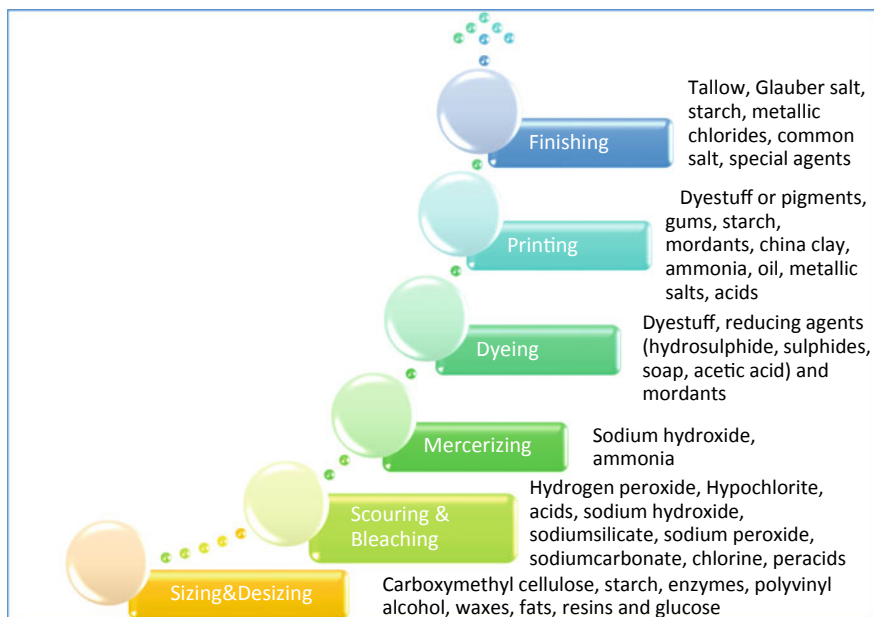


**Fig. 1** Textile chemicals in process sequence

day for groundwater, and these values are very high for the future of the earth [1]. Water contamination is the most unfortunate reason for lack of water because water is wasted knowingly or unknowingly without consuming it, and huge amounts of water become unusable because of the lack of water quality or becoming harmful.

Many sectors affect water contamination with different roles, and the major effect is discharging wastewater of their industrial procedures. In the case of industrial wastewater, the textile industry has the maximum amount of water usage as using 200 L water during pretreatment, coloration, and finishing processes (see Fig. 1) applied for producing 1 kg fabric [2]. Among wet processes, dyeing and finishing operations use around 50% of the water and generate 80% of wastewater [3]. The wastewater of the textile industry which includes high color and toxicity has a very huge amount of contaminant units in it; approximately, 8000 chemicals can be in wastewater, and most of them belong to dyeing [3]. These contaminants can be dyestuffs (acidic, basic, reactive, azo, metal-complex, etc.), finishing agents, bleaching and cleaning agents, lubricants, alkaline and acid auxiliary chemicals, surfactants, metal ions, and fiber coming from textile materials, organic or inorganic compounds, and all of them vary widely in their physical and chemical characters. Wastewater of a desized product can include carboxymethyl cellulose, starch, polyvinyl alcohol, waxes, fats, resins, and glucose [4] with high biological oxygen demand (BOD) which is 35–50% of BOD total, but polyvinyl alcohol and carboxymethyl cellulose are not harmful and do not affect the BOD amount. If a product is bleached, then this process adds hydrogen peroxide, hypochlorite, acids,



caustic soda, chlorine like chemicals [5, 6], and the water characteristic is alkaline with 5% of BOD. For mercerized product, caustic soda can be seen with the high amount, and its characteristics turn to strongly alkaline [7] with low BOD. In wastewater of dyeing processes, dyestuff, reducing agents (hydrosulfide, sulfides, soap, acetic acid), and mordants [8, 9] are seen, and it is strongly colored with fairly high BOD which is 6% of the total BOD. Printing adds dyestuff or pigments, gums, starch, mordants, china clay, oil, metallic salts, and acids into wastewater, and its characteristic can be defined as highly colored and oily with fairly high BOD. When the last process of finishing is applied to the product, chemicals like tallow, Glauber salt, traces of starch, common salt, and special agents [10, 11] can be seen in wastewater that is slightly alkaline with low BOD [3].

Dyestuffs cause the color and toxicity of the wastewater. Especially, cationic dyestuffs that include benzidine or aromatic compounds can be carcinogenic or mutagenic for water creatures and human beings. Anionic and reactive dyestuffs have persistent behavior to be eliminated because of being water soluble and become harmful to nature. Dyestuffs in water act like a photocatalytic material and do not let sunlight to penetrate the water supply; thus, water living habitat gets harm with the change of the oxygen balance; eutrophication which is uncontrolled reproduction of algae in a small water supply is seen and some other species extinct due to suppression of algae [3]. Dyestuff presence in water supplies decreases biodiversity.

Total dissolved solids (TDS) are one of the problems of wastewater, and the reason for this is common salt and Glauber's salt. Even it is at low level, TDS damages the balance of the water habitat because the salt amount changes and osmotic balance is damaged; thus, water creatures can get harm due to dehydration or excess water penetration. Also, the water supply becomes useless for human activities [3].

Oil, grease, clay, silt, and gritty materials can be categorized under suspended solids, and they form a barrier on the surface of the water; thus, oxygen and sunlight inlet are prevented, and the temperature of water habitat decreases. As a result, water creatures get serious harm from these impurities [3].

Toxic effects can be seen for all living things in case of drinking, eating, and respiration, in case of exposure to heavy metals as manganese, copper, arsenic, cadmium, mercury, chromium, zinc, lead, etc., with amounts more than the limitations [3].

Furthermore, impurities can accumulate in pipes and results with clogging unless the wastewater is refined with suitable methods. This can add an economic problem to maintain it. Besides the economic problems, water scarcity and some illnesses such as haemorrhage, dermatitis, an ulcer on the skin, vomiting gastritis, nausea, skin irritation and risk of bladder cancer can be seen due to lack of clean and enough water [12].

These contaminants must be eliminated at refining procedures before discharging not to contaminate the nature and harm all living things. Refining is also needed for reusing wastewater; thus, water consumption is also decreased with reuse policy. This reuse policy provides water, chemical and energy saving, and decreasing waste production.

In this study, general refining methods for wastewater treatment, textile wastewater characteristics, and selection of refining processes depending on wastewater characteristics are explained, and alternative composite structures applicable as well as needs for these alternatives are discussed. Finally, a case study on a novel dyestuff adsorbing nanocomposite is evaluated.

## 2 Wastewater Refining

Refining is impurity elimination from waste to turn it into more suitable forms. In the case of a wastewater refining, it is clarifying wastewater, which is a result of an industrial process, by removing undesired particles from the process environment, end products, and by-products. Refining is very important for both discharging and saving according to regulations and standards because it is a preliminary stage of both of them. Quality of wastewater must be increased; contaminants, color, and odor of the water must be removed, and it is turned into suitable levels. Refinement is a series of clearing processes; refinement wastes as in mud or liquid form must be disposed of suitably, and this needs an extra disposing strategy. There are certain types of refining, but the application of those changes according to characteristics of the wastewater. There are three main types of refining methods as physical refining, oxidative refining, and biological refining. According to the wastewater characteristics, some methods can be applied or all of them can be used in a combination. In a refining step, material elimination starts from bigger particles to tiny particles and chemicals. Generally, first, solid particles are eliminated by using different sizes of grids; then, oxidative/chemical and biological treatments are carried to eliminate small contaminants, color, and odor [13].

Textile wastewater includes many textile fibers, chemicals, and dyestuff, and it is more complex to refine; thus, different refining combinations are applied, and it brings a huge refining process with long time consumption. All these different impurities produce huge chemical loads, and they must be removed carefully for yielding more clear wastewater to discharge in limits or reuse in more suitable applications. According to applied textile processes and characteristics of the resultant wastewater, one or more refining processes that are mentioned in Fig. 2 can be selected, and in these steps, using more functional agents as dye adsorbing composites could decrease the total number of refining steps demanded and time consumption with the increase of efficiencies.

### 2.1 Physical Refining Methods

Physical refining is eliminating the particles in the wastewater by using different sizes of physical equipment. It is generally the primary refining step because, firstly, bigger particles must be removed as fabric pieces, fibers, some metallic particles,

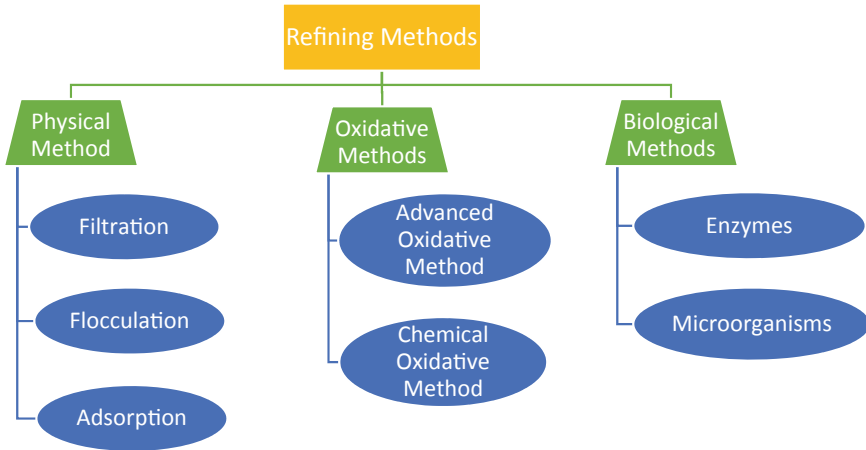


**Fig. 2** Classification of refining methods [13]

and floccules. Physical methods can be classified into three groups as filtration, flocculation, and adsorption.

In filtration, different sizes of sieves and filters are used. According to the ingredient and temperature of the effluent that will be refined, the pore size of sieves and filters alter, and a combination of these with various sizes can be combined. A physical refining system starts from coarser grids to finer filter, and by using in a sequence, particles that can be seen are removed one by one until the only particles that can pass from the finest filter in the refining system. Filtration can be ultrafiltration, nanofiltration, and reverse osmosis [13]. In ultra- and nanofiltration, effluent passes through a filter without any force or effect, and the number of impurities in it is decreased. However, in reverse osmosis, a membrane is used, and the opposite behavior of osmosis mechanism is used. In osmosis, water directly penetrates through the membrane from the diluted region to a more concentrated region without any force, while in reverse osmosis, effluent passes from concentrated region to diluted region by applying pressure on the effluent, and effluent is cleaned and collected at the diluted region. In this sequence of filtration, particle sizes that are removed decrease from ultrafiltration to reverse osmosis and impurities removed step by step.

Flocculation is the precipitation of particles thanks to their density differences or forming precipitation units by using additives to make it faster. Particles collected at the bottom of flocculation pools by waiting certain times and cleaner wastewater are collected from the upper part of the pool. It can be used for disperse dyestuffs, and it has low efficiency at reactive and vat dyestuffs, but it has limited usage and high mud production.

Adsorption is holding impurities on the surface of the adsorbent; thus, particles are removed from wastewater and stay on the adsorbent. When adsorbent is removed, wastewater is cleaned. This method has high discoloration efficiency even at low

color concentrations and low cost [13]. Adsorbent materials and their details will be discussed in the further part of this chapter.

## 2.2 *Oxidative Refining Methods*

Oxidative methods use generally oxidative chemicals, and this class can be known as chemical methods. Different radicals are used to eliminate impurities by oxidizing them. These methods can be applied easily; thus, they are the most commonly used class. This class has two subtitles as advanced oxidative method (AOM) and chemical oxidative methods.

The advanced oxidative method uses hydroxyl radicals which are very strong oxidative, and the generated radicals eliminate organic and inorganic impurities. This method is very useful for textile wastewater and fast [13]. This method can be supported by ultrasonic or hydrodynamic cavitation. Also, photocatalytic oxidation and Fenton reaction which is between  $\text{Fe}^{3+}$  ions and  $\text{H}_2\text{O}_2$  can be in AOM-type refining. In Fenton reaction, a  $\text{Fe}^{2+}$  ion mixture which has pH 2–3 as the acid is prepared, and  $\text{H}_2\text{O}_2$  is added to form hydroxyl radicals [14]. Other Fenton's reagents can be used, but iron salts are the most common ones. Mud formation is a disadvantage of the Fenton method because reagent and dyestuff form a complex molecule and produce floccules [13].

The chemical oxidative method is another method for oxidative methods. It uses oxidative agents as ozone and hydrogen peroxide that attacks to the conjugated double bonds and functional groups at chromophore region of dyestuffs. In this method, effluent is taken into the tank, and the oxidant is added in the reactor, and finally, caustic is added for pH adjustment. In the case of ozone that needs good stabilization conditions as pH and temperature, it removes toxic ingredients, hydrocarbons, phenols, etc., and decreases chemical oxygen demand (COD) of the effluent. For hydrogen peroxide, pH, temperature, peroxidase usage, and strength are parameters that must be paid attention to for suitable removal of dyestuff, especially for acid dyes. To improve these methods, hydrogen peroxide and UV light are used for oxygen. Another chemical is  $\text{NaOCl}$  thanks to its  $\text{Cl}^-$  component for breaking amine bond. Also, coagulation is another option in chemical methods for wastewater that cannot form floccules naturally by waiting as in the flocculation method. Particles coagulate with coagulant chemicals, and coagulated particles are eliminated [14]. If the coagulation occurs by using reaction with ions that are released as  $\text{Al}(\text{OH})_3$  and  $\text{Fe}(\text{OH})_3$  from aluminum and iron electrodes, it is known as electrocoagulation [15].

## 2.3 *Biological Refining Methods*

Biological refining is eliminating impurities by decomposing them in a natural cycle of microorganisms. These methods are very advantageous because they are

environmentally-friendly, relatively lower cost, having lower water consumption, and including non-hazardous metabolites. Efficiency depends on pH, temperature, oxygen concentration, amount of microorganisms, and dyestuff because living things are used, and their metabolism is affected by environmental conditions; thus, it needs attention. Biological refining methods are classified into two groups as methods done by microorganisms and enzymes [13]. If the enzymes such as ligninase (toxicity removal), cellulase (breaking cellulose particles into glucose), peroxidase (removal of color and peroxides), and dehalogenase (dechlorination and removal of chlorophenols) that are used by microorganisms or can degrade the impurities in the wastewater are directly added into the refining baths, then it is enzyme-type methods. Enzymes are specific to their substrates and only deal with them, and if the conditions as temperature, pH, etc., are suitable, they cannot be deformed, and they can be used more than once [16]. If the microorganisms directly used in refining and enzymes that have in their metabolic reactions are used, then it is microorganism-type refining. Also, refining methods with microorganisms can be divided into two subtitles as aerobic and anaerobic refining. For example, bacterial refining can be aerobic or anaerobic, while fungi refining is aerobic generally [17].

Aerobic biological refining methods degrade or convert impurities into less harmful materials by using oxygen with a microorganism, especially at low-strength wastewater which has lower COD than 1000 mg/L [17]. Aerobic refining is very effective, especially at decolorization of dyestuffs by using microorganisms as *Pseudomonas fluorescens*, *Bacillus fusiformis*, *Staphylococcus aureus*, *Enterococcus gallinarum*, *Brevibacillus laterosporus*, etc. [18]. These methods are very good at less odor production and efficient removing, but oxygen need, mud production, clogging, and costs can be adverse sides of aerobic refining methods.

Anaerobic biological treatment does not need oxygen in the degradation of impurities at high strength wastewater which has higher COD than 4000 mg/L. Producing natural gas like methane, having low mud production, and cost can be favorable sides of anaerobic refining methods [17]. With the light of this information, if there is high-strength water, firstly, anaerobic methods are applied, and then, aerobic methods can be added, after the organic material amount of the wastewater is suitable for aerobic microorganisms, to yield the best sides of both methods.

All types of refining methods have some advantages and disadvantages compared to each other, but using alternative environmentally-friendly refining processes that decrease the process amount, chemical, and refining waste, refining cost and time are very valuable and important for total production and environmental concern. It provides an increase in the application of refining with better and more desired options. If refining is easy and economical or it has any advantages over the classical processes, then the refining gains importance, and more companies would like to attend the environmental concern. In most cases, methods or multifunctional materials that can offer all these benefits in a single step are the needs of future applications with growing technologies and keeping fast fashion cycles in a good manner. For these reasons, many studies are concentrated on the development of novel refining processes and multifunctional materials for refining.

### 3 Adsorbent Materials

Adsorbent material usage is one of the alternative refinement methods. They show promise for holding dyestuff and chemical agents. The holding ability of materials depends on the adsorption capacity and ionic characteristics. Thanks to the suitable interaction between adsorbed chemical and adsorbent, the chemical is removed from wastewater and kept in the adsorbent. Adsorbent materials can be natural or polymer-based, i.e., more synthetic ones, but behaviors are the same in principle.

#### 3.1 Properties

The physical properties of adsorbents can be changed according to their raw materials and desired conditions of end usage. First, physical property can be the shape of adsorbent as pellet, rod, molding, or monolith, while the other one is size such as 0.25 and 5 mm of the radius, but pore amount and size are also indicative. To be an effective adsorbent, it must have high stability for thermally and mechanically to withstand the process conditions and showing the same behavior without any loss, structure with pores that make surface area higher, and high capacity to adsorb enough material [19].

#### 3.2 Working Mechanism

Collecting a material or chemical in the interface of a host material is known as adsorption. The substance that is collected is called adsorbate, while the collecting material is adsorbent, and both of them can be solid, liquid, or gas [20]. This collection mechanism changes according to the interaction between adsorbent and adsorbate as chemical or physical. Due to the interaction type, the type of adsorption changes. Physisorption is done by using physical interactions which is the result of energy and entropy decrease as Van der Waals forces, surface adsorption, hydrophobic interactions, hydrogen bond, diffusion into the material network, and these types of adsorptions can be reversible. Chemisorption is done by chemical interactions as ionic or covalent bonding, complexation (coordination), proton displacement, chelation, electrostatic interactions, oxidation/reduction, inclusion complex formation, and it is irreversible, and it has a high range of heat because of strong chemical bonding. Adsorptions are affected by temperature, the concentrations of adsorbate and adsorbent [20–22].

### 3.3 Advantages and Disadvantages

Using adsorbent materials in wastewater treatment processes has some disadvantages such as waste production and weak selectivity, but these can be eliminated with various enhancements or reuse strategies. If the waste adsorbent can be reused in some other processes with different forms as filler, dyestuff source, etc., waste products can be decreased or zeroed, and some modifications on adsorbent can enhance the selectivity of the adsorbent. However, adsorbent usage at refining of wastewater has more advantages than disadvantages as high performance, low cost, wide pH range for process conditions, and ease of operation for treatment [23].

## 4 Adsorbent Composite Production

Adsorbent materials have many advantages compared to each other; however, more properties can be needed to maintain the desired conditions, or sometimes, abilities of the adsorbents must be improved for different cases. In these cases, composite structure can come to screen to yield the abilities of at least two materials or to enhance the functions. With composite production stability, applicability, ease of use, working conditions, cost, end-use, and reusability after waste treatment can be improved. Also, the composite structure can offer lower costs and reduction of process time. Composite structures are yielded by combining at least one layered material such as silica balls and nanotubes and one or two polymer-based materials.

The composite structure can be classified into two groups as micro- and nanocomposites. If polymer component covers around the layered structure without any separation of layers, then it is called microcomposite. Nanocomposites are produced when layered structure deforms by enlarging or separation. If the gap between layers enlarge and polymer component penetrates the enlarged gaps, then it is called intercalated nanocomposites. If the layers are totally separated from each other and polymer component covers individual layers thanks to even distribution of layers, then it is named as exfoliated composite. All types of composites can be used according to end uses, characteristics of the wastewaters, and needed removal amounts, but more uniform composites are produced with exfoliated structures [24].

Structures of composite types are given in Fig. 3, and advantages and disadvantages of them are given in Table 1.

There are three main composite production methods with layered units and polymer units as solution intercalation, melt intercalation, and in situ polymerization.

In situ polymerization method uses a layered unit as clay and monomer units. They are putting in together, and after swelling of layers, monomers are located around the separated or enlarged layers thanks to surface energy and polarity of monomers. Then, curing chemicals are added to turn monomers into polymers. When polymerization occurs, then in situ polymerized composite is formed and layers catch up more polar

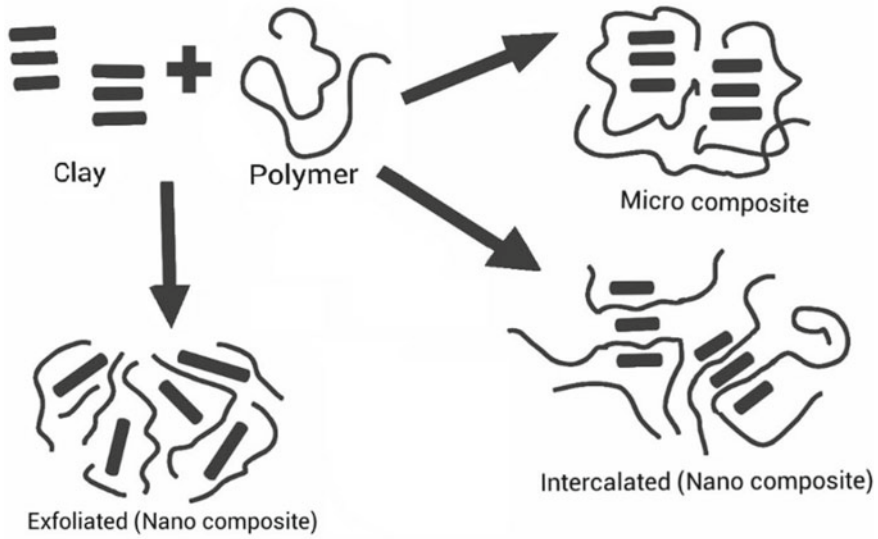


**Fig. 3** Polymer–clay composite structure types

**Table 1** Advantages and disadvantages of composite types

Composite types	Advantages	Disadvantages
Microcomposites	<ul style="list-style-type: none"> <li>• Easier to yield</li> <li>• Showing both properties of polymer and clay in limited amounts</li> </ul>	<ul style="list-style-type: none"> <li>• Minimum clay gap</li> <li>• Less uniformity</li> <li>• Less clay gap</li> <li>• Less polymer entrance</li> <li>• Easier deformation</li> </ul>
Intercalated	<ul style="list-style-type: none"> <li>• Nanocomposite</li> <li>• Bigger clay gap than microcomposite</li> <li>• Better distribution than microcomposite</li> <li>• Uniform properties than micro composite</li> <li>• Better adsorption and performance than microcomposite</li> </ul>	<ul style="list-style-type: none"> <li>• Harder to produce</li> <li>• Needs more time or chemicals to produce make it in short time</li> </ul>
Exfoliated	<ul style="list-style-type: none"> <li>• Nanocomposite</li> <li>• Bigger clay gap than intercalated</li> <li>• Better distribution than intercalated</li> <li>• Uniform properties than intercalated</li> <li>• Best adsorption and performance</li> </ul>	<ul style="list-style-type: none"> <li>• Hardest to produce</li> <li>• Needs more time or chemicals to produce make it in short time</li> </ul>



**Table 2** Advantages and disadvantages of production methods

Production method	Advantages	Disadvantages
In situ polymerization	<ul style="list-style-type: none"> <li>• Suitable for monomers that are sensitive to solutions and temperature</li> </ul>	<ul style="list-style-type: none"> <li>• Extra curing chemicals</li> <li>• Must satisfy polymerization conditions</li> <li>• Less pore enlarging</li> </ul>
Solution intercalation	<ul style="list-style-type: none"> <li>• More pore enlarging than in situ</li> <li>• More uniform distribution than in situ</li> <li>• Intercalated composites</li> </ul>	<ul style="list-style-type: none"> <li>• Chemical release due to solution evaporation</li> <li>• Not suitable for non-soluble or sensitive polymers</li> </ul>
Melt intercalation	<ul style="list-style-type: none"> <li>• More pore enlarging than in situ</li> <li>• More uniform distribution than in situ</li> <li>• Intercalated or exfoliated composites</li> </ul>	<ul style="list-style-type: none"> <li>• Not suitable for temperature sensitive polymers</li> </ul>

monomers inside. For this type of composite structure, polymers as polyamide 6 is suitable [25].

Solution intercalation uses a solution to swell the layered units, and dissolved polymers are added to penetrate gaps of layers. When the solution is evaporated, layers catch up the polymer to form intercalated composites [25].

Melt intercalation is a method for layered units and thermoplastic polymers as polyamide, polystyrene, etc. Layered units and melted polymer are mixed, and penetration of polymer is done thanks to the compatibility of polymer and layers. Due to interaction between layers and polymer, the gap enlarging and penetration increases; thus, both intercalated and exfoliated composites can be formed after annealing under glass transition temperature. The advantage of this method is applicability at the extrusion of melt spinning techniques [25].

The advantages and disadvantages of composite production methods are given in Table 2.

## 5 Raw Materials for Natural Adsorbents

Adsorbent materials can be natural or polymer-based, i.e., more synthetic ones. Natural ones offer further benefits for both the environment and human health. Also, recycling is done by using natural sources to produce adsorbents. For these purposes, various alternatives can be used as agricultural wastes [26], clay minerals, cellulose derivatives, active carbon forms from different wastes [27, 28], and their composites. In this case, natural adsorption capacities can be increased by modifying them or combining them as a composite.

Especially, clay is a very useful material as a layered substance. It has a sandwich-like structure made of clay minerals, and the gap between these layers can be increased, and adsorption abilities can be enhanced. Also, inserting a compatible

polymer structure into these gaps can enhance both adsorption capabilities and gives additional physical, chemical, thermal, or mechanical new properties to the clay. Synthetic [29] or natural polymers can be used, but using natural or more biodegradable polymers can be more environmentally-friendly, and it also promotes reuse of the final product in the preceding production steps. These natural polymers can be chitosan [30], carboxymethyl cellulose [31], and other polymers derivatives as well as activated biochars [26].

## 5.1 Clay

According to AIPEA, clay is a natural material that is made up of fine-grained minerals that pass to plastic state in the appropriate water content and became rigid when it is heated or dried [32]. Clay mineral particles, especially the ones that are smectite, are not exactly at a crystalline state. Smectite crystal is better than normal smectite at bringing the silicate layers together. If the montmorillonite particles are examined under an electron microscope, it will be seen that it does not have a regular shape like real crystalline, but it does have an irregular shape like a ripped paper. The core of the particles is covered with irregular silicate layers, bent, and have worn edges [32]. Between layer stacks, the particles have a weak contact at lots of points. At these 'breaking points,' the particles can be easily crashed, or the rheological attitudes may be affected by the mechanic forces [33]. Layered silicates which are generally used at nanocomposites are members of 2:1 structural pyrosilicate family. Crystalline cape structure of 2:1 phyllosilicates is made of a structure that is compressed between tetrahedral layers that join the sides of octahedral layers of magnesium or aluminum hydroxides. The layer thickness is 1 nm, and the lateral diameter varies between 300 (Å) and several microns. These layers get into stack form with the interlayers that are formed between the layers, or the Van der Waals spaces which are known as gates. The isomorphic replacement of  $\text{Si}^{+4}$  with  $\text{Al}^{+3}$  at tetrahedral layers and  $\text{Al}^{+3}$  with  $\text{Mg}^{+2}$  at the octahedral layer generates an excessive negative charge. This negative charge is balanced with the  $\text{Ca}^{+2}$  and  $\text{Na}^{+}$  cations which are placed between the layers. This type of layered silicates is characterized by a middle-level surface charge which can be named as cation exchange capacity (CEC), and this charge varies from one layer to another (see Fig. 4) [32].

Because of the water absorbency property of silicate layers, these layers and water-repellent polymer matrices cannot make good interaction. To avoid this, the clay surfaces should be modified. To modify the clay, there are many types of mechanisms which are getting into reaction with acids, the attachment of organic and inorganic ions, ion exchange using organic and inorganic cations, plasma, ultrasound, burning, etc. Modified clays are also used as rheological control factor, at removing organic pollutants from water, air, and oil with adsorption, and at cosmetics and dyeing fields [34]. The process which makes clays organophilic is done with changing inorganic alkali cations at the clay surface with the desired organic cation. To make the middle

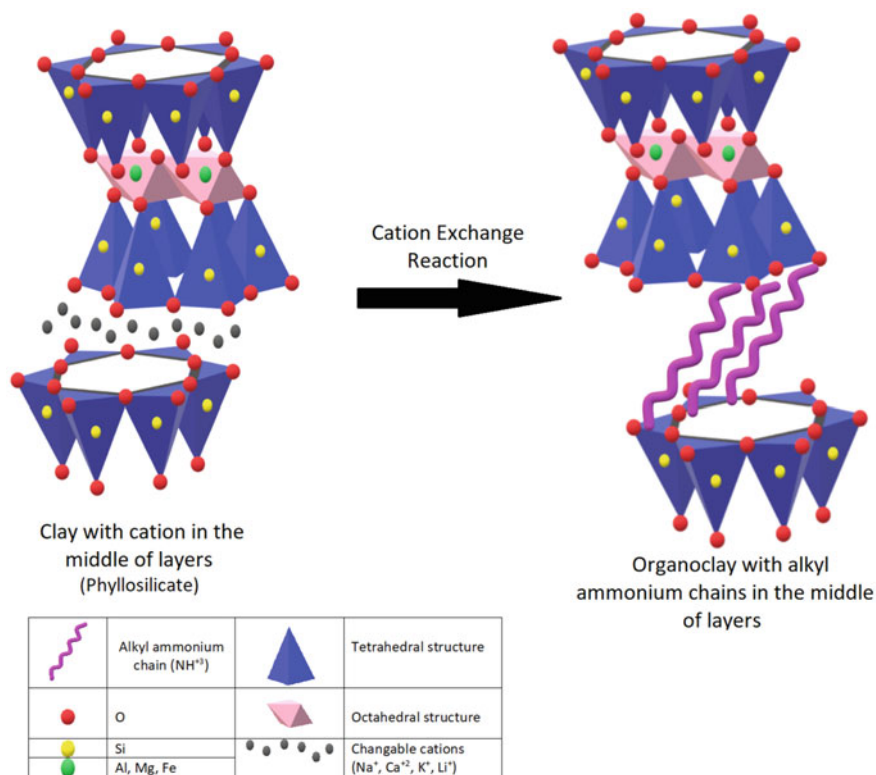


**Fig. 4** Cation exchange reaction between the alkali ammonium ions and layered silicates and between the changeable cations that are inside the polymer-layered silicate nanocomposites

layers more organophilic, hydrate cations at the layers are changed with surface-active agents such as alkali ammonium and alkali phosphonium. The clays that are organically modified, organophilic, and have less surface energy are more compatible with organic polymers so these polymers can get into the middle layers. When the inorganic changeable cations are changed by the organic onium ions which are at the middle layer surfaces, the polarity of the polymer pairs and the surface polarity of the clay and the middle layers of the clays enlarge. Thereby, when organo-modified silicates (organoclays) and ions that have long alkali chains are used, dyestuffs, polymers, and other such chemicals can penetrate more decent [35].

The primary change of metallic cations with organic cations takes place in the aqueous medium. The hydrophobic organic tails going away tendency from the aqueous medium and the tendency to hydration of little inorganic cations in water make a repulsive power for the reaction. The neutralization of the negatively charged layers occurs when the positively charged ions settle inside gaps of the inner layers. Van der Waals force is formed between oxygen and alkali chain. As a result of the primary adsorption of ammonium cations, three cases take place at the inner layer

of the silicate. Molecules can penetrate inner layers due to breaking the water in the inner layer by cations, and it is called hydrophobic adsorption [36]. Van der Waals or hydrophobic interaction can be seen with ammonium cation alkali chains and adsorbed nonpolar molecules at gaps of the inner layer. When organic cations are placed at inner layers, they enlarge layer gaps [37].

Secondary adsorption occurs with Van der Waals forces which are between adsorbed organic molecules and aliphatic chains of changeable cations. That is why the secondary adsorption between molecules that have a low polarity or nonpolar molecules and the long-chained ammonium montmorillonite complexes increases with the increment of the basal gaps and primary adsorbed organic ions amount [38].

At the experiments that are done with alkali ammonium ions that have different alkali chain lengths which are used as a surface-active agent, it is seen that the longer chained alkali ammonium ions (C18-C20) increase the distance between the silicate layers more than the shorter chained alkali ammonium ions (C9-C10). Also, between unary, binary, trilogy, and quart onium ions, quart alkali ammonium ions are the most effective ions that increase one layer distance to another one best [39]. The reason for this is quart ammonium ions make a strong bond with MMT. This force increases with the increment of the displaced components of the ammonium cations [40].

The sum of equivalent mass number of changeable cations (meg) at 100 g of the mineral is called the cation exchange capacity (CEC), and it is a significant parameter to nominate the most suitable clay type for defined end-use [41].

Bentonite which has a general formula of  $\text{Al}_4\text{Si}_8\text{O}_{20}(\text{OH})_4.n\text{H}_2\text{O}$  is clay that shows the strong colloidal property, has high plasticity, has a soft handle, and can be easily shaped. Also, it is an important ion exchanger that swells when it gets into the water, can be activated by acid, darkens the drilling muds, and has wide surface area [42, 43]. Inside the bentonite, there are natural clay minerals such as kaolin and illite and non-clay minerals such as gypsum, quartz, rutile, calcite, dolomite, and volcanic ash. They are found in nature in many colors such as white, gray, green, yellow, and pink [42].

The most distinguishing property of bentonites is holding water inside their structure as presented in Fig. 5. Taking water in its structure and widening its crystalline structure is called swelling. Swelling is directly proportional to the type and amount of cations between the 2:1 segments. At these segments, generally, there are  $\text{Na}^+$  and  $\text{Ca}^{+2}$  cations, and while the  $\text{Na}^+/\text{Ca}^{+2}$  equimolar ratio increases, the swelling also increases [44].

The bentonite which can swell five times when in contact with water is accepted as good in trade, but better bentonites can swell 10–20 times. The swelling property of bentonite is lost after a particular temperature. The bentonite which has high ionization density has a dry density of 2.7–2.8 g/cm<sup>3</sup>, and the dust form has a density of 1.6–1.7 g/cm<sup>3</sup> [42].

Intercalation of dye molecules (especially organic dyes) in between layers of inorganic clays are done with different purposes and applications. Bergman et al. reported the metachromatic behavior of methylene blue that is cationic dye stuff on clay which is Wyoming montmorillonite as first [38]. After that study, interaction between organic molecules and clay particles is researched with many studies.

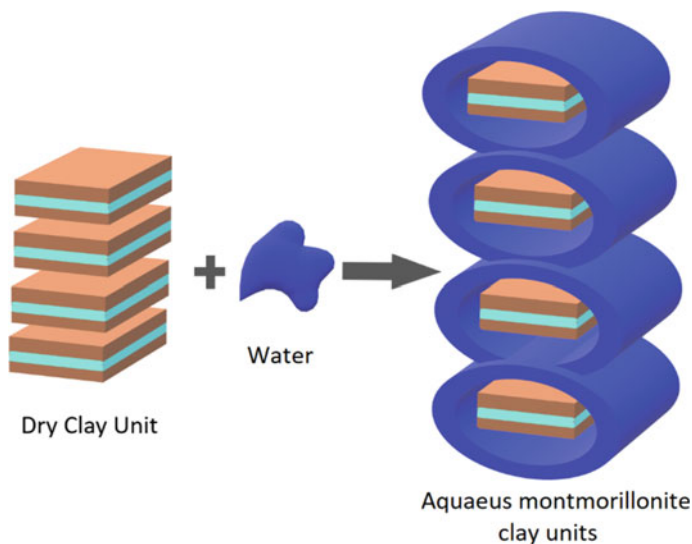


**Fig. 5** Change in the structure of bentonite when it is exposed to water

Bannani Karim et al. used Morocco clay which is characterized by diffraction as adsorbent material for searching the adsorption kinetic of basic red (BR46) with isotherm and thermodynamic parameter at different dye at different dye concentrations, adsorbent weight, and pH. Chemical composition of clay was identified by using XRF as 53.11% SiO<sub>2</sub>, 16.95% Al<sub>2</sub>O<sub>3</sub>, 5.94% Fe<sub>2</sub>O<sub>3</sub>, 3.51% CaO, 2.51% MgO, 0.2% SO<sub>3</sub>, 4.64% K<sub>2</sub>O, 0.26% Na<sub>2</sub>O, and 0.09% P<sub>2</sub>O<sub>5</sub>. After the experiments increasing adsorption amount was observed with increasing initial pH and dye concentrations and with 40 mg adsorbent maximum removal was seen [45].

Vimonses et al. worked with three different natural clays: bentonite, kaolin and zeolite, and a material that is produced by burning of the clays with its effects for removing anionic dyes from aqueous solutions. Experiments were analyzed with Brunauer–Emmett–Teller (BET), differential temperature analysis (DTA), thermogravimetric analysis (TGA), and UV-visible spectrophotometer. According to results, mixtures 2, 6, and 9 had the most suitable removing capacity. High dye removing efficiency was yield with burning at 300 °C for 1.5 h. Increasing the ratio of removing dye was observed with increasing initial dye concentration [46].

Li et al. studied with the purpose of understanding principles of swelling clays (montmorillonite SWy-2, Na montmorillonite, SHCa-1) at removing methylene blue, explaining the mechanism of methylene blue adsorption to verify the usage of methylene blue for specific surface area (SSA) and cation exchange capacity (CEC) determination. With the use of UV-visible spectrophotometer, X-ray diffraction (XRD), chromatography, FTIR, and TG-DTG analyses, it is observed that load intensity was a limiting factor for MB adsorption and swelling clays with high CEC adsorbed more MB [47].

Ten and Li evaluated adsorption of methylene orange52 ( $C_{14}H_{14}N_3NaO_3S$ ) by using raw and activated montmorillonite with HCl. With using BET and XRD at experiments, it was examined that adsorption capacity of modified clay with HCl because of substitution of  $Fe^{2+}$  and  $Al^{3+}$  ions at montmorillonite with  $H^+$  ions as a result of activation with HCl, the distance between layers of clays are decreased, and crystallization degree of raw clay is more than activated clay with HCl [48].

Karagözoğlu et al. worked on kinetic, isotherm, and thermodynamic parameters of Astrazon Blue (FGRL) adsorption from aqueous solutions with different concentrations between 100 and 300 mg/L, temperature (303–323 °K) and adsorbent dosages by using sepiolite, flying clay, and the carbonated seed of apricot and analyzed by using Perkin Elmer UV-visible spectrophotometer. It was observed that the adsorbed dyestuff amount for each clay increased when initial dye concentration and adsorbent amount increase. With the use of thermodynamic parameters, it also came to light that adsorption amount increased when the temperature was increased, and adsorption processes are endothermic [49].

Gürses et al. examined changes of remaining methylene blue which is a cationic dyestuff from aqueous solutions by using montmorillonite and nontronite clay according to pH, temperature, initial dye concentration, mixture ratio, and adsorbent amount. Firstly, the chemical composition of clay was determined. In this study, it was understood that adsorption tends to be a balance of approximately 60 min. Maximum dye removing with 100 mg/L initial concentration was 58.2 mg/g. Increasing in dye concentration increased the adsorption capacity. Adsorption capacity increased at the range of 20–40 °C, while it decreased at the range of 40–60 °C. At pH 3 and 7, minimum adsorption value was observed, while the maximum adsorption value was seen at pH 1 and 5.6 [50].

Weng and Pan searched on methylene blue adsorption characteristics of active clay on the mud that was formed from a waste of an oil producer for food. The structure of clay was determined by SEM. Removing of methylene blue was increased with increased pH. Adsorption of methylene blue was increased with increased temperature. The maximum adsorption capacity of active clay which is treated under high pressure is  $2.44 \times 10^{-4}$  mol/g, pH 5.5, and 25 °C [51].

## 5.2 Cellulose and Its Derivatives

Cellulose is a widely used polymer around the world in various forms because it is a very common polymer, and it is easy to reach work on. It has many types, and all modifications can be done according to the usage.

Carboxymethyl cellulose (CMC) is anionic water-soluble cellulose ether that is used in various industries including personal care, food, chemicals, pharmaceuticals, textile, drilling fluids as well as paper. Carboxymethyl cellulose (CMC) is nearly always present in the market as the sodium salt of carboxymethyl cellulose (Na-CMC), and it is water-soluble and preferred to use in this form, a property enhanced by its ionic nature. When it is acidic, it is insoluble. It has an average degree of

substitution (DS) of 0.75, and 4000 cP is its maximum viscosity for 1% solution. The viscosity of CMC increases below pH 4, due to the presence of sodium salt of weak acid groups, when free acid is formed. If all COOH groups of CMC have been reacted for salt formation, its pH would be 8.25. Na-CMC has higher moisture absorption than other cellulose ethers, directly proportional to its DS, thanks to its ionic character [34]. Thanks to its strong anionic character, Na-CMC is also used for removal of cationic dyestuff from textile dyeing effluents, and its usefulness for removal of various dyestuffs is presented [52, 53].

The first step is treating cotton fiber with sodium hydroxide. In this step, negatively charged oxygen atom is produced by removing the hydrogen atom from the hydroxyl group, and a reactive form of cellulose is produced which is called alkali or soda cellulose. These sites of cellulose are used for reaction of chloroacetate. Secondly, soda cellulose is treated with the sodium salt of chloroacetic acid under alkaline conditions. As shown in Fig. 6, hydroxyl groups of cellulose chain are using for reaction of chloroacetate to produce an ether linkage, and hydrochloric acid is formed at the end of the reaction [54, 55]. The first substitution occurs on the primary alcohols, and then, the second substitution is seen on the secondary alcohols. The substitution will occur more rapidly in the regions where crystallinity is lower. Moreover, very inhomogeneous carboxymethyl group distribution is seen in the early stages of the reaction. Carboxymethyl group distribution becomes more homogeneous when the reaction time is extended [56].

The resulting material which is carboxymethyl cellulose is very swellable and has highly acidic carboxyl groups that enhance the values in elongation at break, moisture regain, soil release, water retention, and tensile strength [57, 58]. CMC that is suitable for being an adsorbent for dye removal from aqueous solution in a broader pH range has low DS value, and it is water insoluble [59].

Salama and his friends examined the removal of methyl orange dye from aqueous solutions by using Carboxymethyl cellulose-g-poly(2-(dimethylamino) ethyl methacrylate) (CMC-g-PDMAEMA) in hydrogel form as an adsorbent and finding the adsorption kinetics of CMC-g-PDMAEMA. At the study, high viscosity CMC sodium salt is used, and FTIR spectroscopy is done to observe the structural changes of CMC-g-PDMAEMA and CMC hydrogel, and the effect of pH on dye adsorption is observed. As a result of the study, increase of the pH decreases the adsorption capacity of the hydrogel, and it is seen that the adsorption process occurs by the chemical interaction between the bioadsorbent surfaces and the dyestuff [60].

Cai et al. had research on the hydrolysis degree effect of hydrolyzed polyacrylamide grafted carboxymethyl cellulose (CMC-g-HPAM) on dye removal efficiency. In the study, series of CMC-g-HPAM is produced and it is used as flocculants to remove methylene blue dye from aqueous solution. As a result, using FTIR-spectroscopy, characterization of CMC-g-HPAM is done. The flocculation performance of the CMC-g-PAM, CMC-g-HPAM and CMC are compared, and CMC-g-HPAM made higher flocculation performance for removal of methylene blue [61].

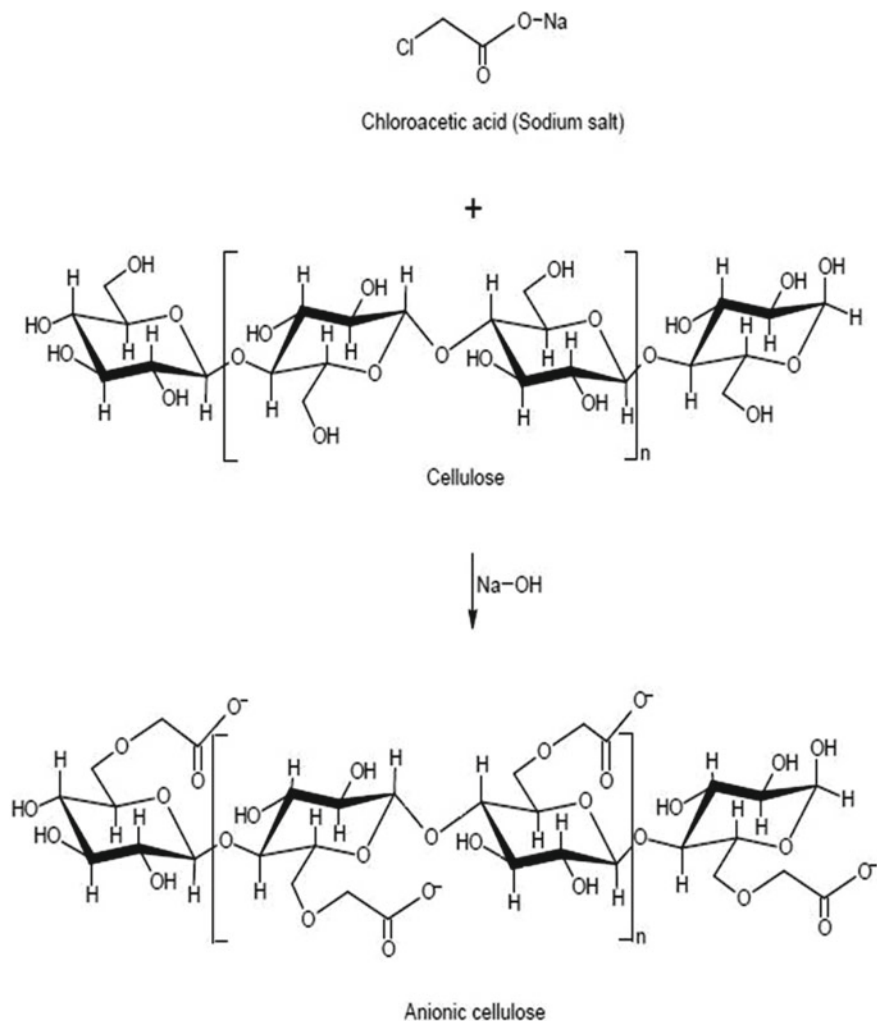


**Fig. 6** Reactions of cellulose with CAA

Zhang et al. had researched the sorption behavior of carboxymethyl cellulose for methylene blue and its reuse in secondary sorption. In the study, the carboxymethyl cellulose is prepared, and the sorption of methylene blue is done at different pHs. FTIR, SEM, and 'Y' potential measurement test methods are used to find that methylene blue removal is pH dependent but temperature independent [52].

Wang et al. studied on the subject of synthesizing carboxymethyl cellulose/organic montmorillonite (CMC/OMMT) nanocomposite at different weight ratios and using the synthesized nanocomposite at the removal of Congo red dye. At the experiment, CMC/OMMT nanocomposite preparation and adsorption experiments are



done. FTIR, XRD, TEM, SEM, TG, and UV-vis tests are done to figure out the best absorbency of Congo red dye. As a result, the best absorbency occurred at a weight ratio of CMC to OMMT was 1:1, having a reaction temperature of 60 °C and a reaction time of 6 h [53].

### 5.3 Chitosan and Its Derivatives

Chitosan is a soluble form of chitin which has the second biggest polymer supply in the world following cellulose. To form chitosan, approximately, 50% of chitin is deacetylated (see Fig. 7). This deacetylation amount that is mentioned at the chitosan definition can change according to polymer origin of chitin polysaccharide. When  $\text{-NH}_2$  group in D-glucosamine is protonated, chitosan turns into polyelectrolyte forms in an acidic media. It has many usage areas including protein and depollution recovery as flocculent. It is very unique material due to being the only cationic pseudo-natural polymer. Thanks to the solubility property of chitosan, it is applicable in many areas with various forms [62].

Szygula et al. studied the removal of Acid Black 1, Reactive Black 5, and Acid Violet 5 which are sulfonated azo dyes via coagulation with chitosan. At acidic solutions, removing of dyestuff was related to the neutralization of charges. It was obvious that with the use of chitosan, the efficiency of amine groups was increased, while the contact time needed to reach equilibrium was decreased, and the coagulation–flocculation mechanism was affected by initial pH values and the amount of coagulant, while stirring did not make any change [64].

Wang and Wang evaluated the adsorption behavior of Congo red dye which is an anionic dyestuff by using a nanocomposite that includes *N*, *O*-carboxymethyl chitosan/montmorillonite with the aim of recovery of anionic dyestuff and effects of molar ratio on recovery. They used FTIR, XRD, and SEM for testing their results. According to SEM results when molar ratio was increased, the adsorption capacity also increased, and maximum adsorption was seen at a 5:1 ratio. Besides, decreasing pH increased the dye adsorption thanks to increasing the attraction between nanocomposite and dyestuff, and when the temperature was increased, adsorption capacity increased because the composite swelled and bigger space was opened for bigger dyestuffs. Finally, it was observed that the adsorption equilibrium of Congo red dyestuff by *N*, *O*-CMC-MMT was well fit with Langmuir and pseudo-second-order models [65].

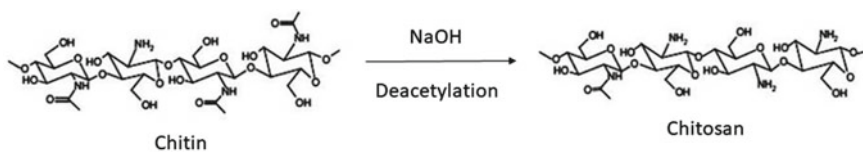


Fig. 7 Chitin and chitosan structure with deacetylation reaction

Bhattacharyya and Ray worked on removing synthetic dyes from waters via micro- and nanocomposites of bentonite filled with chitosan and acrylic copolymer. They used FTIR, XRD, SEM, DTA, and TGA for the evaluation of their results. The best swelling ratio in water was yield with a comonomer ratio of acrylic acid and acrylamide 7.5:1, and the highest adsorption for methyl violet and Congo red dye was yield with chitosan which is 12 wt% of total monomer weight in a polymethacrylic acid gel. The highest swelling of clay including hydrogel samples was 2 wt% nano-sized clay (NF2) and 4 wt% micro-sized clay (MF4). When all samples were treated with methyl violet and malachite green dyes with different concentrations, adsorption amount from high to low was, respectively, NF2, MF4, and F0. Furthermore, it was seen that methyl violet adsorption is less than malachite green, and adsorption characteristics were well-fitting with first- and second-order kinetics, and the combined Langmuir–Freundlich model [66].

Bulut and Karaer examined adsorption of a composite including cross-linked chitosan and bentonite for methylene blue which is a cationic dyestuff to remove the dyestuff from aqueous solution. By using FTIR, it was seen that the maximum adsorption capacity of the dyestuff was 95.24 mg/g at 298 °K, and thermodynamic and kinetics of the process were well-fitting with Langmuir model [67].

Liua et al. used a composite including cross-linked chitosan and bentonite to removing Amino Black 10B(AB10B) which is an anionic azo dye and adsorption behavior. The results of the study were tested with FTIR, SEM, XRD, and TGA. It was observed that removing AB10B decreased when pH and dye concentration of the solution were increased while the removal increased when contact time and dosage of adsorbent were increased. Time for reaching the equilibrium was extended when the initial dye concentration was increased. Moreover, kinetic and equilibrium behavior were well-fitting, respectively, with the Langmuir model and pseudo-second-order kinetic model. Maximum adsorption capacity values were yield at 313 °K with natural pH as 350.9 mg/g and at 293 °K with pH 2 as 323.6 mg/g. As understood from this data, relatively high temperatures and low pH are more suitable for adsorption of the dyestuff [68].

Guo et al. studied for removing of dyestuff from wastewater by a composite including chitosan and CTAB-modified bentonite. 1CTS–10 CTAB-bentonite was prepared and used for weak acid scarlet adsorption which resulted in more than 85% adsorption efficiency; thus, it was a very good adsorbent composite that was reusable for three cycles. For the testing stage, FTIR and XRD are used, and it was seen that the adsorption behavior of the composite was well-fitting with Langmuir and Temkin models [69].

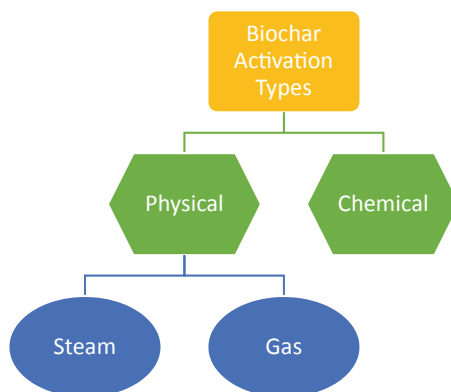
Mahdavinia and Karami synthesized a nanocomposite that is magnetic carboxymethyl chitosan-poly(acrylamide)/laponite RD with improved dye adsorption capacity. They used X-ray diffraction, transmittance electron microscopy, thermogravimetric analysis, vibrating sample magnetometer, and scanning electron microscopy techniques for the testing stage. It was clear that water absorbency is related to magnetic laponite RD content, and when the amount of magnetic clay increased, the swelling capacity and salt sensitivity decreased, while dye removing and adsorption capacity at acidic medium increased. Besides, analyses were done

according to Langmuir and Freundlich models, and it was understood that the composite could be used many times with the same dye adsorption capacity [70].

#### 5.4 Activated Biochars and Alternative Biomaterials

Biomass is turned into a carbon-based end product by the pyrolysis process, and as a result, biochar is formed. It has some advantages as being a low-cost product and providing a recycle for the waste of agriculture and forest, so it adds value to waste [71]. Biomass is decomposed in oxygen-free media with very high temperatures as 350–650 °C. Biochar is produced in a charcoal form with volatile gases in two forms. The first one is gas that could turn into bio-oil with condensation, and the second one is gas as CO, CO<sub>2</sub>, CH<sub>4</sub>, and H<sub>2</sub> that cannot turn into bio-oil. Pyrolysis can be categorized as slow, intermediate, and fast due to its heating rate, maximum temperature, and time, and with differences, characteristics of biochar can be changed. The slow one is more advantages because of being simple and suitable for agricultural products and small production amounts, but other options can be selected according to the needs of the end product and usage area [72]. To enhance the properties of biochar as pore and surface area increasing, functional group adding, and enhancing the capacity, some modification can be done by some additives (see Fig. 8). If this modification is chemical, it is known as chemical activation, and it can enhance the full process as decreasing the steps of the process (carbonization + activation), lowering the needed temperatures for desired properties, and increasing the capacity of catalytic oxidation [71]. Also activation can be done via physical methods such as steam or gas activation. Steam activation is the application of steam after thermal carbonization. If the activation is done by using CO<sub>2</sub>, N<sub>2</sub>, NH<sub>3</sub>, air, O<sub>2</sub> gases, or a mixture of these, then it is gas activation. Both of them can enhance the porosity but micro- or mesoporous structures by gas activation [73].

**Fig. 8** Activation methods of biochar



Active biochar/carbon structures that have well-distributed pores, high surface area, and good surface properties use the physisorption methods but oxygen around the surface can enhance the absorption according to adsorbate characteristics.

Radaei et al. produced activated carbon with 572.53 m<sup>2</sup>/g surface area from the waste of pomegranate by using 37% phosphoric acid acids for the removal of Reactive Blue 19 dyestuffs. Their adsorbent whose amount is 3.5 g/L could adsorb maximum 98.16% dyestuff under conditions with pH 11, 5 min of contact time, and 300 mg/L initial dyestuff concentration [27].

Kahka and Piri used a waste of *Citrullus colocynthis* which is a kind of watermelon, to yield a bio-adsorbent for reactive red dyestuff. The waste of the plant is modified by using sodium hypochlorite. The best condition for maximum adsorption is with pH 2, 1.75 g/L initial adsorbent amount, 90 mg/L initial dyestuff concentration, and 70 min of contact time, and they could yield 36 mg/L adsorption capacity [28].

Jin et al. convert municipal solid wastes into biochar by using pyrolysis for removing arsenic (As(V)) that is a heavy metal. They examined the effects of potassium hydroxide on the activation of biochar. They observed that activated form has very high adsorption capacity than nonactivated biochar as 30.98 mg/g which is 1.3 times of it because this activation brings functional groups and more surface area to the pure biochar [71].

Rajapaksha et al. formed biochar with steam activation from an invasive plant (*Sicyos angulatus* L.) for sulfamethazine (SMT) in water. They observed that the most effective parameter is process pH for biochar properties. The best adsorption which is 37.7 mg/g is yielded at activated one with pH 3, and this capacity referred to 55% growth compared to pure biochar [74].

Li et al. investigate the formation of biochar from *Enteromorpha prolifera* (EPAC) in one step with oily sludge addition for methylene blue dyestuff. With this production, they yielded better surface area, pore, and adsorption capacity as 910 mg/g and prove the importance of pH levels [75].

Zhang and Lu studied on biochar formation from coconut shell at 450 degree for 2 h with wet impregnation and calcination for Reactive Brilliant Blue KN-R remove. Their biochar is modified with TiO<sub>2</sub>, and its crystals are dispersed suitably and removal ability enhanced than untreated [76].

Ramie bars are used by Cai et al. for removing Safranin T. Their adsorbent is prepared by pyrolysis of ramie at 500 degree for 20 h after titanium butoxide is treated. With this modification, pore volume, surface area, and adsorption increase than pristine biochar thanks to homogenous TiO<sub>2</sub> particles [77].

Chicken feathers are a source of biochar that belongs to Li et al. for Rhodamine B removal. They used pyrolysis for 1 h at 450 degrees with tetrabutyl titanate treatment. This method increased surface area and degradation rate due to the TiO<sub>2</sub> particle surface of biochar [78].

## 5.5 Other Polymers

Other polymers, especially biopolymers for the natural cycle, are mostly used in the form of hydrogels, bead pellets, etc., for being an adsorbent, and they have very advantageous usage in wastewater refinement processes of the textile industry. Some studies are summarized below:

Ekici and Guntekin assert that low-temperature dyestuff removal can be done with their hydrogel. They could yield 111–122 mg dyestuff adsorption per gram of adsorbent by using polyampholytes (PAHs) hydrogels in simultaneous Remazol-type dyestuff removal studies at 35 °C and 20 °C. They had dyestuff adsorption ability from 94 to 98% [79].

Inal et al. studied on methylene blue dyestuff removal by using hydrogels that are acrylamide–crotonic acid. When hydrogels which consist of only acrylamide, adsorption can be increased by increasing pH. Maximum adsorption was yielded with pH 9 for 300-min treatment. For acrylamide–crotonic acid hydrogels, pH 8 causes a decreased adsorption, while pH 7, 9, and 10 bring similar adsorption. When crotonic acid amount in hydrogel structure increased, adsorption amount increased. Desorption can be done by treating colored hydrogels at pH 2 HCl-KCl buffer solution for one hour. Also, their hydrogel did not lose adsorption capacity when it is used 20 times repeatedly [80].

Sudarsan et al. suggested using reusable hydrogels which consist of sodium alginate for methylene blue removal procedure. Condensation of ethylene glycol and acrylic acid and then free-radical polymerization were steps for introducing ionic pendant functionalities on sodium alginate, and pH-tunable hydrogels were prepared. They observed higher swelling at higher pH. Removal amount of tried hydrogels is between 80 and 98%. Also, up to 90% desorption of hydrogels could be done at 0.1 N HCl solution, and they could be reused [81].

Ma and Zhang investigated the adsorption of alizarin red S (ARS) by Fe/Al–alginate composite hydrogel electrode electrocoagulation (EC). They added 2.0% (w/v) sodium alginate solution with scrap iron to 5.0% (w/v)  $\text{Ca}^{2+}$  ( $\text{CaCl}_2 \cdot 2\text{H}_2\text{O}$ ) which is hardening solution at 60 °C for 2 h and then storing at 3% (w/v)  $\text{Al}^{3+}$  ( $\text{AlCl}_3$ ) for the dye degradation study. Initial pH 3 with  $\text{O}_2$  is suitable for the optimal degradation of ARS. COD is removed by the electrode application up to 90% efficiency. Maximum color removal is 99%, and 30 min is the optimum time for electrolysis. These electrodes have better results compared to conventional ones, and they suggest using the ultrasonic application because it accelerates electrocoagulation [82].

Ilgin and Ozay emphasized that they produced hydrogels from poly(acrylamide-co-methacrylamido-4-(2-aminoethyl) morpholine) and poly(Aam-c-MAEM) with four different molar ratios (nAam/nMAEM: 100/0, 95/5, 90/10, 80/20) by using single-step free-radical aqueous polymerization. The produced hydrogel is used for reactive orange (RO) removal which is anionic dyestuff. They used 0.1 mol% MBA as a cross-linker. When the comonomer ratio and initial adsorbent amount increased, the removal ability increased; while temperature and pH of solution increased, the removal percent decreased. Also, maximum removal was done by distilled water.

Salt amount affects removal amount adversely such that Al ion presence in solution has the worst removal performance [83].

Rahimdokht et al. synthesized a photocatalyst as TiO<sub>2</sub>/gum tragacanth hydrogel for the methylene blue dyestuff removal from polluted solutions. The hydrogel was produced by sonication of TiO<sub>2</sub> nanoparticles into gum tragacanth, and they added glutaraldehyde as a cross-linking agent. They yielded maximum efficiency as 88.86% with a pH of 9.02 a 124.34 min removal time [84].

Patel and Patel assert that their Cationic Poly [acrylamide/*N*-vinyl pyrrolidone/*N,N*-diallylpyrrolidinium bromide] [AAm/NVP/DAPB] hydrogels are produced by free-radical solution polymerization with a cross-linker (*N,N*-methylene bisacrylamide), initiator (2,2'-azobis (2-methylpropionamide) dihydrochloride). They used the hydrogels for removal of acid dyestuffs as Acid Yellow, Orange-II and Reactive Golden Yellow. The best swelling was observed at YH5 with higher DAPB amount, and dyestuff removing performance is seen as Acid Yellow < Orange-II < Reactive Golden Yellow [85].

Dey et al. studied on semi-IPN and ester-based hydrogels production for wastewater refining treatments as an adsorbent. They produced their comonomer cross-linker that was poly(ethylene glycol) di-itaconate by functionalizing poly(ethylene glycol) (PEG 1500) with itaconic acid using melt esterification. Then, copolymerization was done by using acrylamide and methylene bisacrylamide. For storage modulus, dyestuff adsorption ability, and the anti-fungal, better results were yielded with ester-based gel than semi-IPN-type gels. Regardless of medium pH, swelling of hydrogel decreased when the PEG amount was increased at semi-IPN gels; thus, dyestuff adsorption decreased [86].

## 5.6 Comparison of All Adsorbent Materials

Clay is easily findable because its source is very high in nature, and it is ready to adsorb thanks to high surface area, but it is very good to modify and produce a composite with many polymer sources. Cellulose and chitosan derivatives are a good example of composite production, especially with clay. They have also very wide sources, but cellulose derivatives have more sources than chitosan derivatives in nature. Chitosan is more likely to form cationic adsorbents, while cellulose derivative is close to slightly anionic characteristics. For further usages of cellulose derivate-based adsorbents, usage conditions, especially temperature, are very important because they are easily flammable, while chitosan derivatives provide flame-retardancy effect. Chitosan and cellulose derivatives need attention for solubility, and they must be turned into suitable forms. Also, chitosan has some viscosity problems because of forming a gel-like solution even with water; thus, it needs extra control in processes. However, it has a very valuable advantage as an antibacterial behavior for further reuse applications of an adsorbent. Biochars are also natural sources, but it needs extra processes to turn them into suitable forms of adsorbent materials and activation of the adsorbent. These processes must need attention not to lose the quality of the

adsorbent. Biopolymers are also good alternatives for using them as hydrogel form or in a composite structure, but adsorption characteristics must be enhanced. Also, biopolymers are the best option for further usages because they are ready to form or reshape in different conditions, but their adsorption is limited.

With the lights of all information, Table 3 is produced for comparison of all adsorbent materials. All of them are valuable and have many different advantages with prior behaviors specific to different usages. However, it is better to combine them in a composite according to characteristics of the waste that would be refined to yield better adsorption and more refining. All of them have reuse option with different conditions that can serve a better cycle for the environment.

**Table 3** Comparison of all mentioned adsorbent materials

Materials	Advantages	Disadvantages
Clay	<ul style="list-style-type: none"> <li>• Natural material with high amount of sources</li> <li>• Ready to adsorb in nature</li> <li>• Cheap</li> <li>• Easy to find</li> <li>• Can be modified easily</li> <li>• Good matrix for composite structures</li> <li>• High surface area</li> <li>• Suitable to many materials</li> </ul>	<ul style="list-style-type: none"> <li>• Need modification to yield high adsorption values than in nature</li> <li>• Only dust form</li> <li>• Non-soluble</li> <li>• Aggregation problem</li> </ul>
Cellulose derivatives	<ul style="list-style-type: none"> <li>• Natural polymer</li> <li>• High source in nature</li> <li>• Can be modified to form composites</li> <li>• Alternative forms provides recycle</li> </ul>	<ul style="list-style-type: none"> <li>• Easily flammable</li> <li>• Non-soluble if not modified</li> </ul>
Chitosan derivatives	<ul style="list-style-type: none"> <li>• Pseudo-plastic structure</li> <li>• Natural polymer</li> <li>• Antibacterial future</li> <li>• Can be amphoteric if it is modified</li> <li>• Flame-retardancy</li> <li>• Can be used as gel or dust form</li> </ul>	<ul style="list-style-type: none"> <li>• Must control viscosity of the solutions</li> <li>• Non-soluble if not modified</li> </ul>
Biochar	<ul style="list-style-type: none"> <li>• Produced from natural sources</li> <li>• Almost all living wastes can be used as source</li> <li>• Provide recycle during production of biochar</li> <li>• High and enhanceable surface area</li> </ul>	<ul style="list-style-type: none"> <li>• Need extra process to turn in to biochar</li> <li>• Need activation</li> <li>• Adsorption values must be increased</li> <li>• Carbonizing needs attention</li> </ul>
Biopolymers	<ul style="list-style-type: none"> <li>• Natural or bio-based materials</li> <li>• Easy to reuse after adsorption by giving shape</li> </ul>	<ul style="list-style-type: none"> <li>• Needs extra process to use at adsorption</li> <li>• Limited usage according to its polymer characteristics</li> </ul>

## 6 An Alternative Composite Structure Study

In the present composite structure study, firstly, chitosan modification is done to turn it into carboxymethyl chitosan. 50 mL NaOH solution (20 wt%) is used to swell 5 g chitosan for 12 h and filtration applied to the mixture. Filtered chitosan is taken into a volumetric flask, and 50 mL ethyl alcohol is added to stir for 30 min. 4 g butanetetracarboxylic acid addition is done, and the mixture is stirred for half an hour 30 min more. After that, cooling is done to make the temperature of the mixture 20 °C, and the mixture is kept at 20 °C for 1 h. Filtration is applied to the treated sample, and distilled water is used for dissolving filtered sample. Further, acetic acid is added to set pH as 7.0. The mixture is poured into ethyl alcohol to yield foam gel precipitation, and pouring is applied to take the white precipitation into Petri dishes. Ethanol with a ratio of 70% is used to wash the precipitate for three times by using, and ethyl alcohol is used for one time. Drying of the CMCTS is done by putting Petri dishes into the oven at 80 °C. Finally, CMCTS is turned into dust form by scraping off from the Petri dishes [30].

In the case of a clay and modified chitosan combination, firstly, 1 g clay is swelled at the 100 mL distilled water. Secondly, the CMCTS solution is prepared with the distilled water which refers to a 5:1 weight ratio of CMCTS-clay at nanocomposite. Further, the CMCTS solution and clay suspension is mixed slowly, and stirring is done at 60 °C for 6 h. Then, washing of nanocomposites is done until the supernatant pH becomes 7.0 by using distilled water. After pH setting, oven at 60 °C is used for drying of composite for 12 h. Finally, the CMCTS-clay nanocomposite is turned into dust form by scraping off [30].

The composite was tried with cationic dyestuff [30, 31] previously, and very high adsorption values are yielded. In this study, anionic dyestuff is used to observe the anionic adsorption and prove the amphoteric characteristic of the composite thanks to the anionic characteristic of the carboxymethyl end group and cationic characteristic of chitosan. Dye bath simulating solution is prepared by using 200 mL pure water and 0.5 g dyestuff which is Nyloset Brilliant Red from Setaş Color Center and anionic dyestuff for nylon dyeing. Water is used to observe the real usage of dyestuff under natural pH instead of observing the full performance of composite by using other solvents. 2 g composite is added to the simulating dye bath, and the bath is mixed with a magnetic stirrer for 12 h. Then, UV-visible spectrophotometer analysis is done for dye bathes before and after the adsorbent addition. Adsorption graph is presented in Fig. 9.

Removal amount is calculated by using Formula 1, and  $R$  refers to removal percent, while  $c_0$  attributes to the initial concentration of solution and  $c_f$  attributes to the final concentration of the solution. As a result, anionic dyestuff removal is 42% as given in Table 4. This result shows that in addition to adsorbing cationic dyestuff, the composite can adsorb anionic dyestuff thanks to its amphoteric characteristic. This also proves that the modification chitosan is applied well enough to hold anionic dyestuff.



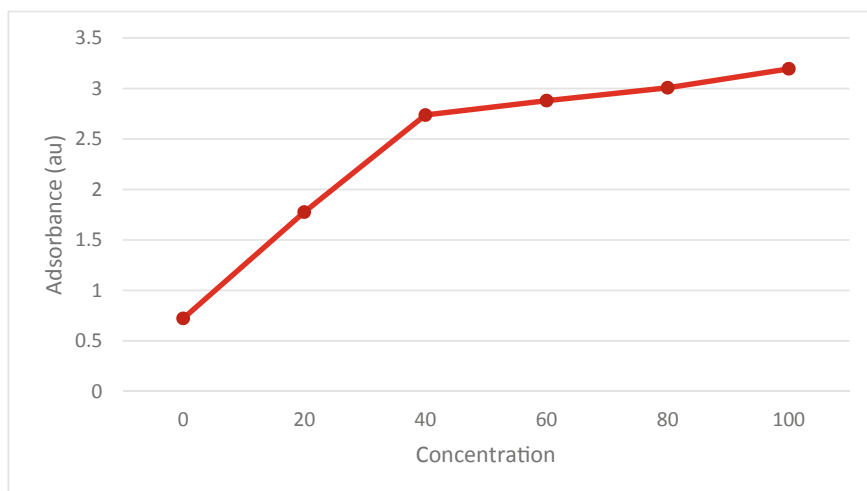


**Fig. 9** Graph of Nyloset brilliant red adsorption

**Table 4** Removal amount comparison in studies of the composite for anionic and cationic dyestuff

	Removal (%)		Reference
Cationic dyestuff (methylene blue)	67.77	[30]	
Anionic dyestuff (Nyloset brilliant red)	42.0	This study	

$$R = \frac{(C_0 - C_f)}{C_0} \times 100\% \quad (1)$$

## 7 Conclusion

The textile industry produces very harmful wastewater with very high amounts. These must be refined before discharging; even the reuse can make a profit for both economies and environment. For the refinement, there are many conventional methods as physical, chemical, and biological treatments, but adsorbent usage is a very promising alternative because of low cost, ease of applicability, and reusability in further cases as dyestuff or filler, etc. These adsorbents can be clay, cellulose and chitosan derivatives, biochars, and other polymers with various forms according to the needs of wastewater characteristics. For better, easier, and faster refining, adsorbents in composite forms are useful. In this chapter, also a study related to a composite adsorbent which is based on modified chitosan and clay for removal of dyestuff and enhancements is evaluated. It is shown that the novel nanocomposite can adsorb both cationic and anionic dyestuffs thanks to its amphoteric structure.

## References

1. White SB, Biernat JF, Duffy K, Kavalar MH, Kort WE, Naumes JS, Slezak MR, Stoffel CR (2010) Water markets of United States and the world: a strategic analysis for Milwaukee Water Council, Wisconsin
2. Agrawal R, Sharan M (2015) Municipal textile waste and its management. *Res J Fam Community Consum Serv* 3(1):4–9
3. Kumar PS, Saravanan A (2017) Sustainable wastewater treatments in textile sector. In: *Sustainable fibers and textiles*
4. Lemeneh DY, Tesema AF (2019) Valuation of polyvinyl alcohol and maize starch as sizing agent for textile processing. *Int J Mod Sci Technol* 4(11):286–293
5. Fu S, Farrell MJ, Ankeny MA, Turner ET, Rizk V (2019) Hydrogen peroxide bleaching of cationized cotton fabric. *AATCC J Res* 6(5):21–29
6. Hossain T, Hossain A, Saha PK, Alam Z (2019) Effect of scouring and bleaching agents on whiteness index and bursting strength of cotton knitted fabric. *Global J Res Eng* 19(1):23–28
7. Patil S, Mahapatra A, Gotmare VD, Patil PG, Bharimalla AK, Arputharaj A (2019) Effect of different mercerization techniques on tactile comfort of cotton fabric. *Indian J Fibre Text Res* 44:217–222
8. Chemchame Y, El Mouden M, Mansar A (2017) Comparison between mordant and alkaline dyeing of wool fiber with dyes from *Rubia tinctorum* plant. *Am J Phys Chem* 6(1):1–5
9. Moniruzzaman M, Mondal MS, Hossain N (2018) The influence of mordant and mordanting techniques on ecofriendly dyeing of cotton fabric by extracted used tea. *J Eng Sci* 9(1):111–117
10. El-Sayed WA, El-Ola SMA, AELSayed NA, Tawila DMN (2017) Multi-functional finishing of woolen fabric. *J Sci Res Sci* 34(1):1–18
11. Moga IC, Iordănescu M, Pricop F, Scarlat R, Dorogan A (2013) Quality monitoring for wastewater generated by the textile finishing. *Ind Textila* 6(4):222–228
12. Raman AAA, Asghar A, Buthiyappan A, Daud WMAW (2017) Treatment of recalcitrant waste. In: *Current developments in biotechnology and bioengineering: biological treatment of industrial effluents*, pp 409–442
13. Holkar CR, Jadhav AJ, Pinjari DV, Mahamuni NM, Pandit AB (2016) A critical review on textile wastewater treatments: possible approaches. *J Environ Manage* 182:351–366
14. Siddique K, Rizwan M, Shahid MJ, Ali S, Ahmad R, Rizvi H (2017) Textile wastewater treatment options: a critical review. In: *Enhancing cleanup of environmental pollutants*
15. Akarsu C (2014) Treatment of industrial wastewater by electrocoagulation process. In: *ISITES*
16. Hakulinen R (1988) The use of enzymes for wastewater treatment in pulp and paper industry—a new possibility. *Water Science Technol* 20(1):251–262
17. Anijiofor Sandra C, Jamil NAM, Jabbar S, Sakyat S, Gomes C (2017) Aerobic and anaerobic sewage biodegradable processes: the gap analysis. *Int J Res Environ Sci* 3(3):9–19
18. Sarayu K, Sandhya S (2012) Current technologies for biological treatment of textile wastewater—a review. *Appl Biochem Biotechnol* 167:645–661
19. Mashall H (2018) Natural nanomaterials. In: *Environmental nanotechnology*, p 133
20. Crini G, Lichtfouse E, Wilson L, Morin-Crini N (2019) Conventional and non-conventional adsorbents for wastewater treatment. *Environ Chem Lett* 17(1):195–213
21. De Gisi S, Lofrano G, Grassi M, Michele N (2016) Characteristics and adsorption capacities of low-cost sorbents for wastewater treatment: a review. *Sustain Mater Technol* 9:10–40
22. Burakov AE, Galunin EV, Burakova IV, Kucherova AE, Agarwal S, Tkachev AG, Gupta VK (2018) Adsorption of heavy metals on conventional and nanostructured materials for wastewater treatment purposes: a review. *Ecotoxicol Environ Saf* 148:702–712
23. Sadegh H, Ali GAM (2018) Potential applications of nanomaterials in wastewater treatment: nanoadsorbents performance. In: *Advanced treatment techniques for industrial wastewater*
24. Liu J, Boo WJ, Clearfield A, Sue HJ (2006) Intercalation and exfoliation: a review on morphology of polymer nanocomposites reinforced by inorganic layer structures. *Mater Manuf Process* 21(2):143–151

25. Şen F, Palancıoğlu H, Aldaş K (2010) Polymeric nanocomposites and usage areas. *Electron J Mach Technol* 7(1):11–18
26. Chen S, Zhou M, Wang HF, Wang T, Wang XS, Hou HB, Song BY (2018) Adsorption of reactive brilliant red X-3B in aqueous solutions on clay–biochar composites from bagasse and natural attapulgit. *Water* 10(703)
27. Radaei E, Alavi Moghadam SMR, Arami M (2014) The study of the adsorption of reactive blue 19 dye by activated carbon from pomegranate residue. *Water and Wastewater* Vol. 25, 4(92):27–34
28. Kähkö MR, Piri J (2016) Adsorption of reactive red dye from wastewater using modified *Citrullus scolosynthis* ash. *Water and Wastewater* 27(3):32–37
29. Şen F, Demirbaş Ö, Çalimli MH, Aygün A, Alma MH, Nas MS (2018) The dye removal from aqueous solution using polymer composite films. *Appl Water Sci* 8(206)
30. Emekdar E, Şahin UK (2018) Design of a zwitter-ionic nanocomposite for dyestuff removal. *IOP Conf Ser Mater Sci Eng* 460(012039)
31. Emekdar E, Şahin UK (2019) Katyonik Atık Suların Arıtılması İçin Tekstil Atıklarından Çevreci Kompozit Üretimi. In: UÇTEK Ulusal Çukurova Tekstil Kongresi, Adana, Turkey
32. Hussin F, Aroua MK, Daud WMAW (2011) Textural characteristics, surface chemistry and activation of bleaching earth: a review. *Chem Eng J* 170(1):90–106
33. Bergaya F, Lagaly G (2006) General Introduction: clay, clay minerals and clay science. In: *Hand book of clay science*, pp 1–18
34. De Paiva LB, Morales AR, Díaz FRV (2008) Organoclays: properties, preparation and applications. *Appl Clay Sci* 42:8–24
35. Yılmazbayhan A (2006) Maleik Anhidritle Graftlanmış Oligomerlerin Ve İPP/Silikat Nanokompozitlerin Tepkimeli Ekstrüzyon Yöntemiyle Sentezi Ve Karakterizasyonu. Hacettepe Üniversitesi Fen Bilimleri Enstitüsü, Ankara
36. Heller-Kallai L, Yariv S (1981) Swelling of montmorillonite containing coordination complexes of amines with transition metal cations. *J Colloid Interface Sci* 79(2):479–485
37. Yariv S (1976) Organophilic pores as proposed primary migration media for hydrocarbons in argillaceous rocks. *Clay Sci* 5(1):19–29
38. Sivathasan J (2007) Preparation of clay-dye pigment and its dispersion in polymers. Thesis dissertation masters by research, RMIT University School of Engineering, MMS ID 9921861231801341
39. Turan D (2012) Organokil esaslı nanokompozit endüstriyel liflerin üretilmesi ve karakterizasyonu. Kocaeli Üniversitesi. Fen Bilimleri Enstitüsü, Kocaeli
40. Maes A, Van Leemput L, Cremers A, Uytterhoeven J (1980) Electron density distribution as a parameter in understanding organic cation exchange in montmorillonite. *J Colloid Interface Sci* 77(1):14–20
41. İpekoğlu B, Kurşun İ, Bilge Y, Barut A (1997) Türkiye bentonit potansiyeline genel bir bakış. In: 2. Endüstriyel Hammaddeler Sempozyumu
42. Demir E (2008) Isıl İşlemin Bir Bentonitin Katyon Değiştirme Kapasitesi, Adsorpsiyon, Gözenekliliği, Yüzey Alanı Ve Yüzey Asitliği Gibi Bazı Fizikokimyasal Özelliklerine Etkisi. Ankara Üniversitesi. Fen Bilimleri Enstitüsü, Ankara
43. Kayır YZ (2007) Bentonit nedir. In: Endüstriyel Fırınlar ve Refrakter Sempozyumu
44. Wentworth SA (1969) Illite. *Clay Sci* 3(6):140–155
45. Karim AB, Mounir B, Hachkar M, Bakasse M, Yaacoubi A (2009) Removal of basic red 46 dye from aqueous solution by adsorption onto Moroccan clay. *J Hazard Mater* 168(1):304–309
46. Vimonses V, Jin B, Chow CW, Saint C (2009) Enhancing removal efficiency of anionic dye by combination and calcination of clay materials and calcium hydroxide. *J Hazard Mater* 171:941–947
47. Li Z, Chang PH, Jiang WT, Jean JS, Hong H (2011) Mechanism of methylene blue removal from water by swelling clays. *Chem Eng J* 168(3):1193–1200
48. Teng MY, Lin SH (2006) Removal of methyl orange dye from water onto raw and acidactivated montmorillonite in fixed beds. *Desalination* 201:71–81

49. Karagozolu B, Tasdemir M, Demirbas E, Kobya M (2007) The adsorption of basic dye (Astrazon Blue FGRL) from aqueous solutions onto sepiolite, fly ash and apricot shell activated carbon: kinetic and equilibrium studies. *J Hazard Mater* 147:217–228
50. Gürses A, Doğan Ç, Yalçın M, Açıkyıldız M, Bayrak R, Karaca S (2006) The adsorption kinetics of the cationic dye, methylene blue, onto clay. *J Hazard Mater* 131:217–228
51. Weng CH, Pan YF (2007) Adsorption of a cationic dye (methylene blue) onto spent activated clay. *J Hazard Mater* 144:355–362
52. Yan H, Zhang W, Kan X, Dong L, Jiang Z, Li H, Cheng R (2011) Sorption of methylene blue by carboxymethyl cellulose and reuse process in a secondary sorption. *Colloids Surf A* 380:140–153
53. Wang MM, Wang L (2013) Synthesis and characterization of carboxymethyl cellulose/organic montmorillonite nanocomposites and its adsorption behavior for Congo red dye. *Water Sci Eng* 6(3):272–282
54. Bilgen M (2006) Wrinkle recovery for cellulosic fabric by means of ionic crosslinking. Thesis dissertation MSc. Textile Chemistry, NCSU, USA
55. Gordon S, Hsieh YL (eds) (2006) Cotton: science and technology. Woodhead Publishing Series in Textiles, Woodhead Publishing Limited, Cambridge, England, ISBN-13: 978-1845690267
56. Borsa J, Ravichandran V, Obendorf SK (1999) Distribution of carboxyl groups in carboxymethylated cotton fibers. *J Appl Polym Sci* 72(2):203–207
57. Rác I, Borsa J, Obendorf SK (1998) Carboxymethylated cotton fabric for pesticide-protective work clothing. *Text Res J* 68(1):69–74
58. Parikh DV, Sachinvala ND, Calamari TA, Negulescu I (2003) Carboxymethylated cotton for moist wound healing. *AATCC Rev* 3(6)
59. Begum HA, Mahbub MKB (2003) Effectiveness of carboxymethyl cellulose for the removal of methylene blue from aqueous solution. *Dhaka Univ J Sci* 61(2):193–198
60. Salama A, Shukry N, El-Sakhawy M (2015) Carboxymethyl cellulose-g-poly (2-(dimethylamino) ethyl methacrylate) hydrogel as adsorbent for dye removal. *Int J Biol Macromol* 73:72–75
61. Cai T, Yang Z, Li H, Yang H, Li A, Cheng R (2013) Effect of hydrolysis degree of hydrolyzed polyacrylamide grafted carboxymethyl cellulose on dye removal efficiency. *Cellulose* 20(5):2605–2614
62. Rinaudo M (2006) Chitin and chitosan: properties and applications. *Prog Polym Sci* 31(7):603–632
63. Cheaburu-Yilmaz CN, Yilmaz O, Vasile C (2015) Eco-friendly chitosan-based nanocomposites: chemistry and applications. In: *Eco-friendly polymer nanocomposites*, New Delhi, Springer, pp 341–386
64. Szyguła A, Guibal E, Ruiz M, Sastre AM (2008) The removal of sulphonated azo-dyes by coagulation with chitosan. *Colloids Surf A* 330:219–226
65. Wang L, Wang A (2008) Adsorption behaviors of Congo red on the *N, O*-carboxymethyl-chitosan/montmorillonite nanocomposite. *Chem Eng J* 143:43–50
66. Bhattacharyya R, Ray SK (2014) Micro- and nano-sized bentonite filled composite superabsorbents of chitosan and acrylic copolymer for removal of synthetic dyes from water. *Appl Clay Sci* 101:510–520
67. Bulut Y, Karaer H (2015) Adsorption of methylene blue from aqueous solution by crosslinked chitosan/bentonite composite. *J Dispersion Sci Technol* 36(1):61–67
68. Liu Q, Yang B, Zhang L, Huang R (2015) Adsorption of an anionic azo dye by cross-linked chitosan/bentonite composite. *Int J Biol Macromol* 72:1129–1135
69. Guo J, Chen S, Liu L, Li B, Yang P, Zhang L, Feng Y (2012) Adsorption of dye from wastewater using chitosan-CTAB modified bentonites. *J Colloid Interface Sci* 382(1):61–66
70. Mahdavinia GR, Karami S (2015) Synthesis of magnetic carboxymethyl chitosan-g-poly (acrylamide)/laponite RD nanocomposites with enhanced dye adsorption capacity. *Polym Bull* 72(9):2241–2262
71. Jin H, Capareda S, Chang Z, Gao J, Xu Y, Zhang J (2014) Biochar pyrolytically produced from municipal solid wastes for aqueous As(V) removal: adsorption property and its improvement with KOH activation. *Biores Technol* 169:622–629

72. Manyàa JJ, Azuara M, Manso JA (2018) Biochar production through slow pyrolysis of different biomass materials: seeking the best operating conditions. *Biomass Bioenerg* 117:115–123
73. Tan X-F, Liu S-B, Liu Y-G, Gu Y-L, Zeng G-M, Hua X-J, Wang X, Liu S-H, Jiang L-H (2017) Biochar as potential sustainable precursors for activated carbon production: multiple applications in environmental protection and energy storage. *Biores Technol* 227:359–372
74. Rajapaksha AU, Vithanage M, Ahmad M, Seod D-C, Cho J-S, Lee S-E, Lee SS, Ok YS (2015) Enhanced sulfamethazine removal by steam-activated invasive plant-derived biochar. *J Hazard Mater* 290:43–50
75. Li X-Y, Han D, Xie J-F, Wang Z-B, Gong Z-Q, Li B (2018) Hierarchical porous activated biochar derived from marine macroalgae wastes (*Enteromorpha prolifera*): facile synthesis and its application on methylene blue removal. *Roy Soc Chem Adv* 8:29237–29247
76. Zhang S, Lu X (2018) Treatment of wastewater containing reactive brilliant blue KN-R using TiO<sub>2</sub>/BC composite as heterogeneous photocatalyst and adsorbent. *Chemosphere* 206:777–783
77. Cai X, Li J, Liu Y, Yan Z, Tan X, Liu S, Zeng G, Gu Y, Hu X, Jiang L (2018) Titanium dioxide-coated biochar composites as adsorptive and photocatalytic degradation materials for the removal of aqueous organic pollutants. *J Chem Technol Biotechnol* 93:783–791
78. Li H, Hu J, Zhou X, Li X, Wang X (2018) An investigation of the biochar-based visible-light photocatalyst via a self-assembly strategy. *J Environ Manag* 217:175–182
79. Ekici S, Guntekin G (2018) Utilization of polyampholyte hydrogels for simultaneous removal of textile dyes from aqueous solutions. *Sep Sci Technol* 53(11):1777–1790
80. Inal M, ÇAĞDAŞ TUNALI BE, Yiğitoğlu M (2017) Akrilamid-Krotonik Asit İç İç Geçmiş Ağ Yapılı Hidrojellerinin Metilen Mavisinin Adsorpsiyonunda Kullanımı. *Uluslararası Mühendislik Araştırma ve Geliştirme Dergisi* 9(2)
81. Sudarsan S, Franklin DS, Sakthivel M, Chitra G, Sridharan TB, Guhanathan S (2018) Ecofriendly pH-tunable hydrogels for removal of perilous thiazine dye. *J Polym Environ* 26:3773–3784
82. Ma SS, Zhang YG (2016) Electrolytic removal of alizarin red S by Fe/Al composite hydrogel electrode for electrocoagulation toward a new wastewater treatment. *Environ Sci Pollut Res* 23:22771–22782
83. Ilgin P, Ozay O (2017) Novel stimuli-responsive hydrogels derived from morpholine: synthesis, characterization and absorption uptake of textile azo dye. *Iran Polym J* 26:391–404
84. Rahimdokht M, Pajootan E, Ranjbar-Mohammadi M (2018) Titania/gum tragacanth nanohydrogel for methylene blue dye removal from textile wastewater using response surface methodology. *Polym Int* 68(1):134–140. 10. <https://doi.org/1002/pi.5706>
85. Patel YN, Patel MP (2012) Novel cationic poly[AAm/NVP/DAPB] hydrogels for removal of some textile anionic dyes from aqueous solution. *J Macromol Sci Part A Pure Appl Chem* 49:490–501
86. Dey A, Bera R, Chakrabarty D (2017) Synthesis of poly(ethylene glycol) di-itaconate and investigation of its influence on acrylamide based hydrogels meant for water treatment. *Polymer* 116:178–190

# Treatment of Textile Waste Water Using Low-Cost and Innovative Materials



K. Amutha

**Abstract** Clothing is a basic necessity of human but the industries that produce clothing pose a serious environmental pollution in many ways. One such problem is the effluents from the wet processing of textile materials. The complex nature of textile effluent makes the recycling process challenging and also expensive. The extensive use of water for the wet processing of textiles and the scarcity of water resources demand efficient and cost-effective methods for the treatment of textile effluent. Agro-residual and plant materials were effectively used by researchers to develop low-cost effluent treatment. Also, some species of microbes could be used effectively for effluent treatment. Activated carbon is another low-cost adsorbent used effectively for textile effluent treatment. This chapter explores the low-cost and innovative materials that could be used for the treatment of textile waste water.

**Keywords** Textile effluent · Nanotechnology · Treatment methods · Biosorption · Bioremediation

## 1 Introduction

The term ‘textile’ sounds colourful and fascinating. Dyes and pigments are used by mankind for colouration of food, textiles, pottery, paper, etc. The colour imparts aesthetic property to the textiles. Until the industrial revolution by 1850 in Europe, natural dyes were extensively used for colouration. And also the difficulties and disadvantages with the natural dyes paved way to the growth of synthetic dyes by 1900. Since then synthetic dyes rule the dye industry market worldwide. Some of these dyes are associated with health hazards of human and aquatic life, ranging from mild to acute or chronic.

The textile industrial chain is characterized by large and complex structure. Broadly, the manufacturing processes could be categorized as dry (spinning, knitting, weaving, and garment production) and wet (sizing, desizing, scouring, bleaching,

---

K. Amutha (✉)

Department of Textiles and Apparel Design, Bharathiar University, Coimbatore, Tamilnadu, India  
e-mail: [amuthatad@buc.edu.in](mailto:amuthatad@buc.edu.in)

mercerizing, dyeing, printing and finishing operations) with strong interconnection. These processes are associated with wastewater, solid wastes, emissions to air and noise pollution. Among these, the major environmental concern of the textile industry is the effluent or the waste water [21].

The dyeing and finishing processes account for high levels of environmental contamination as the process effluents contain large and diverse quantities of colour, organic and inorganic contaminants and other hazardous chemicals including heavy metals [24].

The textile industry is one of the leading polluters of surface water and consumes about 200–270 tons of water to produce 1 ton of textile product [6]. The harmful chemicals present in textile effluents react with many disinfectants especially chlorine and form by products that are often carcinogens [18].

Huge amount of wastewater loaded with high amount of chemicals from textile industries that are discharged into surface water is a major source of environmental pollution. Suitable waste water treatment must be done to reduce the pollution load. The textile wastewater effluent consists of chemicals including chlorinated solvents, hydrocarbon solvents, oxygenated solvents, oils, waste fabrics drenched in grease and oil, and dyestuffs and pigments [20].

The situation has become better due to stringent regulations by the government and increase in awareness among the stakeholders of textile dyeing industry. Fashion brands have become environmental conscious and started implementing sustainable production across the textile supply chain. These oblige the wet processing industry to follow zero liquid discharge (ZLD). The effluent treatment plant (ETP) is the only possible way to recycle the waste water and achieve ZLD.

This chapter elucidates the nature of the textile waste water, classification of textile waste water treatment methods and the use of low-cost and innovative materials for waste water treatment that are different from conventional methods.

## 2 Nature of Textile Waste Water

Textile industry employs a wide array of chemicals for the wet processing of textiles and the unfixed or residual chemicals are present in the waste water in varied quantities. All these chemicals have to be removed from the waste water before discharge.

The term wet processing of textiles includes all the processes such as sizing, desizing, scouring, bleaching, mercerizing, dyeing, printing and finishing. Each of these processes is specific and uses different chemicals and auxiliaries. Hence, the effluent produced by these processes and its characteristics are also variable. Table 1 shows the various wet processes and the relevant effluent characteristics in detail.

The textile wastewater or effluent is highly complex in nature as it contains unfixed dyes and other chemicals of different characteristics. The quantity of these chemical compounds in the waste water also varies considerably from one process to the other. The waste water from dyeing or printing process may be highly coloured while that

**Table 1** Nature of textile waste water [4, 10, 21]

Process	Possible pollutants	Waste water characteristics				
		Volume	BOD	COD	Alkalinity	Others
Sizing	Starch, glucose, PVA, resins, fats and waxes	Small	High	Medium		Metals, cleaning waste, yarn waste
Desizing	Starch, CMC, PVA, resins, fats and waxes, pectins, ammonia	Very small	High (30–50% of total)	High		Biocides, anti-static compounds
Scouring	Caustic soda, waxes, soda ash, sodium silicate and fragments of cloth	Very small	High (30% of total)		High	Dark colour
Bleaching	Hypochlorite, chlorine, caustic soda, hydrogen peroxide, acids	Small	Low (5% of total)		High	High suspended solids
Mercerizing	Sodium hydroxide, cotton wax	Small	Low (less than 1% of total)	Low	High	High dissolved solids
Dyeing	Dye stuff, mordant, formaldehyde, acetic acid, detergent, reducing agents and wetting agents	Large	Fairly high (6% of total)	High	High	Strong colour, highly toxic, high pH, high dissolved solids (TDS)
Printing	Dye, starch, gum oil, urea, solvents, binders, thickeners, mordants, cross-linking agents, acids and metallic salts	Very small	Fairly high	High		Oily appearances, high toxicity, strong colour, high pH, high TDS

(continued)



**Table 1** (continued)

Process	Possible pollutants	Waste water characteristics				
		Volume	BOD	COD	Alkalinity	Others
Finishing	Traces of starch, tallow, salts, resins, spent solvents, waxes, softeners, chlorinated compounds	Very small	Low		Low	High toxicity

from processes like sizing, desizing, scouring and bleaching may not be coloured. Hence, a clear understanding of the effluent characteristics is necessary to choose the right treatment process.

The major pollutants identified in the textile waste water are high pH or alkalinity, colour, nutrients (nitrogen and phosphorus), inorganic salts and refractory organics. The azo and other chromophoretic groups in the dye matrix render geno toxicity to the biodiversities in the environment [11].

### 3 Classification of Textile Waste Water Treatment Methods

The textile waste water is complex and its characteristics varies according to the process and the recipe used for the process. Hence, a single treatment method or a single stage process may not be sufficient for the water recycling.

Synthetic dyes used in textile dyeing are of different types (azo, acid, basic, vat, reactive, direct, disperse dye, etc.) and have different molecular structures. Hence, a decolouration treatment adopted for one dye may not be suitable for other thereby making the process very specific.

The textile waste water is treated at three different stages: primary, secondary and tertiary. At each stage, various treatment methods can be used which is shown in Fig. 1 [21]. Figure 2 shows the classification of various waste water treatment methods.

### 4 Low-Cost Materials for Textile Waste Water Treatment

Among various water treatment methods, adsorption is supposed as the best one due to its inexpensiveness, universal nature and ease of operation. Many waste materials used include fruit wastes, coconut shell, scrap tyres, bark and other tannin-rich

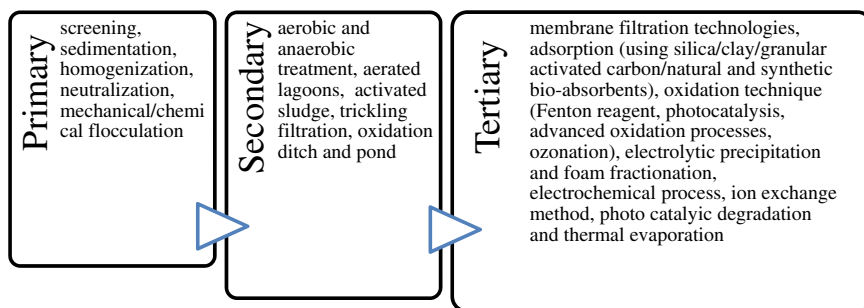


**Fig. 1** Three stages in textile waste water treatment. *Content source* [21]

materials, sawdust and other wood type materials, rice husk, petroleum wastes, fertilizer wastes, fly ash, sugar industry wastes, blast furnace slag, chitosan and seafood processing wastes, seaweed and algae, peat moss, clays, red mud, zeolites, sediment and soil, ore minerals, etc. These adsorbents have been found to remove various organic pollutants ranging from 80 to 99.9% [2].

Industrial and agricultural waste materials like sawdust, ash, sun flower seed shells, corncob, lignin and seashell were used as low-cost sorbents in removal of anionic and cationic dyes from textile wastewaters [22]. Activated carbon is an effective sorbent but it is expensive. Hence, sorbents from waste materials would be cost effective in waste water treatment.

**Activated carbon** remains the most widely studied adsorbent, and it has been found to adsorb a variety of materials such as metals, dyes, phenols, and a host of other organic compounds and bio-organisms, and is therefore used for the removal of pollutants from wastewaters by adsorption. These low-cost alternative adsorbents may be classified in two ways (Fig. 3), either on basis of their availability (i.e., natural materials such as wood, peat, coal, lignite, etc.; industrial/agricultural/domestic wastes or byproducts such as slag, sludge, fly ash, bagasse flyash, red mud, etc.; and synthesized products) or depending on their nature, i.e., inorganic and organic [8].

**Water hyacinth**, an aquatic weed that poses many environmental problems, has been successfully used as a biosorption material to remove various pollutants in textile waste water. The different parts of water hyacinth plant—the root, stem, leaves and the biomass of water hyacinth were employed by researchers for dye absorption. For improved biosorption property, the water hyacinth was treated with acid/alkali which in turn showed better removal of metal ions than the untreated plant materials [15].

**Phytoremediation** is considered to be a possible method for the removal of pollutants present in wastewater and recognized as a better green remediation technology. Water hyacinth can be effectively used in the waste water treatment for removal of heavy metals, organic and inorganic matters [17]. Aquatic weed like water hyacinth has negative impacts on the environment but its use in waste water treatment makes it sustainable.

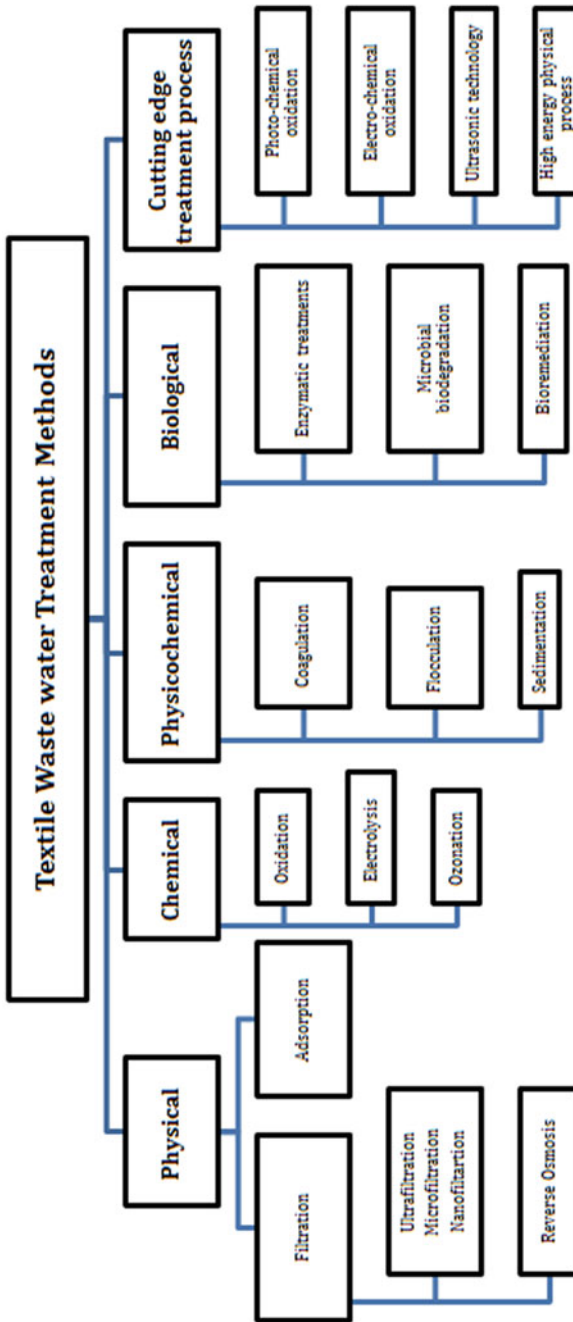
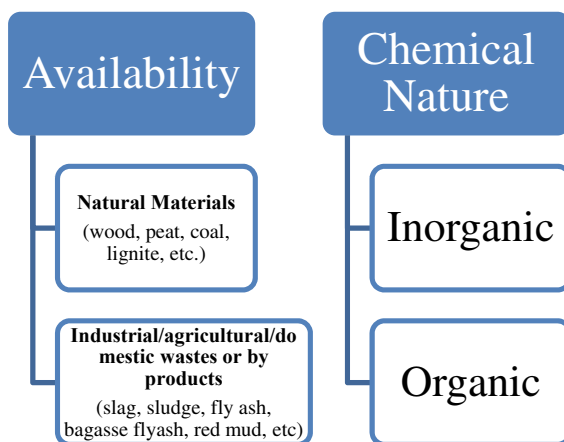


Fig. 2 Various methods for textile waste water treatment

**Fig. 3** Classification of low-cost alternative adsorbents



**Algal bioremediation** is an eco-friendly, cost-effective and precise technique for recovery of metal compounds from waste water. **Cyanobacteria** are an efficient tool used for removal of toxic pollutants from waste water in a sustainable way [19].

**Bacillus species** isolated from processed food (pickles) and characterized by biochemical reactions was used for the treatment of textile effluent. The crude effluent collected was first diluted to 10, 50 and 90% and then subjected to biological (aerobic) treatment. The dye degradation rate was observed to be 87.7% and 93.3% at 50 and 90%, respectively, with the spore formers while the culture supernatant could degrade the crude dye at 34% and the 90% diluted effluent by 98%. The treatment was effective with spore forming Bacillus than with the non-spore forming organisms [13].

Azo dye effluent was treated using both adapted (*Aspergillus* sp., *Penicillium* sp., *Fusarium* sp. and *Mucor* sp.) and non-adapted (*Aspergillus* sp., *Penicillium* sp., *Fusarium* sp. and *Rhizopus* sp.) **fungal strains** by bioremediation. The adapted fungal strains were screened from effluent sample while the non-adapted fungal strains were screened from soil, water and fungal fruiting bodies. The bioremediation using adapted fungal consortium exhibited better results, 75% colour reduction and 50% COD reduction while it was 67% and 34%, respectively with non-adapted fungal consortium [16].

**Pseudomonas sp. SU-EBT** had been used for both decolourization of Congo red dye and detoxification of textile industry waste water. The decolourization efficiency was observed to be 97 and 90% for recalcitrant Congo red dye. The optimum pH and temperature for the decolourization was 8.0 and 40°C, respectively. 50% reduction in COD within 60 h was observed. Phytotoxicity study revealed nontoxic nature of the degradation metabolites to *Sorghum bicolor*, *Vigna radiata*, *Lens culinaris* and *Oryza sativa* plants as compared to Congo red and textile industry effluent [23].

**Orange peel** biomass has been used in the preparation of activated carbon which in turn was used for the decolourization of auramine yellow dye used in the textile industry. Maximum decolourization was observed at pH of 2. The decolourization efficiency of 95% was achieved in 200 min. Increase in pH of the dye solutions

**Table 2** Application of magnetic nanoparticle/nanocomposite in waste water treatment. Content Source (9)

Magnetic nanoparticle/nanocomposite	Properties	Applications
Nanomagnetite	Amphoteric surface activity, easy dispersion ability, high metal ion adsorption capacity	As adsorbents for removal of <ul style="list-style-type: none"> <li>• heavy metals such as arsenic, lead, mercury, cadmium and chromium from waste water</li> <li>• azo and anthraquinone dyes</li> </ul>
Substituted nanomagnetite (Mn, Co and Ni)	High adsorption capacity, catalytic nature, ion-exchange, high pore volume	
Nanosized magnetite with surface functionalization	Effective adsorbents, superparamagnetic, high metal ion adsorption capacity	
Nanosized magnetite as part of composites with inorganic moieties (TiO <sub>2</sub> , SiO <sub>2</sub> ) or supported magnetite on clay and carbon	New functional hybrid materials with the synergy of all the components, large uniform nanopore structures	

caused a decline in decolourization activity. Among the tested quantities of orange peel, optimum activity was observed for 0.6 g/100 mL [14].

**Nanosized magnetite** has emerged as an adsorbent of pollutants in water remediation. Magnetic nanoparticles and nanocomposites are used as low-cost materials in the treatment of contaminated water. The characteristics of these nanomaterials are related to their ability to eliminate heavy metal ions and dyes from wastewater. Different magnetic materials, from raw nanomagnetite to magnetite combined with several compounds, have been studied. Magnetic activated carbons exhibited high surface areas and porosities and can be easily manipulated by an external magnetic field. Application of magnetic nanoparticle or nanocomposite in waste water treatment is given in Table 2 [9].

## 5 Innovative Materials for Textile Waste Water Treatment

Two different raw **clay** materials from Tunisia, standard kaolinite and palygorskite had been used as adsorbent for the removal of a reactive red dye (RR 120) found in textile industry effluents. The study indicated that the nature of clay is the dominant factor in controlling the efficiency of dye removal compared to other factors such as porosity, surface area and cationic exchange capacity of the clay [1] (Table 3).

**Boron doped diamond (BDD)** have been used as anode in the electrochemical treatment of textile waste water from Brazilian textile industry for removal of chemical oxygen demand (COD) and colour. COD was reduced under different operating conditions such as current density, temperature, Na<sub>2</sub>SO<sub>4</sub> concentration, flow rate

**Table 3** Application of clay for dye removal. Content Source (1)

Clay	Outcomes
Tabarka clay: mixture of kaolinite (62%) and illite (38%)	Shows a better adsorption capacity than Fouchana and palygorskite
Fouchana clay: mixture of smectite (60%), kaolinite (30%), and illite (10%)	Exhibits highest rate of desorption
Standard kaolinite (KGa-2)	Exhibits the lowest specific surface and shows the highest adsorption capacity for anionic dye
Standard palygorskite (PFI-1)	Provides a large surface to the adsorption; has the lowest capacity for adsorption of RR 120 dye

which reduced the time of depuration and subsequently the costs. This method could be effectively used as an alternative for pre-treatment of textile effluents for COD and colour removal [12].

**Nanotechnology** is one of the most advanced techniques for waste water treatment. To ensure high quality of water, advanced technologies are required and nanotechnology is a suitable option. Nanomaterials used for effluent treatment may be of three classes as listed in Table 4. Nanoparticle photocatalysts can be used for treatment of both toxic pollutants and heavy metals, where the modification in catalyst material can provide the capability of using visible region of solar light instead of high cost artificial ultraviolet radiation [3] (Table 4).

A **new coagulant** obtained through polymerization of *Acacia mearnsii* de Wild tannin extract has been characterized in the removal of two dangerous dye pollutants: Alizarin Violet 3R and Palatine Fast Black WAN. This coagulant is lab-synthesized according to the etherification of tannins with glycidyltrimethyl ammonium chloride and formaldehyde and its performance in dye removal in terms of efficiency was high. A reasonably low coagulant dosage (ca. 50 mg/L) reaches high capacity levels

**Table 4** Nanomaterials and their application in waste water treatment. Content Source (3)

Type of nanomaterial	Nanomaterials	Processes
Nanoadsorbents	Activated carbon, carbon nanotubes, graphene, manganese oxide, zinc oxide, titanium oxide, and magnesium oxides	Removal of heavy metals
Nanocatalysts	Photocatalyst, electrocatalyst, Fenton based catalyst and chemical oxidant	Removal of both organic and inorganic contaminants
Nanomembranes	Carbon nanotube membranes, electrospun nano fibres and hybrid nanomembranes	Removal of dyes, heavy metals and foulants
Integrated nanotechnology and biological processes	Algal membrane bioreactor, anaerobic digestion, microbial fuel cell	Waste water purification

(around 0.8 for Alizarin Violet 3R and 1.6 for Palatine Fast Black WAN mg dye/mg of coagulant) and pH and temperature are not extremely affecting variables [5].

Fenton oxidation process and aerobic Sequencing Batch Reactor (SBR) combined with Fenton process were employed to study the degradation of textile wastewater in Spain. The obtained results showed the feasibility of both processes to achieve suitable water qualities for internal reuse, according to RD 1620/2007 (Spanish Normative for wastewater reclamation and reuse) [7].

## 6 Conclusion

The complex nature of textile wastewater requires customized treatment methods to meet specific needs. The cost of wastewater treatment is high which increases the operating cost of the wet processing industry. Hence, the use of low-cost innovative materials for treatment is the need of the industry. Moreover, the method of treatment should be sustainable that allows recovery and reuse of the treated water.

## References

1. Abidi N, Duplay J, Jada A, Errais E, Ghazi M, Semhi K, Trabelsi-Ayadi M (2019) Removal of anionic dye from textile industries' effluents by using Tunisian clays as adsorbents. Zeta potential and streaming-induced potential measurements. *C R Chim* 22(2–3):113–125
2. Ali I, Asim M, Khan TA (2012) Low cost adsorbents for the removal of organic pollutants from wastewater. *J Environ Manage* 113:170–183
3. Anjum M, Miandad R, Waqas M, Gehany F, Barakat MA (2019) Remediation of wastewater using various nano-materials. *Arab J Chem* 12(8):4897–4919
4. Arslan S, Eyvaz M, Gürbulak E, Yüksel E (2016) A review of state-of-the-art technologies in dye-containing wastewater treatment—the textile industry case. *Text Wastewater Treat* 1–28
5. Beltrán-Heredia J, Sánchez-Martín J, Rodríguez-Sánchez MT (2011) Textile wastewater purification through natural coagulants. *Appl Water Sci* 1(1–2):25–33
6. Bhatia D, Sharma NR, Kanwar R, Singh J (2018) Physicochemical assessment of industrial textile effluents of Punjab (India). *Appl Water Sci* 8(3):83
7. Blanco J, Torrades F, De la Varga M, García-Montaña J (2012) Fenton and biological-Fenton coupled processes for textile wastewater treatment and reuse. *Desalination* 286:394–399
8. Gupta VK, Carrott PJM, RibeiroCarrott MML, Suhas (2009) Low-cost adsorbents: growing approach to wastewater treatment—a review. *Crit Rev Environ Sci Technol* 39(10):783–842
9. Horst MF, Lassalle V, Ferreira ML (2015) Nanosized magnetite in low cost materials for remediation of water polluted with toxic metals, azo-and antraquinonic dyes. *Front Environ Sci Eng* 9(5):746–769
10. Kanu I, Achi OK (2011) Industrial effluents and their impact on water quality of receiving rivers in Nigeria. *J Appl Technol Environ Sanitation* 1(1):75–86
11. Karthikeyan S, Titus A, Gnanamani A, Mandal AB, Sekaran G (2011) Treatment of textile wastewater by homogeneous and heterogeneous Fenton oxidation processes. *Desalination* 281:438–445
12. Martínez-Huitle CA, dos Santos EV, de Araújo DM, Panizza M (2012) Applicability of diamond electrode/anode to the electrochemical treatment of a real textile effluent. *J Electroanal Chem* 674:103–107

13. Murugalatha N, Mohankumar A, Sankaravadivoo A, Rajesh C (2010) Textile effluent treatment by *Bacillus* species isolated from processed food. *Afr J Microbiol Res* 4(20):2122–2126
14. Paul JJ, Surendran A, Thatheyus AJ (2020) Efficacy of orange peel in the decolourization of the commercial auramine yellow dye used in textile industry. *Indian J Biochem Biophys (IJBB)* 57(4):481–485
15. Priya ES, Selvan PS (2017) Water hyacinth (*Eichhorniacrassipes*)—an efficient and economic adsorbent for textile effluent treatment—a review. *Arab J Chem* 10:S3548–S3558
16. Rajendran R, Karthik SS, Prabhavathi P, Sridevi BV, Gopi V (2011) Comparative analysis of bioremediation potential of adapted and non-adapted fungi on azo dye containing textile effluent. *Pak J Biol Sci PJBS* 14(11):610–618
17. Rezaia S, Ponraj M, Talaiekhazani A, Mohamad SE, Din MFM, Taib SM et al (2015) Perspectives of phytoremediation using water hyacinth for removal of heavy metals, organic and inorganic pollutants in wastewater. *J Environ Manag* 163:125–133
18. Saini RD (2017) Textile organic dyes: polluting effects and elimination methods from textile waste water. *Int J Chem Eng Res* 9:121–136
19. Singh M, Pant G, Hossain K, Bhatia AK (2017) Green remediation. Tool for safe and sustainable environment: a review. *Appl Water Sci* 7(6):2629–2635
20. Sivaram NM, Gopal PM, Barik D (2019) Toxic waste from textile industries. In: *Energy from toxic organic waste for heat and power generation*. Woodhead Publishing, UK, pp 43–54
21. Srebrenkoska V, Zhezhova S, Risteski S, Golomeova S (2014) Methods for waste waters treatment in textile industry. In: *International scientific conference “UNITECH 2014”*, Gabrovo
22. Suteu D, Zaharia C, Muresan A, Muresan R, Popescu A (2009) Using of industrial waste materials for textile wastewater treatment. *Environ Eng Manage J* 8(5):1097–1102
23. Telke AA, Joshi SM, Jadhav SU, Tamboli DP, Govindwar SP (2010) Decolorization and detoxification of Congo red and textile industry effluent by an isolated bacterium *Pseudomonas* sp. SU-EBT. *Biodegradation* 21(2):283–296
24. Zaharia C, Suteu D, Muresan A, Muresan R, Popescu A (2009) Textile wastewater treatment by homogenous oxidation with hydrogen peroxide. *Environ Eng Manag J* 8(6):1359–1369



# Photo-Catalytic-Assisted Method for Treating Industrial Dye House Effluents



Manickam Parthiban and Gunasekaran Devanand

**Abstract** The use of photo-catalyst for the degradation of synthetic and organic pollutants such as dyes and chemicals has emerged as an effective method for the wastewater treatment. Similarly, Titanium-Di-oxide (Titanium-Di-oxide) has been widely used as a photo-catalyst in many environmental and energy applications due to its efficient photo-activity, high stability, low cost and safety to the environment and humans. Photo-catalysis is a promising technique for the degradation of various hazardous chemicals that are present in dye house effluent. The reason might be the light source that is provided for the reaction. The cost of photo-catalysis in UV light may be costlier but India being a tropical country and having abundance of sunlight; the photo-catalysis in sunlight is attractive and cost-effective option for textile industries. This chapter describes the benefits of using Titanium-Di-oxide and reduces graphene oxide (RGOT) as an efficient catalyst for the degradation of the dye house effluent. The degradation experiments have been conducted, and RGOT catalyst was found to be more efficient.

**Keywords** Titanium-Di-oxide · Reduced graphene oxide · Nano-composite · Photo-catalysis · Modification · Degradation · Hazardous · Organic pollutants

## 1 Introduction

The quick development of worldwide populace just as industrialization has prompted an attending increment in ecological contamination. This has exceptionally negative impacts on normal components that are fundamental for life on earth, for example, air and water. It turns out to be extremely pivotal consequently to discover maintainable approaches to relieve contamination to give a spotless and safe climate for people.

---

M. Parthiban (✉)

Department of Fashion Technology, PSG College of Technology, Coimbatore, Tamil Nadu, India  
e-mail: [parthi111180@gmail.com](mailto:parthi111180@gmail.com)

G. Devanand

Department of Textile Technology, KSR College of Technology, Tiruchengode, Tamil Nadu, India

Photograph catalysis has pulled in overall interest because of its capability to utilize sun-based energy not exclusively to take care of natural issues yet additionally give an inexhaustible and practical fuel source. A proficient photograph impetus changes over sunlight-based energy into synthetic energy which can be utilized for ecological and energy applications, for example, water treatment, air refinement, self-cleaning surfaces, hydrogen creation by water cleavage and CO<sub>2</sub> transformation to hydrocarbon energize. Examination in the advancement of productive photograph reactant materials has seen critical improvement over the most recent twenty years with an enormous number of exploration papers distributed each year. Upgrades in the exhibition of photograph synergist materials have been a great extent corresponded with propels in nanotechnology [1].

Numerous materials that have been read for photograph catalysis, Titanium-Dioxide (Titanium-Di-oxide:titania), have been widely explored on the grounds that it has many merits, for example, high photograph synergist action, brilliant physical and synthetic strength, minimal effort, non-destructive, non-toxicity and high accessibility [2]. The photograph synergist movement of titania relies upon its stage. It exists in three glass-like stages; the anatase, rutile and brookite. The anatase stage is metastable and has a higher photocatalytic action, while the rutile stage is all the more synthetically stable yet less dynamic. A few titania with a combination of both anatase and rutile stages show higher exercises contrasted with unadulterated anatase and rutile stages. When titania is illuminated with light of adequate energy, electrons from the valence band are elevated to the conduction band, leaving an electron insufficiency or opening, h<sup>+</sup>, in the valence band and an overabundance of negative charge in the conduction band. The free electrons in the conduction band are acceptable diminishing specialists while the resultant openings in the valence band are solid oxidizing specialists and can both partake in redox responses [3, 4].

At the point when titania is illuminated with light of adequate energy, electrons from the valence band are elevated to the conduction band, leaving an electron inadequacy or opening, h<sup>+</sup>, in the valence band and an overabundance of negative charge in the conduction band. The free electrons in the conduction band are acceptable decreasing specialists while the resultant openings in the valence band are solid oxidizing specialists and can both partake in redox responses. Titania anyway experiences various downsides that limit its commonsense applications in photo-catalysis. Right off the bat, the photo-generated electrons and openings exist together in the titania molecule and the likelihood of their recombination is high. This prompts low paces of the ideal substance changes concerning the consumed light energy [5, 6]. The generally enormous band hole energy (~3.2 eV) requires bright light for photo-activation, bringing about a low productivity in using sunlight-based light. UV light records for just about 5% of the sun-powered range contrasted with obvious light (45%) not able to withstand these, on the grounds that titania is non-permeable and has a polar surface, and it shows low retention capacity for non-polar natural poisons. There is additionally the test to recuperate nano-sized titania particles from offered water in respects of both monetary and well-being concern. The Titanium-Di-oxide nanoparticles likewise experience the ill effects of collection and agglomeration which influence the photo-activity just as light ingestion. A few systems

have been utilized in the open writing to defeat these disadvantages. These systems target broadening the frequency of photo-activation of Titanium-Di-oxide into the obvious district of the range subsequently expanding the usage of sun-based energy; forestalling the electron/opening pair recombination and consequently permitting more charge transporters to effectively diffuse to the surface; expanding the retention partiality of Titanium-Di-oxide toward natural contaminations just as forestalling the accumulation and agglomeration of the nano-titania particles while facilitating their recuperation from treated water. A few audits have been distributed as of late on the improvement of methodologies to dispose of the constraints of titania photo-catalysis. The majority of these anyway center around poison expulsion from wastewater, water parting for hydrogen creation, CO<sub>2</sub> transformation and response components. In this part, we survey a portion of the techniques that have been explored to beat the restrictions of Titanium-Di-oxide for general photo-catalytic applications and the degree of progress that these procedures have had the option to accomplish in the business [7].

The material business needs huge amounts of water of good quality in its major preparing steps, which for the most part suggest the usage of an enormous number of synthetics, for example, natural dyestuffs, surfactants, chelating special-ists, pH controllers and so on. These cycles create exceptionally harmful wastewater, whose treatment is regularly troublesome because of the presence of some non-biodegradable species with complex structure. Material industry wastewater is vigorously accused of unconsumed colors, surfactants and here and there hints of metals. These effluents cause a ton of harm to the climate. The poisonous impacts of dyestuffs and other natural mixes, just as acidic and antacid pollutants, from modern foundations on the overall population are broadly acknowledged. As of now, the colors are primarily fragrant and heterocyclic mixes, with shading show gatherings and polar gatherings. The structure is more muddled and stable, bringing about more noteworthy trouble to debase the coloring wastewater. Subsequently, there is impressive interest in creating option and more practical techniques for wastewater treatment [8].

## 2 Technologies Available for Treating Dye House Effluents

Material colors and other mechanical colors structure one of the critical natural mixes that cause an expansion in ecological threats. About 1–20% of the general color creations of the world is squandered during the coloring measures and is delivered in material streams. In this manner, there is an expanding worry for decolorization of color streams. For disposal of color contaminations business, actual innovations (adsorption on dynamic carbon, ultrafiltration, invert assimilation, coagulation with compound components and particle trade in engineered retentive pitches) can be utilized effectively. Nearly these techniques are non-destructive as they exclusively move natural mixes from water to the next stage which causes optional contamination. An unnatural weather change brought about by huge scope emanation of carbon

dioxide ( $\text{CO}_2$ ) in the environment and the exhaustion of petroleum products are two basic issues to be tended to sooner rather than later. Extraordinary exertion has been made to diminish  $\text{CO}_2$  emanations. Advances including carbon catch and land sequestration have quickened in the previous decade. Shockingly, a large portion of the related cycles requires incidental energy input, which may bring about the net development of  $\text{CO}_2$  outflow. Moreover, there are numerous vulnerabilities with the drawn out underground stockpiling of  $\text{CO}_2$ . In such manner, the photo-catalytic decrease of  $\text{CO}_2$  to deliver hydrocarbon energizes, for example, methane ( $\text{CH}_4$ ) is esteemed as an alluring and reasonable methodology in lessening  $\text{CO}_2$  emanations and settling the energy emergency. Numerous sorts of semiconductor photo-catalysts, for example, Titanium-Di-oxide,  $\text{ZrO}_2$ , CdS and blends thereof have been generally read for this reason.

## ***2.1 Titanium-Di-oxide as Photo-Catalyst***

By far the most researched photo-catalytic material is anatase Titanium-Di-oxide because of its long-term thermodynamic stability, strong oxidizing power, low cost and relative non-toxicity [9, 10]. However, the rapid recombination of electrons and holes is one of the main reasons for the low photo-catalytic efficiency of Titanium-Di-oxide. Moreover, its wide band gap of 3.2 eV confines its application to the ultraviolet (UV) region, which makes up only a small fraction ( $\approx 5\%$ ) of the total solar spectrum reaching the earth's surface. In order to utilize irradiation from sunlight or from artificial room light sources, the development of visible-light-active Titanium-Di-oxide is necessary. In the past few years, carbon-based Titanium-Di-oxide photo-catalysts have attracted cosmic interest for improved photo-catalytic performance.

### **2.1.1 Significance of Photo-Catalytic Treatment**

Titanium-Di-oxide photo-catalysis is a serious oxidation measure with key preferences, over other water therapy advancements, including the absence of mass exchange constraints, activity at encompassing conditions and the possible utilization of sun-based radiation (e.g., modest, plentiful and clean wellspring of energy). This technique has extraordinary points of interest:

- First this cycle can be completed under surrounding conditions and may prompt absolute mineralization of natural carbon to  $\text{CO}_2$ ;
- Second, photograph impetus, typically Titanium-Di-oxide, is non-harmful, modest and can be upheld on reasonable materials.

Also, the UV radiation needed for photo-catalytic cycles may come from a counterfeit source or from the sun. Since, Titanium-Di-oxide can just utilize a general little part (under 5%) of the sun-oriented range for photo-catalytic oxidation, likewise, the utilization of high-energy UV light is not just expensive yet in addition can

be hazardous [11]. Graphene has attracted extensive consideration photo-catalysis because of its fantastic conductivity and enormous surface region. Its wonderful electron catch stockpiling transport properties improve the charge detachment proficiency of Titanium-Di-oxide. Then, its huge explicit surface zone builds absorptivity. This extraordinarily advances the photo-catalytic evacuation effectiveness for natural toxins. Huang et al. have arranged a graphene/Titanium-Di-oxide composite for photo-degradation.

Except if shading materials are appropriately taken out, color wastewater essentially influences photosynthetic movement in amphibian life to diminish light infiltration. Heterogeneous photo-catalysis is an effective procedure to wreck natural contaminations in water [12]. The usage of consolidated photo-catalysis and sunlight-based advances to accomplish, with ease, the mineralization of toxins present in water has as of late drawn consideration, and numerous fruitful inventive sun-oriented pilot scale reactors have been created. Late examinations on Titanium-Di-oxide photo-catalysis have been situated toward the photo-catalyst immobilization as a dainty film. This strategy empowers mechanical application by taking out most of the issues experienced [13]. Due to the special appropriate ties of graphene, for example, improvement of adsorption of pollutants, light assimilation force and predominant electrical properties, it has been accounted for that grapheme-based semiconductor nano-composites are considered as photo-catalysts for corruption of poison [14].

## ***2.2 Modification of Titanium-Di-oxide Photo-Catalysts Using Graphene***

An enormous number of exploration work has been distributed on Titanium-Di-oxide adjustment to improve its photo-catalytic properties. These alterations have been done from multiple points of view which incorporate metal and non-metal doping, color refinement, surface change, creation of composites with different materials and immobilization and adjustment on help structures. The properties of adjusted Titanium-Di-oxide are in every case naturally not the same as the unadulterated Titanium-Di-oxide with respect to light assimilation, charge detachment, adsorption of natural contaminations, adjustment of the Titanium-Di-oxide particles and simplicity of division of Titanium-Di-oxide particles. Graphene, specifically, has been viewed as a very appealing part for the planning of composite materials. Since it is not able to withstand its huge hypothetical explicit surface region, graphene has a broad two-dimensional  $\pi$ - $\pi$  formation structure, which enriches it with fantastic conductivity of electrons. Transporters in perfect graphene sheets have been accounted for to act as massless Dirac fermions. When joining Titanium-Di-oxide nano-crystals with graphene, energized electrons of Titanium-Di-oxide could move from the conduction band (CB) to graphene through a permeation system. The hetero-junction framed at the interface (named Schottky boundary) isolates the

photo-induced electron-opening sets, along these lines smothering charge recombination. The improvement of photo-catalytic movement of graphene-based semiconductor–metal composites was first exhibited by Kamat and associates in 2010. Following that, Zhang et al. Shen et al., and Zhou et al. done one-venture aqueous techniques to plan graphene–Titanium-Di-oxide half breed materials and demonstrated that the composites showed improved photo-activity toward natural corruption over uncovered Titanium-Di-oxide. Fan et al. created P25 graphene composites by three diverse arrangement techniques, i.e., UV-helped photo-catalytic decrease, hydrazine decrease and aqueous strategy, all of which had essentially improved photo-catalytic execution for H<sub>2</sub> advancement from methanol fluid arrangement when contrasted with unadulterated P25. Supposedly, the investigation on the utilization of graphene–Titanium-Di-oxide composites on the photo-reduction of CO<sub>2</sub> is as yet in its earliest stages. This prompts our incredible interest in contemplating the function of graphene in the composite toward the photo-reduction of CO<sub>2</sub> into CH<sub>4</sub> gas under noticeable light illumination [15].

### 2.2.1 Non-metal Doping of Titanium-Di-oxide Nanoparticles

Titanium-Di-oxide nanoparticles have been completely doped at the O locales with non-metals, for example, C, B, I, F, S and N. Non-metal dopants are accounted for to be more fitting for the augmentation of the photo-catalytic action of Titanium-Di-oxide into obvious area contrasted with metal dopant. This can be credited to the pollution states which are close to the valence band edge, notwithstanding, they do not go about as charge transporters, and their part as recombination focuses may be limited. From Fig. 2, it has been noted that the band and hole energy is a narrowing component for TiO<sub>2</sub> [16]. The doped non-metal with the O2p states moves the valence band edge upward and limits the band–hole energy of the doped Titanium-Di-oxide photo-catalyst. The nitrogen and carbon-doped Titanium-Di-oxide nanoparticles have been accounted for to show more noteworthy photo-catalytic action under obvious light illumination contrasted with other non-metal dopants. N-doped Titanium-Di-oxide (N-TiO) has all the earmarks of being the most proficient and widely researched photocatalyst for non-metal doping. Zeng et al. revealed the readiness of an exceptionally dynamic-changed N-Titanium-Di-oxide nanoparticle through a novel secluded calcination technique. The magnificent photo-catalytic execution of the photocatalyst was attributed to brilliant crystallinity, solid light gathering and quick partition of photo-generated transporters.

In addition, the upgrade of charge division was ascribed to the arrangement of paramagnetic [O-Ti<sup>4+</sup>-N<sub>2</sub>-Ti<sup>4+</sup>-VO] group. The surface oxygen opportunity actuated by vacuum treatment caught electron and elevated to create super oxygen anion extremist which was a fundamental dynamic animal groups in photocatalytic measure. The photocatalytic action of CO<sub>2</sub> decreases under noticeable light over altered N-Titanium-Di-oxide photo-catalyst was analyzed, and it has been discovered that the band–hole of N-Titanium-Di-oxide photo-catalyst marginally diminishes by expanding N content. Moreover, the sub-band energies identified with the

contamination energy level were seen in the N-Titanium-Di-oxide photo-catalyst in light of the interstitial N species and the sub-band-hole energies were found to have diminished from 2.18 eV with 10 wt% N-Titanium-Di-oxide photo-catalyst. Interestingly, the substitution of O by N is troublesome in light of the range of N (17.1 nm) being higher contrasted with O (14 nm) and the electro neutrality can be kept up by oxygen opening, that are given by substitution of three oxygen opportunities by two nitrogen particle. N-Titanium-Di-oxide photo-catalyst decreases the oxygen energy opening from 4.2 to 0.6 eV, recommending that N favors the development of oxygen opportunities.

Conversely, O particles (14 nm) could be subbed effectively by F molecules (13.3 nm) on account of their comparative ionic span. Yu et al. detailed that the F-doped Titanium-Di-oxide (F-Titanium-Di-oxide) can assimilate obvious light because of the high-thickness expresses that were assessed to be underneath the maxima valence band, despite the fact that there was no move in the band edge of Titanium-Di-oxide. A synergistic impact among fluorine and hydrogen in hydrogenated F-doped Titanium-Di-oxide which empowered light assimilation in UV, noticeable and infrared light enlightenment with upgraded electrons and openings partition were also studied. Surface opening and  $Ti^{3+}$  focuses on the hydrogenated F-doped impetus combined with upgraded surface hydrophobicity and encouraged the creation of surface-bound and free hydroxyl revolutionaries. Species present on the outside of the impetus set off the arrangement of new  $Ti^{3+}$  involved states under the conduction band of the hydrogenated F-doped Titanium-Di-oxide, subsequently narrowing the band-hole energy.

Enhanced photo-catalytic execution of N-doped Titanium-Di-oxide over unadulterated Titanium-Di-oxide has likewise been credited to productive partition of electron-opening sets just as an expanded making of surface extremists, for example, hydroxyl. The band-hole can likewise be limited by doping Titanium-Di-oxide with S, since substitution of S into Titanium-Di-oxide can be performed effectively because of bigger sweep of S (18 nm) contrasted with O particles (14 nm). S fuse in Titanium-Di-oxide has been accounted for to change the cross section dividing of the Titanium-Di-oxide with a decrease in the band-hole width from 3.2 to 1.7 eV taking into consideration higher photo-catalytic action. N, S and C co-doped Titanium-Di-oxide tests photo-catalytic decrease of Cr(IV) demonstrated that the co-doping and calcination assumed a significant function in the microstructure and photo-catalytic movement of the impetuses. The co-doped examples calcined at 500 °C indicated the most noteworthy exercises credited to the synergistic impact in upgrading crystallization of anatase and (N, S and C) co-doping.

The carbon-doped Titanium-Di-oxide (C-Titanium-Di-oxide) is accounted for 44 photo-impetuses—applications and attributes be more dynamic than N-Titanium-Di-oxide, in this way, C-Titanium-Di-oxide has gotten exceptional consideration. Noorimotlagh et al. examined the photograph synergist evacuation of nonylphenol (NP) compound utilizing obvious light dynamic C-Titanium-Di-oxide with anatase/rutile. It was discovered that the doping of C into Titanium-Di-oxide cross section may improve the noticeable light use and influence the auxiliary properties of the as-combined photograph impetuses. Also, it was accounted for that after C doping and

changing the calcination temperature, and the band-hole was limited from 3.17 to 2.72 eV and from 2.72 to 2.66 eV, separately. C-Titanium-Di-oxide with a distance across of around 200 nm and the cylinder divider was made out of anatase Titanium-Di-oxide, formless carbon, glasslike carbon and carbon component doping into the cross section of Titanium-Di-oxide. The C-Titanium-Di-oxide nanotubes showed much preferred execution in photo-catalytic action over exposed Titanium-Di-oxide under UV and obvious light. The got results were credited to the C doping, which limited the band-hole energy of Titanium-Di-oxide, expanded the obvious light adsorption toward longer frequency and obstructed charge recombination [16].

### 2.2.2 Graphene-Based Nano-composites for Effluent Treatment

The plan and arrangement of graphene-based composites containing metal oxides and metal nanoparticles have stood out for photo-catalytic exhibitions. For instance, Tan et al. arranged a novel graphene oxide-doped-oxygen-rich Titanium-Di-oxide (GO-O Titanium-Di-oxide) mixture heterostructure and assessed its movement for photo-reduction of CO<sub>2</sub> under the light of low-influence energy-sparing sunshine bulbs. It was discovered that the photo-stability of O<sub>2</sub>—Titanium-Di-oxide was fundamentally improved by the expansion of GO, at which the subsequent mixture composite held a high reactivity. The photo-activity accomplished was about 1.6 and 14.0 folds higher than that of exposed O<sub>2</sub>—Titanium-Di-oxide and the business Degussa P25, separately. This high photo-catalytic execution of GO-O Titanium-Di-oxide was credited to the synergistic impact of the obvious light responsiveness of O<sub>2</sub>—Titanium-Di-oxide and an improved detachment and move of photo-generated charge transporters at the close interface of GO-O Titanium-Di-oxide hetero-junctions. This investigation is accounted to have opened up additional opportunities in the advancement of novel, cutting-edge hetero-junction photo-catalysts. Additionally examined photo-reduction of CO<sub>2</sub> with H<sub>2</sub>O fume in the gas stage under the light of a Xe light utilizing Titanium-Di-oxide/nitrogen (N)-doped decreased graphene oxide (Titanium-Di-oxide/NrGO) nano-composites. They found that the amount and design of N dopant in the Titanium-Di-oxide/NrGO nano-composites firmly impacted the photo-catalytic effectiveness, and the most elevated reactant movement was noticed for Titanium-Di-oxide/NrGO nano-composites with the most elevated N doping content. In addition, altered Titanium-Di-oxide/rGO exhibited a synergistic impact, upgrading CO<sub>2</sub> adsorption on the impetus surface and advancing photo-generated electron move that brought about a higher CO<sub>2</sub> photo-reduction pace of Titanium-Di-oxide/NrGO. Qu et al. arranged the graphene quantum specks (GQDs) with high quantum yield (about 23.6% at an excitation frequency of 320 nm) and GQDs/Titanium-Di-oxide nanotubes (GQDs/Titanium-Di-oxide nanoparticles) nano-composites and the photo-catalytic action was tried toward the debasement of methyl orange. It was discovered that the GQDs stored on Titanium-Di-oxide nanoparticles can grow the noticeable light retention of Titanium-Di-oxide nanoparticles and upgrade the action on photo-catalytic corruption of methyl orange under UV-vis light illumination ( $\lambda = 380\text{--}780$  nm). Moreover, the photo-catalytic movement



of GQDs/Titanium-Di-oxide nanoparticles was around 2.7 occasions as higher than that of exposed Titanium-Di-oxide nanoparticles. Tian et al. detailed the readiness of N, S co-doped graphene quantum specks (N, S-GQDs)—decreased graphene oxide-(rGO)—Titanium-Di-oxide nanotubes (Titanium-Di-oxide NT) nano-composites for photo-degradation of methyl orange under obvious light illumination. It was discovered that the S-GQDs+rGO + Titanium-Di-oxide nano-composites all the while indicated an all-encompassing photo-response range, improved charge detachment and transportation properties. Also, the clear rate consistent of N, S-GQDs+rGO + Titanium-Di-oxide NT is 1.8 and 16.3 occasions higher contrasted with rGO + Titanium-Di-oxide NT and unadulterated Titanium-Di-oxide NT, individually. Recommending that GQDs can improve the use of sun-powered light for energy transformation and ecological treatment.

In any case, its huge band–hole energy, ca. 3.2 eV restricts its retention of sunlight-based radiation to the UV light reach which represents just about 5% of the sun-powered range. Besides, the photo-catalytic action of Titanium-Di-oxide is likewise restricted by the fast recombination of the photograph produced electron-opening sets. At the point when utilized in water treatment applications, Titanium-Di-oxide has a helpless partiality toward natural contaminations, particularly hydrophobic natural poisons. A few systems have been utilized to lessen its band–hole energy, its electron-opening recombination rates just as upgrade its retention of natural toxins. In this section, we survey the absolute latest works that have utilized the doping, design and auxiliary alteration of Titanium-Di-oxide particles for applications in photo-catalysis. Moreover, we examine the viability of these dopants or potentially modifiers in upgrading Titanium-Di-oxide photo-activity just as some point of view on the eventual fate of Titanium-Di-oxide photo-catalysis.

The composites of GO/RGO outperform electron-openings sets recombination rate and diminish energy hole by changing valence band level (VBL) and conduction band level (CBL) bringing about better adsorption of light radiation that upgrades photo-degradation execution of metal oxides and polymers-based composites. This audit will be the principal endeavor to thoroughly investigate the impact of photo-catalytic exercises on stacking of GO/RGO with metals oxides and polymer-based composites. Besides, the impact of pH, starting color fixation, portion of photo-catalyst and impact of surface charge on composite surface for viable debasement have additionally been analyzed.

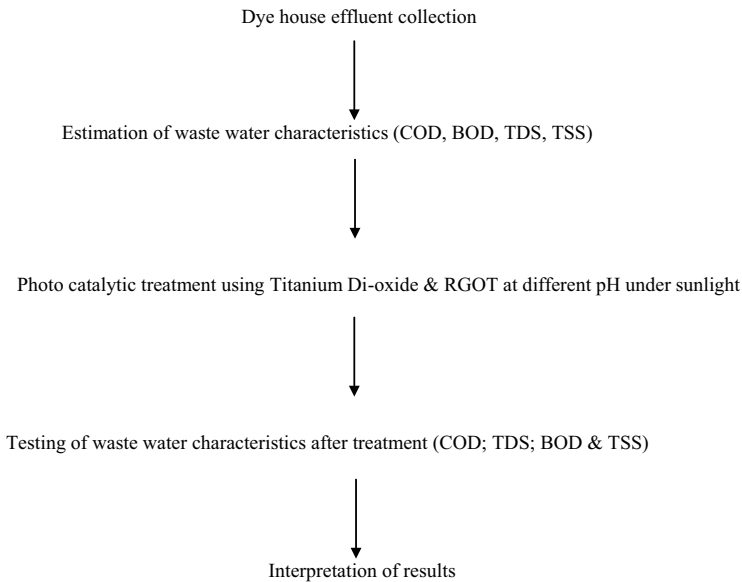
Anatase Titanium-Di-oxide particles with a normal width of 12 nm were consistently scattered on the rGO sheet. Slow hydrolysis response was effectively achieved using ethylene glycol and acidic corrosive-blended solvents combined with an extra cooling step. The readied RGO-Titanium-Di-oxide nano-composites displayed prevalent photo-catalytic movement ( $0.135 \mu\text{mol gcat}^{-1} \text{h}^{-1}$ ) in the decrease of  $\text{CO}_2$  over graphite oxide and unadulterated anatase. The cozy contact among Titanium-Di-oxide and RGO was proposed to quicken the exchange of photo-generated electrons on Titanium-Di-oxide to RGO, prompting a compelling charge against recombination and in this manner upgrading the photo-catalytic action. Besides, our photo-catalysts were discovered to be dynamic much under the illumination of low-power

energy-sparing lights, which delivers the whole cycle monetarily and for all intents and purposes possible [17].

### 3 Materials and Methods

For treating the dye house effluents, RGOT and  $\text{TiO}_2$  have been widely used. The effluents are treated using recently developed RGO-based binary, ternary and quaternary nano-composites. The photo-catalytic activities of RGO-based ternary nano-composites such as RGO/dual semiconductors, RGO/metal/semiconductor and RGO/dual metal-free semiconductors have proven positive results, and the plausible photo-catalytic pathway for generation of free radicals by RGO-based is helpful to develop a new RGO-based photo-catalysts to treat dye house effluents with superior activity and minimized production costs.

#### 3.1 Work Flow Diagram



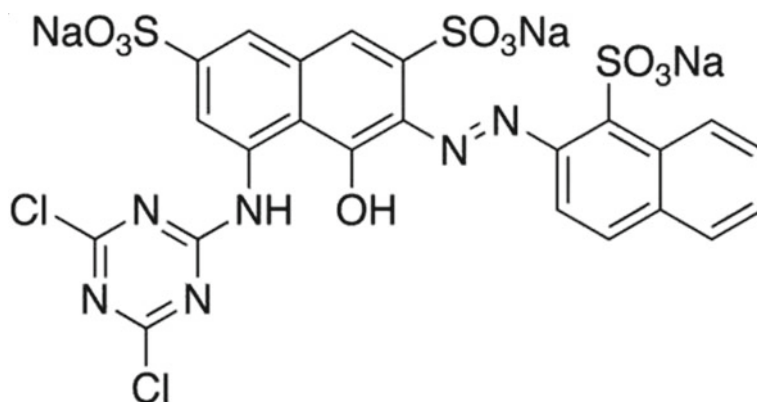


**Fig. 1** Molecular structure of Procion red dye

## 3.2 Materials

The effluent was collected from a local dyeing industry. The dye house recipe is given below.

### 3.2.1 Dye Characteristics

Form—Powder. Color—Red.  
 Odor—Odorless.  
 Solubility (Water)—80 g/l (at RT).  
 pH (value)—6.0–8.0 (Fig. 1).

### 3.2.2 Catalysts Used

**Titanium-Di-oxide:** Titanium-Di-oxide was sourced from the laboratory house of the industry.

**RGOT:** Reduced graphene oxide was synthesized by doping Titanium-Di-oxide and the resultant doped catalyst, namely RGOT was used for the above process.

### 3.2.3 Instruments Used

pH Meter

The pH of the solution was monitored using a digital pH meter. pH was adjusted using HCL solution for making it neutral and basic, respectively. The meter was calibrated using a buffer solution periodically (Fig. 2).

**Fig. 2** pH meter**Fig. 3** Magnetic stirrer

### Magnetic Stirrer

A magnetic stirrer was used for constant mixing of the catalyst throughout the solution (Fig. 3).

### Aerator

Aerator was continuously used in experiments containing both UV and sunlight. The aeration helped in producing more oxygen that will help the dye to degrade.

**Fig. 4** UV spectrophotometer



#### UV Spectrophotometer

The UV spectrophotometer was used to analyze the UV spectrum of the samples (Fig. 4).

### 3.2.4 Methodology

#### Preparation of Test Solution

For each experiment conducted, a bulk solution was prepared and the experiment was conducted for solution of 1000 ml with 1 g of catalyst in it.

#### Testing of Effluent Characteristics

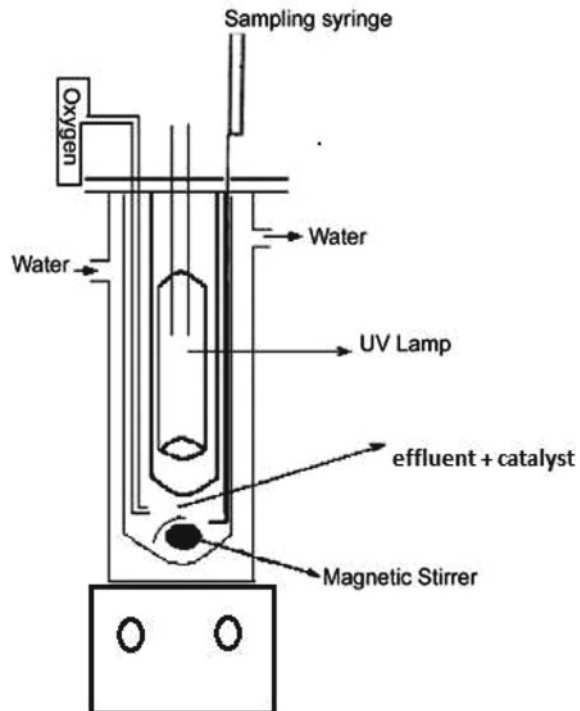
The sourced effluent is tested for its characteristics namely COD, BOD, TSS and TDS (Table 1).

### 3.2.5 Photo-Catalytic Treatment

The photo-catalytic treatment was conducted using Titanium-Di-oxide and RGO P<sub>25</sub> catalyst. Various parameters like pH, light source and concentration of catalyst were analyzed. All the experiments were conducted for 100 ml solution with 0.1 g of catalyst in it. In Fig. 5, the UV photo reactor model is shown. In this method,

**Table 1** Characteristics of raw effluent

S.No.	Characteristics in mg/L	Test method	Result	Standard
1.	Total dissolved solids	Gravimetric	23622	2100
2.	Chemical oxygen demand	Open reflux	3200	250
3.	Biochemical oxygen demand	Dilution	1080	30
4.	Total suspended solids	Gravimetric	328	100

**Fig. 5** UV photo reactor

the oxygen is given through an aerator. The aerator along with the stirring of the catalyst mixes the catalyst throughout the effluent uniformly. This will enhance the degradation of the dye at a higher rate. The UV lamp will provide the light source, and it is covered by glass ware so that water does not penetrate the tube. An opening is given for the syringe to collect the samples.

Figure 6 represents the fish tank model for sunlight reaction. In this model, aeration along with shaking is given for the reaction. This will enhance the reaction at a faster rate giving better results. As sunlight has UV spectrum, visible spectrum and infrared spectrum, the reaction will be faster in sunlight.

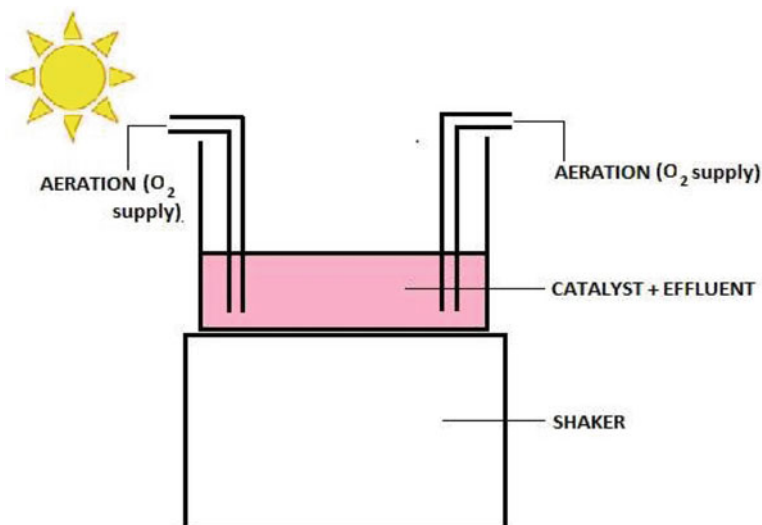


**Fig. 6** Photo reactor for sunlight

### 3.2.6 Textile Wastewater

Wastewater from dyeing units is often rich in color, containing residues of reactive dyes and chemicals, such as complex components, many aerosols, high chroma, high COD and BOD concentration as well as much more hard degradation materials.

With the continuous growth of population in the cities and towns, service utilities are under pressure to provide the increasing demand for wastewater and water supply services. But with limited freshwater resources in many areas, alternative water sources need to be explored. Wastewater reuse is increasingly seen as an option to augment freshwater resources, but to win public confidence the reliability of the technology to produce safe reusable water must be demonstrated. Reuse of wastewater will help maintain environmental quality and help relieve the unrelenting pressure on natural freshwater resources. The existing method of wastewater treatment does not produce effluent of safe and reusable quality, and therefore advanced treatment technology needs to be further explored. The various effluent organic matters (EfOMs), pathogenic microorganisms and persistent organic (POPs) present in the effluent from the wastewater treatment plant should be removed before reuse [9].

## 4 Results and Discussion

### 4.1 Sample Preparation

Graphene oxide (GO) was synthesized by chemical exfoliation of graphite powder following modified Hummers' method. 400 mg GO was first added in 100 mL methanol and ultrasonicated for 1 h. Later, 2 g Titanium-Di-oxide was added to the GO suspension and stirred for an hour. The obtained homogeneous suspension was then transferred to a Teflon-lined autoclave and subjected to solvothermal treatment at 393 K for 8 h. The resultant composite was filtered, washed repeatedly with distilled water and dried in vacuum at 333 K. The sample prepared by this procedure is denoted as RGOT.

### 4.2 Characterization of RGOT Catalyst

Fourier transform infrared (FT-IR) spectra were recorded using Shimadzu DR-8101A spectrometer in transmittance mode after making a pellet with IR grade KBr. The powder X-ray diffractograms (XRD) were recorded using an analytical X'Pert Pro X-ray diffractometer with Cu K $\alpha$  source with a wavelength of 1.54 Å operating at 20 mA and 50 kV. The morphology of the catalysts was evaluated by JOEL 2010 F transmission electron microscope (TEM) equipped with ED and SAED operating at 200 kV. The band gap measurements were carried out using UV-visible DRS spectrophotometer (Jasco V650 model).

#### 4.2.1 FTIR

GO powder presented different bands arising from oxidized groups. The band around 1720 cm<sup>-1</sup> is attributed to stretching vibrations from C=O of -COOH groups. The peak at 1620 cm<sup>-1</sup> is due to C=C from unoxidized sp<sup>2</sup> bonds. The band at 1220 cm<sup>-1</sup> can be assigned to C-OH stretching vibrations, and the band around 1050 cm<sup>-1</sup> corresponds to C-O stretching vibrations. The FT-IR spectra of Titanium-Di-oxide showed a broad band below 700 cm<sup>-1</sup> which is attributed to the Ti-O-Ti stretching and bending vibrational modes and another broad band at around 3400 cm<sup>-1</sup>, which is due to the O-H stretching frequency from the surface hydroxyl group. All the characteristic peaks of GO and Titanium-Di-oxide are present in the RGOT composite. These results imply that Titanium-Di-oxide can be susceptible to the interaction with the functional groups of RGO in the nano-composite. When GO was reduced to RGO, all the peaks arising from oxygen containing functionality were substantially reduced, indicating a reduction of the oxygen content in the sample. Figure 7 shows the FT-IR spectra of graphite, GO, Titanium-Di-oxide and RGOT nano-composite.



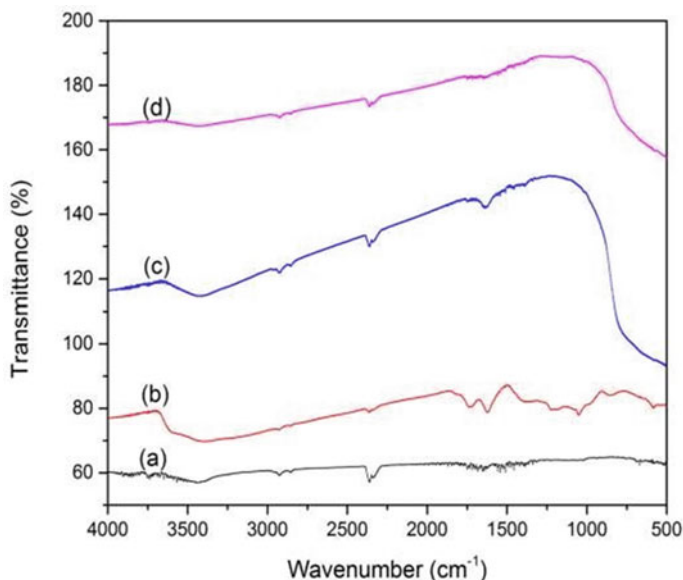


Fig. 7 FT-IR spectra of graphite, GO, Titanium-Di-oxide and RGOT nano-composite

#### 4.2.2 XRD

XRD pattern of the graphite shows a broad diffraction peak at  $2\theta$  of  $26.4^\circ$  corresponding to a d-spacing of  $3.37 \text{ \AA}$  which can be indexed to (002) plane, a typical diffraction peak of graphitic carbon. The peak intensity reduced drastically in GO, and a new strong and sharp diffraction peak at  $2\theta$  of  $10.3^\circ$  was seen with an interplanar distance of  $8.5 \text{ \AA}$  indicating the complete oxidation of graphite to GO. For RGOT nano-composite, the peaks located at  $25.4^\circ$ ,  $37.9^\circ$ ,  $48.0^\circ$ ,  $53.9^\circ$  and  $55.2^\circ$  can be indexed to (101), (004), (200), (105) and (211) crystal planes of anatase Titanium-Di-oxide [JCPDS no. 21-1272]. However, the diffraction peaks of GO were not distinguishable in the XRD pattern of RGOT, which may be due to the masking of the GO peaks by the high intensity peaks of crystalline Titanium-Di-oxide. These results indicate that the modification with RGO did not influence the lattice structure of Titanium-Di-oxide. Figure 8 shows the XRD patterns of graphite, GO powders and RGOT nano-composite.

#### 4.2.3 TEM

The morphology of the RGOT composite was investigated by TEM. It can be clearly seen that the graphene sheet is decorated by Titanium-Di-oxide nanoparticles. The lattice resolved image and the SAED pattern of the Titanium-Di-oxide in the composite, indicating its single crystalline anatase phase with the perfect lattice

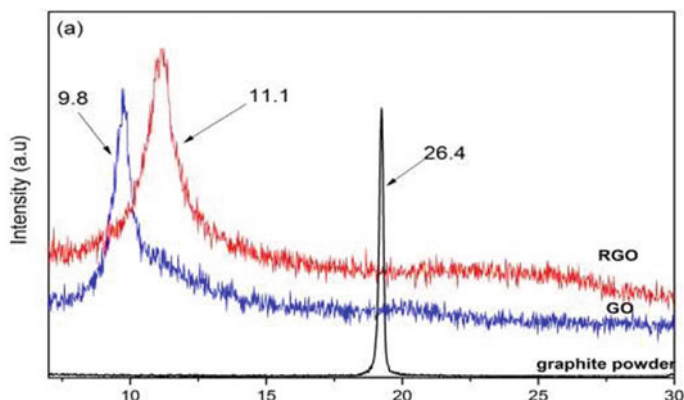


**Fig. 8** XRD patterns of graphite, GO powders and RGO nano-composite

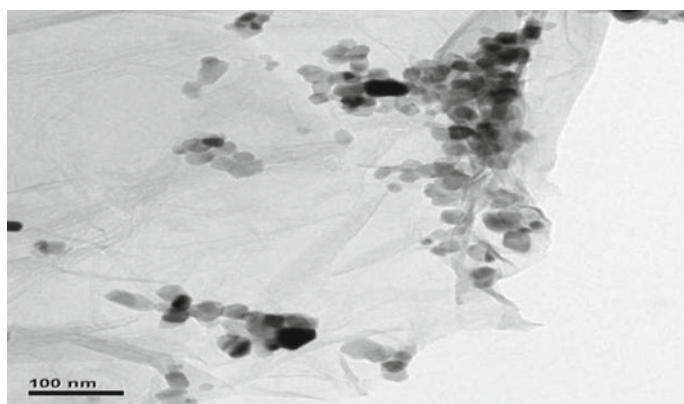


**Fig. 9** Presence of exfoliated RGO flakes and Titanium-Di-oxide nano-composite

spacing of 0.362 nm [(101) anatase]. This is in agreement with the results of the XRD pattern shown in Fig. 8. The TEM image (Fig. 9) shows the presence of exfoliated RGO flakes and Titanium-Di-oxide nanoparticles embedded in them indicating the formation of the composite.

### **4.3 Photocatalytic Activity Test**

Photocatalytic experiments were carried out in a glass tank of 6 L capacity. The dye sample of desired concentration along with the required amount of the catalyst was sonicated for 10 min and later mechanically stirred in dark for 30 min to ensure the establishment of an adsorption/desorption equilibrium of dye on the catalyst

surface. A small amount of sample was collected, filtered and considered as initial concentration of the effluent solution. After the adsorption study, it is then kept in sunlight at an intensity of 70,000 lx. After the zero time reading was taken. Aliquots were taken at regular intervals and then filtered through a Millipore syringe filter of 0.45  $\mu\text{m}$ , and the decolorization was determined through absorbance at maximum wavelength ( $\lambda_{\text{max}}$  538 nm) using UV-visible spectrophotometer (Shimadzu1800, Japan). The rate of decolorization efficiency ( $E$  %) was calculated using the formula (1) given below:

$$E(\%) = \frac{(C_0 - C)}{C_0} \times 100 \quad (1)$$

where  $C_0$  is the initial concentration and  $C$  is the concentration of treated dye samples at various time intervals. The photo-degradation efficiency of the catalyst was determined in terms of chemical oxygen demand (COD), biological oxygen demand (BOD), total dissolved solids (TDS) and total suspended solids (TSS).

#### ***4.4 Process Conditions for Different Reactions Using $\text{TiO}_2$ and RGoT Catalyst***

The collected dye house effluent was treated using the above catalyst at various conditions as per the procedure mentioned below:

##### **4.4.1 Condition 1 (Under Dark Conditions)**

- Catalyst: Titanium-Di-oxide
- Catalyst weight: 0.1 g/100 ml
- Lightness: dark
- pH: 500 times—8.2, 100 times—10.7, raw—13.5
- Duration of reaction: 3 h (Fig. 10).

##### **4.4.2 Condition 2 (Under Sunlight)**

- Catalyst: Titanium-Di-oxide
- Catalyst weight: 0.1 g/100 ml
- Lightness: sunlight
- pH: 500 times—8.2, 100 times—10.7
- Duration of reaction: 3 h (Fig. 11).



**Fig. 10** Reaction with Titanium-Di-oxide in dark



**Fig. 11** Reaction with Titanium-Di-oxide in sunlight

#### 4.4.3 Condition 3 (Under Different pH in Sunlight)

- Catalyst: Titanium-Di-oxide
- Catalyst weight: 0.1 g/100 ml
- Lightness: sunlight
- pH: acidic—4, neutral—7.31
- Duration of reaction: 3 h (Fig. 12).

#### 4.4.4 Condition 4 (in Sunlight)

- Catalyst: RGOT 20%
- Catalyst weight: 0.1 g/100 ml
- Dye concentration: 100 times diluted from raw effluent
- pH: 10.3
- Duration of reaction: 3 h (Fig. 13).



**Fig. 12** Reaction with Titanium-Di-oxide in sunlight under different pH



**Fig. 13** Reaction with RGOT in sunlight

#### 4.4.5 Condition 5 (in UV Light)

- Catalyst: RGOT 20%
- Catalyst weight: 0.1 g/100 ml
- Dye concentration: 100 times diluted from raw effluent
- pH: 10.3
- Duration of reaction: 1 h
- Light: UV light (360 nm) (Fig. 14).

#### 4.4.6 Condition 6 (in UV Light)

- Catalyst: Titanium-Di-oxide
- Catalyst weight: 0.1 g/100 ml
- Dye concentration: 100 times diluted from raw effluent
- pH: 10.3; Duration of reaction: 1 h



**Fig. 14** Reaction with RGOT in UV light



**Fig. 15** Reaction with Titanium-Di-oxide in UV light

- Light: UV light (360 nm) (Fig. 15).

#### 4.4.7 Condition 7 (in Sunlight)

- Catalyst: Titanium-Di-oxide
- Catalyst weight: 1 g/1000 ml
- Dye concentration: 100 times diluted from raw effluent

**Fig. 16** Reaction with Titanium-Di-oxide in sunlight



- pH: 10.3
- Aeration and shaker are used (Fig. 16).

#### 4.4.8 Condition 8 (in Sunlight)

- Catalyst: RGOT 20%
- Catalyst weight: 1 g/1000 ml
- Dye concentration: 100 times diluted from raw effluent
- pH: 10.3
- Duration of reaction: 1 h
- Light: sunlight
- Aeration and shaker are used (Fig. 17).

Based on the treatment conditions, the samples were assessed for its decolorization efficiency and wastewater parameters, namely COD, BOD, TDS and TSS, and the treated samples were compared with the original values and the effluent characteristics were determined accordingly.



**Fig. 17** Reaction with RGOT in sunlight

**Table 2** Treated effluent character estimation

S.No.	Effluent characteristics (mg/L)	Before treatment (mg/L)	After treatment (mg/L)	
			Titanium-Di-oxide	RGOT
1.	COD	3200	20	60
2.	BOD	1080	24	21
3.	TDS	23,622	$6 \times 10^{-8}$	$4 \times 10^{-8}$
4.	TSS	328	0	0

#### 4.5 Effluent Characteristics of Treated Sample

The effluent characteristics were drastically reduced after the treatment with the abovementioned catalyst, namely  $\text{TiO}_2$  and RGOT catalyst. The above catalyst provides best results for treating the dye house effluents (Table 2).

#### 4.6 Decolorisation Efficiency

Similarly, the decolorization efficiency was tested using UV spectrophotometer. Figures 18 and 19 represent the efficiency of decolorization under sunlight for Titanium-Di-oxide and RGOT at various pH and found to be excellent for the treated samples.

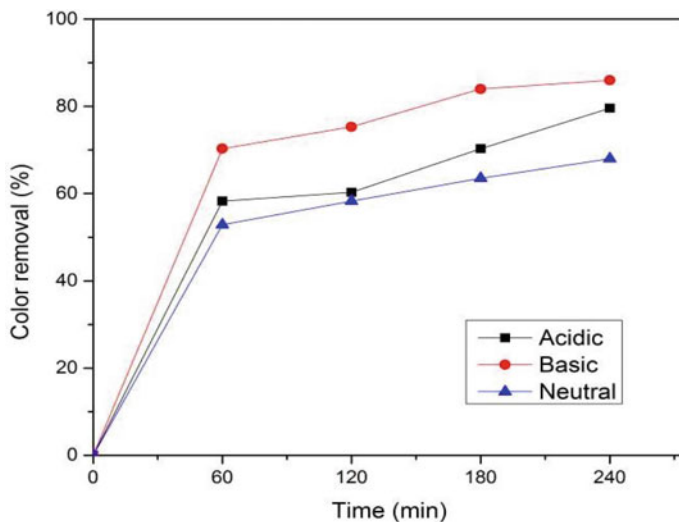


**Fig. 18** pH versus color removal (%) for Titanium-Di-oxide photocatalyst for 1000 mL of solution with 1 g/L of catalyst under sunlight at various pH



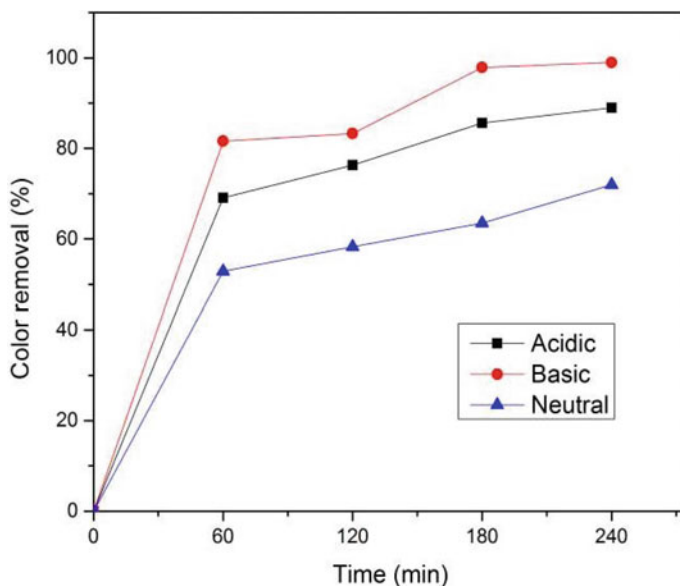


**Fig. 19** pH versus color removal (%) for RGOT nano-composite photo-catalyst for 1000 mL of solution with 1 g/L of catalyst under sunlight at various pH

## 5 Conclusion

From this chapter, it has been found that Titanium-Di-oxide and RGOT are found to be efficient catalyst for the degradation of the dye house effluent. The degradation experiments have been conducted, and RGOT catalyst was found to be more efficient. The highest degradation was found for RGOT catalyst under sunlight in alkaline pH with 94.44%, and the effluent was degraded 92.54% for Titanium-Di-oxide catalyst under sunlight in alkaline pH. In the presence of Titanium-Di-oxide catalyst, under optimized conditions, the COD of the treated sample is reduced from 3200 to 20 mg/L in, the BOD of the treated sample is reduced from 1080 to 24 mg/L, the TDS of the treated sample is reduced from 23622 mg/L to  $6 \times 10^{-8}$  mg/L, and the TSS is found to be reduced from 328 to 0 mg/L. In the presence of RGOT catalyst, under optimized conditions, the COD of the treated sample is reduced from 3200 to 60 mg/L in, the BOD of the treated sample is reduced from 1080 to 21 mg/L, the TDS of the treated sample is reduced from 23622 mg/L to  $4 \times 10^{-8}$  mg/L, and the TSS is found to be reduced from 328 to 0 mg/L.

## References

1. Ganesan NM, Senthil TS, Muthukumarasamy N, Balasundaraprabhu R (2014) The role of pH on the structural properties and photocatalytic applications of Titanium-Di-oxide nanocrystals prepared by simple sol-gel method. *Int J Chem Tech Res* 6(5):3078–3082
2. Jeni J, Kanmani S (2011) Solar nanophotocatalytic decolorisation of reactive dyes using titanium dioxide 8(1):15–24
3. Zhang J, Xiong Z, Zhao XS (2011) Graphene-metal-oxide composites for the degradation of dyes under visible light irradiation. *J Mater Chem* 21:3634–3640
4. Montaser YG, Farah JY, Fathy AM (2007) Enhancement of decolorization rate and COD removal from dyes containing waste water by the addition of hydrogen peroxide under solar photocatalytic oxidation. *Desalination* 217:74–84
5. Pekakis PA, Xekoukoulotakis NP, Mantzavinos D (2006) Treatment of textile dyehouse wastewater by Titanium-Di-oxide Photocatalysis. *Water Res J* 40:1276–1286
6. Barka N, Qourzal S, Assabbane A, Nounah A, Ait-Ichou Y (2010) Photocatalytic degradation of an azo reactive dye, reactive yellow 84, in water using an industrial titanium dioxide coated media. *Arab J Chem* 3:279–283
7. Mahvi AH, Ghanbarian M, Nasser S, Khairi A (2009) Mineralization and discoloration of textile waste water by Titanium-Di-oxide nano particles. *Desalination* 239:309–316
8. Rauf MA, Meetani MA, Hisaindee S (2011) An over view on the photocatalytic degradation of azo dyes in the presence of Titanium-Di-oxide doped with selective transition metals. *Desalination* 276:13–27
9. Shon HK, Phuntsho S, Vigneswaran S (2008) Effect of photocatalysis on the membrane hybrid System for waste water treatment. *Desalination* 225:235–248
10. Dong Y, Chen J, Li C, Zhu H (2007) Decoloration of three azo dyes in water by photocatalysis of Fe(III)–oxalate complexes/hydrogen peroxide in the presence of inorganic salts. *Dyes Pigm* 73:261–268
11. Yaacoubi A, Nejmeddine A (2007) Treatment of textile industry waste water by supported photocatalysis. *Dyes Pigm* 74:439–445
12. Irawaty W, Soetaredjo FE, Ayucitra A (2014) Understanding the relationship between organic structure and mineralization rate of Titanium-Di-oxide-mediated photocatalysis. *Procedia Chem* 9:131–138
13. Egerton TA, Purnama H (2014) Does hydrogen peroxide really accelerate Titanium-Di-oxide, UV-C photocatalyzed decolouration of azo-dyes such as reactive Orange 16. *Dyes Pigm* 6:101, 280–285
14. Chun H, Yizhong W (1999) Decolorization and Biodegradability of photocatalytic treated azo dyes and wool textile waste water. *Chemosphere* 39(12):2107–2115
15. Sameiro M, Goncalves T, Pinto EMS, Nkeonye P, Oliveria-Campos AMF (2005) Degradation of C.I. Reactive Orange 4 and its simulated dyebath waste water by heterogeneous photocatalysis. *Dyes Pigm* 64:135–139
16. Akram TM, Ahmad N, Shaikh IA (2016) Photocatalytic degradation of synthetic textile effluent by modified sol-gel, synthesized mobilized and immobilized Titanium-Di-oxide and Ag-DoP ed Titanium-Di-oxide. *Poly-Environ Stud* 25(4):1391–1402
17. Sivakumar T, Thamaraselvi K, Brindh A, Elangovan E (2019) Photocatalytic degradation of reactive dyes over titanates. *J. Nanosci. Nanotechnol.* 19(12):2087–2098

# Advanced Oxidation Processes (AOP)—Effective Innovative Treatment Methods to Degrade Textile Dye Effluent



R. Sukanya Devi, Bhaarathi Dhurai, S. Sundaresan, and A. Selvakumar

**Abstract** Textile industry is the second largest consumer and polluter of water for processing fibres, yarns, fabrics and garments. There are wide range of dyestuffs and chemicals used in the treatment of textile materials to enhance several properties. In early days, the dye wastewater effluent was discharged to the nearby fresh-water bodies or land. Due to the increase in awareness and necessity for sustainable processes, there are many treatment methods to treat the textile effluent. The processes include physico-chemical treatment, and secondary and tertiary treatment methods are adopted widely which basically work on coagulation and sedimentation, adsorption, biological degradation of dyes. In these processes, the residual sludge is a great problem, and the textile effluent treatment process results in piled up sludge which consists of majority of dyes and other salts. The degradation of the dyes in the sludge takes several years, and to speed up the degradation of dyes, advanced oxidation processes are currently under research, and few technologies are used in effluent treatment plants. The generation of hydroxyl radical species and exposure of textile effluent to these radicals decolourize and degrade the organic compounds. There are several processes to generate the hydroxyl radicals like ozonation, UV treatment, photocatalytic treatment, electrochemical oxidation process, Fenton process, etc. The biodegradability of the by-products after AOPs increases 6–8 times. This chapter will discuss in detail about the above-said treatment methods, their efficacy in treatment of dye decolourization and reduction of pollution load. Each process has its own advantages and disadvantages in terms of decolourization, operational cost, sludge generation and so on. The adaptation of suitable technology will also be discussed briefly.

**Keywords** Textile effluent · Dye degradation · Advanced oxidation process · Ozonation · Photocatalysis

---

R. Sukanya Devi (✉) · B. Dhurai · S. Sundaresan · A. Selvakumar  
Department of Textile Technology, Department of Fashion Technology, Kumaraguru College of Technology, Coimbatore, Vellore Institute of Technology, Chennai, India  
e-mail: [sukanyadevi.r.txt@kct.ac.in](mailto:sukanyadevi.r.txt@kct.ac.in)

## 1 Introduction

Textile industries have their root which dates back to many centuries, and it is a major contributor for the country's economy in terms of industrial production, employment and exports. The Indian textile industry dates back to centuries, and it contributes to 14% of India's industrial production, 4% GDP and 17% of the country's export [1]. The industry provides direct employment to over 35 million people, and it is the second largest employment provider. The structure of the textile industry is complex [2]. The textile industry has different sectors from fibre manufacturing, spinning, weaving, knitting, wet processing and garmenting. The wet processing industry utilizes huge amount of water for pre-treatment, dyeing and printing of the fabrics. Figure 1 illustrates the input/output analysis of a typical wet processing industry [2].

The two major problems with textile wet processing industries include (i) enormous consumption of water and (ii) discharge of dyes and allied organic chemicals. The environmental law for the dyeing effluent in India is very stringent, and this necessitates the need for efficient treatment methods that must follow zero liquid discharge (ZLD). Most common effluent treatment plants (CETP's) in India set for the ZLD are generating hundred tons of hazardous solid waste per day as sludge (residual dyes and waste salts). These secondary pollutants and their disposal is a serious problem, and thus, there is need to shift from ZLD towards zero waste plants. This can be attained by focusing on complete removal of dyes and other organics

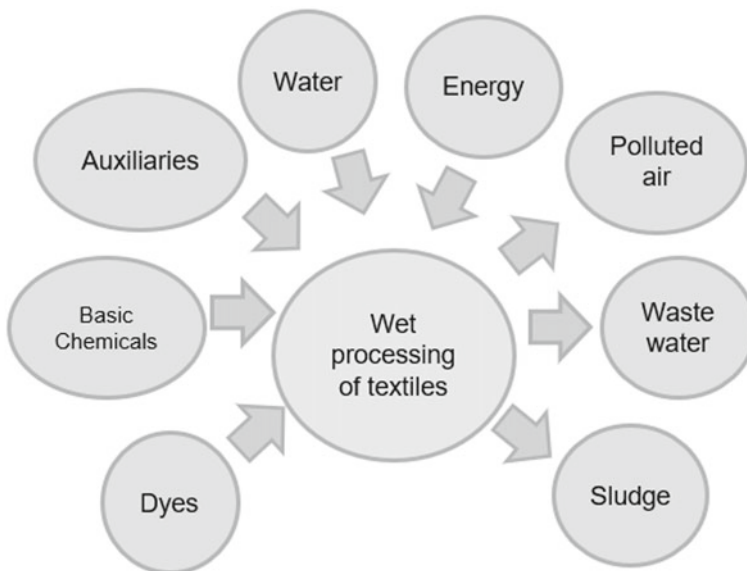


**Fig. 1** Input/output analysis of a typical wet processing industry

from the effluents before their discharge on to the soil and water bodies, in addition to water recovery.

In general, the unutilized dyes from the processing industry are harmful for the ecology, since these effluents discharged are coloured and contain high concentrations of pollutants like organic dyes, salts. They also contribute higher biological oxygen demand/chemical oxygen demand (BOD/COD) values [3, 4]. The use of dyes will not be abandoned as humans are aesthetically interested in dyed textile. Many types of dyes are used to treat different fibres in the manufacture of textiles. The textile chemical processing sector consumes large quantities of water and chemicals for pre-treatment and dyeing processes of textile materials, which in turn leads to large amount of wastewater contribution [5, 6]. It is already known and acceptable that those group of pollutants posing numerous problems (affectation of photosynthesis in water plants, carcinogenicity, etc.) and therefore decolourization of textile effluents become a major environmental concern [7]. The effluents from textiles contain large amount of recalcitrant unfixed dyes (as acid dyes, basic dyes, reactive dyes, sulphur dyes, disperse dyes, chrome dyes, optical brightener) which include the dyes which are not fixed or unreacted to the fibre of different textiles during the process (fibres as wool and nylon, cotton and viscose, polyester and acrylic) and are considered emerging contaminants. Synthetic dyes, in the dyeing effluent, are carcinogenic and mutagenic in nature, and they must be removed from the dyeing effluent before the effluent is discharged.

There are wide number of chemical structures of synthetic dyes. The effluent consists of wide range of chemical reagents which are used in the dyeing and finishing processes, contains different chemical structures and different concentration and compositions of both organic and inorganic compounds, which causes a serious problem when they are discharged to the environment [8, 9]. The chemical classes of dyes employed more frequently on industrial scale are the azo which contributes about 60–70% of the total dyes used and also other classes like, anthraquinone, indigoid, sulphur, phthalocyanine derivatives and triphenylmethyl (trityl).

Removal of various toxic dyes requires a complex series of hybrid physico-chemical (coagulation sorption, reverse osmosis and ion exchange) and biological processes (aerobic and anaerobic biodegradation). The dyes in the effluent exhibit complex structures and are dependent on the types of dyes used, and this makes their removal difficult even after combining various hybrid processes. Several methods available or reported in the literature to address the above issues are provided in Table 1.

Lately, the inclusion of advanced oxidation processes (AOP) in the treatment train has been suggested for the treatment of textile industry effluent. AOPs involve the generation of hydroxyl radicals, exploiting the high reactivity and unselectively of the intermediate hydroxyl radicals ( $\text{OH}^*$ ) to attack the organic molecules at accelerated rate constants vs. standard oxidation processes (KOH, organic substance, usually in order of  $10^6$ – $10^{11} \text{ M}^{-1} \text{ S}^{-1}$ ) [24, 25]. In wastewater treatment, AOP refers mainly to processes that yield  $\text{OH}^*$  through ozone ( $\text{O}_3$ ), hydrogen peroxide ( $\text{H}_2\text{O}_2$ ) and UV light simultaneously, or their combination as  $\text{O}_3$ ,  $\text{O}_3/\text{UV}$ ,  $\text{O}_3/\text{H}_2\text{O}_2$ ,  $\text{UV}/\text{H}_2\text{O}_2$ . Other interesting technologies include ozonation alone is often considered as an AOP in

**Table 1** Various treatment processes for cotton textile process effluents with their merits and demerits

Process	Advantages	Disadvantages	References
Coagulation/flocculation	Removal of insoluble dyes	Fouling due to sludge generation	[10]
Adsorption using activated carbon	Control over suspended solids and organic substances	Cost of activated carbon used	[11]
Biodegradation	Effective elimination of oxidizable substances	Poor biodegradability of dyes	[12]
Ozonation	Effective dye decolourization	No significance in terms of the COD removal; cost of ozonation systems	[13]
Electrochemical oxidation process	Well suited for different volumes and pollution loads	Excess iron hydroxide sludge formation	[14, 15]
Ultra-filtration and micro filtration	Low pressure	Pre-treatment for NF or RO and reduce fouling on NF and RO	[16]
Nano filtration	Effective filtration of low molecular weight organic compounds and divalent ions from monovalent salts	Not efficient for separation of monovalent salts, fouling	[17–20]
Reverse osmosis	Effective removal of mineral salts and hydrolyses reactive dyes and other chemical auxiliaries	Requires high pressure, fouling	[21–23]

wastewater due to the formation of hydroxyl radicals in the presence of organic matter in high concentration. Introduction of a homogeneous (dissolved ions as  $\text{Fe}^{2+}$ ,  $\text{Mn}^{2+}$ ,  $\text{Cu}^{2+}$ ) or heterogeneous (i.e.  $\text{MnO}_2$ ,  $\text{Ni}_2\text{O}_3$ ,  $\text{Fe}_2\text{O}_3$ ,  $\text{CuO}$ ,  $\text{Al}_2\text{O}_3$ ,  $\text{TiO}_2$ ) catalyst can serve as an opportunity to accelerate the ozonation reaction and the decomposition of the target compounds [26]. For instance, it is showed that the combined ability of ozone and a catalyst/adsorbent shows high potential in elimination of dyes from wastewater. These AOPs used for the removal of dyes from wastewater effluents are conducted on industrial wastewater treatment plants effluents and designed as end-of-the-pipe solution.

Table 2 shows the characteristics of the dye bath and wash water effluent (raw effluent and before/after each process) (26). The TDS levels at RO reject and the ME evaporator inlet/concentrate are so intense and require an alternate methods to reduce the pollutant. Many new treatment methods are suggested and are under laboratory trials. One such process is the advanced oxidation treatment, which has a promising results, and some processes are already in use. Advanced oxidation processes are wide range of technologies which are used/investigated mainly to

**Table 2** Characteristics of the Wastewater and dye bath effluent of various treatment units

Parameters	Details of samples									
	Dye bath raw effluent	Wash water (raw effluent)	Primary outlet	Secondary outlet	RO inlet	RO permeate	RO reject			
pH	10.5–12	8–9.5	7–7.5	7–7.50	6.50	5.8	6.80			
Turbidity (NTU)	50–60	20–40	10–15	<2	NIL	NIL	<5			
TSS, mg/L	400–500	<50	<20	<10	NIL	NIL	<2			
TDS, mg/L	23,000–26,000	2000–2400	2300–2500	2300–2500	2500–2700	<100	16,000–18,000			
BOD, mg/L	400–600	250–400	150–200	<30	<10	<2	<100			
COD, mg/L	1500–3000	800–1000	650–900	100–130	<50	<5	1000–1200			
Chloride, mg/L	9000–12,000	750–1000	750–1000	750–1000	750–1000	<50	5000–7000			

degrade the organic pollutants present in air and water. These are effectively studied in treatment of wastewater from domestic sewage and widely on the industrial effluents. These systems mainly generate oxidizing agents, and these agents react with the pollutant and degrade them. There are various ways and means to produce the most effective oxidizing agents, and this chapter will unveil the types of advanced oxidation processes and their effectiveness. There may be a single process used to degrade the effluent or combination of several oxidation process for effective degradation of the pollutants.

## 2 Advanced Oxidation Processes

Oxidation is the loss of electrons by a molecule, atom or ion during any chemical reaction, and the opposite reaction of gaining electrons by a molecule, atom or ion is termed as reduction. In general, oxidation and reduction occur together, with one species losing electron and the other gaining electron, and this process is termed as redox reaction. Hydrogen peroxide and sodium hydrosulphite are classic examples for the use as oxidizing agent and reducing agent, respectively, in textile wet process. Though hydrogen peroxide is a good oxidizing agent, the reaction rate is dependent on the thermodynamics, and the process kinetics is slower [27, 28]. The reaction rate can be increased by generation of free radicals like hydroxyl radicals ( $\cdot\text{OH}$ ), and the reaction rates are much higher than the oxidizing agents generated by  $\text{H}_2\text{O}_2$ .

Advanced oxidation processes are an effective alternative for the treatment of contaminated wastewater (underground as well as from industry) resources containing non-biodegradable harmful substances as well as to purify and disinfect drinking water [29]. Table 3 provides the oxidation potential of various commonly used oxidants [30] (Fig. 2).

**Table 3** Comparison of oxidation potential

Oxidizing species	Oxidation potential (V)
Fluorine	2.87
Free hydroxyl radical ( $\text{OH}\cdot$ )	2.8
Sulphate radical	2.60
Ozone ( $\text{O}_3$ )	2.08
Hydrogen peroxide ( $\text{H}_2\text{O}_2$ )	1.78
Permanganate	1.68
Hypochlorite	1.49
Chlorine dioxide ( $\text{ClO}_2$ )	1.57
Chlorine ( $\text{Cl}$ )	1.36



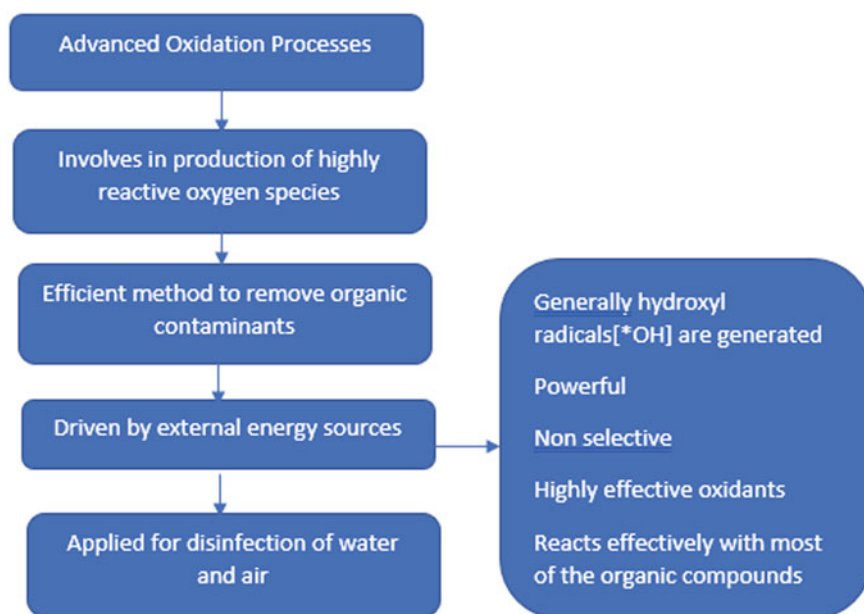


Fig. 2 Advanced oxidation process [30]

## 2.1 Types of Advanced Oxidation Process

There are many types of advanced oxidation processes, and classification is made according to the mode of release of the oxidizing agents [30] (Fig. 3).

## 3 Chemical AOPs

### 3.1 Ozonation

Ozone consists of three oxygen atoms and is a very unstable gas, due to its unstable nature, the gas readily converts to oxygen, and during this transformation, a free oxygen atom or free radical is being released. The free radical form of oxygen generated will be highly reactive, also has a shorter life time, and it can survive only for few milliseconds.

Ozone is a colourless gas, and the smell of the ozone gas is similar to the odour of the air after thunderstorm. Ozone is a great disinfectant and efficient in treating bacteria and viruses [31], and it is already used for water purification nowadays, replacing chlorine. Apart from this, ozone is used to eliminate taste and odour problems, by reducing the concentration of sulphur, iron, manganese in water. The iron,

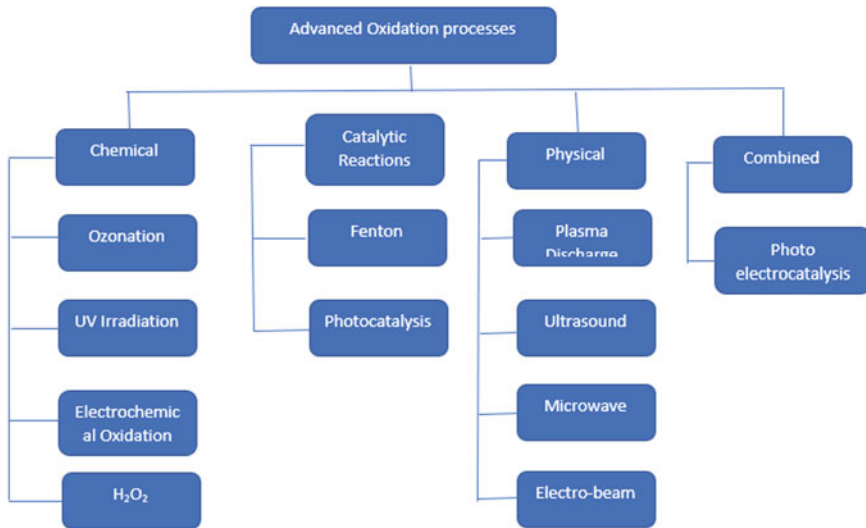


**Fig. 3** Types of advanced oxidation process [30]

manganese and sulphur present in the water are oxidized by ozone to form respective metal oxides or elemental sulphur which are in the insoluble form, and these particles can then be removed later by filtration process. Other organic pollutant and chemicals can be eliminated either by chemical oxidation or by coagulation. Since ozone is highly unstable, it will convert into lower molecular compounds within a time frame of very few seconds to few minutes. The efficiency and rate of degradation are highly dependent on the water temperature, pH and water chemistry.

### 3.1.1 Ozonation Process

Ozone can be generated in the following ways

- Corona Discharge—type ozone generators (simulation of the lightning)
- Ultraviolet rays—type ozone generators (simulation of the UV rays from the sun)
- Electrolytic and chemical reactions.

Figure 4 [32] is the general process flow of treating wastewater using ozone. In general, an ozonation process includes passing of clean, dry air through a high voltage electric discharge. For treating very small quantity of wastewater, UV ozonation is preferred, and for large-scale treatment systems, corona discharge type ozone generator or other bulk ozone-generating methods are used. The clean and dry air is passed through electric discharge for instance corona discharge, which produces an ozone concentration of roughly around 1% or 10,000 mg/L. The vacuum is created in raw wastewater by passing it through a venturi throat, and the vacuum attracts the ozone gas into the wastewater stream, and hence, the air is bubbled up. Post filtration

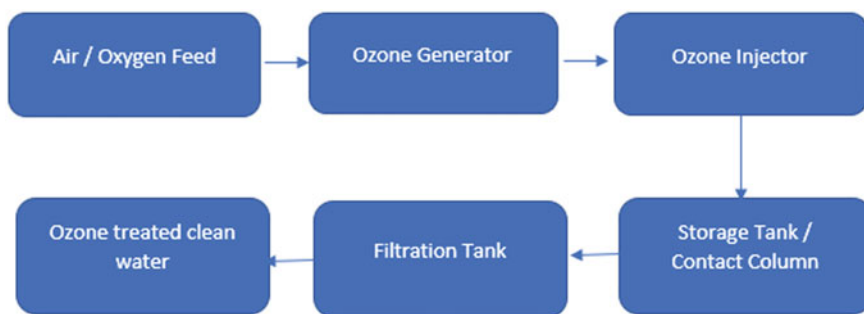


**Fig. 4** Ozonation process

is essential as insoluble metal oxides are created due to the oxidation of metals by ozone.

Ozone is used to treat bacteria, viruses and protozoans as it is effective over a wide range of pH, and it has a strong germicidal property than chlorination. It is also a very strong oxidizing agent which reacts in a shorter time. The main advantage of this treatment process is there is no addition of chemicals to the wastewater. Ozone treatment process can be used to eliminate a wide range of organic, inorganic, microbes and taste, odour problems. Higher equipment cost and operational cost are the main drawback of this process. In addition to this, there is a difficulty to have highly efficient professional for the operation and maintenance of the equipment. The by-products generated during ozonation are still being evaluated as some by-products reported to be carcinogenic which may include certain types of aldehydes, carboxylic acids, ketones and brominated by-products. Hence, post filtration process is necessary which may be an activated carbon filter. Prior to ozonation, the system requires a pre-treatment process to reduce the hardness and prevent the formation of carbonate scaling, which may be achieved by the addition of polyphosphate to the wastewater. When compared to chlorine, solubility of ozone in water is very less, and to make it soluble and form a homogenous mixer, special mixing techniques are adopted. Ozone generation may lead to potential fire hazards and toxic in nature.

Ozone can be effective when combined with hydrogen peroxide, which will generate free hydroxyl radical. When these free radicals are in contact with organic pollutants, they decompose them into simpler substances [33, 34].

### 3.1.2 Ozone Degradation in Textiles

Ozonation ( $O_3$ ) is a promising and efficient method of treatment of textile wastewater as it is a very strong oxidizing agent that is able to degrade many substances including dyes, and ozone is not affected by any textile auxiliaries and saline water [35]. Chromophores which are the colourants in the dye are the target for the ozone and decompose them even if there are other chemicals and auxiliaries present in the

wastewater. The complex dye compounds are converted into simpler compounds which can be further treated using biological treatment.

### 3.2 UV AOPs

Sunlight is a major source which is used as disinfectant to kill the growth of microorganisms [36]. In textiles, light fastness is an important parameter that is to be checked in the dyed and printed fabrics, as light could deteriorate the colour to fade. Hence, this can be used as a source of degradation of organic dye compounds present in the textile wastewater. The sunlight is in the wave form and is classified as the visible light, ultraviolet and infrared rays. Out of which, ultraviolet rays are the most powerful one which is used to oxidize the compounds present in the polluted water. Generally, ultraviolet irradiation is a photolysis process, and the principle of degradation of organic pollutant is by absorption of photons from the UV irradiation by the compounds present in the wastewater, and the oxidation process continues due to the energy released. The quantum yield and rate of the compound are responsible for the photolysis rate of UV radiation [37]. UV irradiation can be used in advanced oxidation processes, since the agents such as hydrogen peroxide, ozone and chlorine form free radicals when they are exposed to UV. In addition to that, the UV treatment produces or simplifies the organic pollutants into simpler and less refractory organic compounds or converts it to water, carbon dioxide and mineral acids. UV radiation-based free radical generation is very powerful in generating oxidation species like hydroxyl radical when hydrogen peroxide exposed direct UV photolysis, photo-Fenton reactions or heterogeneous photocatalysis.

In direct photolysis, the mechanism of degradation happens through the absorption of incident ray from the UV irradiation on the contaminant. For an effective direct photolysis of the process, the contaminant in the wastewater should strongly absorb the UV light, but not all the contaminant has good absorbency. To obtain a very effective process, UV can be combined with hydrogen peroxide or ozone or hydrogen peroxide/ozone. In combined process, UV irradiation with hydrogen peroxide produces hydroxyl radical which can degrade the organic contaminants in the wastewater. Generally, most of the textile dyestuffs consist of double bonds or conjugated double bonds. The dyes with double bond consist of carbon, nitrogen or oxygen atoms.

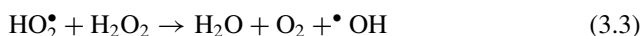
The degradation of organic and inorganic compounds in wastewater of environmental concern is extensively studied, and hydroxyl radical-driven photooxidation process such as UV/hydrogen peroxide, UV/ozone, UV/ozone/H<sub>2</sub>O<sub>2</sub> and photocatalytic reactions shows significant results in degradation of the organic pollutants than direct photolysis [38]. The photooxidation processes are discussed in detail.

### 3.2.1 UV/H<sub>2</sub>O<sub>2</sub>

In photooxidation process, the free radical hydroxyl is generated from hydrogen peroxide in the presence of UV irradiation. This process is the combination of H<sub>2</sub>O<sub>2</sub> and UV light in a synergistic effect to degrade organic dyes and chemicals present in the textile wastewater and other pathogenic microorganisms in aqueous solutions [39]. The successful degradation of the dyes and chemicals is obtained due to the generation of hydroxyl radicals from the UV/H<sub>2</sub>O<sub>2</sub> process.



The decomposition of the hydrogen peroxide is induced by the photoreaction and is the initiation of the reaction starts as per Eq. (3.1). Equations (3.2) and (3.3) indicate the propagation of the reactions



The net reaction of the propagation as observed in reactions (3.2) and (3.3) is the decomposition of hydrogen peroxide into molecular oxygen and water. Since the wash water (water used for pre-treatment and washing) may contain hydrogen peroxide after bleaching of the textile materials, the residual peroxide may be used for this photooxidation process only if the solution contains active peroxide compounds. The termination of this chemical reaction may be of different reactions like radical-radical recombination.

The decomposition of H<sub>2</sub>O<sub>2</sub> involves more complex mechanisms, and the explanation of this decomposition is found in the literature and includes species like HO<sub>2</sub><sup>-</sup>; HO<sub>2</sub><sup>•-</sup> and O<sub>2</sub><sup>•-</sup> in the chain decomposition mechanism. The efficiency of the UV/H<sub>2</sub>O<sub>2</sub> photooxidation is highly dependent on the generation of hydroxyl radical which in turn is dependent on the UV absorption capacity of the hydrogen peroxide and the chemical constituents and characteristics of the textile wastewater subjected to degradation [40]. The optical property of the effluent and the specific constituents present in it plays a significant role in generation of hydroxyl radical. The chemicals in the effluent are responsible for the transmittance resulting in reduction of hydroxyl radical generation. In addition to this, the presence of natural organic matter, inorganic ions and organic acid can reduce the degradation efficiency of specific contaminants.

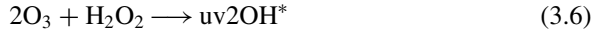
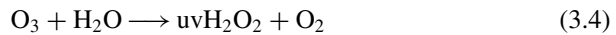
The effluent absorption capacity can be measured by measuring the UV radiation transmittance of the effluent at 254 and 172 nm. Strong absorbance values of UV light by effluent are due to the presence of natural organic matter and aromatic compounds. In such cases, the treatment of organic contaminants with higher UV radiation absorbance results in lower transmittance at these UV light wavelengths, will be more difficult to degrade and is costly.

The modelling or design of an UV/H<sub>2</sub>O<sub>2</sub> oxidation process for a wastewater treatment plant is not easily done using the complete theoretical approach. The main reasons for this are as follows:

- The characteristics of the effluent are complex and variable.
- It is expensive to conduct full effluent characterization.
- Requires advanced numerical solutions to overcome complex mathematical model for practical applications.
- Better and quite precise results can be obtained by a simplified model which considers all the uncertainties that are involved in the process design.

### 3.2.2 UV/Ozone

Combining UV and O<sub>3</sub> [41] and treating wastewater are a proven technology. This technology is more advantageous than the individual ozone and UV treatment as it has advantages of both by generating hydroxyl radical when UV light when reacts with the ozone. The reactions are as follows



The hydroxyl radical which is formed either completely degrades the organic pollutant in the wastewater to CO<sub>2</sub> and water or to simpler degradable compounds which can be easily digested in the further biological process.

Since ozone is highly unstable and reactive, it is produced separately and passed through the UV lamp reactor. The UV lamps are placed inside a quartz sleeves to achieve better transmission of UV light. In non-contact type, a transparent separator film is used to separate the UV lamp and the effluent.

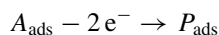
### 3.3 Electrochemical Oxidation Process

In the electrochemical oxidation process, free hydroxyl radicals are generated, which will attack the organic pollutants in the wastewater. There are two types of electrochemical oxidation process

1. Direct Electrochemical Oxidation process.
2. Indirect Electrochemical Oxidation Process.

### 3.3.1 Direct Electrochemical Oxidation Process

In direct electrochemical oxidation process, the hydroxyl radicals are formed at the surface of the electrode. In direct electrochemical oxidation process, the organic pollutants are oxidized once they are adsorbed by the anodic surface without discharge of any other substance other than the electron which is called as the clean reagent. These surface-controlled reactions are also known as anodic oxidation process which take place the near surface of the anode, and hence, the electrode plays an important role in the process [42].



where  $A_{\text{ads}}$  is the pollutant adsorbed by the anode and  $P_{\text{ads}}$  is the oxidized adsorbed pollutant. Direct electrochemical oxidation process has a lower kinetics that is highly dependent on the electrocatalytic activity of the anode. Higher reaction rates can be obtained by using metals such as Pt and Pd and also metal oxides like iridium dioxide, ruthenium-titanium dioxide and iridium dioxide [43]. Table 4 shows the oxygen potential of different anodes [44].

When organic pollutant wastewater gets oxidized on the electrodes, there are two different scenarios observed, a soft oxidation of organics where several species and polymers were formed as by-products of the direct electrolytic process by the anodes (class 1 electrodes). The oxygen evolution over potential is observed to be lower in these cases. However, in bulk electrolysis, there was a contradiction, using class 2 electrodes, the electrolysis of the organic wastes was harsh, and they were easy to mineralize into carbon dioxide gas without any production of polymers with very few or almost no refractory species. The oxygen evolution over potential (OEP) was also higher.

It is observed that there are different types of behaviour with the electrolytic oxidation of water to free hydroxyl radicals and their interaction with the electrode surface [45]. In bulk electrolysis, the potential applied in the cell is large, and the reactions take place over the oxygen evolution over potential, and first stage conversion or oxidation of water to free hydroxyl radical is expected, and however, the behaviour

**Table 4** Oxygen evolution potential of different anodes

Electrodes	Class	Oxygen evolution potential	Conditions
RuO <sub>2</sub>	1	1.47	0.5 M H <sub>2</sub> SO <sub>4</sub>
IrO <sub>2</sub>	1	1.52	0.5 M H <sub>2</sub> SO <sub>4</sub>
Pt	1	1.60	0.5 M H <sub>2</sub> SO <sub>4</sub>
Oriented pyrolytic graphite	1	1.70	0.5 M H <sub>2</sub> SO <sub>4</sub>
SnO <sub>2</sub>	2	1.90	0.05 M H <sub>2</sub> SO <sub>4</sub>
PbO <sub>2</sub>	2	1.90	1 M H <sub>2</sub> SO <sub>4</sub>
BDD	2	2.30	0.5 M H <sub>2</sub> SO <sub>4</sub>

of these radicals is observed to be entirely different. In the case of active electrode (Class I electrodes), the generated hydroxyl radical reacts with the surface of the electrode enabling the oxidation of organic pollutants by direct transfer of electrons from the electrode surface. The oxidation in direct electrolysis happens due to the transfer of electrons and chemical oxidation of the pollutant at the anode surface and not with the reaction of hydroxyl radicals generated. The conversion of organic pollutant to different simpler compounds or species is dependent on the electrodes used. For example, if graphite is used as electrode, it results in electrode burning, resulting in very low removal efficiencies. In case of certain electrodes like Platinum, Titanium, Iridium dioxide electrodes, results in formation of the oxides which in turn chemically attack the organic pollutant resulting in different simpler compounds and efficiency. Apart from breaking down of dyes into simpler compounds it is observed that there is a decrease in the Total Dissolved Solids (TDS) and Chemical Oxygen Demand (COD) values of the treated effluent using different electrodes [46].

In bulk electrolysis, the non-active electrodes (Class 2 electrodes) and the hydroxyl radicals generated do not react at the anodic surface instead it reacts directly with the organic pollutants in the electrochemical cell and very near to the electrode, as the span of hydroxyl radical is short. Since the reaction zone is very small, very often researchers consider it as direct electrolysis reaction, although it is a mediated electrochemical oxidation reaction.

In direct electrolysis, it is important to consider the processes that happen on the electrode surface and how the mass transfer of organic pollutants from the solution happens near the electrode surface and their reactions take place. The following stages should be completed for effective oxidation at the electrode surface to take place.

- Transfer of the organic pollutants from the bulk solution to the electrode surface
- Mediated oxidation by hydroxyl radicals at the electrode surface
- From the electrode surface, oxidized product has to be transferred to the bulk solution [47].

Figure 5 [47] explains the above-mentioned stages.

During direct electrode oxidation, the main point of concern is the formation of polymer layer on the anodic surface. Moreover, the direct electrochemical oxidation is fixed based on the anodic potential, before the  $O_2$  evolution results in decrease in catalytic activity also known as poisoning effect. This effect is dependent on the nature of the organic pollutants, their adsorption capacity, concentration of aromatic organic compounds like phenols, chlorophenols, etc. [48].

### 3.3.2 Indirect Electrochemical Oxidation Process

In indirect electrochemical oxidation process, the hydroxyl radicals are formed at the bulk solution. In indirect electrochemical oxidation, a mediator is generated at the anode or at the cathode, which is responsible for the reaction to happen [49]. Chlorine, hydrogen peroxide are the mostly used mediators; however, any salt present in the



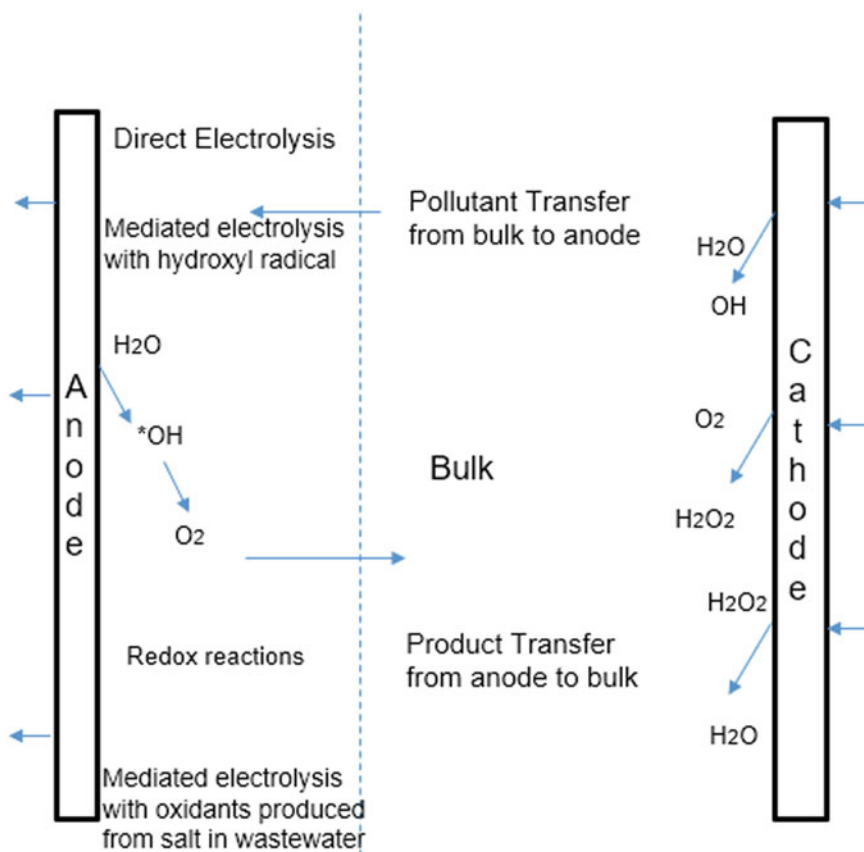


Fig. 5 Mass transport controlled processes in anodic oxidation

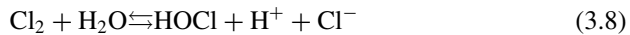
wastewater can be a mediator. The textile wastewater consists of excess amounts of chlorines and sulphates which can be used as mediators in the indirect electrochemical oxidation process. There is not only bulk electrochemical oxidation that happens, and it is also associated with other types of oxidation process, but bulk is the effective one.

The production or activation of the mediator can be accomplished in four ways

- Activation by available salts in wastewater
- Chemical activation by addition of oxidizing agents
- Activation by photolysis
- Activation by sonication.

The later three processes are combined processes which increase the efficiency of the oxidation process which splits up the organic pollutants. Since textile wastewater contains salt, the process is discussed in detail. During bulk process, chlorine

is generated on the surface of the anode, and it undergoes many speciation reactions. These reactions are highly influenced by the pH resulting in chlorine (3.7) hypochlorite (3.8) and hypochlorous acid (3.9) which are strong oxidants



Though the oxidants are powerful, there are several drawbacks associated with this process. The formation of organo-chlorinated species by chlorine with many functional groups of the pollutant creates new compounds which are hazardous than the wastewater. Similarly, production of chlorates due to electrochemical reactions or chemical reactions slows down the kinetics at room temperature. In certain electrochemical reactions using electrodes like boron doped diamond electrodes, perchlorates are formed due to electrolysis, action of hydroxyl radicals are hazardous and prevent usage of these electrodes in wastewater containing huge chlorides.

### 3.4 Hydrogen Peroxide

Hydrogen peroxide is a very strong oxidizing agent and is used in textiles for bleaching or removal of natural colour from the cotton fibre. And has a molar mass is 34.0147 g/mol. The commercially available hydrogen peroxide has a wide range of concentration from 3% (household use) to 60% for some industrial uses. Normally, for wastewater treatment applications, 30–50% concentrations are most common.

Hydrogen peroxide has been widely used to treat the industrial wastewater to reduce the BOD and COD. It is mainly used to predigest the wastewater which contains moderate and high levels of toxic compound, inhibitory or recalcitrant to biological treatment. Though the cost of the process is higher than the physical or biological means, in specific applications, the usage is justified. The specific applications are as listed below

- It is applied as a pre-treatment process of high strength and low flow wastewaters, prior to discharge to a treatment system, where biological treatment is practically impossible
- Enhances the separation of organic pollutants by flotation and settling processes
- Provides supplemental supply of dissolved oxygen (DO) when there is any temporary overload or equipment failure in the biological treatment systems.

Hydrogen peroxide process can be applied as a standalone treatment of wastewater or as an enhancement to existing physical or biological treatment processes based on the effluent characteristics. The conversion of  $\text{H}_2\text{O}_2$  to hydroxyl radical is possible

by combined AOPs like  $O_3$ /hydrogen peroxide, UV/ $H_2O_2$ , UV/ $H_2O_2$ /ozone, etc. The combination of UV/ $H_2O_2$  has been discussed earlier in this chapter. To reduce the cost of  $H_2O_2$  processes, research is going on to produce the  $H_2O_2$  prior to the advanced oxidation process by cathodic generation of  $H_2O_2$ .

### 3.5 Fenton Reagent

Fenton, in the year 1894, discovered the Fenton reaction that the activation of hydrogen peroxide is possible by  $Fe^{2+}$  salts to oxidize tartaric acid. In late 1960s, studies were carried out to oxidize the organic pollutants. Fenton process is an efficient advanced oxidation process, involving generation of hydroxyl radical due to the reaction between hydrogen peroxide and aqueous ferrous ions. The principle of removal or degradation of the organics is by radical oxidation and flocculation. The hydroxyl radical generated during the reaction of ferrous ion catalysing the hydrogen peroxide effectively oxidizes the organics in the effluent, and effective results can be obtained like generation of  $CO_2$ , water and other inorganic salts, while ferrous ions generated in the wastewater by Fenton act as a flocculant.

There are two mechanisms suggested for degradation of organic pollutants by Fenton process [50].

One mechanism considers active hydroxyl species ( $*OH$ ) produced in Fenton reaction degrades the organic pollutants.

Second mechanism considers generation of strong oxidizing iron substance like  $FeO^{2+}$  and  $FeO^{3+}$  in Fenton reaction instead of hydroxyl radical generation. Hydroxyl radical merely involves in initiating the reaction [51].

The Fenton process is normally operated at the pH 3, and the oxidation activity of hydroxyl radical is dependent on the pH of the solution. In general, the oxidation potential and the oxidation capacity of the hydroxyl radical increase with decrease in the pH. The activity of Fenton reagent is less due to increase in the pH because of lack of  $Fe^{2+}$  species which results in the formation of ferric hydroxides and iron oxohydroxides which are inactive. Moreover, auto decomposition of hydrogen peroxide happens at higher pH levels

Fenton is highly considered in wastewater treatment due to its high performance and simple operating conditions like room temperature and atmospheric pressure. It is also non-toxic, and the hydrogen peroxide in the wastewater can be broken down to simple compounds like water and oxygen. Though it has several advantages, the process involves maintenance of pH, higher consumption of hydrogen peroxide and formation of ferric sludge that hinders the oxidation during the process. To overcome these problems, both homogeneous and heterogeneous catalysts are used to replace the  $Fe^{2+}$  are under current research.

### 3.5.1 Electro-Fenton Process

The Electro-Fenton process is an effective advanced oxidation process which involves generation of hydroxyl radical in an electrocatalytic process [52]. Electrochemistry offers an excellent method to generate and to control the concentration of Fenton's reagents. The hydrogen peroxide is synthesized in the solution to be treated, and regeneration of  $\text{Fe}^{2+}$  is possible by the electrochemical process which overcomes the drawbacks of the chemical Fenton process.

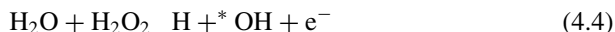
At acidic pH of 3, hydrogen peroxide generation is achieved by two electron reduction of  $\text{O}_2$  from the compressed air in an electrochemical cell. This provides reduction in cost of the reagents, transport and storage of the reagents.



Hence, it is sufficient to add the ferrous or ferric iron to the solution to proceed with the Fenton reaction, to generate the hydroxyl radical. The Fenton reagent then generates ferric iron that is reduced at the cathode with same potential that generates the hydrogen peroxide.



Similarly, at the anode, water is oxidized to oxygen, and  $\cdot\text{OH}$  is produced at the surface of the high-oxygen over voltage anode from water oxygen [53].



Hence, there is a continuous and controlled generation of Fenton reagent in an electrochemical cell which leads to continuous generation of hydroxyl radical without any accumulation of the Fenton reagent, thereby eliminating the wastage reactions. The rate of production of the Fenton reagent can be controlled by either the applying suitable current between the electrodes or by using a three-electrode cell which can control the potential of the cathode.

When compared to the chemical Fenton process, the electrochemical Fenton process provides some advantages [54].

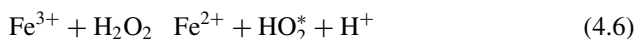
- On-site production of hydrogen peroxide
- Higher removal rate of the organics since there is continuous regeneration of  $\text{Fe}^{2+}$  at a low and constant concentration
- Realizing the various forms of organic degradation methods like Fenton and anodic oxidation, flocculation and electric adsorption.

However, the generation of  $\text{H}_2\text{O}_2$  is very slow because oxygen has less solubility in water at lower pH, and the current efficiency is also low at lower pH. In addition to this,

the efficiency of the process also depends upon the electrode, catalyst concentration, electrolytes, current density, dissolved oxygen levels and temperature.

### 3.5.2 Photo-Fenton

Ultraviolet radiation treatment process with Fenton reagents is known as photo-Fenton process. This process combines hydrogen peroxide and  $\text{Fe}^{2+}$  or  $\text{Fe}^{3+}$  ion and UV radiation resulting in production of more hydroxyl radicals. The main advantage of this process eliminated the drawbacks of the Fenton process and increases the degradation rate of the organic contaminants. In the classical Fenton process, the  $\text{Fe}^{3+}$  ions in the reactor are accumulated, and the reaction does not take place, until all  $\text{Fe}^{2+}$  ions are exhausted. But in the photo-Fenton process, as mentioned in the equations (Eqs. 4.5 and 4.6), the continuous generation of ferrous ions takes place by the photo-reduction process of ferric ions. Hence, the generation of free hydroxyl radical happens due to the reaction between the regenerated ferrous ions, hydrogen peroxide and ferric ion, and the reaction continues this same manner [55].



The photo-Fenton process is effective at pH in the range of 3.0, during the hydroxy  $\text{Fe}^{3+}$  complexes are highly soluble and  $\text{Fe}(\text{OH})^{2+}$  is also highly photoactive. The photo-Fenton reactions are more efficient than the chemical Fenton process because of higher removal rate of the organic pollutants. To reduce the cost of the process, it is also suggested to use sunlight instead of UV irradiation; but the results in terms of degradation of organic pollutants are not satisfactory. Due to the generation of carbonic acid by conversion of carbonate and bicarbonate species, which is less reactive to hydroxyl radicals, the pH conditions at 3 are reported to be favourable.

The photo-Fenton process shows a better degradation of organic pollutants at low concentration, as high concentration pollutants reduce the penetration and absorption of UV radiation of iron complex and in turn require higher concentration of hydrogen per oxide and longer radiation time. The efficient of photo-Fenton process can be improved by addition of several organic ligands like Ethylenediaminetetraacetic acid(EDTA), Ethylenediamine-N,N'-disuccinic acid (**EDDS**), oxalate and organic carboxylic acid and used along with  $\text{Fe}^{3+}$  under photocatalytic reactions. The effects achieved by these ions are stated as follows

- Since iron ligands have wider UV light wave length absorption in comparison with the other  $\text{Fe}^{3+}$  complexes, which reduces the ferric ion to ferrous ion.
- regeneration of more amount of hydroxyl radical
- promotes hydrogen peroxide activation and increases the generation of hydroxyl radicals
- improving iron resolution to pH 7

- This can be operated over a wide range of solar radiation spectrum.

When compared with chemical Fenton process, the photo-Fenton has many advantages such as reduction in dosage of catalyst resulting in reduced sludge formation but the cost of UV lamps, longer time for UV irradiation and higher energy consumption are the major drawbacks of this process [56].

### 3.5.3 Sono-Fenton Process

The sound waves with the frequency higher than the upper limit of human ears (above 20,000 Hz) are known as ultrasonic sound waves. These sound waves create expansion and compression cycles, and during expansion cycle, it creates acoustic cavitation. These cavities oscillate in size, following the frequency cycles created by ultrasonic sound waves. At certain condition, the cavitation bubble undergoes implosion, creates increase in hundreds of atmospheric pressure and thousands of temperature measured in Kelvin. When ultrasonic sound waves are applied to wastewater treatment system, it decomposes the organic contaminants either by free hydroxyl radicals formed by pyrolysis or by pyrolytic cleavage.

The combination of Fenton reagent and ultrasound is known as the sono-Fenton treatment process which promises high efficient degradation of organics. Ultrasound creates higher hydroxyl radical due to cavitation and explosion of the water molecule which enhances the Fenton oxidation rate. In addition to the generation of hydroxyl radical, ultrasound enhances constant stirring and mass transfer effects so as to diffuse the reactants in the solution and improves the efficacy of Fenton reaction. The limitations of sono-Fenton process are its high cost and energy intensive process.

### 3.5.4 Fenton-Like Process

Fenton-like processes use zero valent iron instead of ferrous sulphate and are classified as heterogeneous and homogeneous Fenton-like processes. Adding a suitable solid catalyst to the Fenton reagent replaces  $\text{Fe}^{2+}$  and forms heterogeneous Fenton-like processes. The use of combination of other metal ion or metal ion-organic ligand complexes and hydrogen peroxide are termed as homogeneous Fenton-like processes. Since the Fenton-like systems show a significant result in terms of efficient degradation of organic pollutants and reduction in sludge generation, the various process parameters like pH, hydrogen peroxide concentration, catalyst concentration, etc., are studied extensively [57].

### 3.6 Photocatalytic Reaction

The reactions that use both light and a catalyst are termed as photocatalytic reactions, and it means a substance which alters the rate of reaction by its presence. Hence, photocatalyst is a substance which is used to enhance the rate of any chemical reaction induced on exposure to light, and this phenomenon is called photocatalysis. The catalyst used is semiconductors, and when exposed to sunlight or artificial light source with sufficient energy, it absorbs the light rays and acts as catalyst to induce chemical reactions to happen [58].

#### Fundamentals of Photocatalysis

When the semiconductor is exposed to light, electron–hole pair is generated, and photo reduction and oxidation take place, and hydroxyl ion is generated. Hydroxyl radical being a strong oxidant reacts with the organic pollutant and degrades it [58] (Fig. 6).

Semiconductors are materials which have a conductivity in between conductors and insulators and can conduct electricity when exposed to light, even at room temperature. These conductors act as catalyst under light and work as photocatalysts. A photocatalyst when exposed to desired wavelength of sunlight or illuminated produces pair of holes and electrons. The electron of the valence band gets excited, and the excess energy of the excited electron promotes it to the conduction band. This results in creation of negative electron and positive hole pair. At such conditions, the semiconductor attains photo-excitation, and the difference in energy between the conduction band and the valence band is termed as the energy band gap. The hole in the semiconductor breaks the water to free hydroxyl radical and hydrogen gas. On the other hand, the electron reacts with the oxygen molecule and creates super oxide anion. Until the semiconductor is exposed to light, this cycle continues, and

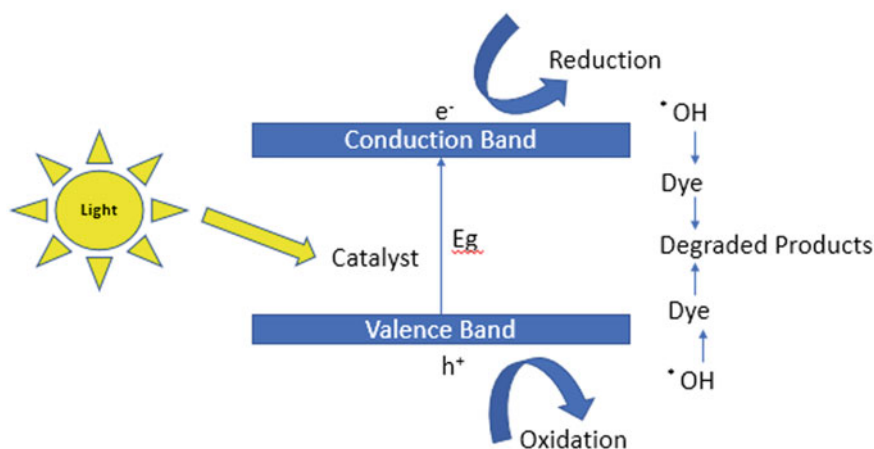


Fig. 6 Photocatalytic reaction

the importance of the photocatalytic reaction is that the semiconductor provides both oxidation and reduction environment simultaneously. The reaction rate of the electron and hole is determined by the semiconductor and substrate. The interaction between the semiconductor and the substrate is dependent on the band gap of the conduction band, valence band and the redox reactions. The reactions may be of any of these four ways

1. **By Reduction:** This occurs as a result of the redox potential of the substrate becomes lower than that of the redox potential of the conduction band of the photocatalyst.
2. **By Oxidation:** This occurs when the redox potential of the substrate becomes higher than the redox potential in the valence band of the photocatalyst.
3. **Neither oxidation nor reduction:** This happens while the redox potential of the substrate becomes greater than conduction band and lower than the valence band of the photocatalyst.
4. **By reduction and oxidation:** This happens when the redox potential of the substrate becomes lower than the conduction band and higher than the valence band.

The applications of photocatalysts are decolourization of colourants, antifouling of membranes, antifouling, sterilization, to conserve and store energy self-cleaning properties, treatment of pollutants in air and water and so on.

Based on appearance of the physical state of the reactants, the photocatalytic reactions are classified into two types

- **Homogeneous photocatalysis:** The physical state of the semiconductor and substrate is of same phase, i.e. solid, liquid or gas.
- **Heterogeneous photocatalysis:** The physical state of the semiconductor and substrate is of different phase, i.e. solid, liquid or gas.

The efficiency of the photocatalytic reactions is based on the semiconductors selected. Several metal oxides are widely studied and used as photocatalyst. In recent years, the metal oxides are converted to nano particles and are used in photocatalytic reactions. Similarly, nano plasmons, hybrid nano fibres with nano semiconductors are extensively used as photocatalyst in laboratory studies.

### Metal Oxides

Earlier metal oxides were used in electronics since they can carry charges when exposed to light. It also has wide application in treatment of wastewater. These metal oxides are best suitable because of their electronic structure and light absorption characteristics and charge transport properties. Photocatalytic reactions mediated by semiconductor have gained huge importance as the problem related to fast charge recombination is eliminated. The metal oxides like titanium dioxide and zinc oxide are widely studied against the dyestuffs belonging to azo dyes. Similarly, other metal oxides like vanadium oxide, tungsten oxide, molybdenum and cerium oxide,



**Table 5** Energy band gap of different semiconductors

Photocatalyst	Band gap (eV)	Photocatalyst	Band gap (eV)
ZnS	3.7	WO <sub>3</sub>	2.8
SnO <sub>2</sub>	3.5	B <sub>2</sub> WO <sub>6</sub>	2.78
SrTiO <sub>3</sub>	3.4	V <sub>2</sub> O <sub>5</sub>	2.7
ZnO	3.2	NaBiO <sub>3</sub>	2.62
TiO <sub>2</sub> anatase	3.2	CdS	2.4
Fe <sub>2</sub> O <sub>3</sub>	3.1	WSe <sub>2</sub>	1.2
TiO <sub>2</sub> rutile	3.02	Si	1.1
SiC	3.0		

cadmium oxide, cadmium sulphide are also used to study the removal or decolourization of the colourants such as acid orange, alizarin, methylene blue, congo red as photocatalyst.

The formation of hydroxyl radical, perhydroxyl ion or oxygen gas through multi-step reduction was detected by ESR spin trapping technique enabled the mineralization of the organic colourants into carbon dioxide, ammonia, nitrates and sulphates. In many research works, the photocatalytic treatment against several dyes like congo red, methylene blue, methyl red, alizarin S, etc., is studied using titanium dioxide nano particles as the catalyst. The comparison between commercially available titanium dioxide and zinc oxide and the nano particles of titanium dioxide and zinc oxide reveal that the efficiency is enhanced due to the nano size, large surface area and the crystallinity [58] (Table 5) [59].

## 4 Physical AOPs

### 4.1 Electrohydraulic Discharge (Plasma)

Application of plasma in wastewater treatment is receiving increased interest from researchers to degrade organic pollutants and inactivate the microbes. Plasma reactors are classified based on where the electrical discharge is generated like [60]

1. Generation of plasma directly in water
2. Generation of plasma directly in the water along with the bubbles applied externally (bubble discharge reactors)
3. Electrical discharge created over the water bulk or film in the gaseous phase
4. In the form of water drops or mist (gaseous phase)
5. Combination of all the above types
6. Non-contact treatment.

Based on the electrical discharge, the plasma reactors are known as

- (1) electrohydraulic discharge plasma reactors
- (2) bubble discharge plasma reactors
- (3) gas phase discharge plasma reactors
- (4) spray discharge plasma reactors
- (5) hybrid plasma reactors.

The classification is based on the total plasma–water interface, and the larger the interface higher will be the degradation of the organic pollutants. Another classification of plasma reactors is based on discharge

1. Corona and streamer discharge
2. Glow discharge
3. Dielectric barrier discharge (DBD)
4. Arc discharge.

Out of which, the most used is the pulsed corona discharge and pulsed arc discharge. Non-thermal plasma can be either applied above the water surface or applied underwater. Non-thermal plasma interacts with water to generate wide range of reactive species like hydroxyl radical, ozone, hydrogen peroxide, oxygen and hydrogen gas and also emit UV, visible light and generate shockwaves. The main advantage of plasma-based AOP is the generation of free hydroxyl radicals and another reactive species without the addition of other chemicals and UV lamps [61].

This technology is widely considered for wastewater treatment due to the following

- No requirement of external chemicals
- Environmental compatibility
- Effective process
- Simple and ease of operation at ambient temperature and pressure.

However, full-scale commercialization is hindered due to the usage of high voltage discharge resulting in high power consumption than other treatment methods.

## ***4.2 Ultrasound***

Ultrasonic treatment also known as sonolysis or sonochemistry is a promising field in advanced oxidation processes for removal of organic pollutant without the addition of any chemicals. The categorization of ultrasonic treatment is based on their frequency used.

High-frequency ultrasonic irradiation (2–10 MHz)

Low-frequency ultrasonic irradiation (20–100 kHz).

The ultrasonic reactions take place because of high irradiation of sound from 20 kHz to 1 MHz which leads to the formation of cavitation bubbles and explosions from acoustical wave form having expansion and compression. When the size of the

bubble reaches the critical resonance size, they implode violently and generate high atmospheric pressures (500–10,000 atm) and transient high temperatures (3000–5000 K). This subsequently leads to the dissociation of water molecules into highly reactive hydroxyl radicals, which eventually split into oxygen and react with the organic pollutants (Eqs. 5.1 and 5.2)



- The hydroxyl radical generated may further react with oxygen to form peroxide and hydrogen peroxide. Ultrasonic treatment either alone or combinedly used in treatment of organic pollutant efficiently, but still these treatments are not successful for industrial applications due to the following reasons
- Difficulty in scaling up for industrial use
- Highly energy intensive.

Similarly, adoption of these technologies has its own unique advantages like

- Operational simplicity
- Cleanliness
- Sludge free, safe and clear
- Ability to penetrate through cloudy water with poorly soluble and high suspended solid wastewater
- Coupling of sonolysis with other advanced oxidation processes will be efficient in treatment of wastewater.

The coupling of ultrasound with UV irradiation (sono-photolysis), other potential oxidants like ozone and hydrogen peroxide, with other catalysts (sono-catalysis) or with UV/catalysts (sono-photocatalysis) received increased attention in laboratory research. These combined or hybrid processes can yield additional advantages (Fig. 7).

### 4.3 Microwave

Microwave used for various heating applications is a part of electromagnetic spectrum occurring at 300 MHz to 300 GHz frequency, is now widely used in improving the chemical reactions. The rapid and effective heating properties of microwave lead to its usage in wastewater treatment of organic pollutants. However, the energy produced by microwave is insufficient in disrupting the chemical bond of certain organic pollutants. In several studies, microwave is effectively used to remove the ammonia completely in lab scale and 80% removal of ammonia in pilot-run. But

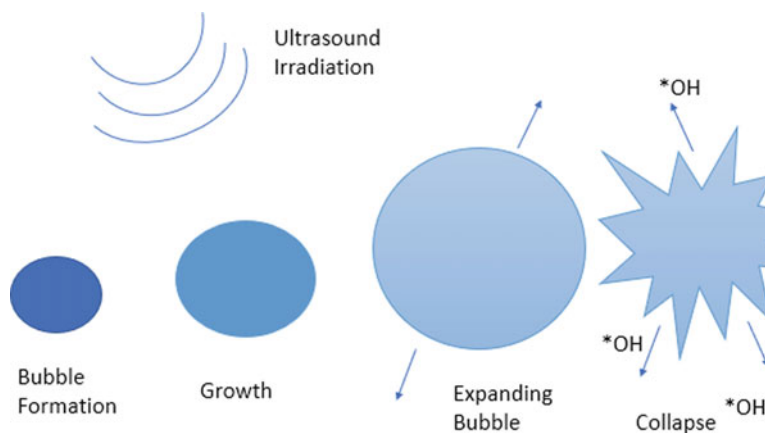


**Fig. 7** Ultrasound advanced oxidation process

microwave can be combined with other oxidants to enhance the rate of chemical reactions and can be used to induce selective heating of the contaminants through internal molecule vibration. The main advantage of combined microwave-assisted process with oxidants is the stimulation of free radicals from oxidants and the rapid polarization of the pollutant. The two major oxidants used with microwave are hydrogen peroxide and persulphate. The combination of microwave with titanium dioxide and granular activated carbon (GAC) can also be used to degrade the contaminants.

Microwave-assisted Fenton reaction or Fenton-like reaction show a better efficiency for the treatment of wastewater and soil pollutants.

#### **4.4 Electron Beam**

An electron beam source creates electrons of high acceleration, which penetrate the water surface results in the generation of electronically excited species in wastewater along with other reactive ionic species and free radicals. The accelerated electrons are reportedly penetrated to a maximum of 7 mm from the water surface, and the penetration is dependent on the energy of the incident electrons. The reaction process in electron beam does not require any catalyst, activators or additives, the rate of reaction, low temperature and low specific energy requirement are the main benefits of this process. Apart from these, the main advantage of electron beam is that it is able to direct radiation to the specific point of action, free choice of electron energy with power, facility to match process requirements, implementation of high dosage rates, able to control and disconnect the radiation source at any point of time and finally the availability of high beam powers. However, the electron beam process does not seem to be profitable due to the fact that the capital costs are higher for an electron

accelerator, the risk of liberation of potential X-rays and necessary precautions to be taken.

## 5 Conclusion

During the last few years, several advanced oxidation processes are studied, and few have been established to industrial scale. The combination of hybrid processes like electro-photo-catalysis, electro-photo-Fenton, UV/O<sub>3</sub>/H<sub>2</sub>O<sub>2</sub> and so on are showing better degradation efficiency but converting the laboratory scale process to pilot scale and to industrial scale is a challenge. The efficiency of the hybrid processes has to be improved with minimum capital cost and reduced operating and energy cost. The generation of sludge and their disposal remains unresolved in textile and other industries, and these processes would offer a solution to the industry.

### Appendix: Application of Sustainable and Low-Cost Sludge-Based Adsorbents for Textile Dye Degradation

This appendix enumerates a short description of the articles (Journals/Books/chapters/ standards) referred for relevant data in preparing this book chapter including tables.

S.No.	Journal title	Volume/Issue article title	Year of publication	Page no.	Content referred in the current book chapter
1	Water Science and Technology	30	1994	255–263	Table 1: Various treatment process for cotton textile process effluents with their merits and demerits
2	Dyes Pigments	47	2000	207–218	
3	Ozone Science Engineering	17	1995	149–161	
4	Soil and Sediment Contamination	10(6)	2001	577–591	
5	Water Research	31	1997	868–876	
6	Desalination	116	1998	65–80	
7	Desalination	70	1988	157–167	
8	Separation Science and Technology	34	1999	2501–2519	

(continued)

(continued)

S.No.	Journal title	Volume/Issue article title	Year of publication	Page no.	Content referred in the current book chapter
9	Chemical Engineering and Processing	41	2002	601–609	
10	Desalination	143	2002	11–20	
11	Separation Science and Technology	26	1991	1295–1313	
12	Water Science and Technology	40	1999	37–144	
13	Water Research	35	2001	567–572	
14	Catalysis Today	53(1)	1999	51–59	
15	Modern Applied Science	3	2009	146–160	
16	Water	11(2)	2019	205	Table 3: Comparison of oxidation potential
17	Journal of the Mexican Chemical Society [online]	58(3)	2014	256–275	Table 4: Oxygen evolution potential of different anodes
18	Applied Catalysis B Environmental	198	2016	347–377	Table 5: Energy band gap of different semiconductors

## References

1. Meena ML, Dangayach GS, Bhardwaj A (2014) Measuring quality of work life among workers in handicraft industries of Jaipur. *Int J Ind Syst Eng*
2. Chavan RB (2001) Indian textile industry—environmental issues. *Indian J Fibre Text Res* 26:11–21
3. Babu BR, Parande AK, Kumar SA, Bhanu SU (2011) Treatment of dye effluent by electrochemical and biological processes. *Open J Saf Sci Technol* 1:12–18
4. Babu BR, Parande AK, Raghu S, Prem Kumar T (2007) Cotton textile processing: waste generation and effluent treatment. *J Cotton Sci* 11:141–153
5. Brillas E, Martínez-Huitle CA (2015) Decontamination of wastewaters containing synthetic organic dyes by electrochemical methods. An updated review. *Appl Catal B Environ* 166–167:603–643. <https://doi.org/10.1016/j.apcatb.2014.11.016>

6. Muhammad A, Shafeeq A, Butt MA, Rizvi ZH, Chughtai MA, Rehman S (2008) Decolorization and removal of COD and BOD from raw and biotreated textile dye bath effluent through advanced oxidation processes (AOPS). *Braz J Chem Eng* 25(3):453–459. <https://doi.org/10.1590/S0104-66322008000300003>
7. Robinson T, McMullan G, Marchant R, Nigam P (2001) Remediation of dyes in textile effluent: a critical review on current treatment technologies with a proposed alternative. *Biores Technol* 77(3):247–255. [https://doi.org/10.1016/S0960-8524\(00\)00080-8](https://doi.org/10.1016/S0960-8524(00)00080-8)
8. Cruz-González K, Torres-López O, García-León A, Guzmán-Mar JL, Reyes LH, Hernández-Ramírez A, Peralta-Hernández JM (2010) Determination of optimum operating parameters for Acid Yellow 36 decolorization by electro-Fenton process using BDD cathode. *Chem Eng J* 160(1):199–206
9. Pala A, Tokat E (2002) Colour removal from cotton textile industry wastewater in an activated sludge system with various additives. *Water Res* 36:2920–2925
10. Gaehr F, Hermanutz F, Oppermann W (1994) Ozonation— an important technique to comply with new German laws for textile wastewater treatment. *Water Sci Technol* 30:255–263
11. Arslan I, Balcioglu IA, Bahnemann DW (2000) Advanced chemical oxidation of reactive dyes in simulated dye house effluents by ferrioxalate-Fenton/UV-A and TiO<sub>2</sub>/UV-A processes. *Dyes Pigm* 47:207–218
12. Adams CD, Fusco W, Kanzelmeyer T (1995) Ozone, hydrogen peroxide/ozone and UV/ozone treatment of chromium and copper complex dyes: decolourization and metal release. *Ozone Sci Eng* 17:149–161
13. Lin SH, Peng FC (1994) Treatment of textile wastewater by electrochemical method. *Water Res* 28:277–282. Onianwa PC (2001) Roadside topsoil concentrations of lead and other heavy metals in Ibadan, Nigeria. *Soil Sediment Contam* 10(6):577–591
14. Lin SH, Chen ML (1997) Treatment of textile wastewater by chemical methods for reuse. *Water Res* 31:868–876
15. Ghayeni SB, Beatson PJ, Schneider RP, Fane AG (1998) Water reclamation from municipal wastewater using combined microfiltration-reverse osmosis (ME-RO): preliminary performance data and microbiological aspects of system operation. *Desalination* 116:65–80
16. Erswell A, Brouchaert CJ, Buckley CA (1988) The reuse of reactive dye liquors using charged ultrafiltration membrane technology. *Desalination* 70:157–167
17. Xu Y, Lebrun R, Gallo PJ, Blond P (1999) Treatment of textile dye plant effluent by nanofiltration membrane. *Sep Sci Technol* 34:2501–2519
18. Akbari A, Remigy JC, Aptel P (2002) Treatment of textile dye effluent using a polyamide-based nanofiltration membrane. *Chem Eng Process* 41:601–609
19. Tang C, Chen V (2002) Nanofiltration of textile wastewater for water reuse. *Desalination* 143:11–20
20. Watters JC, Biagtan E, Sener O (1991) Ultrafiltration of textile plant effluent. *Sep Sci Technol* 26:1295–1313
21. Rott U, Minke R (1999) Overview of wastewater treatment and recycling in the textile processing industry. *Water Sci Technol* 40:37–144
22. Ciardelli G, Ranieri N (2001) The treatment and reuse of wastewater in the textile industry by means of ozonation and electroflocculation. *Water Res* 35:567–572
23. Andreozzi R (1999) Advanced oxidation processes (AOP) for water purification and recovery. *Catal Today* 53(1):51–59
24. Munter R (2001) Advanced oxidation processes—current status and prospect. *Proc Est Acad Sci Chem* 50(2):59–80
25. Khamparia S, Jaspal DK (2017) Adsorption in combination with ozonation for the treatment of textile waste water: a critical review. *Front Environ Sci Eng* 11(1):8
26. Kumar MR, Saravanan K, Shanmugam R (2009) Recycling of woven fabric dyeing wastewater practiced in Perundurai common effluent treatment plant. *Mod Appl Sci* 3:146–160
27. Gautam RK, Chattopadhyaya MC (2016) Advanced oxidation process-based nanomaterials for the remediation of recalcitrant pollutants. In: *Nanomaterials for wastewater remediation*, Chap. 3. Butterworth-Heinemann, Boston, pp 33–48

28. Brugnera MF, de Araújo Souza BC, Zanoni MVB (2016) Advanced oxidation process applied to actinobacterium disinfection. In: Actinobacteria: basics and biotechnological applications, vol 353
29. Miklos DB, Remy C, Jekel M, Linden KG, Drewes JE, Hübner U (2018) Evaluation of advanced oxidation processes for water and wastewater treatment—a critical review. *Water Res* 139:118–131. <https://doi.org/10.1016/j.watres.2018.03.042>. Epub 2018 Mar 22. PMID: 29631187
30. Amor C, Marchão L, Lucas MS, Peres JA (2019) Application of advanced oxidation processes for the treatment of recalcitrant agro-industrial wastewater: a review. *Water* 11(2):205
31. Klemeš JJ (2009) Water footprint, water recycling and food-industry supply chains. In: Handbook of waste management and co-product recovery in food processing
32. Yin GQ, Lo KV, Liao PH (2008) Microwave enhanced advanced oxidation process for sewage sludge treatment: the effects of ozone addition. *J Environ Eng Sci* 7(2):115–122. <https://doi.org/10.1139/s07-042>
33. Merenyi G, Lind J, Naumov S, von Sonntag C (2010) Reaction of ozone with hydrogen peroxide (peroxone process): a revision of current mechanistic concepts based on thermokinetic and quantum-chemical considerations. *Environ Sci Technol* 44(9):3505e3507. <https://doi.org/10.1021/es100277d>
34. Merenyi G, Lind J, Naumov S, von Sonntag C (2010) The reaction of ozone with the hydroxide ion: mechanistic considerations based on thermokinetic and quantum chemical calculations and the role of HO<sub>4</sub>· in superoxide dismutation. *Chemistry* 16(4):1372–1377. <https://doi.org/10.1002/chem.200802539>
35. Bilińska L, Blus K, Gmurek M, Ledakowicz S (2019) Coupling of electrocoagulation and ozone treatment for textile wastewater reuse. *Chem Eng J*
36. Song K, Mohseni M, Taghipour F (2016) Application of ultraviolet light-emitting diodes (UV-LEDs) for water disinfection: a review. *Water Res* 94:341–349. <https://doi.org/10.1016/j.watres.2016.03.003>
37. Ibrahim N, Zainal SFFS, Aziz HA (2019) Application of UV-based advanced oxidation processes in water and wastewater treatment, Chap. 14. IGI Global
38. Makhatova A, Mazhit B, Sarbassov Y, Meiramkulova K, Inglezakis VJ, Pouloupoulos SG (2020) Effective photochemical treatment of a municipal solid waste landfill leachate. *PLOS ONE*
39. Kumar V, Singh K, Shah MP (2021) Advanced oxidation processes for complex wastewater treatment. Elsevier BV
40. Mierzwa JC, Rodrigues R, Teixeira ACSC (2018) UV-hydrogen peroxide processes. Elsevier BV
41. Mishra N, Reddy R, Kuila A, Rani A, Nawaz A, Pichiah S (2017) A review on advanced oxidation processes for effective water treatment. *Curr World Environ*
42. (2010) *Electrochemistry for the environment*. Springer Science and Business Media LLC
43. Gheraout D, On the dependence of chlorine by-products generated species formation of the electrode material and applied charge during electrochemical water treatment. *Desalination*, 20110401
44. Barrera-Díaz C et al (2014) Electrochemical advanced oxidation processes: an overview of the current applications to actual industrial effluents. *J Mex Chem Soc* 58(3):256–275 [online]. ISSN 1870-249X
45. Comninellis C, Chen G (2010) *Electrochemistry for the environment*. Springer, New York
46. Devi RS, Geethakarthis A (2020) Electro-chemical coagulation treatment for the degradation of reactive blue 25 dye effluent using different electrodes. In *AIP Conference Proceedings*, vol 2270, no 1, p 060006. AIP Publishing LLC
47. Rodrigues de Oliveira G, Suely Fernandes N, Vieira de Melo J, Ribeiro da Silva D, Urgeghe C, Martínez-Huitle CA (2011) Electrocatalytic properties of Ti-supported Pt for decolorizing and removing dye from synthetic textile wastewaters. *Chem Eng J*
48. Stupar SL (2017) Direct and indirect electrochemical degradation of acid blue 111 using irOx anode. *Int J Electrochem Sci*
49. Panizza M, Cerisola G (2009) Direct and mediated anodic oxidation of organic pollutants. *Chem Rev*



50. Hammami S, Degradation of Acid Orange 7 by electrochemically generated (\*)OH radicals in acidic aqueous medium using a boron-doped diamond or platinum anode: a mechanistic study. *Chemosphere* 200810
51. Xu M, Wu C, Xhou Y (2020) Advancements in Fenton process for wastewater treatment. <https://doi.org/10.5772/intechopen.90256>
52. Oturan N, Oturan MA (2018) ElectroFenton process: background, new developments, and applications. Elsevier BV
53. Behfar R, Davarnejad R (2019) Pharmaceutical wastewater treatment using UV-enhanced electro-Fenton process: comparative study. *Water Environ Res*
54. Muruganandham M, Suri RPS, Jafari S, Sillanpää M, Lee G-J, Wu JJ, Swaminathan M (2014) Recent developments in homogeneous advanced oxidation processes for water and wastewater treatment. *Int J Photoenergy*
55. Ameta R, Chohadia AK, Jain A, Punjabi PB (2018) Fenton and photo-fenton processes. Elsevier BV
56. Cruz-Gonzalez K, Determination of optimum operating parameters for Acid Yellow 36 decolorization by electro-Fenton process using BDD cathode. *Chem Eng J* 20100515
57. Prousek J, Palacková E, Priesolova S, Marková L, Alevová A (2007) Fenton- and fenton-like AOPs for wastewater treatment: from laboratory-to-plant-scale application. *Sep Sci Technol* 42:1505–1520. <https://doi.org/10.1080/01496390701290151>
58. Ameta R, Solanki MS, Benjamin S, Ameta SC (2018) Photocatalysis. Elsevier BV
59. Mamba G, Mishra AK (2016, May) Graphitic carbon nitride (g-C<sub>3</sub>N<sub>4</sub>) nanocomposites: a new and exciting generation of visible light driven photocatalysts for environmental pollution remediation. *Appl Catal B Environ* 198:347–377. <https://doi.org/10.1016/j.apcatb.2016.05.052>
60. Vanraes P, Nikiforov AY, Leys C, Electrical discharge in water, Chap. 16
61. Tijani JO, Fatoba OO, Madzivire G, Petrik LF (2014) A review of combined advanced oxidation technologies for the removal of organic pollutants from water. *Air Soil Pollut, Water*

# Treatment of Textile Wastewater Using Biochar Produced from Agricultural Waste



R. Sivaranjane and P. Senthil Kumar

**Abstract** The material business creates gigantic measures of wastewater which must be dealt with adequately in an offer to forestall water shortage through reuse. Biosorption through farming lignocellulosic squanders and side effects has been identified as a feasible substitute to ebb and flow innovations applied to evacuate poisonous metal particle and natural toxins from water and wastewater. The current examination underscores the utilization of rural and agro-enterprises-based build-ups as minimal effort biosorbents. The investigation expects to return to the status of biosorption and different late advances made in this field. Biochar as a steady carbon-rich material demonstrates extraordinary potential to deal with water/wastewater contaminants. Its application is increasing expanding enthusiasm because of the accessibility of feedstock, the straightforwardness of the readiness techniques, and their upgraded physico-substance properties. The viability of biochar to expel natural and inorganic toxins relies upon its surface region, pore size dispersion, surface useful gatherings, and the size of the particles to be evacuated, while the physical design and surface properties of biochar rely upon the idea of feedstock and the arrangement technique/conditions. The ebb and flow audit talks about on the various strategies for biochar creation and gives a review of ebb and flow uses of biochar in wastewater treatment.

**Keywords** Biochar · Biosorption · Toxic pollutants · Wastewater · Separation · Pollution

---

R. Sivaranjane

Department of Chemical Engineering, St. Joseph's College of Engineering, Chennai 600119, India

R. Sivaranjane · P. Senthil Kumar

Department of Chemical Engineering, Sri Sivasubramaniya Nadar College of Engineering, Chennai 603110, India

P. Senthil Kumar (✉)

SSN-Centre for Radiation, Environmental Science and Technology (SSN-CREST), Sri Sivasubramaniya Nadar College of Engineering, Chennai 603110, India

e-mail: [senthilchem8582@gmail.com](mailto:senthilchem8582@gmail.com); [senthilkumarp@ssn.edu.in](mailto:senthilkumarp@ssn.edu.in)

© The Author(s), under exclusive license to Springer Nature Singapore Pte Ltd. 2021

205

S. S. Muthu (ed.), *Advances in Textile Waste Water Treatments*, Sustainable Textiles: Production, Processing, Manufacturing & Chemistry, [https://doi.org/10.1007/978-981-16-0065-4\\_8](https://doi.org/10.1007/978-981-16-0065-4_8)

## 1 Introduction

In recent times, the effluent which is let out from different industries namely textile, printing, leather, dyeing, and paper and pulp industries contains toxic substances which have the potential to pollute the surface water, groundwater, and soil [1]. As the demand for safe water increases, the waste effluent released from the industries needs to be addressed at the earliest [2]. A textile industry on the whole makes use of a variety of dyes for the purpose of colouring. Separate dyes are employed in the process of manufacturing, and the cationic dye plays a key role. A vast amount of waste sludge and polluted water is generated by the textile industry. On the contrary, the effluent released from the textile industry contains complex substances when compared to the other effluent from various industries [3]. The effluent let out from the dyeing industry is dreadful, alkaline in nature, and it denotes the presence of high concentration of aromatic contaminants as well as other complex substances within it [4]. The industrial effluent accounts for about 15% of the dye lost during the various activities that take place inside the industries namely manufacturing and processing operations [5]. The effluent which is released from the textile industry denotes the presence of high COD level and a low BOD level in them [2].

The intensity of colour which is present in contaminated water is extremely harmful even when the concentration is very low [3]. The presence of small quantity of dye solution can be a great threat to aquatic systems. The textile discharge is also carried with itself an enormous amount of organic substances which needs to be concentrated before it is let out into any water bodies. About 800,000 tons of 10,000 different synthetic dyes are produced yearly on an average, and this dyeing industry happens to release 140,000 tons of variety of synthetic dyes which has a great negative impact on environment. It has also been noted that the textile industry gives rise to a huge volume of sewage and as a result it has gained attention amongst researchers in recent years [6]. The effluent can be effectively treated by employing various sources of agricultural waste. In general, agricultural waste refers to any type of organic squanders which is got rid by human beings during agricultural production, and the waste material includes plant waste, livestock manure, and certain domestic waste [7].

Biochar is generally preferred on comparison with other adsorbent because of its low cost and its ability to concentrate enormous amount of pollutants. Textile industry generates a huge quantity was wastewater during the manufacturing process. Disposal of textile effluent has to be concentrated on a large scale before it is let out into the environment because the effluent from this industry contains many complex substances as well as some heavy colours within it. Many techniques like adsorption, ion exchange, photocatalysis, membrane filtration, oxidation process, chemical precipitation are available to treat the dyes let out from textile industries [8]. This effluent when let out into the environment causes serious illness and pollution to animals and mankind. So, treating this effluent becomes a great challenge, and various researches are being carried out in this issue. Amongst the various techniques available for treating wastewater, the adsorption technique seems to be the most facile

method because of its unique properties like high sorption capacities, low operating cost, and easier to operate on comparing it with other techniques [2].

### ***1.1 Various Methodologies Available for Wastewater Treatment***

The various methodologies which are available for the treatment of effluent are categorized as follows.

- Physical Treatment.
- Chemical Treatment.

#### **Physical Treatment**

There are number of techniques which are available to treat the coloured effluent which is being discharged from textile industries. Few methods namely membrane filtration, adsorption, electro dialysis, and reverse osmosis will fall under this category. All these methods have some defects. Of these methods, the membrane filtration method has a major drawback on comparison with other technologies because the membrane tends to be fouled very easily. In this method, the membrane has to be monitored constantly to prevent fouling, and periodic replacement of the membrane is required for effective functioning of the system. Of all these available techniques, the adsorption process seems to be more effective because of its low operating cost and distinctive properties [9].

#### **Chemical Treatment**

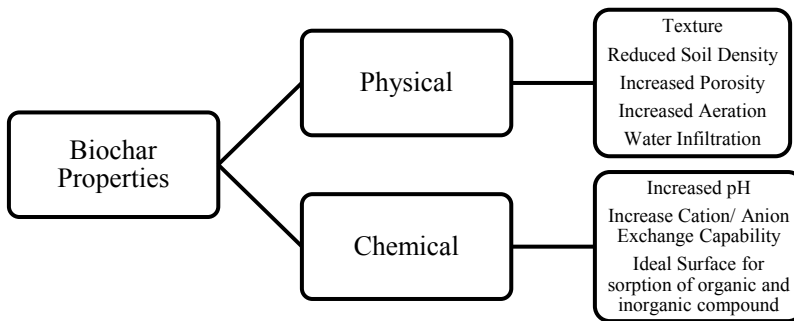
The dyes present in the effluent let of from the textile industries can also be treated by subjecting them to coagulation and flocculation methods. This method also involves the addition of some organic polymers. This method is generally very expensive in nature. The major drawback of this method is that it involves sludge formation at the final stage of the process which in turn is pH dependent [9].

### ***1.2 What Is Biochar?***

Biochar is a charcoal that is made to be used as soil manure. It is not like a charcoal that is available in stores which contains a number of ingredients. It can be made from all forms of organic matter including wood and dried manure. It is produced through a process known as pyrolysis which is the heating or burning of a biomass such as wood and oxygen limited environment. The liquid and gases that are present in the biomass are released during pyrolysis leaving a very small amount of carbon and a small amount of inorganic ash, and this remaining carbon material when used as a soil amendment is called as biochar. Biochar has number of benefits that results in

improved soil fertility and better crop yields. Biochar is very porous, and as a result, it has a very large surface area. This porous surface makes a great home for beneficial microbes and helps them to thrive and multiply. Biochar can be inoculated with beneficial microbes simply by adding it to compost worm castings or compost tea before application to the garden. The increased microbial will in turn feed earthworms and increase their numbers and the amount of castings they leave in the garden. Biochar also has high cation exchange capacity which attracts positively charged nutrients, and as a result, biochar attracts and holds onto nutrients and prevents them from leaching from the soil. Biochar improves soil structure and soil aeration. Agricultural wastes, rice husks, bagasse, paper products, animal manures, and even urban green waste can be used as major feedstock for preparing biochar.

### 1.3 Properties of Biochar



### 1.4 Benefits of Biochar

The benefits of biochar are listed below:

- Suppressed methane emission
- Reduced nitrous oxide emission
- Reduced leaching of nutrients
- Reduced fertilizer requirement
- Reduces soil acidity
- Stored carbon for a very long time.

### 1.5 Biochar Preparation

Pyrolysis is the most common method that is widely adopted for the preparation of biochar on a large scale. As the name suggests, pyrolysis is a process in which the

compound is transformed into a simple complex or compounds possessing a higher molecular weight, and the process is normally carried out at a temperature ranging between 400 and 800 °C. Pyrolysis in turn differs from the natural combustion process, and this process exclusively takes place in the absence of air, and there is nil chance of oxidation to occur. The by-products of obtained as a result of this process include biochar, bio-oil, and syngas.

The production of biochar involves the use of different agricultural feedstock by subjecting the feedstock to the pyrolysis process at different temperatures. This pyrolysis process is taking place inside a furnace under nitrogen environment. The obtained samples were further sieved for the purpose of size reduction, and they were cleansed with DI water to eliminate any contaminants present within it. The thus obtained samples were further oven dried for later use [10]. The pyrolysis technique is considered to be the most favourable one for the production of biochar on a large scale. This technique can be further classified into conventional slow pyrolysis, fast pyrolysis, and microwave assisted pyrolysis which in turn is completely based on their operating conditions. These pyrolysis techniques cause a great variation in composition of solids, liquids, and gases which in turn is completely dependent upon its operating parameters like heating rate, temperature, and the residence time [11]. Biochar can be significantly prepared by adopting carbonization technique in which the temperature varied from 200 to 400 °C, respectively [12].

### 1.5.1 Conventional Pyrolysis

Magnetic biochars are generally prepared by adopting conventional pyrolysis method. In this method, heat transfer between the materials is mainly due to conduction, convection, and radiation methods. This method in turn involves the use of two other processes namely carbonization and activation. In this process of carbonization, a non-porous char is produced when the temperature is between 600 and 900 °C in the presence of an inert atmosphere. After this stage, it undergoes an activation process in which the char contacted with an oxidizing gas namely CO<sub>2</sub> or steam at a temperature of 600–1200 °C [13].

### 1.5.2 Biomass Pyrolysis

Wooden or agricultural biomass stored in a dedicated storage facility is transported to the pyrolysis reactor via a bucket feeder. The raw biomass is pre-dried inside the feeder through the use of hot and dry air flowing through the cross flow. Biomass pre-drying has a positive impact on the reduction of the moisture content inside the material by few percent. Pre-dried and pre-heated biomass gets into the pyrolysis reactor where the following process takes place. All the moisture accumulated on the raw biomass has to evaporate in order to initiate the carbonization process depending on the type of biomass and moisture accumulated in the process material. In the next

stage, the biomass is degasified in the temperature range of 370–400 °C. Within this range, the removal of volatile particle seems to be more efficient.

### **1.5.3 Torrefaction**

The roasting of wood or other biomass to remove moisture and low energy volatiles thereby increasing the density of the biomass. Torrefaction is basically a pre-treatment process which is employed for moisture removal, biomass densification and to enhance the property of biomass. Torrefaction process on combination with any pre-treatment methods will yield better quality of biomass [14]. This process produces a solid material which is rich in carbon content. The primary purpose of this torrefaction process is to produce biochar. Torrefaction is an upcoming methodology which is used to expel the volatiles by utilizing different decomposition reactions which in turn improves the quality of biomass. This process of torrefaction can be further subdivided into two types namely wet and dry torrefaction. The wet torrefaction method has the potential to produce energy dense product within a very short period of time owing to its high heat transfer rate when it is kept inside an aqueous media. Torrefaction can deliver biochar with high calorific value, and it can be used as a substitute for fossil fuel [11].

### **1.5.4 Microwave Assisted Pyrolysis**

Microwave aided pyrolysis is one of the most productive thermochemical forms in the creation of biochar, bio-oil, and syngas, and it has been effectively applied to plant remains. The major advantage of pyrolysis is that it gives higher product yield. It is also one of the most effective and cost saving techniques for the production of biochar. Microwave technology utilizes electromagnetic wave, and this wave causes movement of molecules, and it delivers heat. The technological benefit microwave-helped pyrolysis over traditional pyrolysis is larger biomass particles are subjected to uniform microwave heating, and due to the absence of agitation in fluidization process, it produces a clean product. There are few contrast between the conventional and microwave pyrolysis method. The traditional pyrolysis method utilizes ordinary heating methodology, while the microwave method requires some pre-treatment before subjecting to heating. On subjecting the finally produced biochar to any chemical or thermal processing, it has the ability to get transformed into activated carbon material [11].

## ***1.6 Effluent Treatment by Utilizing Biochar as Adsorbent***

By employing wheat straw as an agricultural waste, biochar was prepared by following pyrolysis technique at a temperature of 200 °C. The resulting biochar

proved to be an outstanding material for treating the cationic dye namely methylene blue dye present in the effluent [15]. Biochar obtained from waste chicken bones proved itself to be an excellent material for eliminating rhodamine B dye [16]. The biochar derived by using a variety of crop residues showed better results which was extremely very helpful in the elimination of methyl violet dye present in wastewater [1]. Agricultural waste namely sunflower seed hull rejected from food industry upon further processing was further made use of to extract methyl violet dye from aqueous solution [17]. Biochar produced by using agricultural waste namely rice husk was used to get rid of the reactive black dye which is present in textile effluent [18]. Agricultural squander rice straw was converted into a biochar by pyrolysis method, and this biochar was further activated, and the final product was used to adsorb methylene blue and crystal violet dye [19]. Pomelo peel waste was scrap, and this material was further activated to eliminate methyl orange dye [20]. The biochar derived from persimmon fruit peel was used to adsorb basic blue dye from aqueous solution, and this biochar proved to be a promising adsorbent material [21]. The elimination of Basic Blue 41 and Basic Red 09 dyes was studied by making use of biochar derived from groundnut pod. The biochar was obtained by pyrolysis method [3]. Biochar extracted from coffee husk showed excellent sorption capacity towards the termination of variety of dyes present in wastewater. This biochar was acquired by pyrolysis method at a temperature of 450 °C, and it was further exposed to chemical activation [22]. Biochar extracted from agricultural waste namely corn cob was used to get rid of the methylene blue dye present in wastewater. The biochar was achieved by following pyrolysis technique in which the corn cob sample was pyrolysed at 500 °C for 2 h [8]. Agricultural waste proves to be a low-cost-effective adsorbent for eliminating any toxins present in the wastewater. By taking into consideration, cocoa pod husk as a source of agricultural waste biochar was acquired by pyrolysis method. This cocoa pod husk after getting pyrolysed at 550 °C was then subjected chemical activation, and the final puce product obtained was used to eliminate dyes present in the textile effluent [23]. Biochar obtained from milled raw grass straw confirmed that it can be used as an adsorbing material for the removal of methylene blue dye. This biochar from straw underwent certain chemical modifications to enhance the adsorptive capacity of the material. Pyrolysis technique was adopted to derive biochar from the agricultural waste, and this method was carried out in the presence of nitrogen flow [24]. Biochar was got from pine cone by choosing pyrolysis method. The biochar was obtained at a temperature of 500 °C. This eco-friendly biochar adsorbent showed excellent removal capacity of methylene blue dye [25]. Crab shell was found to be a good source of squander and the biochar derived from crab shell showed extraordinary sorption capacity towards both anionic and cationic dyes namely congo red and malachite green [26]. The biomass from eucalyptus bark was further processed, and this in turn resulted in biochar which was employed to eliminate the MB dye [27]. An agro waste namely bael shell was made use of to produce biochar which in turn was found to be used in treating wastewater which had a high concentration of patent blue dye associated with it. This biochar was obtained on pyrolysing the bael shell at a temperature of 500 °C [28]. A low-cost squander peanut shell was subjected to KOH activation and the resulting biochar found its application in the removal of



MB dye, and it showed a good sorption capacity [29]. Arjun fruit was used for the production of biochar. Biochar was obtained by pyrolysing the fruit at 500 °C for 3 h, and the obtained biochar was employed to remove the congo red dye from the effluent [30]. Cassava slag was used to treat aqueous solution containing Rhodamine B and the biochar obtained from this cassava slag by hydrothermal carbonization technique. This biochar also showed tremendous adsorption capacity, and it was utilized for treating a variety of dye solution [7]. *Strychnos potatorum* seed powder showed good sorption capacity towards the elimination of methylene blue dye [31]. Orange peel was taken as a source of agricultural waste, and orange peel was further activated by using sulphuric acid. The activated powder had good pore characteristics, and this low-cost eco-friendly material was widely employed to eliminate MB dye present [32]. Adsorption studies were carried out by utilizing raw tamarind seeds and surface modified tamarind seeds. The surface modification was done by using sulphuric acid. The tamarind seeds obtained from kitchen waste should outstanding performance towards the removal of methylene blue dye solution [33]. Adsorption of methylene blue dye onto cashew shell proved to be very significant in which the cashew shell was surface modified to enhance the pores within it which facilitated the number of vacant sites available for the process of adsorption to take place [34]. The activated carbon or the biochar obtained from corn cob by following microwave assisted pyrolysis proved to be a low-cost and eco-friendly adsorbent which played a major role in getting rid of the MB dye present in aqueous solution. The sorption process was spontaneous and exothermic in nature [5]. Microwave assisted pyrolysis technique was applied to the agricultural waste material namely saw dust. The biochar obtained as a result of pyrolysis was further used for the separation of dye solution present in the aqueous solution [2]. Cashew nut shell modified with sulphuric acid was used to extract all the pollutants present in wastewater. Surface modification increased the number of vacant site available in the bisorbent [35]. Adsorption of pollutant from aqueous solution using sulphuric acid modified *Caryota urens* seeds was explained [36]. A most facile methodology was adopted for the evacuation of pollutants present in aqueous solution. Coffee bean was further treated, and the activated carbon was derived which in turn was used for the recovery of pollutants [37]. A novel and very effective type of low-cost adsorbent namely *S. potatorum* seeds was surface modified, and this material helped in expelling the pollutant from aqueous solution. The surface modification was observed using FTIR and SEM analyses [38]. A study affirmed that hydrothermal carbonization of urban food waste was utilized to produce biochar, and this biochar was very helpful to eliminate Acridine Orange and Rhodamine 6G dyes from adulterated water [39]. A low-cost-effective adsorbent obtained from tomato waste was used to evacuate pollutants present in aqueous solution. Carbonization technique was employed to obtain biochar from tomato waste [40]. Hydrothermal conversion and pyrolysis method were employed to produce biochar from various agricultural wastes like pinewood, peanut shell, and bamboo biomass. The biochar obtained from pyrolysis method yielded a good result than that of HTC method. The biochar obtained from the above-mentioned agricultural waste was significantly effective in eliminating the methylene blue dye present in wastewater [41]. Two different fruit shells namely Rutaceae vila and Vilvam fruit

were used as an agricultural mode of adsorbent to eliminate crystal violet dye from aqueous solution. Hence, it was proved that these two materials had a great potential to treat textile effluent [42]. Agricultural waste *Cinnamomum camphora* sawdust was used as a source of biosorbent to expel malachite green dye from aqueous solution. This *C. camphora* sawdust was further subjected to surface modification with the help of an organic acid namely oxalic acid, citric acid, and tartaric acid, respectively. Surface modification in turn provided a large number of vacant sites which helped in the effective termination of the dye solution [43]. Chemical modification of cotton waste resulted in biochar which in turn was further employed to remove methylene blue and other contaminants existing in aqueous solution [44]. The fruit waste from sour cherry (*Prunus cerasus* L.) stones was modified to obtain activated carbon. This material showed outstanding performance on elimination yellow 18 which is a basic textile effluent. The activated carbon utilized for the adsorption of yellow 18 was well described by Langmuir isothermal fit [45]. Bamboo was transformed into biochar by subjecting it to chemical modification. This chemically modified bamboo showed significant adsorption capacity, and it was employed to reject methylene blue dye from aqueous solution. The sorption process was well defined using Langmuir fit [46]. Pine cone was converted into activated carbon by exposing it chemical modification. The resulting material thus obtained was very potential to get rid of methylene blue dye [47]. Biochar samples were collected from Hornbeam sawdust by undergoing pyrolysis technique. The different samples were collected at a temperature of 500, 600, 700, and 800 °C. The higher the temperature the more porous the material is. This biochar was further employed to evacuate disperse orange 30 dye from aqueous solution [48]. Raw eucalyptus seeds were picked as precursor, and these seeds were further surface modified to upgrade the porosity of the raw eucalyptus seeds. The surface modification was in turn followed by ultrasonication process to attain uniform particle size distribution. The final powdered activated carbon material derived by this process was utilized to knock out malachite green from aquatic system [6]. The agro waste biomass corn pith was collected from agricultural field was found to be an effective precursor for eliminating malachite green dye from aqueous solutions. This waste biomass was treated with conc  $H_2SO_4$  to increase the availability of the pores in corn pith, and the Langmuir monolayer sorption capacity was computed as 488.3 mg/g, and the equilibrium data obeyed pseudo-first order kinetic model [49]. A macro alga named *Sargassum wightii* was used as a source of biomass and the solid waste which remains after oil expulsion was further deployed as adsorbent material to detach the methylene blue dye molecules present in wastewater system. The equilibrium data was well explained by Freundlich isotherm and pseudo-second-order model. The sorption of dye molecules onto the surface of the biomass were managed by film diffusion and particle diffusion, respectively. The thermodynamic study helped in concluding that the process was spontaneous and exothermic in nature [50]. The agro waste biomass acquired from raw tea filtrate was engaged in the sorption process. The biomass was subjected to two surface modification process namely chemical modification and ultrasonication process. The end product obtained as a result of these two processes is powdered activated carbon material which played a vital role to pull out the azo dye Solochrome Black T, the sorption

system followed pseudo-second-order kinetic model, and the thermodynamic data revealed that the process is exothermic and spontaneous [51]. Cassia fistula seeds underwent physical and chemical modification to yield activated carbon. This AC material was used as an adsorbent for the expulsion of pollutant existing in wastewater. The equilibrium data responded very well to pseudo-first-order kinetic model [52]. Biosorbent was developed from dried *Spirulina platensis* algae by exposing the algae to ultrasonication and sulphuric acid. On doing so, sorption capacity of the biomass can be upgraded. The biosorbent derived from the above-mentioned algae revealed good sorption capacity, and it also helped in the expulsion of the pollutant namely copper ions present in aqueous solutions [53]. Surface modified eucalyptus seeds were engaged in the removal of pollutant from aqueous solution. Surface modification improves the porosity of the material, and it also enhances the adsorption capacity of the biomass utilized for expulsion of the pollutant present in the system [54]. The biomass from *Lantana camara* fruit was used in expulsion of pollutant from aqueous solution. The tincture from *L. camara* fruit was utilized as a capping agent in the preparation of nanoparticles which was obtained by following co-precipitation method [55]. The eucalyptus seeds were gathered and then subjected to dehydration process to eliminate the moisture present in the seeds, and the final biomass obtained was utilized to evict the pollutant present in the system, and the maximum sorption capacity was determined to be 76.94 mg/g [56]. Eucalyptus seeds were recognized as a very potential source of biomass, and these seeds underwent chemical modification to increase the active sites available in the eucalyptus seeds. This low-cost biosorbent was very helpful to reject the pollutants present in the wastewater system, respectively [57]. *C. urens* seeds were selected as a source of agro-based biomass material which was very effective to clear the pollutants present in the aqueous system. This *C. urens* seeds underwent H<sub>2</sub>SO<sub>4</sub> modification and ultrasonication process which rendered a uniform particle size and also hiked the number the active sites available for the sorption process. The equilibrium data fitted extremely well into Freundlich and pseudo-first-order models, and the monolayer sorption capacity of the pollutant was determined to be 93.7 and 175.9 mg/g, respectively, for the above two mentioned modified *C. urens* seeds [58]. The biochar acquired from Cassia fistula seed was eco-friendly, and it was utilized to get rid of pollutant present in aqueous system. The biochar was prepared by subjecting the seeds to physical and chemical treatment. The biochar synthesized by adopting chemical method showed better sorption capacity of about 303.5 mg/g when compared to the one (115.4 mg/g) obtained from physical method [59]. An agro waste from periwinkle shells was utilized as a precursor and carbon source. The periwinkle shells underwent chemical activation technique in the presence of KOH, and finally, the biochar thus obtained by this methodology was utilized to expel Remazol Brilliant Violet-5R [60]. Activated carbon (AC) extracted from Durian peel was made use to knock out Basic Green 4 dye present in the system. The activated carbon was produced by carbon dioxide activation under nitrogen atmosphere or vacuum pyrolysis. The AC produced by vacuum pyrolysis gave better results. Results were much higher when the AC was further treated with HCl [61] (Table 1).

### ***1.7 Pros of Biochar***

- Upon acidic treatment, biochar enhances the functional groups present on the surface of the activated material.
- Upgrades the take up of organics.
- When loaded with foreign material, it improves the oxygen ability.
- It enhances the pore volume of the material and also the BET surface area.
- Activated bed life can be extended rapid oxidation of organics by microbes before the material can take over the adsorption sites.

### ***1.8 Cons of Biochar***

- The metal ion intake drops down very rarely.
- Oxygen surface functional group reduces during the chemical treatment.
- Due to the formation of polycyclic aromatic hydrocarbons (PAHs), lower quality products are produced.
- Pore volume has a negative impact on the uptake of organics which may let out undesired gases like sulphur dioxide and nitrogen dioxide.
- Biochar is not a fertile artificial soil.
- Biochar does not always show a sign of positive effect on soil fertility.
- It tends to enhance the organic loss from humus.

### ***1.9 Challenges of Biochar***

- Soil pH is one of the main reasons which prevent the utilization of biochar to farming soils. Most kinds of biochar are of antacid nature, and its application to agrarian soil may adversely influence the accessibility of soil supplements because of increase in soil pH. In high pH (soluble) soils, an expansion in soil pH is not alluring as yields just endure a specific scope of soil pH.
- Long-term evacuation of yield deposits, similar to stems, leaves and seed units, to be utilized for creation of biochar can decrease the health of the soil by reducing the quantity of soil micro-organisms and disturbing inside nutrient cycling.
- The fine debris related with biochar is the ideal hot spot for dust, representing a hazard for respiratory sicknesses.
- Some biochars can go about as a wellspring of contaminants, for example, substantial metals, volatile organic compounds (VOCs), polycyclic aromatic hydrocarbons (PAHs), and dissolved organic carbon (DOC).
- The sorption of pesticides and herbicides by the biochar can lessen their adequacy.
- Yields may decrease due to the sorption of water and supplements by the biochar, which diminishes the accessibility of these assets for the crops.
- Biochar has likewise been appeared to hinder germination.

**Table 1** Utilization of biosorbent from various sources for dye removal

Biosorbent	Adsorbate	Adsorption kinetics fit	Isothermal fit	Sorption capacity (mg/g)	Dose (g/L)	pH	Time (min)	Initial conc (mg/L)	Refs.
Sludge derived biochar	Methylene blue	Pseudo-second-order	Langmuir isotherm	–	6	11	–	50	[4]
NZVI-AC	Malachite green	Pseudo-first order	Langmuir isotherm	187.3	0.5	9	60	–	[6]
Biochar residues from various source	Methylene blue	Pseudo-second-order	Langmuir isotherm	9.5	8	5–9	120	5	[12]
Corn cob biochar	Methylene blue	Pseudo-first order	Freundlich isotherm	82.71	0.2	7	90	25	[60]
Saw dust	Methylene blue	Pseudo-second-order	Freundlich isotherm	58.14	3	7	90	25	[61]
Wheat straw	Methylene blue	Pseudo-second-order	Langmuir isotherm	46.6 62.5 400	100 200 400	3, 7, 11	120	80	[15]
Magnetite-modified chicken bone biochar	Rhodamine B	–	Freundlich isotherm	113.31	–	10	–	40	[16]
Crop Residue	Crystal violet	–	Langmuir isotherm	–	–	9	–	–	[1]
Agricultural waste	Methyl violet	Pseudo-second-order	Freundlich isotherm	92.59	0.3	7	135	100	[17]
Rice straw	Methylene blue Crystal VIOLET	Pseudo-second-order	Langmuir isotherm	90.91 44.64	0.2–1	7	15 20	50	[19]

(continued)

Table 1 (continued)

Biosorbent	Adsorbate	Adsorption kinetics fit	Isothermal fit	Sorption capacity (mg/g)	Dose (g/L)	pH	Time (min)	Initial conc (mg/L)	Refs.
Pomelo peel waste	Methyl orange	Pseudo-second-order	Langmuir isotherm	163.105	1	3	70	150	[20]
Persimmon fruit peel	Methylene blue	Pseudo-second-order	Langmuir isotherm	303	–	7	180	2	[21]
Arachis hypogaea shell	Basic blue 41 Basic red 09	Pseudo-first-order Pseudo-second-order	Sips model	22.322 40.655	2 1	8	240	50	[3]
Corn cob	Methylene blue	Pseudo-second-order	Langmuir isotherm	16.50	–	–	–	5 10 50 80	[8]
Ryegrass by-products	Methylene blue	Pseudo-first-order Pseudo-second-order Avrami model	Sips model	28.7 67.19	–	–	–	150	[24]
Pine cone	Methylene blue	Pseudo-second-order	Langmuir isotherm	106.4	0.2–1	5.1–11.3	120	10–50	[25]
Calcium rich biochar from crab shell	Malachite green Congo red	Pseudo-first-order	Langmuir isotherm	12,502 20,317	–	3–10	–	–	[26]
Eucalyptus bark based biochar	Methylene blue	Pseudo-second-order	Langmuir isotherm	–	0.2–0.6	11.3	15–150	10–100	[27]
Bael shell biochar	Patent blue	Pseudo-second-order	Freundlich isotherm	3.7	–	2.7–10.4	–	–	[28]

(continued)

Table 1 (continued)

Biosorbent	Adsorbate	Adsorption kinetics fit	Isothermal fit	Sorption capacity (mg/g)	Dose (g/L)	pH	Time (min)	Initial conc (mg/L)	Refs.
Peanut shell biochar	Methylene blue	Pseudo-second-order	Langmuir isotherm	208	-	2-10	-	100-500	[29]
Arjun fruit biochar	Congo red	Pseudo-second-order	Langmuir isotherm	4.81	12	7	30-480	20-100	[30]
Cassava slag biochar	Rhodamine B	Pseudo-second-order	Freundlich isotherm	105.3	4	2-12	-	-	[7]
Strychnos potatorum seeds	Methylene blue	Pseudo-second-order	Langmuir isotherm	78.84	3	-	60	50-250	[31]
Orange peel	Methylene blue	Pseudo-second-order	Freundlich isotherm	-	4	8	45	50	[32]
Tamarind seeds	Methylene blue	Pseudo-second-order	Langmuir isotherm	16.611 34.483	6	8	120	25-125	[33]
Cashew nut shell	Methylene blue	Pseudo-second-order	Freundlich isotherm	5.311	5-30	2-10	10-90	20-100	[34]
Corn cob	Methylene blue	Pseudo-first-order	Freundlich isotherm	82.71	8	7	90	25	[5]
Saw dust	Methylene blue	Pseudo-second-order	Freundlich isotherm	58.14	3	3-9	90	25	[2]

## 2 Case Study

A case study was performed to improve the soil fertility and to bring down the emission of carbon in Nepal. Nepal being an agrarian country, most of the country's population is directly being involved in agriculture. Agricultural use of biochar can assist countryman to make use of biomass and simultaneously alter the soil to enhance its water holding limit, upgrade microbial action. Biochar counters were set up in the field locales at Amarapuri VDC, Nawalparasi and Kusma, Parbat. Soil examination report recommended that the soil at the site has low phosphorus content, moderate measure of natural nitrogen and potassium, and low micronutrients. Proper soil revision practices were prescribed to local people to manage the soil nutrients [62].

### 2.1 Future Scope

Biochar has caused high yield enhancements on tropical and acidic humid soils. Biochar can enhance water quality, reduce soil emissions of greenhouse gases, reduce nutrient leaching, reduce soil acidity, and reduce irrigation and fertilizer requirement.

Introducing biochar at village includes biochar stoves and small-scale product units. Biochar can be integrated into new organic systems for farming, building, clothing, electronics, and consumer products. Biochar can initiate multiple cascades to optimize and recycle materials desired for future use.

### 2.2 Conclusion

The use of dyes on a large scale leads to environmental pollution on a large extent. Several different techniques are available to treat the dyes which are released from the textile industries. Out of the many methods available, it is concluded that adsorption technique is most feasible and preferred technique by the researchers because of its low operating cost and its unique properties. Agricultural waste utilizing various materials was employed from the production of biochar on a large scale. The biochar demonstrated a very high removal capacity, and it proved itself as one of the effective biosorbents which can be utilized to eliminate various pollutants and dyes present in wastewater. As a result, biochar assures soil quality, and it plays a vital role to eliminate various forms of pollutants present in the soil. Utilization of agricultural squanders (biochar) was employed to produce bioenergy, to enhance soil fertility and to decrease the carbon content.



## References

1. Xu R, Xiao S, Yuan J, Zhao A (2011) Adsorption of methyl violet from aqueous solutions by the biochars derived from crop residues. *Biores Technol* 102:10293–10298. <https://doi.org/10.1016/j.biortech.2011.08.089>
2. Suganya S, Senthil Kumar P, Saravanan A, Sundar Rajan P, Ravikumar C (2017) Computation of adsorption parameters for the removal of dye from wastewater by microwave assisted sawdust: theoretical and experimental analysis. *Environ Toxicol Pharmacol* 50:45–57. <https://doi.org/10.1016/j.etap.2017.01.014>
3. Jegan J, Praveen S, Bhagavathi Pushpa T, Gokulan R (2020) Sorption kinetics and isotherm studies of cationic dyes using groundnut (*Arachis hypogaea*) shell derived biochar a low-cost adsorbent. *Appl Ecol Environ Res* 18(1):1925–1939. [https://doi.org/10.15666/aeer/1801\\_1925\\_1939](https://doi.org/10.15666/aeer/1801_1925_1939)
4. Fan S, Wang Y, Wang Z, Tang J, Tang J, Li X (2017) Removal of methylene blue from aqueous solution by sewage sludge-derived biochar: adsorption kinetics, equilibrium, thermodynamics and mechanism. *J Environ Chem Eng* 5(1):601–611. <https://doi.org/10.1016/j.jece.2016.12.019>
5. Tharaneedhar V, Senthil Kumar P, Saravanan A, Ravikumar C, Jaikumar V (2017) Prediction and interpretation of adsorption parameters for the sequestration of methylene blue dye from aqueous solution using microwave assisted corncob activated carbon. *Sustain Mater Technol* 11:1–11. <https://doi.org/10.1016/j.susmat.2016.11.001>
6. Senthil Kumar P, Varjani SJ, Suganya S (2017) Treatment of dye wastewater using an ultrasonic aided nanoparticle stacked activated carbon: kinetic and isotherm modelling. *Biores Technol* 250:716–722. <https://doi.org/10.1016/j.biortech.2017.11.097>
7. Wu J, Yang J, Huang G, Xu C, Lin B (2020) Hydrothermal carbonization synthesis of cassava slag biochar with excellent adsorption performance for Rhodamine B. *J Cleaner Prod* 251:119717. <https://doi.org/10.1016/j.jclepro.2019.119717>
8. Suwunwong T, Hussain N, Chantrapromma S, Phoungthong K (2020) Facile synthesis of corncob biochar via in-house modified pyrolysis for removal of methylene blue in wastewater. *Mater. Res. Express* 7:015518. <https://doi.org/10.1088/2053-1591/ab6767>
9. Mohammed MA, Shitu A, Ibrahim A (2014) Removal of Methylene Blue using low cost adsorbent: a review. *Res J Chem Sci* 4(1):91–102
10. Sun Y, Gao B, Yao Y, Fang June, Zhang Ming, Zhou Yanmei, Chen Hao, Yang Liuyan (2014) Effects of feedstock type, production method, and pyrolysis temperature on biochar and hydrochar properties. *Chem Eng J* 240:574–578. <https://doi.org/10.1016/j.cej.2013.10.081>
11. Yu KL, Lau BF, Show PL, Ong HC, Ling TC, Chen W-H, Poh NE, Chang J-S (2017) Recent developments on algal biochar production and characterization. *Biores Technol* 246:2–11. <https://doi.org/10.1016/j.biortech.2017.08.009>
12. Sun L, Wan S, Luo W (2013) Biochars prepared from anaerobic digestion residue, palm bark, and eucalyptus for adsorption of cationic methylene blue dye: characterization, equilibrium, and kinetic studies. *Biores Technol* 140:406–413. <https://doi.org/10.1016/j.biortech.2013.04.116>
13. Noor NM, Othman R, Mubarak NM, Abdullah EC (2017) Agricultural biomass-derived magnetic adsorbents: preparation and application for heavy metals removal. *J Taiwan Inst Chem Eng* 78:168–177. <https://doi.org/10.1016/j.jtice.2017.05.023>
14. Rashidi A, Yusup S (2020) A mini review of biochar synthesis, characterization, and related standardization and legislation. <https://doi.org/10.5772/intechopen.92621>
15. Li G, Zhu W, Zhang C, Zhang S, Liu L, Zhu L, Zhao W (2016) Effect of a magnetic field on the adsorptive removal of methylene blue onto wheat straw biochar. *Biores Technol* 206:16–22. <https://doi.org/10.1016/j.biortech.2015.12.087>
16. Oladipo AA, Ifebajo AO (2018) Highly efficient magnetic chicken bone biochar for removal of tetracycline and fluorescent dye from wastewater: two-stage adsorber analysis. *J Environ Manage* 209:9–16. <https://doi.org/10.1016/j.jenvman.2017.12.030>
17. Hameed BH (2008) Equilibrium and kinetic studies of methyl violet sorption by agricultural waste. *J Hazard Mater* 154:204–212. <https://doi.org/10.1016/j.jhazmat.2007.10.010>

18. Saba B, Jabeen M, Mahmood T, Aziz I (2014) Treatment comparison efficiency of microbial amended agro-waste biochar constructed wetlands for reactive black textile dye. IPCBEE 65. <https://doi.org/10.7763/IPCBEE.2014.V65.3>
19. Abd-Elhamid AI, Emran M, El-Sadek MH, El-Shanshory AA, Soliman HMA, Akl MA, Rashad M (2020) Enhanced removal of cationic dye by eco-friendly activated biochar derived from rice straw. Appl Water Sci 10:45. <https://doi.org/10.1007/s13201-019-1128-0>
20. Zhang B, Wu Y, Cha L (2019) Removal of methyl orange dye using activated biochar derived from pomelo peel wastes: performance, isotherm, and kinetic studies. J Dispersion Sci Technol 125–136. <https://doi.org/10.1080/01932691.2018.1561298>
21. Ates A, Oymak T (2019) Characterization of persimmon fruit peel and its biochar for removal of methylene blue from aqueous solutions: thermodynamic, kinetic and isotherm studies. Int J Phytorem 607–616. <https://doi.org/10.1080/15226514.2019.1696745>
22. Kosaiyakanon C, Kungsanant S (2019) Adsorption of reactive dyes from wastewater using cationic surfactant-modified coffee husk biochar. Thaijo 18(1). <https://doi.org/10.32526/enmrj.18.1.2020.03>
23. Córdova BM, Santa Cruz JP, Ocampo M TV, Huamani-Palomino RG, Baena-Moncada AM (2020) Simultaneous adsorption of a ternary mixture of brilliant green, rhodamine B and methyl orange as artificial wastewater onto biochar from cocoa pod husk waste. Quantification of dyes using the derivative spectrophotometry method. New J Chem 44:8303. <https://doi.org/10.1039/D0NJ00916D>
24. da Silva EO, dos Santos VD, de Araujo EB, Guterres FP, Zottis R, Flores WH, de Almeida ARF (2020) Removal of methylene blue from aqueous solution by ryegrass straw. Int J Environ Sci Technol. <https://doi.org/10.1007/s13762-020-02718-9>
25. Dawood S, Sen TK, Phan C (2017) Synthesis and characterisation of slow pyrolysis pine cone bio-char in the removal of organic and inorganic pollutants from aqueous solution by adsorption: kinetic, equilibrium, mechanism and thermodynamic. Biores Technol 246:76–81. <https://doi.org/10.1016/j.biortech.2017.07.019>
26. Dai L, Zhu W, He L, Tan F, Zhu N, Zhou Q, He M, Hu G (2018) Calcium-rich biochar from crab shell: an unexpected super adsorbent for dye removal. Biores Technol 267:510–516. <https://doi.org/10.1016/j.biortech.2018.07.090>
27. Dawood S, Sen TT, Phan C (2016) Adsorption removal of Methylene Blue (MB) dye from aqueous solution by bio-char prepared from *Eucalyptus sheathiana* bark: kinetic, equilibrium, mechanism, thermodynamic and process design. J Desalin Water Treat 57(59):28964–28980. <https://doi.org/10.1080/19443994.2016.1188732>
28. Roy K, Verma KM, Vikrant K, Goswami M, Sonwani RK, Rai BN, Vellingiri K, Kim K-H, Giri BS, Singh RS (2018) Removal of Patent Blue (V) dye using indian Bael shell biochar: characterization, application and kinetic studies. Sustainability 10(8):2669. <https://doi.org/10.3390/su10082669>
29. Han X, Chu L, Liu S, Chen T, Ding C, Yan J, Cui L, Quan G (2015) Removal of Methylene Blue from aqueous solution using porous biochar obtained by KOH activation of peanut shell biochar. BioResources 10(2):2836–2849
30. Vikrant K, Roy K, Goswami M, Tiwari H, Giri BS, Kim K-H, Tsang YF, Singh RS (2020) The potential application of biochars for dyes with an emphasis on azo dyes: analysis through an experimental case study utilizing fruit-derived biochar for the abatement of congo red as the model pollutant. Biochar Appl Agric Environ Manage. [https://doi.org/10.1007/978-3-030-40997-5\\_3](https://doi.org/10.1007/978-3-030-40997-5_3)
31. Senthamarai C, Senthil Kumar P, Priyadarshini M, Vijayalakshmi P, Vinoth Kumar V, Baskaralingam P, Thiruvengadaravi KV, Sivanesan S (2012) Adsorption behavior of Methylene Blue dye onto surface modified *Strychnos potatorum* seeds. Environ Progress & Sustain Energy 32(3):624–632. <https://doi.org/10.1002/ep.11673>
32. Senthil Kumar P, Fernando PSA, Tanvir Ahmed R, Srinath R, Priyadarshini M, Vignesh AM, Thanjiappan A (2014) Effect of temperature on the adsorption of Methylene Blue dye onto sulfuric acid-treated orange peel. J Chem Eng Commun 201(11):1526–1547. <https://doi.org/10.1080/00986445.2013.819352>

33. Senthil Kumar P, Sivaranjane R, Vinothini U, Raghavi M, Rajasekar K, Ramakrishnan K (2014) Adsorption of dye onto raw and surface modified tamarind seeds: isotherms, process design, kinetics and mechanism. *J Desalin Water Treat* 52(13–15):2620–2633. <https://doi.org/10.1080/19443994.2013.792016>
34. Senthil Kumar P, Abhinaya RV, Gayathri Lashmi K, Arthi V, Pavithra R, Sathyaselvabala V, Dinesh Kirupha S, Sivanesan S (2011) Adsorption of methylene blue dye from aqueous solution by agricultural waste: equilibrium, thermodynamics, kinetics, mechanism and process design. *Colloid J* 73:651. <https://doi.org/10.1134/S1061933X11050061>
35. Senthil Kumar P, Ramalingam S, Abhinaya RV, Thiruvengadaravi KV, Baskaralingam P, Sivanesan S (2011) Lead(II) adsorption onto sulphuric acid treated cashew nut shell. *J Sep Sci Technol* 46(15):2436–2449. <https://doi.org/10.1080/01496395.2011.590174>
36. Saravanan A, Senthil Kumar P, Annam Renita A (2018) Hybrid synthesis of novel material through acid modification followed ultrasonication to improve adsorption capacity for zinc removal. *J Clean Prod* 172:92–105. <https://doi.org/10.1016/j.jclepro.2017.10.109>
37. Suganya S, Senthil Kumar P (2017) Influence of ultrasonic waves on preparation of active carbon from coffee waste for the reclamation of effluents containing Cr(VI) ions. *J Ind Eng Chem* 60:418–430. <https://doi.org/10.1016/j.jiec.2017.11.029>
38. Senthil Kumar P, Senthamarai C, Sai Deepthi ASL, Bharani R (2013) Adsorption isotherms, kinetics and mechanism of Pb(II) ions removal from aqueous solution using chemically modified agricultural waste. *Can J Chem Eng* 91(12):1950–1956. <https://doi.org/10.1002/cjce.21784>
39. Parshetti GK, Chowdhury S, Balasubramanian R (2014) Hydrothermal conversion of urban food waste to chars for removal of textile dyes from contaminated waters. *Biores Technol* 161:310–319. <https://doi.org/10.1016/j.biortech.2014.03.087>
40. Önal E, Özbay N, Yargıç AŞ, Şahin RZY, Gök Ö (2014) Performance evaluation of the bio-char heavy metal removal produced from tomato factory waste. In: *Progress in exergy, energy, and the environment*, pp 733–740. [https://doi.org/10.1007/978-3-319-04681-5\\_70](https://doi.org/10.1007/978-3-319-04681-5_70)
41. Huff MD, Kumar S, Lee JW (2014) Comparative analysis of pinewood, peanut shell, and bamboo biomass derived biochars produced via hydrothermal conversion and pyrolysis. *J Environ Manage* 146:303–308. <https://doi.org/10.1016/j.jenvman.2014.07.016>
42. Priya R, Nithya R, Anuradha R, Kamachi T (2014) Removal of colour from crystal violet dye using low cost adsorbents. *Int J Chem Tech Res* 6(9):4346–4351
43. Wang Y, Zeng G et al (2014) Removal of malachite green dye from wastewater by different organic acid-modified natural adsorbent: kinetics, equilibriums, mechanisms, practical application, and disposal of dye-loaded adsorbent. *Environ Sci Pollut Res* 21:11552–11564. <https://doi.org/10.1007/s11356-014-3025-2>
44. Ding Z, Hu X, Zimmerman AR, Gao B (2014) Sorption and cosorption of lead (II) and methylene blue on chemically modified biomass. *Biores Technol* 167:569–573. <https://doi.org/10.1016/j.biortech.2014.06.043>
45. Angin DD (2014) Utilization of activated carbon produced from fruit juice industry solid waste for the adsorption of Yellow 18 from aqueous solutions. *Biores Technol* 168:259–266. <https://doi.org/10.1016/j.biortech.2014.02.100>
46. Guo J-Z, Li B, Liu L, Lv K (2014) Removal of methylene blue from aqueous solutions by chemically modified bamboo. *Chemosphere* 111:225–231. <https://doi.org/10.1016/j.chemosphere.2014.03.118>
47. Özhan A, Şahin Ö, Küçük MM et al (2014) Preparation and characterization of activated carbon from pine cone by microwave-induced ZnCl<sub>2</sub> activation and its effects on the adsorption of methylene blue. *Cellulose* 21:2457–2467. <https://doi.org/10.1007/s10570-014-0299-y>
48. Ates F, Un UT (2013) Production of char from hornbeam sawdust and its performance evaluation in the dye removal. *J Anal Appl Pyrol* 103:159–166. <https://doi.org/10.1016/j.jaap.2013.01.021>
49. Jothirani R, Senthil Kumar P, Saravanan A, Narayan AS, Dutta A (2016) Ultrasonic modified corn pith for the sequestration of dye from aqueous solution. *J Ind Eng Chem* 39:162–175. <https://doi.org/10.1016/j.jiec.2016.05.024>

50. Senthil Kumar P, Pavithra J, Suriya S, Ramesh M, Anish Kumar K (2014) *Sargassum wightii*, a marine alga is the source for the production of algal oil, bio-oil, and application in the dye wastewater treatment. *Desalin Water Treat* 55(5):1342–1358. <https://doi.org/10.1080/19443994.2014.924032>
51. Suganya S, Senthil Kumar P (2018) Kinetic and thermodynamic analysis for the redemption of effluents containing Solochrome Black T onto powdered activated carbon: a validation of new solid-liquid phase equilibrium model. *J Mol Liq* 259:88–101. <https://doi.org/10.1016/j.molliq.2018.03.004>
52. Hemavathy RRV, Kumar PS, Suganya SS, Swetha V, Varjan SJ (2019) Modelling on the removal of toxic metal ions from aquatic system by different surface modified *Cassia fistula* seeds. *Biores Technol* 281:1–19. <https://doi.org/10.1016/j.biortech.2019.02.070>
53. Gunasundari E, Senthil Kumar P (2017) Adsorption isotherm, kinetics and thermodynamic analysis of Cu(II) ions onto the dried algal biomass (*Spirulina platensis*). *J Ind Eng Chem* 56:129–144. <https://doi.org/10.1016/j.jiec.2017.07.005>
54. Pearlin Kiruba U, Senthil Kumar P, Prabhakaran C, Aditya V (2014) Characteristics of thermodynamic, isotherm, kinetic, mechanism and design equations for the analysis of adsorption in Cd(II) ions-surface modified *Eucalyptus* seeds system. *J Taiwan Inst Chem Eng* 45:2957–2968. <https://doi.org/10.1016/j.jtice.2014.08.016>
55. Nithya K, Sathish A, Senthil Kumar P, Ramachandran T (2018) Fast kinetics and high adsorption capacity of green extract capped superparamagnetic iron oxide nanoparticles for the adsorption of Ni(II) ions. *J Ind Eng Chem* 59:230–241. <https://doi.org/10.1016/j.jiec.2017.10.028>
56. Pearlin Kiruba U, Senthil Kumar P, Sangita Gayatri K, Shahul Hameed S, Sindhuja M, Prabhakaran C (2014) Study of adsorption kinetic, mechanism, isotherm, thermodynamic, and design models for Cu(II) ions on sulfuric acid-modified *Eucalyptus* seeds: temperature effect. *J Desalin Water Treat* 56(11):2948–2965. <https://doi.org/10.1080/19443994.2014.966279>
57. Senthil Kumar P, Saravanan A, Kumar KA, Yashwanth R, Visvesh S (2015) Removal of toxic zinc from water/wastewater using eucalyptus seeds activated carbon: non-linear regression analysis. *Inst Eng Technol* 10(4):244–253. <https://doi.org/10.1049/iet-nbt.2015.0087>
58. Anbalagan S, Senthil Kumar P, Selvam SRP, Sankaranarayan A, Dutta A (2016) Influence of ultrasonication on preparation of novel material for heavy metal removal from wastewater. *Korean J Chem Eng* 33:2716–2731. <https://doi.org/10.1007/s11814-016-0109-3>
59. Hemavathy RV, Senthil Kumar P, Kanmani K, Jahnav N (2020) Adsorptive separation of Cu(II) ions from aqueous medium using thermally/chemically treated *Cassia fistula* based biochar. *J Clean Prod* 249:119390. <https://doi.org/10.1016/j.jclepro.2019.119390>
60. Bello OS, Ahmad MA (2011) Removal of Remazol Brilliant Violet-5R dye using periwinkle shells. *J Chem Ecol* 27(5):481–492. <https://doi.org/10.1080/02757540.2011.600696>
61. Nuithitikul K, Srikhun S, Hirunpraditkoon S (2010) Kinetics and equilibrium adsorption of Basic Green 4 dye on activated carbon derived from durian peel: effects of pyrolysis and post-treatment conditions. *J Taiwan Inst Chem Eng* 41:591–598. <https://doi.org/10.1016/j.jtice.2010.01.007>
62. Bhatt VD (2014) A case study on production of biochar to enhance the soil fertility, reduced carbon emission in context of climate change in Western Nepal. <https://doi.org/10.13140/RG.2.1.3397.9367>